Twelfth International Symposium on
REACTOR DOSIMETRY

May 8-13, 2005 Gatlinburg, TN, USA

Program
and
Book of Abstracts

ASTM INTERNATIONAL

EWGRD

ATOMIC ENERGY SOCIETY OF JAPAN

Twelfth International Symposium on

REACTOR DOSIMETRY

May 8-13, 2005
Park Vista Resort
Gatlinburg, TN, USA

INTRODUCTION

The Symposia in this series are held approximately every three years to provide a forum for the interchange of state-of-the-art techniques, data, and standardization of radiation metrology. This Symposium is jointly sponsored by ASTM International, the European Working Group on Reactor Dosimetry (EWGRD), and the Atomic Energy Society of Japan (AESJ). It is organized by ASTM Committee E10 on Nuclear Technology and Applications and EWGRD.

The Symposium theme is dosimetry for the assessment of irradiated reactor materials and reactor experiments, featuring radiation metrology techniques, data bases, and standardization. Under this theme, papers will be presented in the following areas:

- Reactor surveillance and plant-life management
- Data evaluation, uncertainty analysis, and adjustment methods
- Retrospective dosimetry and decommissioning
- Dosimetry for assessment of reactor structural materials
- Neutron and gamma-ray transport calculations
- Dosimetry for core characterization and reactor physics
- Characterization of neutron and gamma-ray environments
- Damage correlation and exposure parameters
- Monitoring of irradiation experiments
- Nuclear data for dosimetry
- Benchmarking, calibrations, and standards
- Fusion and high-energy neutrons
- Advanced reactors and accelerator neutron sources
- Irradiation processing and testing of electronics
- Experimental techniques, new developments, and optical methods
- Dosimetry for space nuclear power

The Symposium is organized into oral and poster presentations, informal round-table workshops, and tutorials. The meeting language is English. No translations will be provided.

SPONSORS

The organizers wish to acknowledge the support of their sponsors:

- Sandia National Laboratories
- Thermo Electron/RMP
- UT-Battelle (Oak Ridge National Laboratory)
- Canberra Industries
- National Institute of Standards and Technology
- U.S. Department of Energy

SYMPOSIUM ORGANIZING COMMITTEE OFFICERS:

ASTM Symposium Chairman	David W. Vehar, SNL
ASTM Symposium Secretary	James M. Adams, NIST
ASTM Program Chairman	David M. Gilliam, NIST
ASTM Workshop Sessions Chair	Mary Helen Sparks, WSMR
ASTM Subcommittee E10.05 Chairman	Patrick J. Griffin, SNR
ASTM Committee E10 Chairman	Roger E. Stoller, ORNL
EWGRD Chairman	Pierre D'hondt, SCK·CEN
EWGRD Scientific Secretary	Jan Wagemans, SCK·CEN
EWGRD Workshop Chairman	Willem Voorbraak, NRG

LOCAL ORGANIZING COMMITTEE:

Douglas L. Selby, Oak Ridge National Laboratory, Chairman
Tony Gabriel
Louis Mansur
Larry Miller
Randy Nanstad
Igor Remec

OTHER PROGRAM COMMITTEE MEMBERS AND SESSION CHAIRS:

ASTM: Allan Carlson, Arnold Fero, Mike Flanders, Larry Greenwood, Alireza Haghighat, Ayman Hawari, Craig Heimbach, E. Parvin Lippincott, Louis Mansur, Igor Remec, Frank H. Ruddy, Wes Sallee, James Stubbins, Jehudah Wagschal, John G. Williams.

EWGRD: Hamid Ait Abderrahim, Alain Alberman, Antonio Ballesteros, Bertram Boehmer, M. Brumovsky, A. Fernandes, J. Hogel, K. Ilieva, M. Marek, K. Noack, Henk Nolthenius, Bohumil Osmera, R. Salomaa, Tom Seren, Dean Thornton, Willem Voorbraak, Sergei Zaritsky, Eva Zsolnay.

SYMPOSIUM ROOM ASSIGNMENTS

Oral Sessions – Ballrooms 3-4
Poster Sessions – Ballrooms 1-2
Presenter Prep – Gardenview C
Workshops 1, 3, 5 – Gardenview A-B
Workshops 2, 4, 6 – Gardenview D-E
Tutuorial A – Gardenview A-B
Tutuorial B – Gardenview D-E
Symposium Office – Le Conte

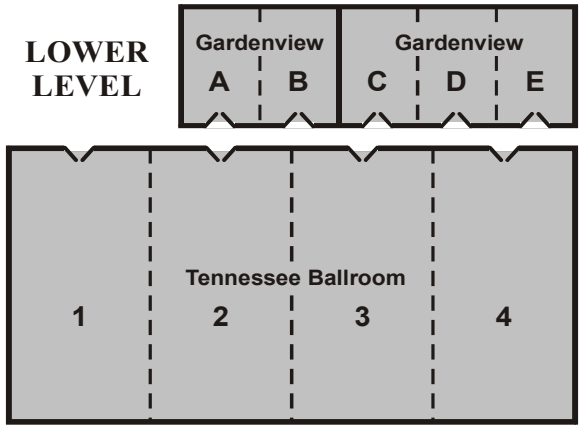

TECHNICAL SESSION SCHEDULE

	Mon	Tue	Wed	Thu	Fri
8:00 AM	[8:00] Coffee **Registration**	[8:00] Coffee	[8:00] Coffee	[8:00] Coffee	[8:00] Coffee
8:30 AM	[8:30] **Opening & Keynote Session** 1 hr 30 min 2 papers	[8:30] **Oral Session 3 Benchmarks & Intercomparison** 1 hr 40 min 5 papers	[8:30] **Oral Session 5 Transport Calculations** 1 hr 40 min 5 papers	[8:30] **Oral Session 6 Adj. Methods Reactor Dosimetry** 1 hr 40 min 5 papers	[8:30] **Oral Session 7 Experimental Techniques** 2 hrs 6 papers
9:00 AM					
9:30 AM					
10:00 AM	**[10:00] Break 20 min**	[10:10] Coffee	**[10:10] Break 20 min**	[10:10] Coffee	**[10:30] Break 20 min**
10:30 AM	[10:20] **Oral Session 1 Power Reactor Surveilllance** 2 hours 6 papers	**Poster Session A** 2 hr 10 min	[10:30] **Workshop Session II** 1 hr 30 min	**Poster Session B** 2 hr 10 min	[10:50] **Workshop Summaries** 30 min
11:00 AM					
11:30 AM					[11:20] **Closing Session** 40 min
12:00 PM			**[12:00]** **(Lunch on Own)**		**[12:00] Adjournment**
12:30 PM	**[12:20]** **Lunch** **1 hr 20 min**	**[12:20]** **Lunch** **1 hr 20 min**		[12:20] **Lunch** **1 hr 20 min**	
1:00 PM			[1:00] **Le Conte** **(Buses depart at 1:00)**		[1:00 - Late] **Technical Tour of SNS and HFIR** **(Oak Ridge National Laboratory)**
1:30 PM					
2:00 PM	[1:40] **Oral Session 2 Test Reactors Accelerators Advanced Sytems** 2 hours 6 papers	[1:40] **Oral Session 4 Cross Sections Nuclear Data Damage Correlations** 2 hours 6 papers		[1:40] **Workshop Session III** 1 hr 30 min	
2:30 PM					
3:00 PM				**[3:10] Break 20 mins**	
3:30 PM	**[3:40] Break 20 mins**	**[3:40] Break 20 mins**		[3:30] **Joint EWGRD/ASTM Committee Meeting**	
4:00 PM	[4:00] **Tutorial Session** 2 hours	[4:00] **Workshop Session I** 1 hr 30 min			
4:30 PM				[4:30] **Workshop Summary Preparation**	
5:00 PM					
5:30 PM		**[5:30] End Session**	[4:30] **Aquarium and Dinner**	**7:00 Banquet**	
6:00 PM	**[6:00] End Session**				
		[7:00-10:00] **Program Committee Meetings**			

SYMPOSIUM SCHEDULE

Sunday, May 8

6:00pm **RECEPTION and REGISTRATION**

Monday, May 9

8:00am **REGISTRATION**

8:30am **OPENING SESSION**
Chaired by: D. Vehar, ASTM Symposium Chairman
P. D'hondt, EWGRD Programme Chairman

K.01 Olkiluoto 3 – A Challenge to the Finnish Nuclear Community
T. Seren, R. Salomaa

K.02 The Spallation Neutron Source: A Powerful Tool for Materials Research
T. E. Mason

10:00am Break

10:20am **ORAL SESSION 1 POWER REACTOR SURVEILLANCE**
Chaired by: J. Adams, M. Marek

1.01 Method for Decreasing the Uncertainty in the Reactor Dosimetry Results Due to the Undefined Positioning of the RPV Surveillance Capsules at the VVER-440 NPP Reactors
É. M. Zsolnay, S. Fehér, F. Oszvald

1.02 Feasibility Study on a Simple Method of Retrospective Neutron Dosimetry for Reactor Internals and Reactor Vessel
K. Hayashi, R. Tayama, Y. Watanabe, T. Nakamura, T. Yamasaki, H. Yuya

1.03 Reactor Dosimetry Issues During Justification of Extension of Service Life of Non-Restorable Equipment of Russian VVER
G. I. Borodkin, N. N. Khrennikov, A. M. Dmitriev, M. I. Miroshnichenko, V. A. Grivizirsky

1.04 Retrospective Dosimetry using Stable Isotopes
A. H. Fero, F. H. Ruddy, R. G. Lott, R. P. Shogan

1.05 Ex-Vessel Fast Neutron Dosimetry for VVER Reactor Pressure Vessels in Czech Republic
J. Hogel

12:20pm Lunch

1:40pm **ORAL SESSION 2 TEST REACTORS, ACCELERATORS, AND ADVANCED SYSTEMS**
Chaired by: D. Selby, A. Fernandes

2.01 Characterizing the Time- and Energy-Dependent Reactor n/γ Environment
P. J. Griffin, S. M. Luker, D. B. King, K. R. DePriest, P. J. Cooper

2.02 Determination of Adjusted Neutron Spectra in Different MUSE Configurations by Unfolding Techniques
M. Plaschy, R. Chawla, C. Destouches, D. Beretz, F. Mellier, H. Serviere, P. Chaussonnet, C. Domergue, J. M. Laurens, H. Philibert

2.03 Spectral Effects and Neutron Multiplicity of an Electron Driven Assembly
W. D. Conwell

2.04 Characterization of Neutron Fields using MCNP in the Experimental Fast Reactor JOYO
S. Maeda, D. Wootan

2.05 Neptunium-Uranium Specimen Irradiation in the Advanced Test Reactor
J. M. Ryskamp, G. S. Chang, M. Ito, M. Saito

2.06 The Advanced High-Temperature Reactor (AHTR): Flux Distribution and Dosimetry
C. W. Forsberg

3:40pm Break

4:00pm **TUTORIALS**

1. **RADIATION EFFECTS IN MATERIALS DOSIMETRY**
Presented by: R. Stoller

2. **NEUTRON SCIENCE**
Presented by: B. Chakoumakos, G. Wignall

Tuesday, May 10

8:00am Coffee

8:30am **ORAL SESSION 3** **BENCHMARKS AND INTERCOMPARISONS**
Chaired by: D. Gilliam, B. Osmera

3.01 Benchmark on the 3-D VENUS-2 MOX-Fuelled Reactor Dosimetry Calculations by DANTSYS Code System
D. H. Kim, C. -S. Gil, J. Chang

3.02 Accurate Determination and Benchmarking of Radiation Field Parameters, Relevant for Pressure Vessel Monitoring - A Review of Some REDOS Project Results
B. Böhmer, B. Ošmera, et al.

3.03 Studying and Benchmarking Thermal Neutron Scattering in Graphite
A. I. Hawari, V. H. Gillette, T. Zhou, I. I. Al-Qasir, B. W. Wehring

3.04 Experimental Benchmark for the New Surveillance Program of WWER-1000
B. Ošmera, M. Mařík, F. Cvachovec, V. Tsofin, S. Lomakin, S. Zaritsky, A. Egorov, E. Brodkin

3.05 Characterization of the Neutron Field in the HSSI/UCSB Irradiation Facility at the Ford Nuclear Reactor
I. Remec, T. M. Rosseel, C. A. Baldwin, E. D. Blakeman

10:10am Coffee will be served in the Poster Session

10:10am **POSTER SESSION A** **POWER REACTOR SURVEILLANCE**
DAMAGE CORRELATIONS AND DAMAGE DOSIMETRY
CROSS SECTIONS AND NUCLEAR DATA
CALCULATIONS AND ADJUSTMENT METHODS

Chaired by: A. Fero, D. Thornton, L. Mansur

A.01 An International Evaluation of the Neutron Cross Section Standards
A. D. Carlson, S. A. Badikov, Chen Zhenpeng, E. Gai, G. M. Hale, F. -J. Hambsch, H. M. Hofmann, T. Kawano, N. M. Larson, S. Oh, V. G. Pronyaev, D. L. Smith, S. Tagesen, H. Vonach

A.02 Analysis of the VENUS-3 PWR Pressure Vessel Surveillance Benchmark Using TRIPOLI-4.3 Monte Carlo Code
Y. K. Lee

A.03 Validation of the Neutron Fluence on the VVER-440 RPV Support Structure
K. Ilieva, S. Belousov, D. Kirilova, B. Petrov, E. Polke

A.04 An Approach to Determining the Uncertainty in Reactor Test Objects using Deterministic and Monte Carlo Methods
R. E. Keith

A.05 Influence of the Multigroup Approximation on VVER-1000 RPV Neutron/Gamma Flux Calculation
S. Belousov, D. Kirilova, M. Mitev, K. Ilieva

A.06 Precision Neutron Total Cross Section Measurements for Natural Carbon at Reactor Neutron Filtered Beams
O. O. Gritzay, V. V. Kolotyi, N. A. Klimova, O. I. Kalchenko, M. L Gnidak, P. N. Vorona

A.07 A New Derivation of the Perturbation Operator Used in MCNP
R. E. Keith

A.08 Improved Surveillance Program Realizing at the WWER-1000 Reactor of Rovno NPP Unit 4
O. V. Grytsenko, E. G. Vasylyeva, V. N. Bukanov, V. L. Dyemokhin, S. M. Pugach

A.09 Track Detector Measurements in RPV of WWER-1000 Mock-Up in the LR-0 Reactor
B. Ošmera, S. Pošta, N. I. Karpunin, S. S. Lomakin,

A.10 Reactor Dosimetry Study of the Rhode Island Nuclear Science Center
N. E. Holden, R. N. Reciniello, J. -P. Hu, J. Leith, T. N. Tehan

A.11 Surveillance Specimen Programmes in Czech NPPs
M. Brumovký, M. Marek, L. Zerola, J. Rataj, P. Novosad, M. Kytka, J. Hogel, J. Brynda

A.12 Calculation of Neutron Fluxes for Radioactive Inventory Analysis of Magnox Power Plant
D. A. Allen, T. A. Lewis, C. Thiruarooran, D. A. Thornton, A. J. Bird, S. Ryecroft

A.13 Radiation Damage Calculation and Database
W. Lu, M. S. Wechsler

A.14 Extensive Revision of the Kernel-Based PREVIEW Program and its Input Data
T. O. Serén, F. Wasastjerna

A.15 Reactor Pressure Vessel Radiation Exposure Monitoring at Khmelnitskaya NPP Unit 2 and Rovno NPP Unit 4 Which Are Set Into Operation
V. N. Bukanov, V. L. Dyemokhin, O. V. Grytsenko, E. G. Vasylyeva, S. M. Pugach, A. M. Pugach

A.16 Investigation of Radiation Transport Modeling Trends in the WSMR MoLLY-G Environments
M. H. Sparks, W. W. Sallee, T. M. Flanders

A.17 Withdrawn

A.18 Interlaboratory Ex-Vessel Dosimetry Measurements and Calculations on VVER-440 of Kola-1
G. I. Borodkin, N. N. Khrennikov, A. Yu. Stolbunov, V. I. Vikhrov, D. Yu Erak, V. N. Kochkin, E. B. Brodkin, A. L. Egorov, S. M. Zaritsky, S. S. Geraschenko, V. I. Tsofin, K. G. Rozanov

A.19 Proton Induced Activation of Mercury: Preliminary Comparison of Calculations and Measurements
I. Remec, D. C. Glasgow, J. O. Johnson, J. R. Haines

A.20 The Effect of the Undefined Positioning of the RPV Surveillance Capsules at the VVER-440 NPP Reactors on the Uncertainty of the Reactor Dosimetry Results
S. Fehér, É. M. Zsolnay, Sz. Czifrus

A.21 Neutronics Tools for the Design of a Spallation Neutron Source
F. X. Gallmeier, T. A. Gabriel, P. D. Ferguson, E. B. Iverson, I. I. Popova

A.22 Coupled Neutron-Gamma Calculations for the LR-0 Experimental Benchmark
G. Hordósy

A.23 Withdrawn

A.24 Comparison of the Results of the Calculational and Experimental VVER-440 Pressure Vessel Dosimetry at Paks NPP for Lifetime Extension
G. Hordósy, Gy. Hegyi, A. Keresztúri, Cs. Maráczy, L. Szalmás, P. Vértes, É. Zsolnay

A.25 Use of CPXSD for Generation of an Effective Multigroup Library for PV Fluence Calculations
F. A. Alpan, A. Haghighat

A.26 Benchmarking of PENTRAN-SSn using the VENUS-2 MOX Problem
G. Longoni, A. Haghighat, C. Yi, J. Huh

12:20pm Lunch

1:40pm **ORAL SESSION 4** **CROSS SECTIONS AND NUCLEAR DATA DAMAGE CORRELATIONS**

Chaired by: A. Carlson, A. Alberman

4.01 Release of the New International Reactor Dosimetry File IRDF-2002
A. Trkov, É. M. Zsolnay

4.02 Nuclear Data Evaluations and Recommendations
N. E. Holden

4.03 Gas Production in Reactor Materials
L. R. Greenwood

4.04 Dosimetry Requirements for Pressure Vessel Steels Toughness Curve in the Ductile to Brittle Range
H. Carcreff, A. Alberman, L. Barbot, F. Rozenblum, D. Beretz, Y. K. Lee

4.05 Radiation Damage Calculations for the SNS Target, Moderators Vessels, and Reflector System
P. D. Ferguson, F. X. Gallmeier, L. K. Mansur, M. S. Wechsler

4.06 Attenuation of Radiation Damage and Neutron Field in RPV Wall
M. Brumovsky, M. Marek, L. Zerola, L. Viererbl, V. N. Golovanov, B. V. Lichadeev, B. M. Raetsky, A. L. Petelin

3:40pm Break

4:00pm **WORKSHOP SESSION I**

A. LWR SURVEILLANCE AND RETROSPECTIVE DOSIMETRY
Chaired by: E. P. Lippincott and S. Zaritsky
B. DOSIMETRY FOR IRRADIATION FACILITIES AT TEST AND RESEARCH REACTORS
Chaired by: A. Hawari and W. Voorbraak

Wednesday, May 11

8:00am Coffee

8:30am **ORAL SESSION 5 TRANSPORT CALCULATIONS**
Chaired by: I. Remec, K. Noack

5.01 Pseudo-Adjoint Model for Reactor Internals Analysis
A. H. Fero, M. V. Perlov

5.02 Measurements and Monte Carlo Calculations of Gamma and Neutron Flux Spectra Inside and Behind Steel-Water Configurations
B. Boehmer, J. Konheiser, K. Noack, I. Stephan, W. Hansen, D. Hinke, S. Unholzer, M. Grantz, H.-C. Mehner

5.03 Advances in Calculation of Fluence to Reactor Structures
E. P. Lippincott, M. P. Manahan Sr.

5.04 Deterministic and Monte Carlo Neutron Transport Calculations for Greifswald-1 and Comparison with Ex-vessel Measured Data
G. I. Borodkin, N. N. Khrennikov, B. Böhmer, K. Noack, J. Konheiser

5.05 Efficacy of Three-Dimensional Adjoint Biasing for a Cyclotron used for Medical Isotope Production in China
R. Pevey, L. F. Miller, B. J. Marshall, L. W. Townsend, B. Alvord

10:10am Break

10:30am **WORKSHOP SESSION II**

A. CROSS-SECTION FILES AND UNCERTAINTIES
Chaired by: P. J. Griffin and E. Zsolnay
B. FUSION AND HIGH ENERGY NEUTRONS
Chaired by: L. Greenwood and TBD

12:00pm Lunch (on your own)

1:00pm **AFTERNOON SOCIAL EVENTS**

Thursday, May 12

8:00am Coffee

8:30am **ORAL SESSION 6** **ADJUSTMENT METHODS**
REACTOR DOSIMETRY

Chaired by: J. Williams, H. Nolthenius

6.01 Sensitivity Analysis and Neutron Fluence Adjustment for VVER-440 RPV
S. I. Belousov, Kr. D. Ilieva

6.02 Generalized Linear Least Squares Adjustment, Revisited
B. L. Broadhead, M. L. Williams, J. J. Wagschal

6.03 Retrospective Measurement of Neutron Activation within the Pressure Circuit Steelwork of a Magnox Reactor and Comparison with Prediction
D. A. Thornton, C. Thiruarooran, D. A. Allen, A. M. Harris, C. G. Holmes, C. R. Harvey

6.04 Comparison of Predicted and Measured Helium Production in US BWR Reactors
L. R. Greenwood, B. M. Oliver

6.05 Shielding Calculations for the Upgrade of the HFIR Beam Line HB-2
C. O. Slater, D. L. Selby, J. A. Bucholz, J. L. Robertson, M. L. Crow

10:10am Coffee will be served in the Poster Session

10:10am **POSTER SESSION B** **TEST REACTORS, ACCELERATORS AND ADVANCED SYSTEMS**
BENCHMARKS AND INTERCOMPARISONS
EXPERIMENTAL TECHNIQUES

Chaired by: M. Flanders, J. Wagemans, I. Remec

B.01 Benchmark Experiments/Calculations of Neutron Environments in the Annular Core Research Reactor
K. R. DePriest

B.02 Spent Fuel Monitoring with Silicon Carbide Semiconductor Neutron/Gamma Detectors
T. Natsume, H. Doi, F. H. Ruddy, J. G. Seidel, A. R. Dulloo

B.04 Measurement of Helium Generation in AISI 304 Reflector and Blanket Assemblies after Long-Term Irradiation in EBR-II
F. A. Garner, B. M. Oliver, L. R. Greenwood

B.05 Development and Test Program for Radiation Hardened Diamond PCDs
D. B. King, S. M. Luker, G. E. Naranjo, P. J. Griffin, R. J. Hohlfelder

B.06 Digital Multiparameter System for Characterisation of Neutron-Gamma Field in the Experimental Reactor LR-O
Z. Bures, J. Kroupa, F. Cvachovec, P. Celeda, B. Osmera

B.07 A Beam-Monitor System for Neutrons and Gamma-Rays in the Medical Irradiation Field of the Kyoto University Research Reactor
Y. Sakurai, A. Maruhashi

B.08 Comparison of Boron-Based Solid State Dosimeter Schemes
M. S. Hallbeck, A. N. Caruso, S. Balkir, W. K. Pitts, J. I. Brand

B.09 Verification of MultiTrans Calculations by the VENUS-3 Benchmark Experiment
P. Kotiluoto

B.10 Application of a Silicon Calorimeter in Fast Burst Reactors
S. M. Luker, K. R. DePriest, P. J. Griffin, D. B. King, G. E. Naranjo, A. J. Suo-Anttila

B.11 The Neutron Spectrum of NBS-1
C. R. Heimbach

B.12 The Validity of the Use of Equivalent DIDO Nickel Dose for Graphite Dosimetry
D. A. Allen, D. A. Thornton, A. M. Harris, J. W. Sterbentz

B.13 Radiation Dosimetry in the BNCT Patient Treatment Room at the BMRR
N. E. Holden, R. N. Reciniello, J. -P. Hu

B.14 Predictions of Radiation Damage in Silicon Carbide Semiconductor Radiation Detectors for Nuclear Reactor Power Monitoring in the GT-MHR
T. E. Blue, B. Lohan, B. Khorsandi, D. W. Miller

B.15 Measurements of Reactor Neutron Spectra Characteristics Using Activation Composite Monitors
B. V. Efimov, A. M. Demidov, V. S. Dikarev, V. S. Ionov

B.16 TRIM Modeling of Displacement Damage in SiC for Monoenergetic Neutrons
B. Khorsandi, T. E. Blue, W. Windl

B.17 Thermal and Epithermal Fluence Rate Measurements in Multipurpose Reactors
W. P. Voorbraak, J. K. Aaldijk, W. E. Freudenreich

B.19 Comparison of Two Methods of Fast Neutron Fluence Measurements in WWER-1000 Surveillance Assemblies
V. A. Nikolaenko, S. M. Zaritsky, I. V. Bachuchin

B.20 Characterization of the Environment Inside a Graphite Thermal Column at the White Sands Fast Burst Reactor Facility
W. W. Sallee, M. H. Sparks, T. M. Flanders

B.21 Neutron and Photon Dosimetry at LR-0 Using Paired Dosemeters
A. C. Fernandes, L. Santos, J. Cardoso, J. Marques, E. Novak

B.22 A New Methodology for Adjustment of Iron Scattering Cross Sections using Time-of-Flight Spectroscopy
M. T. Wenner, A. Haghighat, J. M. Adams, A. D. Carlson, S. M. Grimes, T. N. Massey

B.23 Reactor Dosimetry with Niobium
J. Wagemans, M. Willekens, L. Borms, J. Oeyen, A. Moens

12:20pm Lunch

1:40pm **WORKSHOP SESSION III**

A. ADJUSTMENT METHODS AND UNCERTAINTIES
Chaired by: W. Sallee and T. Seren
B. RADIATION DAMAGE CORRELATIONS
Chaired by: L. Mansur and D. Thornton

3:10pm Break

3:30pm Joint ASTM/EWGRD Symposium Committee Meeting

4:30pm Workshop Summary Preparation

7:00pm **BANQUET**

Friday, May 13

8:00am Coffee

8:30am **ORAL SESSION 7 EXPERIMENTAL TECHNIQUES**
Chaired by: F. Ruddy, J. Hogel

7.01 Neutron Response Function for BC-523A Scintillation Detector in Energy Range 0.5 to 20 MeV
F. Cvachovec, J. Cvachovec, S. Posta, B. Osmera

7.02 Development of a Silicon Calorimeter for Dosimetry Applications in a Water-Moderated Reactor
S. M. Luker, P. J. Griffin, D. B. King, K. R. DePriest, G. E. Naranjo, N. Keltner, A. J. Suo-Anttila

7.03 Measurement and Calculation of WWER-440 Pressure Vessel Templates Activity for Support of Vessel Dosimetry
V. I. Vikhrov, D. Yu Erak, V. N. Kochkin, E. B. Brodkin, A. L. Egorov, S. M. Zaritsky

7.04 Fast Neutron Dosimetry and Spectrometry Using Silicon Carbide Semiconductor Detectors
F. H. Ruddy, J. G. Seidel, A. R. Dulloo

7.05 Retrospective Dosimetry of Fast Neutrons Focused on the Reactions 93Nb (n,n')93mNb and 54Fe(n,p)54Mn
W. P. Voorbraak, J. R. W. Woittiez, J. Wagemans, M. Van Boxstaele, T. Kekki, T. O. Serén

7.06 Space Reactor Shadow Shielding Experiments using Lithium Hydroxide
J. G. Williams, I. Jun, W. W. Sallee

10:30am Break

10:50am **WORKSHOP SUMMARIES SESSION**
Chaired by: M. H. Sparks, W. Voorbraak

11:20am **CLOSING SESSION**
Chaired by: D. Vehar, P. D'hondt

1:00pm **OPTIONAL TECHNICAL TOUR**
Hosted by: D. Selby
Spallation Neutron Source (SNS) facility and the High Flux Isotope Reactor (HFIR) at Oak Ridge National Laboratory

Summaries

OLKILUOTO 3 - A CHALLENGE TO THE FINNISH NUCLEAR COMMUNITY

R. Salomaa

Advanced Energy Systems, Helsinki University of Technology,
P.O.Box 2200, FIN-02015 TKK, Finland
email: Rainer.Salomaa@tkk.fi

Abstract

The Government of Finland granted in 17th February 2005 a license for the construction of a new nuclear power plant in Olkiluoto. The thermal power of the new EPR unit is 4300 MW corresponding to about 1600 MW of electricity. The commercial operation is expected to begin already by mid 2009. Another recent important governmental decision has been the selection of the repository site for the spent nuclear fuel. Presently exploratory excavations involving a test laboratory, ONKALO, are under way in Olkiluoto. The expected time for the application of the final construction license for the repository is 2012. The OL3 project and its current status will be described. The "big" nuclear problems worrying laymen have been acceptably solved in Finland; perhaps, OL3 is leading the way to a wider revival of nuclear power in Europe?

The first four NPP units in Finland were taken into commercial operation in 1977-1982. The present nuclear professionals were mainly educated in the 70´es and 80´es and are, therefore, close to retirement age. The previous decision-in-principle application of a new NPP Unit was filed in 1991, but the Parliament did not ratify the governamental acceptance. As a consequence the Finnish nuclear actors had to adjust to a stagnation period during which the recruitement of new professionals became increasingly difficult and the public acceptance of nuclear energy was lukewarm at best. The scene changed in Finland very quickly from a de facto moratorium into a acute need of new professionals. The whole nuclear community is currently collaborating in both organising training courses for the acute needs of OL3 and in finding longer term solutions for the replacement of retirees. Nuclear education in Finland and its links to international education and training networks will be briefly discussed.

A noteworthy feature OL3 is that it is designed for a 60 year or more operational life-time. Adding to this the time required for handling of the spent fuel, one can conclude that nuclear power will be present in Finland at least for the next hundred years! This time range is considerably longer than the anticipated emergence time of revolutionary fission reactors as presented e.g. by the Generation IV fleet or that of first commercial fusion reactor prototypes. Therefore, it is also worth pondering how to exploit the R&D on new nuclear energy concepts for both recruiting new nuclear professionals for the existing NPP needs and, on the other hand, for the advancement of the new concepts.

The Spallation Neutron Source: A Powerful Tool for Materials Research

T.E. Mason
Associate Laboratory Director for the Spallation Neutron Source
Oak Ridge National Laboratory

The wavelengths and energies of thermal and cold neutrons are ideally matched to the length and energy scales in the materials that underpin technologies of the present and future: ranging from semiconductors to magnetic devices, composites to biomaterials and polymers. The Spallation Neutron Source (SNS) will use an accelerator to produce the most intense beams of neutrons in the world when it is complete in 2006. The project is being built by a collaboration of six U.S. Department of Energy laboratories. It will serve a diverse community of users drawn from academia, industry, and government labs with interests in condensed matter physics, chemistry, engineering materials, biology, and beyond. The design goals, current status, and anticipated scientific capabilities of SNS will be summarized.

Method for Decreasing the Uncertainty in the Reactor Dosimetry Results Due to the Undefined Positioning of the RPV Surveillance Capsules at the VVER-440 NPP Reactors

Zsolnay É. M., Fehér S.
Institute of Nuclear Techniques, Budapest University of Technology and Economics,
Műegyetem rkp. 3-9., H-1111 Budapest, Hungary

Oszvald F.
Paks NPP Ltd., P.O. Box 71, H-7031 Paks, Hungary

ABSTRACT

At the VVER-440 NPP reactors the RPV surveillance specimens and the neutron monitors are situted in the surveillance capsules in undefined positions, relative to the active core (details see in the corresponding paper presented at this symposium). The geometrical discrepancies resulted in a large uncertainty in the dosimetry results, i.e. in determination of the neutron exposition of the specimens. To improve the accuracy of the dosimetry results deriving from the RPV surveillance programme developed by the constructor of the NPP, the ^{54}Mn activites – from the nuclear reaction ^{54}Fe(n,p)^{54}Mn – measured on the irradiated specimens between 1986-1990, were used. These measurements resulted in the average relative axial fast neutron fluence rate distributions at the places of the specimens, and they were fitted to the absolute neutron fluence rate values above 0.5 MeV, determined from the responses of the corresponding neutron monitors. The possible spectral differences at the different irradiation positions were also investigated and considered. Important improvement has been reached in the accuracy of the dosimetry results by this method.

After the old surveillance chains were used up, a new RPV surveillance programme was introduced at the Paks NPP in 1992. In frame of this new programme the neutron monitors have been situated in the mid position, on the top of the specimens. Consequently, the geometrical uncertanties of the surveillance capsules relative to the active core, can influence the neutron exposition of the specimens only. The neutron monitors in this case always measure the axial distribution of the neutron fluence rate at the mid positions of the specimens in the capsules, independently of the geometrical configuration of the capsules, considered. The exposition rates of the specimens and of the neutron monitors within the same capsule were determined and analysed together with their uncertainties, using the special Monte Carlo code developed for this purpose. The results have shown that the uncertainties of the investigated exposition rates have significantly decreased as compared with the ones obtained from the old RPV surveillance programme. Averaging the exposition values of more capsules situated in the vicinity of the geometrical position with maximum neutron fluence rate, lead to further reduction of the uncertainties of the corresponding results.

This paper presents the methods outline above, and the results achived.

Feasibility study on a simple method of retrospective neutron dosimetry for reactor internals and reactor vessel

Katsumi Hayashi, Ryuuichi Tayama, Yoshio Watanabe, Tomomi Nakamura.
Hitachi Ltd.
3-2-1, Saiwai-cho, Hitachi, Ibaraki, 317-8511, Japan

Tadashi Yamasaki, Hideki Yuya
Chubu Electric Power Co., Inc.
20-1, Kitasekiyama, Ohdaka-cho, Midori-ku, Nagoya, Aichi, 459-8522, Japan

OBJECTIVE

Accurate estimation on the neutron flux distribution in reactor vessel is necessary to predict the material lifetime, maintenance dose and radioactivity at decommissioning phase. For these purposes, precise calculation using 3D Sn method and Monte Carlo method [*1*][*2*] are preferable. Simultaneously, measured data is indispensable to assure the calculated results for necessary position. For this purpose, retrospective dosimetry [*3*] is one of good approach for plant in operation. Because the sampling of the metal and following procedure of gamma or beta counting is time and cost consuming in retrospective dosimetory, therefore number of sampling should be limited. In this paper we present a simple method of retrospective neutron dosimetry that can be used with less time and cost.

APPROACH

Simple direct gamma-ray counting of irradiated structural material was investigated. ^{54}Mn(half life:312days), ^{58}Co(70days) and ^{60}Co(5.27years) are chosen as main nuclides to be measured. ^{59}Fe(44days) and ^{51}Cr(27days) are also supplemental nuclide for checking of short irradiation range. ^{54}Mn and ^{58}Co are produced by fast neutron and ^{60}Co, ^{59}Fe and ^{51}Cr are by thermal neutron. Detector was chosen to be HgI2 or CdZnTe from three reasons, namely, (1) detector should be small enough to insert in limited space between internal structures, (2) it should have high efficiency to measure in short period, (3) its energy resolution is good enough to distinguish ^{54}Mn(0.835MeV) to ^{58}Co(0.811MeV). To shield background gamma-rays from behind and to limit measuring area, tungsten shield which thickness is 50mm with collimator hole which size is 1mm in diameter is used. Figure 1 shows this collimator shield with detector. Figure 2 shows concept of measuring of BWR shroud.

Figure 3 shows convert procedure from measured photon counts to neutron fluence, DPA and gas production. Detector responses for each geometry, namely, shroud measurement from inside, shroud measurement from outside and reactor vessel measurement from inside etc., are prepared for each nuclide by using MCNP4C Monte Carlo code. Each relative nuclide distribution along the thickness direction is assumed by using the calculated flux distribution and energy spectrum by TORT code [*2*] and each reaction cross section These responses are prepared for unit flux at measuring surface. By using these responses, start time and stop time of counting, decay constant and power histories, we can get neutron fluence. By using these fluences, energy spectra calculated by TORT and energy response of DPA or gas production, we can get DPA or gas production quantity. This process is coded using Visual Basic Editor of Microsoft Corp. Just after measurement, we can start nuclide identification program and subsequent dosimetry program on PC, and desired output of fluence, DPA and gas production are shown on the PC display.

To consider count rate range, dead-time and pulse height distributions of detector at accessible shroud positions are calculated using MCNP4C Monte Carlo code. It is confirmed that we can get sufficient statistics in reasonable count time.

CONCLUSION

Concept design of simple retrospective dosimetry method was performed. By this method, we can measure neutron fluence, DPA and gas production data in reasonable counting time. Because time and cost of this method is much less than sampling method used in ordinal retrospective dosimetry, we can do measurement at many positions and can make measured fluence contour map etc.

REFERENCES

1. L.R.Greenwood and B.M.Oliver, *Retrospective Reactor Dosimetry for Neutron Fluence, Helium, and Boron Measurement*, Reactor Dosimetry in the 21st Century Jan Wagemans et al. (Editors), World Scientific Publishing Co. Pte. Ltd. (2003)
2. T. Tsukiyama et al., *Reliable Estimation of Neutron Flux in BWR Reactor Vessel Using the TORT Code (1) Benchmark Validation Using KKM Measurements*, Reactor Dosimetry in the 21st Century Jan Wagemans et al. (Editors), World Scientific Publishing Co. Pte. Ltd. (2003)
3. M. Kurosawa et al., *Reliable Estimation of Neutron Flux in BWR Reactor Vessel Using the TORT Code (2) Application to Neutron and Gamma Flux Estimation*, Reactor Dosimetry in the 21st Century Jan Wagemans et al. (Editors), World Scientific Publishing Co. Pte. Ltd. (2003)

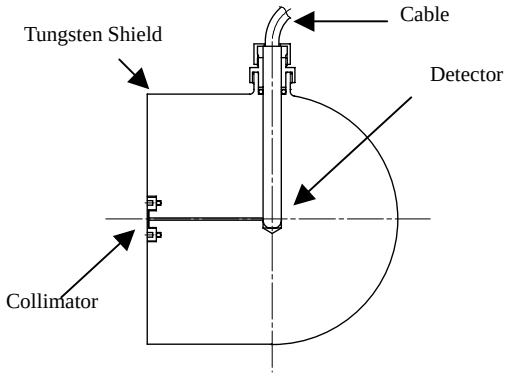

Figure1. Detector and collimator shield

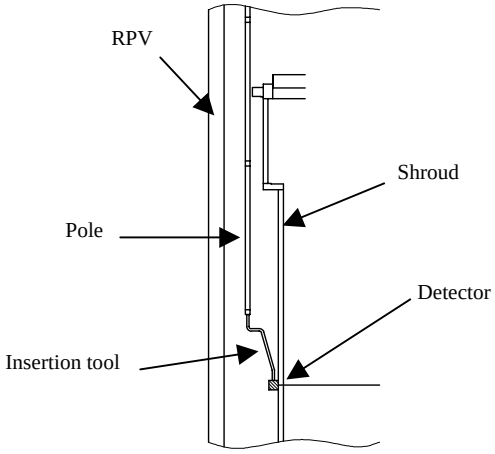

Figure 2. Concept of measuring method

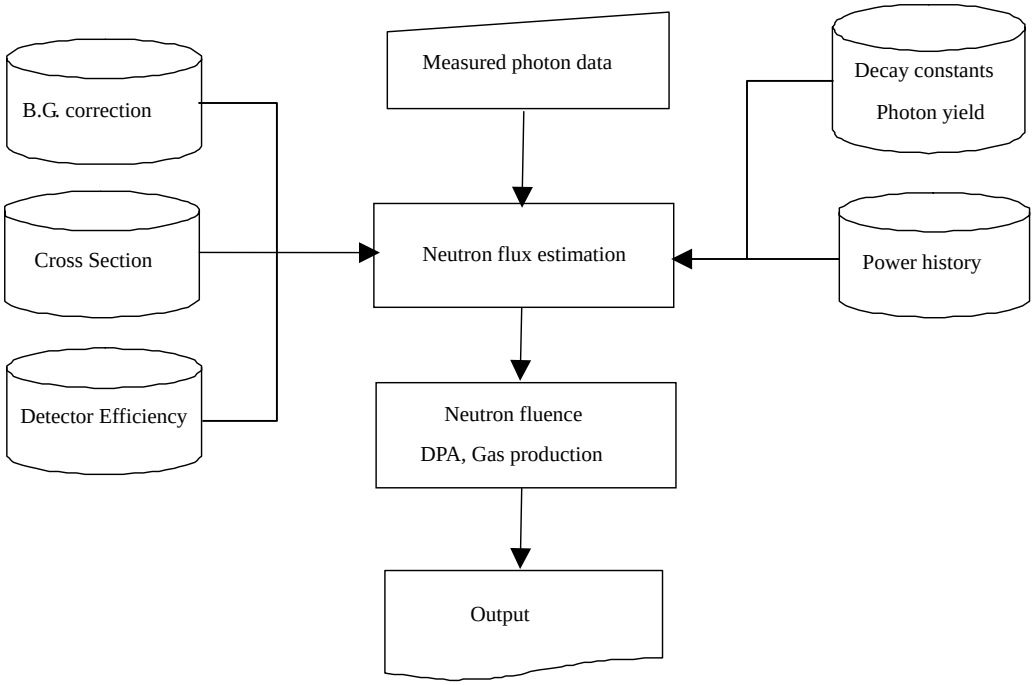

Figure 3. Convert procedure from measured photon counts to neutron fluence, DPA and gas production

Reactor Dosimetry Issues During Justification of Extension of Service Life of Non-Restorable Equipment of Russian VVER

Borodkin, G. I., Khrennikov, N. N. and Dmitriev, A.M.
SEC NRS of GOSATOMNADZOR of Russia
2/8, bld. 5, Malaya Krasnoselskaya ul., 107140 Moscow, Russia

Miroshnichenko, M.I. and Grivizirsky, V.A.
Nuclear, Industrial and Environmental Authority of Russia (former GOSATOMNADZOR of Russia)
34 Taganskaya ul., 109147 Moscow, Russia

The non-restorable equipment of VVER type reactors is a key component during consideration of issues of extension of NPP unit operation. A special attention is paid to structural analysis of equipment (reactor pressure vessel (RPV), support constructions), exposed to reactor irradiation (neutrons and gammas). During expertise of the substantiation of service life of such equipment, a thorough investigation is aimed at analysis of reliability of current evaluation and prediction of radiation exposure in critical points of the equipment. A basis for the expert analysis within the framework of licensing procedure is a system of regulatory documents [*1*] of the Nuclear, Industrial and Environmental Authority of Russia (former GOSATOMNADZOR of Russia). The present work describes actual reactor dosimetry issues within the framework of the licensing expertise procedure. A practice of application of the developed regulatory approach to the estimation of equipment service life proceeding from the accumulated fast neutron fluence is demonstrated.

A detail analysis of evaluation of lifetime of pressure vessels of the first generation of VVER-440 type reactors is presented. The radiation load of these RPVs is considered to be one of the key factors, which regulation allows to manage the RPV lifetime. More over, in some cases (Novovoronezh-4, Kola-2) a value of conservative margin of fast neutron fluence influences directly on the extension of RPV service life. To reduce the conservative margin a comprehensive investigation of neutron dosimetry parameters of RPV should be carried out. New results of calculation and experimental RPV neutron dosimetry investigations performed within expert analysis of safety of the first generation of Russian VVER-440 are discussed in the paper.

The radiation embrittlement of VVER support constructions (especially ferritic steel wall of water tank of first generation of VVER-440) also attracts attention during justification of plant-life extension. The reason of such attention is possible low temperature embrittlement effect at low neutron fluence rate irradiation, for example, analyzed by McElroy [*2*]. In this reference there is a necessity to have reliable evaluations of radiation load of VVER support constructions. Some results of neutron and gamma damage assessments of VVER-440 support constructions are analyzed.

The review of Russian programs of testing of surveillance specimens and templates, used by the Utility for prediction of RPV steel property degradation in extended service life period, is presented. The neutron dosimetry, which accompanies the programs, is evaluated. It is demonstrated, that there is a need of improvement and development of reliable experimental and calculation techniques. The ways of neutron dosimetry improvement are proposed and considered.

The necessity and advantage of research of RPV metal both by cutting out of templates from pressure vessels of operating reactors and by sectioning of pressure vessels of decommissioning VVERs are discussed. One of the promising experimental methods of fast neutron fluence monitoring in such researches is recognized to be niobium-93m activity measurement in probes extracted from irradiated RPV steel fragments.

REFERENCES

1. *The List of Basic Legal Statements and Regulatory Standards used by Gosatomnadzor of Russia for State Regulation of Safety in the Field of Use of Atomic Energy. P-01-01-2003*, GOSATOMNADZOR of Russia, (May 2003).
2. McElroy R.J. et al., *Low Temperature Embrittlement of LWR RPV Support Structures*, Proc. NEA/CSNI Workshop on Safety Assessment of Reactor Pressure Vessels, Espoo, Finland, 8-9 October, 1990, **2**, p. 255.

Retrospective Dosimetry Using Stable Isotopes

Fero, A. H.
Westinghouse Electric Company
Nuclear Services
P. O. Box 158
Interstate 70, Exit 54
Madison, PA 15663-0158 USA

Ruddy, F. H., Lott, R. G., and Shogan, R. P.
Science & Technology
Westinghouse Electric Company
1332 Beulah Road Pittsburgh, PA 15235-5081, USA

In cases where dosimetry information is not available from prepared dosimetry capsules, retrospective dosimetry may be performed by analyzing small samples taken from components of a reactor. Typically, measurements are carried out using available radioactive isotopes, which are produced through activation of major and trace constituents in the component of interest. Unfortunately, the available choice of radioisotopes is very limited and is dominated by isotopes such as 71-day ^{58}Co ([n,p] from nickel) and 312-day ^{54}Mn ([n,p] from iron) that are short-lived compared to the length of time of the reactor exposure. However, the typical neutron exposures in the (1-5)x10^{22} cm^{-2} range can result in significant (5-50%) amounts of isotopic transmutation. For example, more than 12% of the isotope ^{56}Fe in iron will be converted to ^{57}Fe after a thermal neutron fluence of 5x10^{22} cm^{-2}, and the other stable iron isotopes (^{54}Fe, ^{57}Fe, ^{58}Fe) will be transmuted similarly. Thus, iron isotope mass ratio measurements provide a means to estimate the thermal neutron fluence for an irradiated iron-containing sample such as steel. Mass spectrometry measurements can detect changes in the abundances of the iron isotopes to a sensitivity of parts per million, so the expected changes produced by irradiation are easily measurable.

Fast neutron fluences may also be deduced from measurements of stable isotopes. For example, chromium is a major component of some steels. The isotope ^{50}Cr (4.345% abundance) has a 47.12 mb cross section (fission spectrum average) for the (n,p) reaction to produce ^{50}V, which is extremely long-lived (1.4 x 10^{17} year half life). The neutron threshold energy for this reaction is 259.8 keV. If vanadium is present in steel at no more than trace levels, most of the ^{50}V detected in a steel sample can be attributed to fast neutron reactions with chromium. If the vanadium concentration is known or measured, measurement of the amount of ^{50}V can be used to estimate the fast neutron fluence. This reaction and other reactions with different energy responses that produce stable products can be used to provide a measure of neutron energy and fluence for an irradiated sample.

Candidate reactions with potentially measurable stable product yields have been identified. Possible interferences have been evaluated in each case. For example, the presence of vanadium or titanium may interfere with the example ^{50}V reaction given above.

The NJOY code is being used to generate target and product isotope reaction cross sections from the ENDF/B-VI library for some of the reactions of interest. Expected yields of the stable reaction products are being evaluated using the Westinghouse ACT code with neutron fluxes calculated for typical reactor internals structures using the DORT and TORT discrete ordinates transport theory codes and the BUGLE-96 neutron cross section library.

Proof-of-principle mass spectrometry measurements are proposed for selected samples from the Westinghouse inventory of irradiated structural materials, which has accumulated over the years as the result of materials reliability studies on reactor components.

EX-VESSEL FAST NEUTRON DOSIMETRY FOR VVER REACTOR PRESSURE VESSELS IN CZECH REPUBLIC

Josef Hogel, ŠKODA JS Plzen a.s., Czech Republic

The fast neutron fluence monitoring in the reactor cavity is compulsory in Czech Republic for all units of nuclear power plants (NPP).

The monitors are inserted in special holder rack made from aluminium profiles and their insertion and withdrawal is carried out during the refuelling outage. Copper and iron foils are used for the neutron fluence distribution measurement vertically along the core high and azimuthally within the symmetry sector of the core. Dosimeter set containing niobium, nickel, iron, titan, copper and manganese is inserted at the azimuthal maximum of neutron flux density at the core mid-level.

Attenuation coefficients gained at mock-up experiments performed at LR-0 reactor (NRI Øež) were used for the fluence conversion into the reactor pressure vessel (RPV) inner wall and ¼ of its thickness. Their credibility were verified for VVER440 reactors by calculations and the differences between experimental values, both in the reactor cavity and surveillance capsules, and calculated ones were up to 10%. The same calculations will be performed for the VVER1000 reactors after the measurement and evaluation of activation monitors inserted in the surveillance containers. First one was withdrawn from the first unit in April 2004.

All four units of VVER440 in Dukovany have been monitored since the year 1993. The results of measurements strongly influenced the strategy of the core loading. The insertion of highly burned-up fuel elements into the core periphery reduced significantly the fast neutron flux density impinging the RPV.

The following table gives the ratio of evaluated neutron flux densities to the project value at the positions of azimuthal maximum and minimum. First two rows contain the maximal and minimal measured values at NPP Dukovany (EDU). The 3rd and 4th ones give the typical results of monitoring performed by the author of this report at two units of NPP V1 Jaslovske Bohunice (EBO, Slovakia) in the end of eighties of last century. Last row contains the results from measurement performed at Loviisa NPP in 1999 by experts of VTT Chemical Technology, Škoda JS a.s.and NRG Petten. It is necessary to mention, that last two units are operated with the core having dummy peripheral cassettes.

Tab.1: The ratio of evaluated neutron flux densities to project value for different VVER440 units

NPP	Unit/cycle	Core	Azimuthal maximum	Azimuthal minimum	Ratio min / max
EDU min	3/16	Low-leakage	0,56	0,54	0,96
EDU max	2/8	Standard	1,19	0,82	0,69
EBO-V1	1/11	Standard	1,22	0,63	0,51
EBO-V1	2/10	Dummy cassettes	0,32	0,16	0,50
Loviisa	1/22	Dummy cassettes	0,30	0,19	0,63

Irradiation of activation detectors was included into the start up program of both units of Temelin NPP having VVER1000 reactors. The irradiation was performed at constant power level for 100 hours and the dosimeter set was completed by detectors having shorter half-lives. The activity measurements began 40 hours after the reactor shutdown.

The regular fluence monitoring of both units has been performed since their start up.

The experimental verification of attenuation coefficients will be carried out by taking of scarps of inner RPV cladding material and subsequent measurement of induced activity of ^{54}Mn. This activity will be compared with the activities of iron monitors irradiated in the reactor cavity.

This cladding contains also approximately 1% of niobium and from the measured activity of ^{93m}Nb will be assessed the neutron fluence at the take-off position for the whole time of operation of each unit (retrospective dosimetry).

The special device, which will be coupled to the SKIN manipulator used for RPV inspection, is designed and manufactured in Škoda JS a.s.for this purpose. First take off is planed at the 3rd unit of Dukovany NPP in March 2005.

Keywords: Ex-vessel dosimetry, activation measurements, retrospective dosimetry, low-leakage core

Characterizing the Time- and Energy-Dependent Reactor n/γ Environment

Griffin, P. J. [1], Luker, S. M., King, D. B., DePriest, K. R., Cooper, P. J.
Sandia National Laboratories, MS 1146
Albuquerque, NM 87185-1146, USA.

OBJECTIVE

Typical spectrum characterization techniques in reactor environments use integral passive dosimetry metrics to unfold a time-averaged radiation environment. However, the reactor radiation environment is more dynamic. In a reactor pulse, the early radiation has a neutron/gamma component resulting from the prompt fission neutron and gamma radiation and from the neutron-induced secondary gammas. But after the primary reactor pulse, the radiation environment also includes a time-dependent delayed neutron and gamma component. At even later times, the material activation radiation dominates the source term. When active tests are conducted in the reactor, the radiation environment at a particular time may not be well characterized by the time-integrated spectrum characterization provided by the typical radiation transport calculations. When test objects and passive dosimetry are removed from the reactor, they have not only seen the main reactor pulse, but they have also seen the time-dependent delayed fission radiation environment as well as activation gammas. It can be difficult for an experimenter to de-convolute the actual integral radiation environment seen by a test object from the available calculated spectrum characterization data.

The purpose of this paper is 1) to outline a calculational methodology for de-convoluting the time- and energy-dependent radiation environments in a pulsed test reactor field, and 2) to present time-dependent active dosimetry from various dosimeters that can be used to validate the calculational methodology. An inspection of the simultaneous time-dependent response from different types of active dosimeters can also be used to illuminate the difficulties of separating the neutron/gamma response of any dosimeter in the mixed radiation field of a reactor.

CALCULATIONAL APPROACH

Monte Carlo calculations can be used to model the reactor environments. These calculations are typically run in a k-code mode where a normal fission distribution in the reactor fuel represents the fission source term, and the prompt fission neutron/gamma radiation is transported to the test locations. In this transport process, the neutrons will interact with the reactor materials and generate secondary gamma radiation. A typical analysis of the radiation environment stops at this point. However, every fission event does not only have prompt neutron and gamma radiation, but it also has delayed neutron and gamma radiation. The delayed gamma radiation is generated at the same fission sites as were responsible for the prompt neutron/gamma radiation, but it has a time-dependent energy spectrum. The time-integrated delayed gamma radiation is nearly equal in magnitude to the prompt fission gamma radiation [1]. The time-dependent emission rate and energy spectrum for the delayed neutrons has been characterized by Spriggs and Campbell [2]. The time-dependent and energy-dependent delayed gammas have not been as well characterized – but some data can be culled from the literature [3]. These data provide a basis for modeling the time- and energy-dependence of the delayed radiation component.

A radiation pulse from a test reactor typically has a pulse width that can vary from 50 μs in a fast burst reactor to 100 ms in a low energy pulse from a water moderated test reactor. The radiation transport calculations give the results for a very short prompt fission pulse, essentially using a delta function as the source term. Thus, the total reactor radiation environment at a test location must be modeled by doing a time-dependent convolution of the calculated radiation over an

[1] This work was supported by the United States Department of Energy under contract DE-AC04-94AL85000. Sandia is a multiprogram laboratory operated by Sandia Corporation, a Lockheed Martin Company, for the United States Department of Energy

experimentally measured fission time-dependent source profile and incorporating the delayed radiation contributions. Many research reactors use a prompt Cd-based self-powered neutron detector as their power indicator. In water moderated fission reactors this is an excellent metric to use for the time-dependent source profile.

At even later times the radiation environment at a test location may be dominated by activation gammas produced from nearby materials. The activation dose seen by a test object is a combination of the decay gammas from small nearby masses and that produced by larger, more distant, masses. Even trace quantities of high-Z elements in nearby materials can dominate the activation dose seen by test objects. For example, the late-time activation component from the walls of an ionization chamber must be considered in any attempt to compare the calculated-to-experimental ratio of the response of an ionization chamber at times as long as 24-hours after a reactor pulse. The full paper will discuss potential approaches to modeling the activation component of the radiation environment as well as potential pitfalls.

EXPERIMENTAL APPROACH

There is a wide assortment of active dosimeters used by the experimental community. These dosimeters include prompt Cd-based self-powered neutron detectors (SPNDs), fission chambers, ionization chambers, diamond photoconducting detectors (PCD), silicon PIN diodes, Shockey diodes, and more. This paper will compare time-dependent measurements from a range of active dosimeters following pulsed and steady-state reactor operations. The test protocol calls for having a "cold" reactor, one that has not seen an operation for at least 12 hours, conducting a predetermined operations with the active dosimeters, and continuing the measurement for 24-hours after the operation. Figure 1 shows some representative data from a small (20-MJ) pulse in the water-moderated Annular Core Research Reactor (ACRR) at Sandia National Laboratories. Figure 2 shows representative data from a 300-MJ steady-state operation in ACRR. The relative neutron/gamma response of each detector is important in interpreting the late-time response from these various active dosimeters. For example, the SPND is primarily a neutron-sensitive detector. The late-time plateau in the blue SPND curve of Figure 2 represents the noise floor for the dosimeter. The deviation between it and the PCD or ionization chamber at late times is due to the fact that the PCD and ionization chamber are primarily responding to the gamma radiation and the late time gamma-to-neutron ratio is much higher than that during the main reactor pulse.

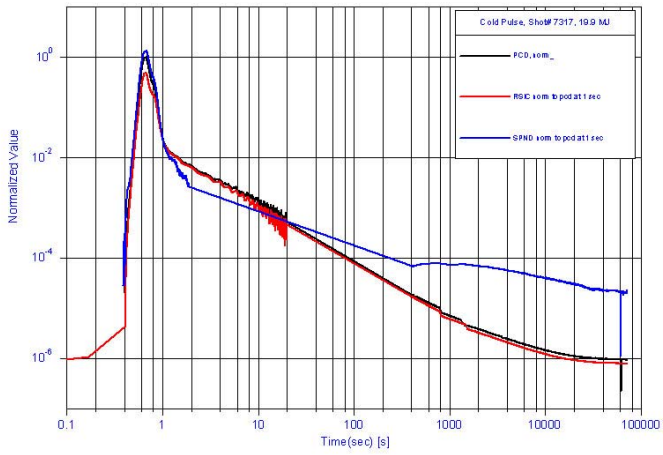

Figure 1: Pulsed Dosimeter Comparison

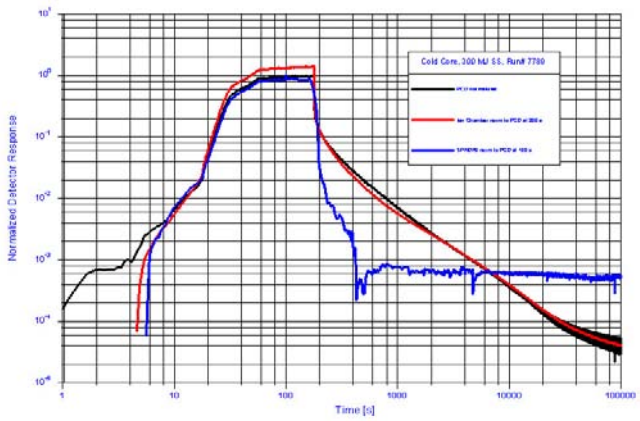

Figure 2: Steady-state Dosimeter Comparison

REFERENCES

1. G. R. Keepin, **Physics of Nuclear Kinetics**, Addison-Wesley Publishing Co., 1965.
2. G. D. Spriggs, J. M. Campbell, V. M. Piksaikin, "An 8-Group Delayed Neutron Model Based on a Consistent Set of Half-Lives," LA-UR-98-1619, Rev. 3,Los Alamos National Laboratory, Los Alamos, NM. Also URL http://public.lanl.gov/jomc/DN_YOC.html
3. Maienshein, Peelle, Zobel, Love, Proceedings of 2nd International Conference Geneva, **15**, 366 (1958).

Determination of adjusted neutron spectra in different MUSE configurations by unfolding techniques

D^r M. Plaschy, P^r. R. Chawla
Paul Scherrer Institute – LRS/NES
CH –5232 Villigen PSI, Switzerland
michael.plaschy@psi.ch

C. Destouches, D^r D. Beretz, F. Mellier, D^r H. Serviere, P. Chaussonnet,
C. Domergue, J.M. Laurens, H Philibert
CEA - Cadarache /DEN/SPEX/LPE
13108 Saint-Paul lez Durance, France
christophe.destouches@cea.fr

The characterization of neutron spectra by unfolding techniques using activation and fission foils is a well-known method developed in the seventies.

In brief, the application of this method requires the definition of a set of stable isotopes which have well known cross-sections for neutronic reactions covering a large range of energies and which, in addition, give rise to appropriate radio-nuclides from the viewpoint of emitted γ's or X-rays (signal easily measured, well defined peak in energy, adequate yield, convenient decay constant, ...). Such a suitably chosen set of materials (foils) is irradiated at a constant flux level in locations where the neutron spectrum is to be determined. Experimental reaction rates and their associated uncertainties are then derived from measured activities and irradiation data. Finally, the adjusted neutron spectrum is deduced by minimisation of an error function (χ^2, for example) using the experimental reaction rates, the calculated spectrum, dosimetry data files and the associated variance-covariance matrices.

Unfolding methods used to deduce the neutron spectrum from a given set of foil irradiations in this manner have suffered in the past from technical limitations: activity measurements of many radio-isotopes were not possible with enough precision, and moreover, some of the uncertainty matrices provided with the dosimetry data files, as well as at times the calculated spectra themselves, were not realistic.

However, the latest developments in calculation codes and dosimetry data files have led us to reconsider the relevance of this method. Thus, in the frame of the MUSE-4 experimental programme, which consists in studying different critical and sub-critical core configurations in the context of Accelerator Driven System (ADS) research, unfolding methods have been applied by the Paul Scherrer Institute (PSI) and by the CEA-Cadarache teams [1] for deriving the neutron spectrum in different reactor core locations of interest using the STAY'SL code [2].

After a brief review of the basic principles of spectrum unfolding, this paper describes the experimental measurement campaign achieved first in a fast critical core, and then in a sub-critical source-coupled configuration. In addition, the choice of the measurement locations is explained (exploration of the lead and voided regions, for example). The strategy used to define the set of foil materials employed, as also the planning of the activity measurements, are then presented. The derivation of the parameters needed for appropriate interpretation of the measured activities is explained, e.g. the calculation of the correction factors for γ self-absorption in the foils. The calculation scheme for obtaining the neutron spectrum using stochastic and deterministic codes, and the reasons leading to the choice of the different dosimetry data files, are described.

The results for unfolded spectra, obtained using the STAY'SL code in conjunction with the experimental activities, are presented, especially for the sub-critical core coupled with the accelerator. The foil isotopes deployed cover a wide range of energies, varying from thermal spectrum ($In^{115}(n,\gamma)$) to almost 20 MeV ($V^{51}(n,2n)$ – 12 MeV threshold)).

Furthermore, sensitivity studies have been carried out with respect to the dosimetry data files and to the neutron spectrum variance-covariance matrixes, and a numerical analysis has been performed for the determination of the most influential data contributing to the final uncertainty in a test case.

Finally, the potential for applying other unfolding codes and methods is assessed, and perspectives for possible presented method upgrades are indicated.

1. M. Plaschy "Etudes numériques et expérimentales de caractéristiques d'un système rapide sous-critique alimenté par une source externe » *Doctoral Thesis N° 2953 (2004), EPFL Lausanne.*
2. Oak Ridge National Laboratory " STAY'SL: Least Squares dosimetry unfolding code system" *Lockheed Martin Energy Research Corporation, PSR-113, 1991.*

Spectral Effects and Neutron Multiplicity of an Electron Driven Assembly

Conwell W. D.
New Mexico Tech,
Socorro, NM 87801, USA.

INTRODUCTION

The fundamental goal of this research is replacing a fast burst reactor (FBR) containing high enriched uranium (HEU) with an equivalent source of neutrons that does not contain HEU. HEU presents a security risk. Replacing the HEU with an assembly of low enriched uranium (LEU is less than 20% enriched by weight with uranium 235) would eliminate security measures that complicate testing and drive up costs. This research characterizes the neutron spectrum of a replacement FBR that does not contain HEU.

A replacement for a FBR must retain its capabilities. The purpose of a FBR is to produce fission spectrum neutrons, as shown in Figure 1, that are characterized by an average energy of 1.98 MeV and a mode of 0.73 MeV. The FBR is small, a metal reactor roughly with the dimensions and shape of a one gallon paint can. This small size allows for a very short pulse width of approximately 45 μsec that produces an isotropic burst of approximately 1E17 neutrons. The reactor can also operate in a steady state mode providing 8 kW sustained with a flux of 6.4E9 n/cm^{2}s at 61 cm from the core centerline.

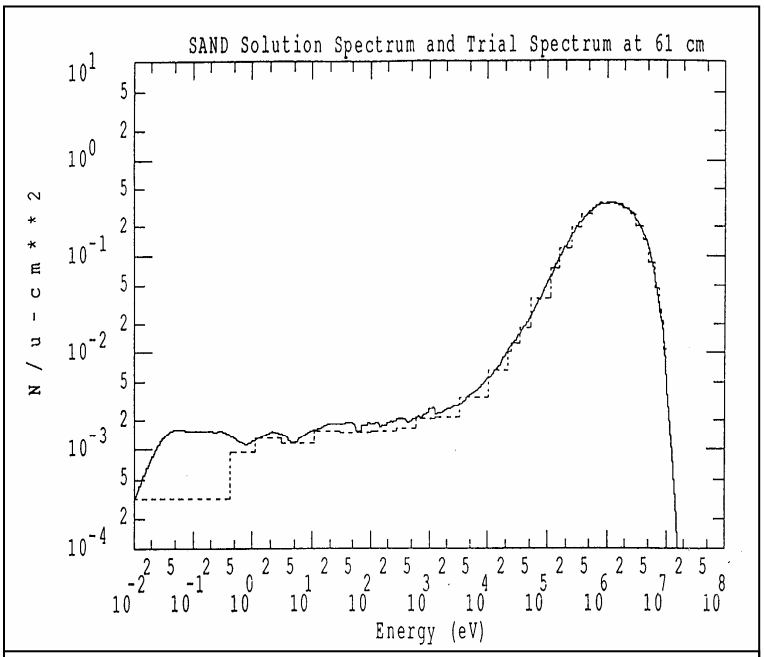

Figure 1: The FBR spectrum in neutrons per unit lethargy per cm squared. The dashed line is a Monte Carlo prediction and the solid line is experimentally determined from activation foils.

Building a replacement reactor out of LEU could increase the mass of the assembly, significantly increasing the pulse width of the reactor pulse. One way to counter this is to drive an LEU assembly with an electron accelerator that produces photo-neutrons, increasing the output of the assembly without slowing down the pulse.

PHOTON INTERACTION

In a LEU assembly, photons below 30 MeV produced by electron bremsstrahlung radiation will deposit energy in the nucleus and produce Giant Dipole Resonant (GDR) neutrons. Assuming the nucleus reaches equilibrium following the inelastic collision with the photon (a good assumption for high-Z nuclei), the nucleus can be viewed classically as evaporating the GDR neutrons, thus the neutrons are produced isotropically and have energy of a few MeV. These processes are well characterized in MCNP5 (Monte Carlo Neutral Particle version 5) below a few tens of MeV for most materials. If a photon of high enough energy strikes a nucleus and the binding energy per nucleon is low enough, one or more neutrons will be

produced. In fissionable nuclei, the photon can also deposit enough energy to fission the nucleus through photo fission. Figure 2 shows the cross section of uranium 238.

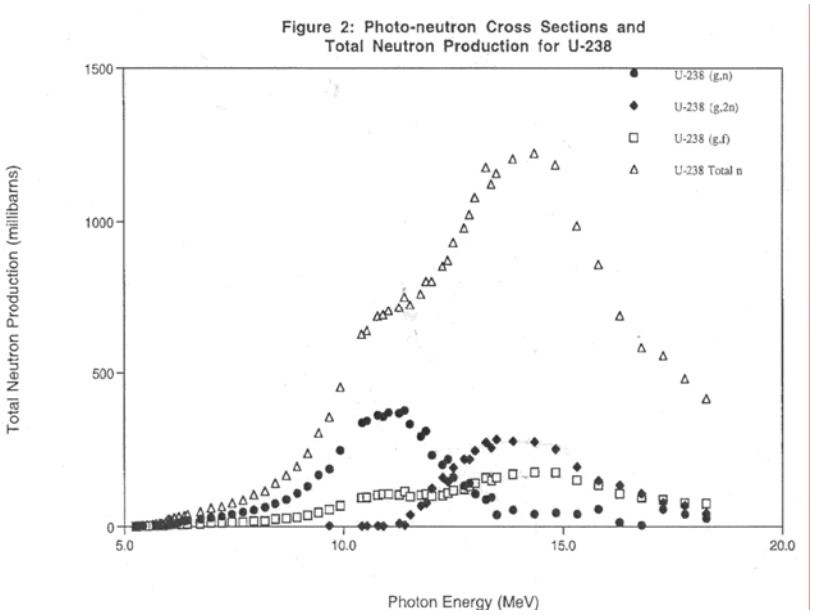

For bremsstrahlung photons above 30 MeV, the quasi-deuteron (QD) absorption mechanism is possible. The photon interacts with the dipole moment of a correlated neutron-proton pair in the nucleus. This results in a direct emission such that the escaping particle does not interact with the nucleus and is characterized by higher emission energy and a forward-peaked angular distribution.
Above 140 MeV (the mass of π^0 meson is 134.97 MeV) it is possible for energetic photons to create pions. The cross sections for these interactions are much smaller than those of GDR and QD, but the neutrons produced by photo-pion reactions are very energetic and forward directed.

CONCLUSION

Since the assembly will be small to meet the pulse width requirements, it is a major concern that the high-energy neutrons in a LEU assembly produced by a high-energy electron beam could contaminate the neutron spectrum and create an anisotropic flux in the direction of the beam line. Also, the target will undergo a tremendous amount of heating due to the relatively short radiation length of the electrons and the need for an extremely high beam current. There may be other results as well. For this research to be successful, the electron beam's effects on the spectrum must be fully understood.

The results of the research will include an analysis of the neutron multiplicity and the neutron spectrum produced by a 200 MeV electron beam deposited into the central cavity of a roughly cylindrical LEU assembly. Critical to the research is fully characterizing the bremsstrahlung radiation that results from the electron beam energy deposition that will be used to characterize the QD neutron and photo-pion neutron production.

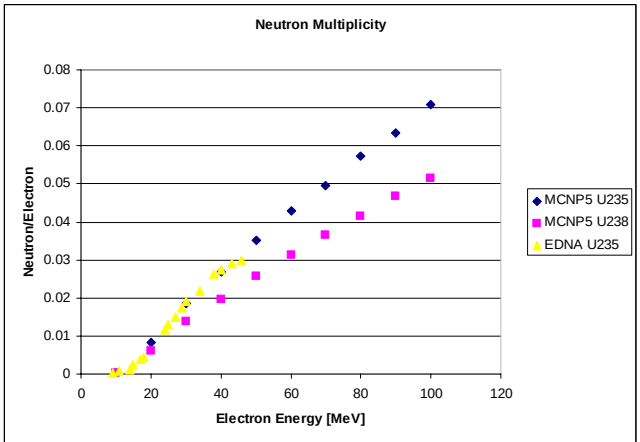

Figure 3. Simulation Using MCNP5 compared to data from Sandia EDNA report.

ACKOWLEDGMENTS

Dr Mike Flanders, Survivability and Vulnerability Assessment Directorate (SVAD) White Sands Missile Range, NM

Dr John Meason, Energetic Materials Research and Testing Center (EMRTC) New Mexico Tech, Socorro, NM 87801

Ms Mary Helen Sparks, Survivability and Vulnerability Assessment Directorate (SVAD) White Sands Missile Range, NM

REFERENCES

Lee J. R. et al. *Design Feasibility of an Externally Driven Nuclear Assembly (EDNA)*, Sandia National Laboratories Albuquerque, New Mexico 1990.
Leo W. R., *Techniques for Nuclear and Particle Physics Experiments*, Springer-Verlag Berlin Heidelberg New York 1994.
Nifenecker H. et al., *Accelerator Driven Subcritical Reactors*, Institute of Physics Publishing Bristol and Philadelphia 2003.
Wangler Thomas P., *Principles of RF Linear Accelerators*, John Wiley & Sons New York 1998.
X-5 Monte Carlo Team, *MCNP - A General Monte Carlo N-Particle Transport Code*, Version 5, University of California Los Alamos National Laboratory 2003.

Characterization of Neutron Fields using MCNP in the Experimental Fast Reactor JOYO

Shigetaka Maeda and David Wootan
O-arai Engineering Center
Japan Nuclear Cycle Development Institute
4002 Narita-cho, O-arai-machi, Ibaraki-ken, 311-1393, Japan

One of the primary missions of the JOYO experimental fast reactor is to perform irradiation tests of fuel and structural materials to support the development of fast reactors. From 1983 to 2000 JOYO was operated with the MK-II irradiation test core. In 2003 the JOYO reactor upgrade to the MK-III core was completed to increase the irradiation testing capability of JOYO. The MK-III core incorporates significant changes to the core size and arrangement, fuel enrichment, and reactor power level compared to the MK-II core. Accurate core calculational methods are required for predicting neutron fluence, related spectral information, and other key performance parameters for new fuels and materials irradiation tests in the MK-III core.

Previous methods applied at JOYO for predicting neutron fields included the MAGI three dimensional diffusion-theory based core management code system for the fuel region and the DORT two dimensional deterministic transport code for ex-core regions [*1*]. Recently Monte Carlo transport calculations using the MCNP code [*2*] have been introduced to account for heterogeneous effects. This paper describes the development of advanced whole-core Monte Carlo analysis methods to provide accurate calculational predictions for the irradiation conditions of the wide variety of JOYO irradiation test locations. The new analysis strategy involves developing efficient calculational models using the continuous energy MCNP code that are optimized for each unique type of test environment. The advantages of the MCNP code are that it provides transport of both neutrons and gamma rays, includes heterogeneous geometry modeling capability, has many options for optimization in space and energy, and can utilize the JOYO core management fuel compositions.

A number of reactor dosimetry measurements have been conducted in JOYO to assure the reliability and accuracy of the neutron flux calculations. Dosimetry tests irradiated in the MK-II operational cycles 34 and 35 providing a full range of environments were selected to verify the new core calculational methods. Shown in Figure 1, these non-fuel test subassemblies included SVIR-1 at core center surrounded by fuel, SVIR-2 in the outer reflector region, SVIR-3 in the in-vessel storage rack, and the M3-3 ex-vessel dosimetry package. The SVIR test subassemblies consisted of 7 steel pins 26 mm in diameter containing materials test specimens and dosimeters. Select pins in each test contained one or more steel dosimeter capsules that were 50 mm in length and 22 mm in diameter. Both bare and vanadium encapsulated wire dosimeters were located in an inner central cavity that was 10 mm in diameter and 10 mm in length. The M3-3 dosimetry capsules were larger than the SVIR capsules, made of aluminum instead of steel, and also included some cadmium covered dosimeter sets.

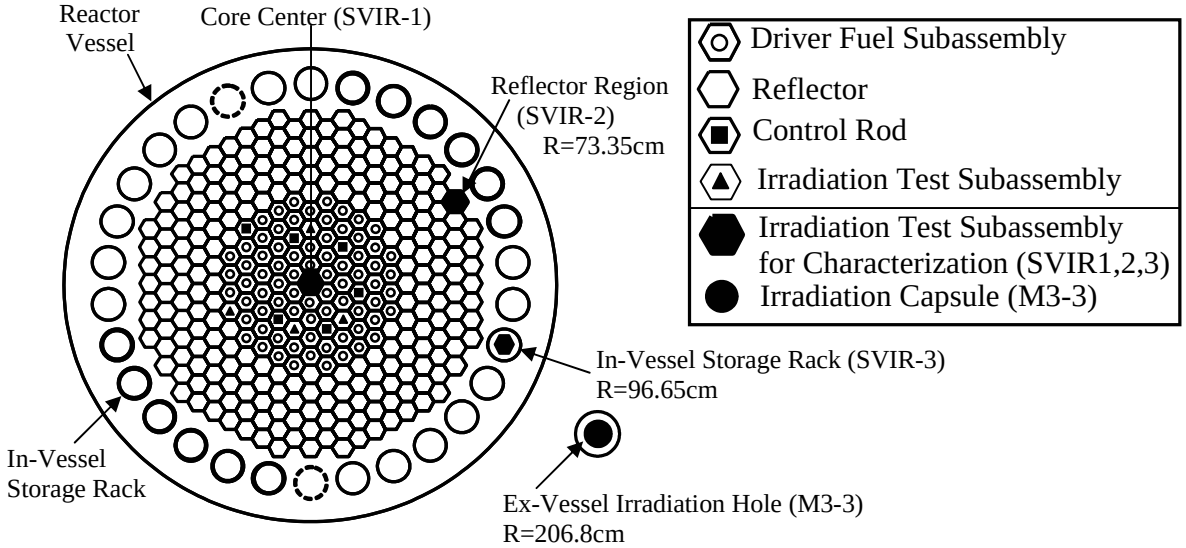

Figure 1. MK-II Cycles 34-35 Characterization Test Subassemblies

The major tasks in optimizing the MCNP whole-core reaction rate calculations included preparing an MCNP model with core management fuel compositions for the MK-II core at the beginning of cycle 35 with radial and axial extents that cover the dosimeter locations, adding the details of each of the test subassemblies containing dosimeters, determining the normalization factor for MCNP tallies, exploring biasing and optimization options, and iterating until adequate statistical uncertainties were obtained. The major variables for the optimization of calculated reaction rates included the weight window mesh description of bins for biasing in energy (to focus on particular energy ranges) and geometry (radial, axial, and azimuthal bins to focus on particular regions), the choice of tally type (point detector or cell volume), the choice of cross sections, and the source description method (kcode or fixed source). The MCNP weight window generator was of limited use since it only provides single tally optimization.

A different optimization scheme was developed for each unique location type, but all involved running MCNP in the "kcode" mode and using three-dimensional mesh based weight windows with three energy bins (<1 MeV, 1-3 MeV, >3 MeV) biased to higher energies. The optimization scheme developed for the M3-3 ex-vessel dosimetry used 20 radial regions biased radially outward and point detector tallies. The optimization scheme developed for the SVIR-2 and SVIR-3 ex-core subassemblies included 14 radial regions biased radially outward, 12 azimuthal regions biased to the vicinity of the SVIR-2 and SVIR-3 subassemblies, and flux volume tallies in each of the dosimeter capsule cavities. MCNP cross sections for both the neutron transport and reaction rates were based on the JENDL-3.3 and JENDL-3.2 sets.

Table 1 shows the initial comparison of measured and MCNP calculated reaction rates for the SVIR-2, -3, and M3-3 ex-vessel dosimeters at core midplane. The optimization results demonstrated that biasing schemes for each location can provide adequate statistical uncertainties for the reaction rates in the less than 1cm^3 volume of the dosimeter capsule cavity.

Table 1. MCNP C/E ratios for MK-II operational cycles 34-35 tests (JENDL-3.2)

Location	Pin #(cm from center)	^{235}U (n,f)	^{10}B (n,a)	^{45}Sc (n,γ)	^{58}Fe (n,γ)	^{54}Fe (n,p)	^{58}Ni (n,p)	^{237}Np (n,f)	^{59}Co (n,γ)	^{181}Ta (n,γ)
SVIR1 Core Center	6 (2.6)	1.04	1.01	1.19	---	0.99	1.01	1.31	---	---
SVIR2 Outer Reflector	1 (71.0)	1.09	1.29	1.25	1.10	0.88	1.03	1.20	---	---
	4 (76.2)	1.09	1.28	1.17	1.17	0.88	1.00	1.19	---	---
SVIR3 In-Vessel Storage	1 (94.1)	0.91	1.03	0.94	0.98	0.86	0.99	1.00	---	---
	2 (94.7)	---	---	---	---	0.96	1.10	---	---	---
	3 (97.2)	0.91	0.97	0.93	---	0.94	1.08	1.06	---	---
	4 (99.2)	---	---	---	---	0.92	1.06	---	---	---
	5 (98.7)	0.86	0.97	0.91	0.81	0.89	1.04	1.00	---	---
	6 (96.1)	---	---	---	---	0.81	0.96	---	---	---
M3-3 Ex Vessel	0 (206.8)	---	---	1.07	1.07	---	1.43	1.25	1.12	1.14

These same methods will be applied to the MK-III core and predictions made for new MK-III core dosimetry tests. A new extensive set of reactor dosimetry measurements in the fuel, reflector, in-vessel storage, and ex-vessel regions is being irradiated during the first two operating cycles of the MK-III core in order to check the validity of the spectrum calculations using the developed methods.

REFERENCES

1. T. Sekine, et al., "Characterization of Neutron Field In the Experimental Fast Reactor JOYO ," Proc. of the 11th Int. Symp. on Reactor Dosimetry, August, 2002, p. 381, Brussels, Belgium (2002).
2. Forrest B. Brown, et al., *MCNP – A General Monte Carlo N-Particle Transport Code Version 5*, LA-UR-030-1987 (2003).

Neptunium-Uranium Specimen Irradiation in the Advanced Test Reactor

John M. Ryskamp-- Idaho National Engineering and Environmental Laboratory
Gray S. Chang-- Idaho National Engineering and Environmental Laboratory
Masahiko Ito—Japan Nuclear Cycle Development Institute
Masaki Saito—Tokyo Institute of Technology

The Protected Plutonium Production (PPP) Project[1] developed by the Tokyo Institute of Technology proposes to achieve the production of inherently protected plutonium, with high portions of ^{238}Pu, by adding ^{237}Np to uranium-based light water reactor fuel. For confirmation of this concept, ^{237}Np-containing U samples will be irradiated in the Advanced Test Reactor (ATR) at the Idaho National Engineering and Environmental Laboratory (INEEL). We will demonstrate ^{238}Pu production in a thermal neutron spectrum. The fabrication of ^{237}Np-U specimens is in progress. Irradiation is expected to start in September 2005.

Minor actinide nuclear data uncertainties lead to uncertainties in the computed nuclide concentrations as a function of fuel burnup. Integral nuclear data measurements in fast neutron spectra have identified problems with some differential nuclear cross sections. For the thermal neutron spectrum suggested for PPP, it is not known how uncertainties in nuclear data will impact the computed nuclide concentrations. Therefore, integral data measurement as a function of burnup should be conducted in a thermal neutron spectrum.

The experiment we are designing will consist of 20 small plates containing small amounts of uranium and neptunium isotopes in various compositions. Argonne National Laboratory-West (ANL-W) in Idaho (USA) will fabricate the plates. These plates will be placed in a thermal neutron spectrum provided by the ATR. After irradiation to various burnup levels, ANL-W will determine the target compositions through radiochemistry analysis. The experimental results will then be compared with neutronics calculations. The comparison should indicate areas where differential nuclear data must be improved.

The axial view of the neptunium experiment is shown in Figure 1. The basket will hold four capsules. Each capsule is designed to hold eight miniplates, for a total of 32 miniplates per basket. The experiment requires irradiation of 18 neptunium-uranium specimens and two natural uranium specimens for a total of 20 specimen plates. The remaining 12 plates will be "dummy" or filler plates consisting of solid aluminum alloy. The composition of each of the 20 plates is shown in Table 1. To measure the fast and thermal fluences, dosimetry flux wires may be included in the basket, or may be embedded within a dummy plate. One design includes a pure iron wire embedded in an aluminum plate to measure the fast fluence and an aluminum wire with 0.1 weight % cobalt embedded in the same aluminum plate to measure the thermal fluence.

One capsule will be removed after approximately 100 effective full power days (EFPDs) (two ATR cycles), another will be removed after 200 EFPD (another two ATR cycles), and the third capsule will be removed after 300 EFPDs (a total of six ATR cycles). The nuclide

concentrations in each plate will then be determined by radiochemistry, along with burnup values based on fission product concentrations.

The first experiment will provide the foundation for future experiments and prove the basic PPP–related processes. If the experiment, calculations, and other considerations support the PPP Project, then further experiments should be performed with fabricated PPP fuel pellets. This fuel could be placed in a few capsules and irradiated in a thermal neutron spectrum. After exposure, the capsules would be removed and undergo chemistry analysis. This would provide the first indication that a PPP fuel form is acceptable for light water reactors.

Reference 1: M. Itoh, M Osaka, M. Saito, and J. M. Ryskamp, "Development of Innovative Nuclear Reactor Technology to Produce Protected Plutonium with High Proliferation Resistance," to be presented at the American Nuclear Society Winter Meeting in Washington DC in November 2004.

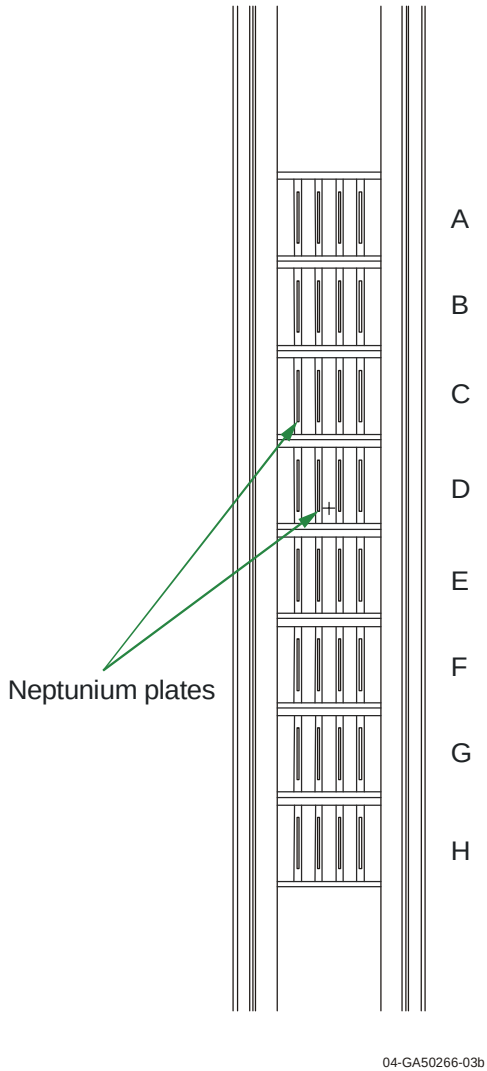

Figure 1. Axial schematic view of neptunium specimen test assembly. (Note: the Y-Z cross-section ratio is not 1:1.)

Table 1. Plate Specimen Specifications and Irradiation Conditions.

Comp. Type	Composition (wt%)	Weight* (mg)	Plate Type	Plate Quantity		Np%	Total Np (mg)	Irradiation Time (EFPD)
1	UO_2: 100	350	A	2	2	0	0	300
2	UO_2: 98, NpO_2: 2	350	B	6	2	2	14	100
		350	B		2	2	14	200
		350	B		1	2	7	300
		2500	C		1	2	50	300
3	UO_2: 95, NpO_2: 5	350	D	6	1	5	17.5	100
		2000	E		1	5	100	100
		350	D		2	5	35	200
		350	D		1	5	17.5	300
		2000	E		1	5	100	300
4	UO_2: 90, NpO_2: 10	350	F	6	1	10	35	100
		1000	G		1	10	100	100
		350	F		2	10	70	200
		350	F		1	10	35	300
		1000	G		1	10	100	300
	*UO_2/NpO_2 Mixture	12000		20	20		695	

—ABSTRACT—

The Advanced High-Temperature Reactor (AHTR): Flux Distribution and Dosimetry

Charles W. Forsberg
Oak Ridge National Laboratory*
P.O. Box 2008
Oak Ridge, TN 37831-6165
Tel: (865) 574-6783
Fax: (865) 574-0382
E-mail: forsbergcw@ornl.gov

File Name: Dose.2005.Abstract
Manuscript Date: September 12, 2004

Twelfth International Symposium on Reactor Dosimetry
Gatlinburg, Tennessee
May 8-13, 2005

Sponsored by:
ASTM International
The European Working Group on Reactor Dosimetry
Atomic Energy Society of Japan

The submitted manuscript has been authored by a contractor of the U.S. Government under contract DE-AC05-00OR22725. Accordingly, the U.S. Government retains a nonexclusive, royalty-free license to publish or reproduce the published form of this contribution, or allow others to do so, for U.S. Government purposes.

---

*Oak Ridge National Laboratory, managed by UT-Battelle, LLC, for the U.S. Department of Energy under contract DE-AC05-00OR22725.

—ABSTRACT—

The Advanced High-Temperature Reactor (AHTR): Flux Distribution and Dosimetry

C. W. Forsberg
Oak Ridge National Laboratory
P.O. Box 2008
Oak Ridge, TN 37831
Tel: (865) 574-6783
forsbergcw@ornl.gov

The Advanced High-Temperature Reactor (AHTR) is a new, large (2400 Mw(t)), passively safe, high-temperature reactor concept that combines three existing technologies: coated-particle graphite-matrix fuels, a clean molten-fluoride salt coolant, and liquid-metal-cooled fast-reactor plant design. Depending upon the application, the peak coolant temperature is between 700 and 1000°C. The fuel is the same fuel that is used in high-temperature gas-cooled reactors. The transparent molten salt coolant is a mixture of fluoride salts with freezing points near 400°C, atmospheric boiling points exceeding 1200°C, and physical properties at operating conditions that are similar to water. Several different salts are being evaluated as the primary coolant, including lithium-beryllium and sodium-zirconium fluoride salts. The reactor operates at near-atmospheric pressure. The plant design is similar to sodium-cooled fast reactors because both types of reactors are low-pressure high-temperature reactors. The AHTR can be used to provide heat for hydrogen production via thermochemical cycles or electricity. An indirect multi-reheat nitrogen or helium Brayton cycle is used for electricity generation. The reactor physics and neutron spectrum are nearly identical to coated-particle gas-cooled reactors because (1) the same fuel is used, (2) the same materials for other incore components are used, (3) the core geometry is similar (except somewhat larger because of the higher power levels), and (4) the molten salts are chosen for their very low neutron cross sections and thus (like helium) do not strongly impact the neutron spectrum. The primary dosimetry difference is that the liquid coolant prevents streaming of neutrons and gamma radiation via coolant channels and other voids from the reactor core and shields the upper vessel heat structure. Neutron activation of the coolant will depend upon the specific salt that is chosen. Figure 1 shows a schematic of the reactor.

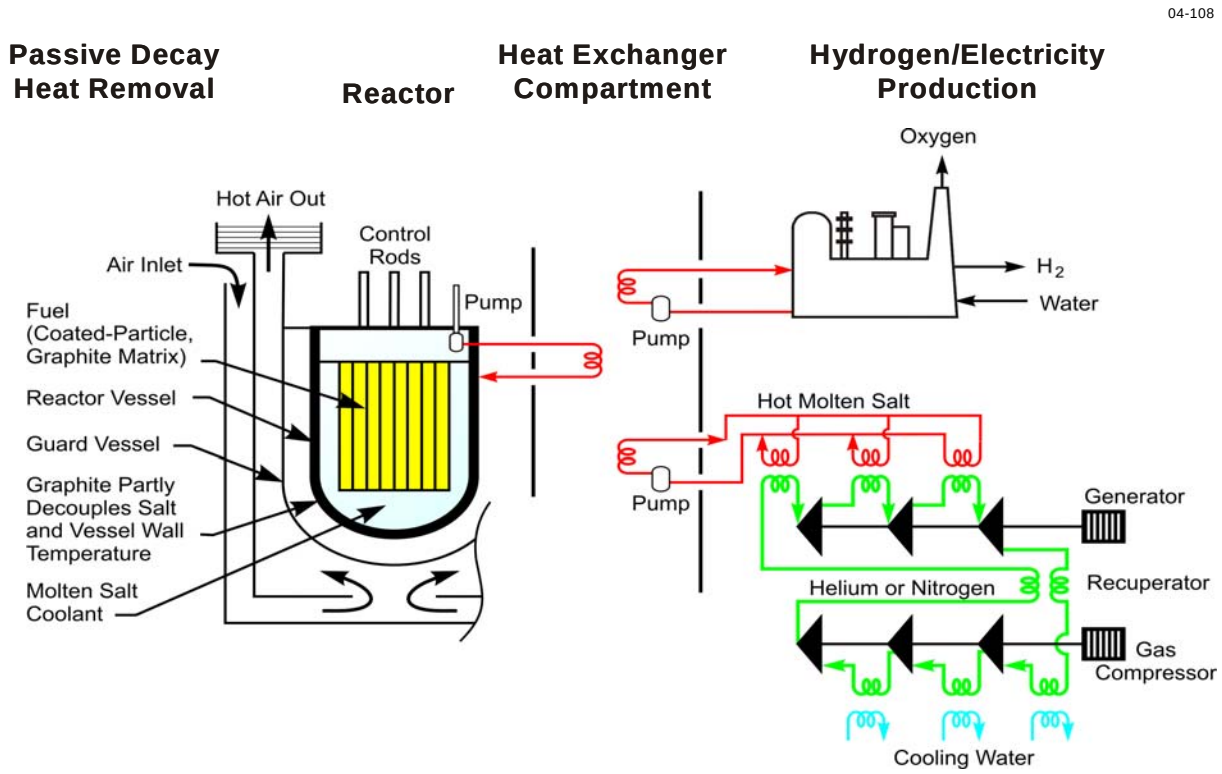

Fig. 1 The Advanced High-Temperature Reactor

Benchmark on the 3-D VENUS-2 MOX-fuelled Reactor Dosimetry Calculations by DANTSYS Code System

Kim, D. H., Gil, C.-S., and Chang, J.
Korea Atomic Energy Research Institute
P.O. Box 105, Yuseong, Daejeon, 305-600, Korea

INTRODUCTION

The OECD/NEA has been preparing the physics benchmark exercises relating to the VENUS-2 reactor loaded with the mixed-oxide (MOX) uranium and plutonium fuel to identify improvements in nuclear data and physics modeling methods. [*1*] The present benchmark calculation on the 3-D VENUS-2 MOX-fuelled reactor dosimetry has been performed by the TRANSX/DANTSYS code system [*2*,*3*]. The nuclear data from the ENDF/B-VI.8 have been processed to MATXS-format 199-group neutron library by NJOY99.90 [*4*]. The nuclear data and the calculational methods will be validated by comparing the results with the experimental measurements released by SCK·CEN.

LIBRARY GENERATION

A MATXS-format multi-group neutron library should be provided for TRANSX/DANTSYS code system. The ENDF/B-VI.8 was adopted for all isotopes constituting the VENUS-2 facility except natural Tin, which was obtained from the ENDL-84 library. The neutron data library with 199-group structure of VITAMIN-B6 [*5*] has been generated by NJOY99.90. The VITAMIN-B6 neutron group structure can be useful for a broader range of applications such as a variety of reactor design and shielding problems including thermal and fast reactor systems.

BENCHMARK CALCULAIONS

The benchmark calculations were carried out using the TRANSX/DANTSYS code system. The 1-D transport calculations for three fuel cells and a Pyrex cell were performed to calculate the region-wise 199-group weighting flux by using the macroscopic cross sections prepared by the TRANSX code. The resulting weighting fluxes were utilized to collapse the 199-group data into 47-group data for 3-D core calculations. For other regions such as barrel, baffle, plexiglass, stainless steel grids, neutron pad, etc., the group collapse was carried out with the built-in P_0 flux.

For 3-D core calculation, the VENUS-2 core was modeled up to the neutron pad in the x- and y-directions. It was assumed that the regions beyond the neutron pad were filled with water. In the z-direction, the core was modeled explicitly from bottom to top with the proper use of homogenization technique for regions having a complex geometrical shape such as the bottom, intermediate, and upper grids. The mesh sizes are ~0.63 cm (a half of the fuel cell pitch) up to the outer baffle region and 1.26 cm outside of the region. Also, the calculation was carried out with P_3S_8 approximation.

The IRDF-90 version 2 dosimeter cross section data were taken to estimate the dosimetry reaction rates for the ^{58}Ni(n,p), ^{115}In(n,n'), ^{103}Rh(n,n'), ^{64}Zn(n,p), ^{237}Np(n,f), and ^{27}Al(n,α) detectors. These data were collapsed into 47 groups with a smoothly varying combination of a Maxwellian thermal spectrum, a 1/E slowing down spectrum, and a fission spectrum (IWT=4 in GROUPR module of NJOY).

The equivalent fission fluxes at 34 measurement positions on the core mid-plane of the reactor were calculated. The equivalent fission fluxes are the reaction rates divided by the ^{235}U fission spectrum averaged cross sections of the corresponding dosimeter. Table 1 shows the equivalent fission fluxes at 100% power in stainless steel zones. Because the measured values are not yet available, the comparative analyses between calculated and measured values will be discussed in the complete paper. In addition, the alterations on weighting fluxes for group collapse and the use of JENDL-3.3 and JEFF-3.0 will be investigated to improve the benchmark results.

Table 1. Equivalent fission fluxes at 100% power in stainless steel zones

[Unit: neutrons/cm2/sec]

Measurement Position *	^{58}Ni(n,p)	^{115}In(n,n')	^{103}Rh(n,n')	^{64}Zn(n,p)	^{237}Np(n,f)	^{27}Al(n,α)
Inner Baffle						
(-4.41, -0.63)	1.40195E+09	1.77367E+09	2.15680E+09	1.35122E+09	2.38683E+09	1.27430E+09
(-4.41, -4.41)	1.68196E+09	2.11329E+09	2.55164E+09	1.62377E+09	2.80841E+09	1.50546E+09
Outer Baffle						
(-39.69, -0.69)	5.68049E+08	6.92703E+08	8.23664E+08	5.50382E+08	9.01658E+08	5.30973E+08
(-39.69, -5.67)	5.39813E+08	6.58547E+08	7.83079E+08	5.22984E+08	8.57273E+08	5.04137E+08
(-39.69, -11.97)	4.40325E+08	5.37756E+08	6.39817E+08	4.26387E+08	7.00726E+08	4.13478E+08
(-39.69, -18.27)	2.56452E+08	3.20657E+08	3.88500E+08	2.47108E+08	4.28989E+08	2.43100E+08
(-37.17, -20.79)	2.65108E+08	3.31948E+08	4.03255E+08	2.55452E+08	4.45749E+08	2.52119E+08
(-30.87, -20.79)	5.24902E+08	6.50032E+08	7.81731E+08	5.07459E+08	8.60030E+08	4.87012E+08
(-24.57, -20.79)	8.34101E+08	1.05115E+09	1.27479E+09	8.04769E+08	1.40721E+09	7.47250E+08
Barrel						
(-49.77, -0.63)	7.54759E+07	9.04592E+07	1.06601E+08	7.26801E+07	1.17015E+08	8.65684E+07
(-49.77, -9.45)	6.54398E+07	7.91832E+07	9.43625E+07	6.28996E+07	1.03920E+08	7.57033E+07
(-47.25, -18.27)	5.97245E+07	7.56742E+07	9.31048E+07	5.70905E+07	1.03839E+08	6.54110E+07
(-45.99, -22.05)	4.91804E+07	6.39214E+07	8.02682E+07	4.68174E+07	9.01746E+07	5.40538E+07
(-44.73, -24.57)	4.31189E+07	5.61620E+07	7.06570E+07	4.10562E+07	7.94193E+07	4.66876E+07
(-42.21, -28.35)	4.01735E+07	5.00769E+07	6.14807E+07	3.84107E+07	6.84707E+07	4.77860E+07
(-38.43, -33.39)	3.55724E+07	4.18392E+07	4.97054E+07	3.42293E+07	5.45123E+07	4.58146E+07
(-35.91, -35.91)	3.57407E+07	4.11890E+07	4.83988E+07	3.44663E+07	5.28598E+07	4.71749E+07
Neutron Pad						
(-58.54, -22.47)	6.08864E+06	7.47105E+06	9.26547E+06	5.79913E+06	1.03423E+07	8.93575E+06
(-46.60, -41.95)	4.29057E+06	5.11510E+06	6.28667E+06	4.09802E+06	6.99326E+06	6.58175E+06

* (x,y) in [cm,cm] co-ordinates with respect to core center

ACKOWLEDGMENTS

This project has been carried out under the Nuclear Research and Development program by Korea Ministry of Science and Technology.

REFERENCES

1. C.Y. Han, C.-H. Shin, H.-C. Kim, J.K. Kim, N. Messaoudi, and B.-C. Na, *VENUS-2 MOX-Fuelled Reactor Dosimetry Calculations: Benchmark Specification*, NEA/NSC/DOC(2004)6, OECD/NEA (2004).
2. R.E. MacFarlane, *TRANSX 2: A Code for Interfacing MATXS Cross-Section Libraries to Nuclear Transport Codes*, LA-12312-MS, Los Alamos National Laboratory (1992).
3. R.E. Alcouffe, R.S. Baker, F.W. Brinkley, D.R. Marr, R.D. O'Dell, and W.F. Walters, *DANTSYS: A Diffusion Accelerated Neutral Particle Transport Code System*, LA-12969-M, Los Alamos National Laboratory (1995).
4. R.E. MacFarlane and D.W. Muir, *The NJOY Nuclear Data Processing System, Version 91*, LA-12740-M, Los Alamos National Laboratory (1994).
5. ORNL, *BUGLE-96: Coupled 47 Neutron, 20 Gamma-ray Group Cross Section Library Derived from ENDF/B-VI for LWR Shielding and Pressure Vessel Dosimetry Applications*, DLC-185, RSIC Data Library Collection, Radiation Shielding Information Center (1996).

Accurate Determination and Benchmarking of Radiation Field Parameters, relevant for Pressure Vessel Monitoring. A Review of some REDOS Project Results

B. Böhmer, B. Ošmera, et al.
FZ Rossendorf , Germany
Nuclear Research Institute , 25068 Rez Czech Republic
osm@ujv.cz

Plant life management needs a reliable estimation of radiation field parameters, including their uncertainty, to avoid the use of conservative approaches. The particular objectives of the REDOS project are the improvements of the RPV monitoring, the improvement of the neutron – gamma calculation methodologies through the LR-0 engineering benchmarks for WWER-1000 and WWER-440, and the accurate determination of radiation field parameters in the vicinity and over the thickness of the RPV. The project was divided in the following four working packages (WP):

WP1 – Review of available experimental data,
WP2 – Experimental programme in WWER-1000 Mock-up,
WP3 – Analytical Area. Analysis of calculated and measured data, conclusions
WP4 – Radiation field parameters in the vicinity of and over the thickness of the RPV.

The project started with a review of existing data, namely with the WWER440 Mock-up No1 and No2 and WWER-1000 Mock-up benchmark experimental data. Collecting of the NPP experimental data was performed for several units of Kozloduy NPP. Photon flux spectra and ratios of neutron / photon fluxes were measured in the WWER-1000 Mock-up.

Collection, evaluation and re-evaluation of the experimental data were carried out for their use in the WPs 3 and 4.

Some results achieved in REDOS have been presented to the 11th ISRD in Brussels 2002 and to the conferences FISA-2003 and ICRS-10/RPS2004.

This paper is mainly devoted to the comparison and analysis of the experimental and calculated LR-0 data (WP-3). The LR-0 benchmark data consist of neutron spectra (VVER-440 Mock-ups) and neutron + photon spectra (VVER-1000 Mock-up) in several points from the barrel simulator to the outer surface of RPV and evaluated integral fluxes, space – energy indices, like the spectral indices and attenuation factors in measuring points. The spectra are presented in the BUGLE format with uncertainties, the photon spectra are available also in a fine energy grid (0.1 MeV).

The recommended source term – core power distribution was calculated pin–by–pin with the MOBY DICK – WIMS-D4 code system (Czech standard code) and is available in the description of all Mock-ups.

The calculations were performed with stochastic and deterministic codes in 8 laboratories (institutes) participating in the project. MCNP as well as other Monte Carlo codes were used in different modes, the 3D, and synthesis modes of deterministic codes were used.

The results of participant calculations of integral fluxes, space – energy indices, a linear functional of spectra (dpa) as well as the calculated spectra were compared between themselves and with experimental results. The results of the comparisons were discussed and analysed. A set of selected results, limited by the volume of the paper, is presented.

Generally, the results of different participants are in good agreement concerning the fast neutron data. There are much more discrepancies for low energy neutrons and photons. The comparison of the measured fast neutron and photon data with the participants calculated results showed also a generally good agreement for neutrons and larger discrepancies for photons.

The work characterises the state of art of up-to-date calculations of neutron and gamma field parameters including spectral data for three realistic mock-ups of VVER-1000 and VVER-440 reactors for the region between the core boundary and the outer surface of the pressure vessel. The unique feature of this work is the benchmarking of calculated detailed neutron and gamma reactor spectra.

Studying and Benchmarking Thermal Neutron Scattering in Graphite

A. I. Hawari, V. H. Gillette, T. Zhou, I. I. Al-Qasir, B. W. Wehring
Department of Nuclear Engineering
North Carolina State University
Raleigh, NC 27695-7909

Generation IV Very High Temperature Reactor (VHTR) concepts, which are currently under study as power and hydrogen production units, are based on graphite moderated and gas cooled nuclear reactors [1]. A demonstration VHTR known as the Next Generation Nuclear Plant (NGNP) is planned to be built at the site of Idaho National Laboratory within the next 10 years [1]. As "thermal" reactors, the design and proper operation of VHTRs will depend on the ability to accurately predict the in-core thermal neutron energy spectrum. Consequently, work is underway to improve the calculation of the thermal neutron scattering cross sections for the graphite moderator, and to benchmark the cross section libraries using a neutron slowing-down-time experiment.

Traditionally, the thermal neutron scattering cross sections for graphite were calculated using computer codes such as GASKET and/or NJOY/LEAPR [2-4]. In these codes, the calculation is performed by utilizing the scattering formulation as developed using the incoherent approximation and assuming a cubic bravais lattice. In this work, we redeveloped the scattering formulation to relax these assumptions and to produce the inelastic scattering cross sections for graphite including exact treatment of the coherent 1-phonon component, which was ignored in the codes mentioned above [5]. Furthermore, to supply the required input (i.e., dispersion relations) for the new formulation, ab inito atomistic simulations combined with lattice dynamics calculations were performed using the VASP and PHONON codes [6,7]. Figure 1 shows the total inelastic thermal neutron scattering cross sections as produced by NJOY/LEAPR and our work at 300 K.

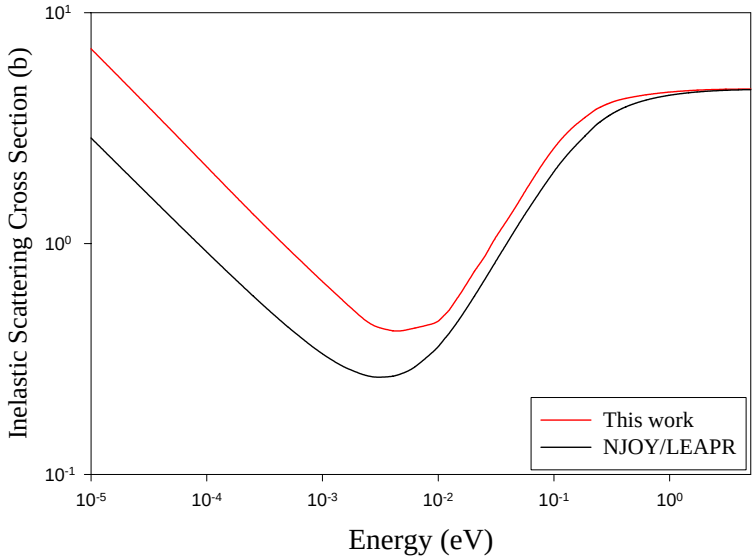

Fig. 1. The total inelastic neutron scattering cross section for graphite at 300 K as calculated using the NJOY/LEAPR code system and the models of this work.

Experimentally, a neutron slowing-down-time benchmark experiment has been designed and is currently set up at the Oak Ridge Electron Linear Accelerator (ORELA) facility of Oak Ridge National Laboratory. The use of this approach in benchmarking allows the measurement of the time-dependent integral reaction rate of a detector that is placed inside or outside a graphite structure, while the neutrons slow down and reach thermal energies [8].

This work is supported by the US DOE NERI grant number DE-FG03-02SF22514.

In this experiment, a 70 x 70 x 70 cm reactor-grade graphite structure is exposed to the neutron beam. ORELA is operated with a pulse frequency of approximately 100 Hz, which produces an effective pulsed source strength of approximately 10^8 n/s and ensures minimal pulse-to-pulse overlap. In addition, a special heating system was designed to allow performing the experiment as the temperature is varied from room temperature to 1000 °C. The entire experimental setup is surrounded by a borated polyethylene enclosure, which has been shown (by MCNP simulations [9]) to minimize the effect of neutron room return. Figure 2 shows an MCNP prediction of the signal (time spectrum) for a Pu-239 detector that is placed outside the graphite. Figure 3 shows the graphite cube and the borated polyethylene enclosure as set up at ORELA. Detectors other than Pu-239 have also been studied and will be used in this work.

In this paper, we will focus on the results of the computational developments and the impact of the cross section data on the predicted time spectra. Experimental design aspects will also be presented and discussed.

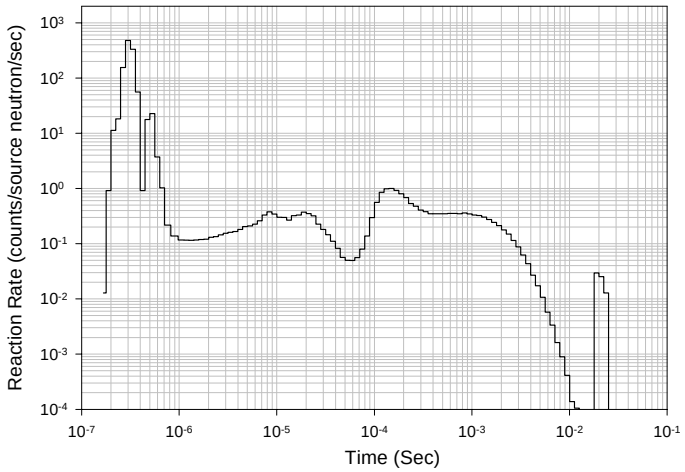

Fig. 2. The expected signal from a Pu-239 detector placed outside the graphite structure. The shape of the curve between 10^{-6} and 10^{-2} seconds is due to the resonances in the Pu-239 fission cross section.

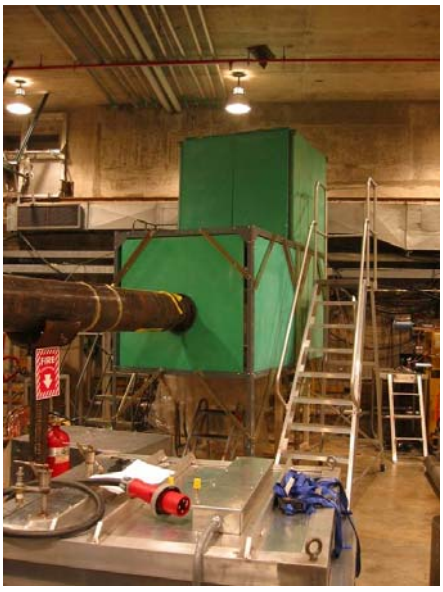

Fig 3. The 70 x 70 x 70 cm graphite cube that is used in the slowing-down-time experiment (left), and the shielded heating system that holds the graphite cube (right).

REFERENCES

1. P. E. Macdonald, "The Next Generation Nuclear Plant – Insights Gained from the INEEL Point Design Studies," Proceedings of the Frédéric Joliot and Otto Hahn Summer School on Nuclear Reactors: Physics, Fuels and Systems, Cadarache, France, (2004).
2. J. U. Koppel, J. R. Triplett, Y. D. Naliboff, *GASKET: A Unified Code for Thermal Neutron Scattering*, General Atomics Report 7417, (1967).
3. R. E. MacFarlane, D. W. Muir, *The NJOY Nuclear Data Processing System, Version 91*, LA-12740M, Los Alamos National Laboratory, (1991).
4. R. E. MacFarlane, *New Thermal Neutron Scattering Files for ENDF/B-VI, Release2*, LA-12639-MS, Los Alamos National Laboratory, (1994).
5. G. L. Squires, *Introduction to the Theory of Thermal Neutron Scattering*, Dover, New York, (1978).
6. G. Kresse, and J. Furthmuller, *Vienna Ab-Initio Simulation Package, VASP the Guide*, Vienna, (2002).
7. K. Parlinski, *PHONON manual, Version 3.11*, Cracow, (2002).
8. A. I. Hawari, J. M. Adams, "*Monte Carlo Assessment of Time Dependent Spectral Indexes for Benhmarking Neutron Transport In Iron*," Reactor Dosimetry in the 21st Century, J. Wagemans, H. A. Abderrahim, P. D'Hondt, and C. De Raet, Ed., Proceeding of the 11th International Symposium on Reactor Dosimetry, Brussels, Belgium, 2002.
9. X-5 Monte Carlo Team, *MCNP – A General Monte Carlo N–Particle Transport Code*, Version 5, LA-UR-03-1987, Los Alamos National Laboratory (2003).

Experimental Benchmark for the New Surveillance Program of WWER-1000

Ošmera B., Mařík M.
Nuclear Research Institute Řež plc
250 68 Řež, Czech Republic

Cvachovec F.
Military Academy
Kounicova 65, 612 00 Brno, Czech Republic

Tsofin V.
EDO "Gidropress"
21 Ordjonikidze Str., 142 103 Podolsk, Moscow Region, Russia

Lomakin S.
SEC of GOSATOMNADZOR
2/8, Building 5, M. Krasnoselskaya Str., 107 140 Moscow, Russia

Zaritsky S., Egorov A., Brodkin E.
RRC "Kurchatov Institute"
Kurchatov sq. 1, 123 182 Moscow, Russia

Modern WWER-1000 units will be equipped with new type of surveillance specimens boxes (SSB), which look like flat containers and locate close to inner surface of reactor pressure vessel (RPV). The experimental and calculation investigations were performed in the WWER-1000 Mock-up assembled in the LR-0 reactor in order to support the dosimetry of this new type SSB. It was the same Mock-up, which was used earlier in experiments for a dosimetry of WWER-1000 RPV without SSB. The model of new SSB was positioned on the inner surface of LR-0 tank (i.e. close to inner surface of RPV model, which is located just out of LR-0 tank) at the symmetry axis of the Mock-up. The dimensions of steel SSB model were 60 x 30 x 3.5 cm (height x width x thickness).

The neutron and photon spectra have been measured with stilbene cylindrical crystal (45 x 45 mm) in the energy range approximately from 0,5 MeV to 10 MeV. The spectra were measured in the Mock-up with SSB at the barrel simulator, before the SSB, behind SSB (before RPV), and in 1/4 of RPV thickness. Measurements in Mock-up without SSB were performed at the barrel simulator, before RPV, in 1/4, 1/2 and 3/4 of RPV thickness and behind RPV. The measurements were performed along the Mock-up axis with two-parametric spectrometer with stilbene scintilator, i.e. the neutron and photon spectra were measured simultaneously.

The spectra were evaluated in fine linearly equidistant (0.1 MeV) energy grid and in the BUGLE format including uncertainties. The experimental values of integral neutron field parameters (attenuations of integral neutron flux densities between different points of Mock-up as well as the spectral indices, i.e. ratios of integral neutron flux densities with different thresholds) were obtained also.

236U and 238U fission rates were measured also with track detectors before the SSB, behind SSB (before RPV), and in 1/4 of RPV thickness.

The Mock-up (LR-0 reactor) power monitoring during measurements was carried out with two fission chambers, one fixed, one moveable axially, so that four orders in power were covered.

The experimental data (spectra, attenuation factors and spectral indices) are compared with calculation results. The sensitivity to parameters of calculation model and method was evaluated also.

Characterization of the Neutron Field in the HSSI/UCSB Irradiation Facility at the Ford Nuclear Reactor

I. Remec, T. M. Rosseel, C. A. Baldwin, and E. D. Blakeman

Oak Ridge National Laboratory, Oak Ridge, TN, USA

(E-mail: remeci@ornl.gov)

Abstract

This article describes the characterization of the neutron field in the US Nuclear Regulatory Commission (US NRC) facility for irradiation of metallurgical specimens.[1] The facility, was located at the University of Michigan's Ford Nuclear Reactor (FNR) in Ann Arbor, Michigan. [NOTE: In 2003 the Ford reactor ceased operation and the HSSI program is in the process of selecting a site where a new facility, similar to the one described above, will be built.] The facility consisted of two capsules (a high-flux and a medium/low flux capsule) used by the University of California, Santa Barbara (UCSB), and two capsules designed and built by the Heavy-Section Steel Irradiation (HSSI) Program, which is conducted by the Oak Ridge National Laboratory. The capsules were reusable and were designed to permit the removal and exchange of metallurgical specimens. Therefore, the dosimetry measurements were performed with the actual capsules and not with the special "dummy" capsules, as was done in previous HSSI experiments.

The characterization of the neutron field in the facility was performed using state-of-the-art methodology. The characterization consisted of the irradiation of neutron dosimeters inside the capsules, the calculation of the neutron field with neutron transport theory, and the least-squares adjustment of the calculated neutron spectra and measured reaction rates to determine the best-estimate neutron-exposure parameters. Two hundred fifty-six reaction rates at 129 different locations in the capsules were obtained from three irradiation experiments. The transport calculations were performed with the TORT code using a three-dimensional model of the facility. The calculations under-predicted the "measured" reactions rates by ~7% and the average absolute difference was ~10%. Hence, the calculations and measurements were in excellent agreement. The least-squares neutron-spectrum adjustment calculations were performed with the computer code LSL-M2. All the reaction rates were applied simultaneously to adjust the calculated fluxes.

The exposure parameters of interest were the neutron fluxes for neutrons with energies greater than 1.0, 0.5, and 0.1 MeV, and the displacement per atom (dpa) rate in iron. These parameters were determined at the location of each dosimeter. To facilitate the preparation of future experiments, the fitting functions were also derived to describe spatial distributions of exposure parameters.

[1] This research is sponsored by the Office of Nuclear Regulatory Research, US Nuclear Regulatory Commission under interagency agreement DOE 1886-N695-3W with the US Department of Energy under contract DE-AC05-00OR22725 with UT-Battelle, LLC.

Release of the New International Reactor Dosimetry File IRDF-2002

Trkov A.
International Atomic Energy Agency, Nuclear Data Section
Wagramer str. 5. A-1400 Vienna, Austria

Zsolnay E. M.
Institute of Nuclear Techniques, Budapest University of Technology and Economics,
Műegyetem rkp. 3-9. H-1111 Budapest, Hungary

ABSTRACT

A new International Reactor Dosimetry File, called IRDF-2002, has been prepared by an international team, coordinated by IAEA NDS [1]. The library contains the best quality data available for reactor dosimetry applications at the time of preparation (closing of data collection was December 2003), namely:

- cross section data for 66 neutron activation (and fission) reactions, accompanied by uncertainties in the form of covariance information;
- total cross sections for three cover materials (B, Cd and Gd), without uncertainty information;
- radiation damage cross sections for some elements and compounds; and
- nuclear data (decay data for the reaction products and isotopic abundances for all the target nuclei of interest).

All data are presented in ENDF-6 format, both in point and in SAND-type 640 group representation.

Integral characteristics of the cross sections and the related uncertainties were calculated and compared with the corresponding experimental values in standard neutron fields: Maxwellian thermal, 1/E, ^{252}Cf fission and 14 MeV neutron spectra [2-5]. Consistency test of the data was made in two reference benchmark neutron spectra (ACRR and SPR-III; SNL, USA) [6].

This paper presents the content and summarizes the main characteristics of the library based on the IAEA TECDOC on IRDF-2002 [1], to be published in the near future.

REFERENCES

[1] O. Bersillon, L. R. Greenwood, P. J. Griffin, W. Mannhart, H. J. Nolthenius, R. Paviotti-Corcuera, K. Zolotarev, E. M. Zsolnay: International Reactor Dosimetry File-2002, IRDF-2002. TECDOC Report. IAEA NDS, 2004. To be published.

[2] MUGHABGHAB, S.F., Thermal neutron capture cross sections, resonance integrals and g-factors, INDC(NDS)-440, IAEA, Vienna, February 2003.

[3] HOLDEN, N.E., Neutron scattering and absorption properties (revised 2003), pp. 198-213 in CRC Handbook of Chemistry and Physics, 84th Edition, Chapter 11, Editor-in-Chief: LIDE, D.R., CRC Press, 2000 NW Corporate Blvd., Boca Raton, Florida 33431, USA (2003).

[4] MANNHART, W., Update of the evaluation of spectrum-averaged cross sections measured in the ^{252}Cf fission neutron field (2001) unpublished results.

[5] ZERKIN, V., EXFOR, Nuclear reaction database retrieval system, IAEA, Vienna, 2003.

[6] P. J. Griffin and R. Paviotti-Corcuera: Summary Report of the Final Technical Meeting on ″InternationalReactor Dosimetry File: IRDF-2002″. Report, INDC(NDS)-448. IAEA Nuclear Data Section, Wagramer Strasse 5, A-1400 Vienna. October 2003.

Nuclear Data Evaluations and Recommendations

Holden, N.E.
Brookhaven National Laboratory
Upton, NY 11973-5000, USA

The published scientific literature is scanned and periodically evaluated for neutron and non-neutron nuclear data and the resulting recommendations are published [*1*,*2*] However, after the literature has been scanned and the appropriate data collected, there are often problems arising with regard to the treatment of the various types of data during this evaluation process and with regard to the method by which some of the recommendations are drawn from the assessment of the collection of individual measurements. Some of the processes and problems will be discussed.

In the case of new chemical elements to be placed on the Periodic Table of the Chemical Elements, there are recent measurements that have reported data about the existence of new chemical elements. There is a process by which that information is reviewed and the conclusion must be drawn as to which set of reported data is the first to have found that new element and whether or not there has been verification of that claim. The result would allow one group to claim discovery and to be given the privilege of supplying the name for this new element. Information reporting new claims of discovery of two new elements, Z = 113 and Z = 115, has appeared in the literature [*3*]. Similarly, an acknowledgement has now been made of two earlier claims of initial discovery that have resulted in the official naming of the element with Z = 110, Darmstadtium, and its addition to the Periodic Table [*4*] and a second element with Z = 111, Roentgenium, which is in the process of being officially approved. Details will be presented.

In the case of radioactive half-lives or radioactive decay constants, problems often arise in connection with the estimation of the systematic error. Underestimating the systematic component of the uncertainty often have the effect that authors will quote their half-life results, such that those results would exclude many other good measurements from consideration, if one would believe their quoted underestimated uncertainties.

Examples will be presented for such long-lived nuclides as ^{176}Lu (where there have been half-life counting experiments, which reported measurements of 3.69 (2) x 10^{10} years [*5*] and also 4.08 (3) x 10^{10} years [*6*]) and ^{187}Re (a liquid scintillation counting measurement of 3.51 (37) x 10^{10} years [*7*] and a cryogenic micro-calorimeter result of 6.2 (6) x 10^{10} years [*8*] have been reported). In the case of Lu, the above two measurements would differ between 13 standard deviations and 19 standard deviations and could not be considered to be estimating the same physical parameter. The methods for treating such problems will be discussed.

For isotopic abundance values, the problems of uncertainties and mass fractionation estimates affect the resulting quoted values. Isotopes may be fractionated substantially by physical, chemical or biological processes, the rates or equilibrium states of which are mass dependent. Processes that differentiate on mass and commonly yield measurable changes in isotopic composition include changes of physical state (e.g., evaporation, condensation, crystallization, melting and sublimation, ion exchange, diffusion and a variety of biological processes. The impact of natural variations of the isotopes on the quoted isotopic composition will be discussed, since it can affect the atomic weight or average mass for the element involved.

When the isotopic abundance values are listed in the isotopic composition of an element, the number of significant figures for a minor isotope are often truncated because of the requirement that the total isotopic composition must add up to unity exactly. Since the number of significant figures of the major isotopes can eliminate some significant figures in the minor isotope, this process can increase the uncertainty, when that minor isotope is used for neutron activation measurements. It may impact the uncertainty for determination of the radioactive decay constant or half-life, when derived from geological measurements using dating methods. This process and some examples will be discussed.

The double beta decay process, when no neutrinos are emitted, has an apparent impact on some physics conservation laws and has been discussed previously [*9*]. The latest update on the previously reported measurement [*10*] of a (0ν, 2β) decay process in ^{76}Ge will be presented.

The estimation of the systematic error and its impact on variance weighting methods will be discussed, as well as the effect of the known (or unknown) psychological problem that is associated with the estimation of the systematic error.

REFERENCES

1. N. E. Holden, "Table of the Isotopes (Revised 2002)", *Handbook of Chemistry and Physics, 85th edition*, section 11, CRC Press Inc., David R. Lide, editor, Boca Raton, FL (2004). pp. 50-201.
2. N. E. Holden, "Neutron Scattering and Absorption Properties (Revised 2003)", *Handbook of Chemistry and Physics, 85th edition*, section 11, CRC Press Inc., David R. Lide, editor, Boca Raton, FL (2004). pp. 202-217.
3. Yu. Ts. Oganessian, V. K. Utyonkoy, Yu. V. Lobanov, F. Sh. Abdullin, A. N. Polyakov, I. V. Shirokovsky, Yu. S. Tsyganov, G. G. Gulbekian, S. L. Bogomolov, A. N. Mezentsev, S. Iliev, V. G. Subbotin, A. M. Sukhov, A. A. Voinov, G. V. Buklanov, K. Subotic, V. I. Zagrebaev, M. G. Itkis, J. B. Patin, K. J. Moody, J. F. Wild, M. A. Stoyer, N. J. Stoyer, D. A. Shaughnessy, J. M. Kenneally, R. W. Lougheed, "Experiments on the Synthesis of Element 115 in the reaction $^{243}Am(^{48}Ca,xn)^{291-x}115$", *Phys. Rev. /C,* **69,** (2004). 021601.
4. N. E. Holden, T. B. Coplen, "The Periodic Table of the Elements", *Chemistry International*, **26**, (2004). pp. 8-9.
5. Y. Nir-El, N. Lavi, "Measurement of the Half-life of ^{176}Lu", *Appl. Radiat. Isot.,* **49.** (1998). pp. 1653-1655.
6. Y. Nir-El, G. Haquin, "Half-life of ^{176}Lu", *Phys. Rev. /C,* **68**, (2003). 067301.
7. E. Cosulich, G. Gallinaro, F. Gatti, S. Vitale, "Detection of ^{187}Re beta decay with a cryogenic micro-calorimeter. Preliminary results", *Phys. Lett. /B,* **295**, (1992). pp. 143-147.
8. S. N. Naldrett, "Half-life of rhenium: geological and cosmological ages", *Can. J. Phys.*, **62**, (1984). pp. 15-20.
9. N. E. Holden, "2002 Review of Neutron and Non-Neutron Nuclear Data", in *Radiation Dosimetry in the 21st Century*, Proc. 11th Int. Symp. Reactor Dosimetry, Brussels, Belgium, August 18-23, 2002, World Scientific Publishing Co., Pte, Ltd., Singapore (2003). pp. 646-653.
10. H. V. Klapdor-Kleingrothaus, A. Dietz, H. L. Harney, I. V. Krivosheina, "Evidence for Neutrino-less Double Beta Decay", *Mod. Phys. Lett. A,* **16**, (2001). pp. 2409-2420.

Invited Paper

Gas Production in Reactor Materials

L. R. Greenwood
Pacific Northwest National Laboratory

This paper presents an overview of the principal nuclear reactions that are known to produce hydrogen and helium in irradiated materials and a summary of the comparison of measurements with predictions in various reactors. Hydrogen and helium are produced in all reactor materials by fast neutron reactions which typically have thresholds above 4 MeV. Selected elements also have thermal neutron gas production reactions that can be quite prolific, such as ^{6}Li, ^{10}B, and ^{14}N. For example, the presence of small boron impurities in reactor steels greatly increases the helium production. Finally, there are a number of elements which produce transmutation products that have high thermal neutron gas production cross sections, most notably ^{59}Ni produced by irradiation of Ni and ^{65}Zn produced by irradiation of Cu or Zn. Since gas production cross sections are isotope-specific, gas production rates can change during irradiation due to transmutation effects or initial rates can be modified by isotopic tailoring of reactor materials.

Total H or He gas production cross sections include a number of different nuclear reactions. For example, helium is produced by reactions such as (n,a), (n,3He), (n,na), (n,pa), and so forth. Consequently, special purpose evaluated cross section files need to be created that add up all possible reaction channels for the routine calculation of gas production. One of the most widely used of these special purpose files in File 533 in ENDF/B-V. The calculation of gas production from fast neutrons also requires an accurate knowledge of the neutron flux spectrum, especially at higher neutron energies above 10 MeV. Failure to include high energy neutrons in sufficiently fine group structure will lead to significant errors in the calculation of gas production from fast neutron reactions.

There has been considerable effort to compare measurements with calculations for pure materials irradiated in a variety of facilities for most common fission or fusion reactor materials. Almost all of the data is for helium rather than hydrogen due to the absence of any helium background in materials and more importantly the stability of implanted helium. In general, materials need to be melted before they release most of the helium. Hydrogen, on the other hand, is difficult to measure for comparison with calculations since most materials contain background levels of hydrogen, there are non-nuclear sources of hydrogen in reactors such as hydrolysis of water, and hydrogen is very mobile at elevated temperatures. Surprisingly, high levels of hydrogen have been seen in some highly irradiated materials with helium bubbles. The most likely explanation is that hydrogen can be trapped in helium bubbles which are observed to form at higher helium levels.

Helium is generally believed to be more important than hydrogen in reactor materials since helium can form bubbles that lead to significant swelling and can prevent weld repair of small cracks that have been observed. However, if high levels of hydrogen are trapped in materials, then the hydrogen may also lead to radiation damage effects.

Dosimetry requirements for pressure vessel steels toughness curve in the ductile to brittle range

H. CARCREFF, A. ALBERMAN, L. BARBOT, F. ROZENBLUM
Commissariat à l'Energie Atomique, Saclay, DEN/DRSN
91191Gif sur Yvette, FRANCE.

D. BERETZ
Commissariat à l'Energie Atomique, Cadarache, DEN/DER
13108 St Paul Lez Durance, FRANCE

Y.K. LEE
Commissariat à l'Energie Atomique, Saclay, DEN/DM2S
91191Gif sur Yvette, FRANCE.

As part of nuclear plant life-time assessment project, a large R&D program has been carried out by Electricité De France (EDF) and the Commissariat à l'Energie Atomique (CEA) from 1995 to 2004, to assess Pressure Vessel (PV) steels toughness curve using very large Compact Tension (CT) specimens (50x125x120 mm) allowing measurements in the ductile to brittle transition range.
For this purpose, four CT specimens were especially manufactured and taken from the heat of a vessel shell ring.

A new high capacity irradiation rig was designed by CEA to meet the CT50 specimens loading requirements in the OSIRIS reactor operated by CEA's Nuclear Energy Division at Saclay research center. This specific rig is the biggest experimental device ever irradiated in the OSIRIS reactor and requires 9 irradiation locations in reflector instead of a single one for a standard device. Large dimensions of the water box containing the irradiation rig, and the rig itself designed to welcome the four specimens, induce a soft neutron spectrum compared with a standard material experiment (smaller specimens).
Moreover, under irradiation, the temperature level at specimens location required to move the device away from the core to limit the energy deposited by gamma heating. Aluminum shields located between the core housing and the water box were used to keep a sufficient fast neutron flux level on the specimens.
Because of the particular conditions of this experiment, dosimetry required important developments.
So the main challenges were :

- to reach the adequate control of temperatures at each CT 50 level to match requested values and associate accuracies,
- to elaborate a relevant calculation scheme for defining a whole irradiation device suitable design in such an environment,
- to keep spectral characteristics as close as possible to the ones encountered in most steel irradiation programs, while preserving a fast neutron flux level leading to an appropriate irradiation time.

After preliminary calculations to select the best location in OSIRIS reflector, a specific TRIPOLI 4 Monte-Carlo transport calculation scheme was performed by CEA to evaluate the nuclear reaction rates, spectrum ratios, nuclear heating levels, and fast neutron flux distributions inside the irradiation device.
On the other hand, spectrum characteristics and neutron flux levels were determined by a comprehensive dosimetry on mock-ups featuring activation foils as well as tungsten and graphite damage monitors.

In spite of neutron spectra significant modification with regard to the experiment size, a very good agreement was found between calculated and measured nuclear reaction rates.
The computed ϕ>1 MeV / ϕ^{f}_{Ni} ratio, a reference parameter in dosimetry, is found within 5 % of experiment.
The iron dpa / ϕ>1 MeV ratio measured to 1800 dpa.barn is a relevant value for usual French PWR vessel neutron spectra. This is in the middle of results range obtained in previous ESTEREL PV steels experimental program [*1*] carried out in OSIRIS and SILOE reactors, being a reference in PV dosimetry.
The target fast neutron fluence was 7.5 10^{19} n.cm^{-2} (E>1 MeV) and required an irradiation time of 340 EFPD in OSIRIS reactor.

The irradiation run is now completed. Actual neutron fluences, after measuring the activity of flux monitors (fissile and activation foils) compiled with dosimetry calibration, are now being processed.

REFERENCE

1. A. Alberman and al, “Neutron spectrum effect and damage analysis of pressure vessel steels irradiations.” *Proceedings of the 9 th International Symposium on Reactor Dosimetry*, (1996). pp. 524-534.

Radiation Damage Calculations for the SNS Target, Moderators Vessels, and Reflector System

Ferguson, P. D. and Gallmeier, F. X.
Spallation Neutron Source, Oak Ridge National Laboratory
Oak Ridge, TN 37830, USA.

Mansur, L. K.
Metals and Ceramics Division, Oak Ridge National Laboratory
Oak Ridge, TN 37830, USA.

Wechsler, M. S.
North Carolina State University
Raleigh, NC 27695, USA.

The Spallation Neutron Source (SNS) [*1*] at Oak Ridge National Laboratory is scheduled to begin operation in June 2006. The SNS is designed to be a 1.4 MW pulsed neutron scattering facility with 1-GeV protons incident on a flowing liquid mercury target. Directly above and below the target are four moderators, three supercritical hydrogen at 20 K and one ambient water. Surrounding the moderators is a heavy water cooled beryllium reflector, with a radius of 32 cm, followed by a heavy water cooled stainless steel reflector. A schematic of the SNS target system is shown in Fig. 1.

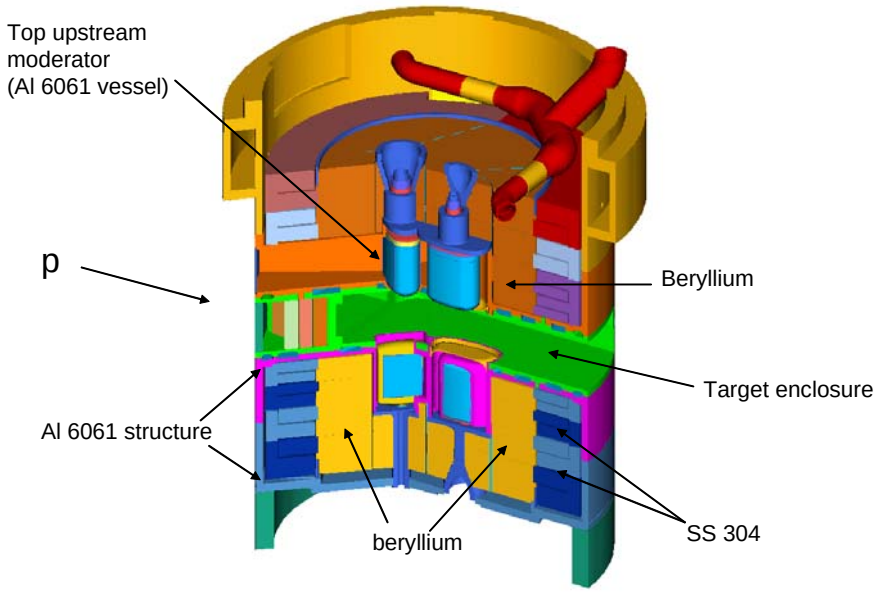

Figure 1. Schematic of the SNS target station

When calculating radiation damage parameters in accelerator driven systems, it is customary to create small tally cells near the region of interest and calculate damage rates inside the cell. However, for complex systems such as the SNS and the Japanese Spallation Neutron Source (JSNS), the region of peak damage rate may not be easily identified. It can also be useful in the design process to understand how radiation damage parameters vary throughout the target system as the radii of replaceable regions are often selected based upon these parameters. For these reasons, the calculation of radiation damage parameters was studied and improvements were implemented.

Radiation damage calculations at the SNS are completed using MCNPX [*2*]. For these calculations, the mesh tally capability of MCNPX was modified to allow material specific cross section folding with neutron or proton fluxes. With the modified mesh tally, any reaction rate for which a cross section exists can be calculated over a large region of interest in a complex geometry. For regions containing multiple materials, one modified mesh tally is performed for each

material within the region with the appropriate cross section specified and the tally histograms can be added together to make the final plot over the entire region. It should be noted that the modified mesh tally performs like the general tally multiplier card (fm card) in MCNPX with some limitations and additional complexity due to the multiple materials within a tally region.

An example of the modified mesh tally applied to the SNS inner reflector plug is shown in Fig. 2. The Monte Carlo geometry is show in Fig. 2(a) with materials showing up as various colors or shades of gray. Because materials vary throughout the system, calculations of the displacement rate for the entire system would be time consuming using the old method. With the modified mesh tally, the displacement rates for the entire system are generated in a single run using multiple mesh tallies, one for each material and particle type of interest. Figure 2(b) is the modified mesh tally plot of the displacement rate in the SNS inner reflector plug. From the plot, it is interesting to note the asymmetry in the direction of the proton beam of the displacement rate, likely due to neutron albedo from the front nose of the target. Just downstream of the moderator positions, at ~+20 cm axial, it is interesting to note the difference in displacement rate in the aluminum plate versus the beryllium. This difference is likely due to the difference in spectrum weighted displacement cross section for this location.

In this paper, the calculation method is described and the SNS target nose is used to verify the modified mesh tally calculations with the old calculation method. The modified mesh tally is then applied to the SNS inner reflector plug and moderators, calculating displacement rate and appm helium/dpa for each material. For the Al 6061 moderators, the silicon production rate is also calculated.

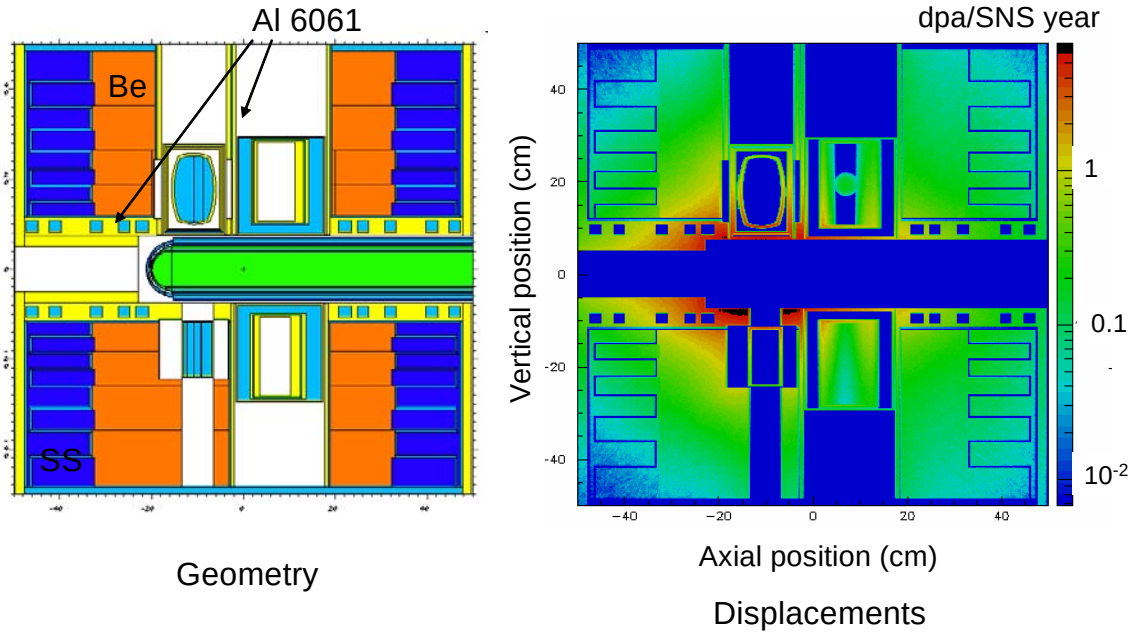

(a) (b)

Figure 2. Monte Carlo model (a) and calculated displacement rate (b) in the SNS inner reflector plug.

ACKOWLEDGMENTS

SNS is managed by UT-Battelle, LLC, under contract DE-AC05-00OR22725 for the U.S. Department of Energy.

SNS is a partnership of six national laboratories: Argonne, Brookhaven, Jefferson, Lawrence Berkeley, Los Alamos, and Oak Ridge.

REFERENCES

1. National Spallation Neutron Source Conceptual Design Report, Oak Ridge National Laboratory, NSNS/CDR-2/VI, 1997.
2. MCNPX, Version 2.4.0, the MCNPX Team, LA-UR-02-5253, Los Alamos National Laboratory, August 2002.

Attenuation of Radiation Damage and Neutron Field in RPV Wall

Brumovsky, M., Marek, M., Zerola, L., Viererbl, L.
Nuclear Research Institute Rez plc
Rez, 250 68, Czech Republic

Golovanov, V.N., Lichadeev, B.V., Raetsky, B.M., Petelin, A.L.
FSUE "SSC RF RIAR"
433510, Dimitrovgrad-10
Ulyanovsk region, Russia

Radiation damage through the RPV wall is typically determined on the basis of neutron field calculations providing a change in fluence coupled with a correlation for embrittlement based on surveillance Charpy V-notch specimen testing. Since the neutron spectrum is changing through the RPV wall and no direct correlation exists between neutron damage and neutron spectrum, the use of dpa to attenuate the fluence has been chosen. The more direct way to measure the real damage is through direct measurement of changes in mechanical properties through a RPV wall. The attempts at using actual decommissioned irradiated vessels have been non-conclusive, primarily because the resultant data are highly scattered and difficult to interpret since the mechanical properties throughout the vessel wall prior to irradiation are unknown. Thus, a mock-up vessel wall experiment could provide the necessary data to discern the changes in properties through a thick irradiated RPV wall connected simultaneously with changes in neutron field in specimens locations.

Irradiation of a block of specimens (minimum dimensions: height = 100 mm, width = 80 mm, depth = 200 mm) representing full RPV VVER-1000 wall (thickness equal to 200 mm) was performed in conditions fully corresponding to the real RPV conditions (temperature, neutron field) in NIIAR Dimitrovgrad.

Irradiation rig was located in the reactor reflector to represent neutron spectrum incident on the RPV inner wall. Target neutron fluence on inner mock-up surface – approx. 6×10^{23} m^{-2} (E_n larger than 0.5 MeV that is approximately equal to 3×10^{23} m^{-2} for E_n larger than 1 MeV). Irradiation temperature was kept on 288 +/- 10 °C throughout all specimen block.

Neutron dosimetry should characterize neutron field (fluence and spectrum) in the whole specimens block in all three directions. Two sets of neutron monitors were used – one set was supplied and fully measured and evaluated by the NIIAR, second set was supplied and evaluated by NRI.

Temperature measurements through the specimens block was performed by a large set of thermocouples located in typical locations – outer surfaces as well as in the block center. Temperature was continuously measured and recorded.

Mainly specimens from VVER-1000 RPV materials (base metals and weld metals) were irradiated. Moreover, several sets of specimens from the IAEA reference steel JRQ were added for a possible comparison with PWR radiation damage data. Additionally, two PWR materials have been selected. The first is a high copper weld metal, and the second is a low copper base metal.

Irradiation experiment was finished in December 2003 and first neutron monitors were measured and evaluated. Preliminary results are shown in Fig.1. Further activation measurements and supplementary calculations are in progress as well as mechanical tests of unirradiated and irradiated specimens.

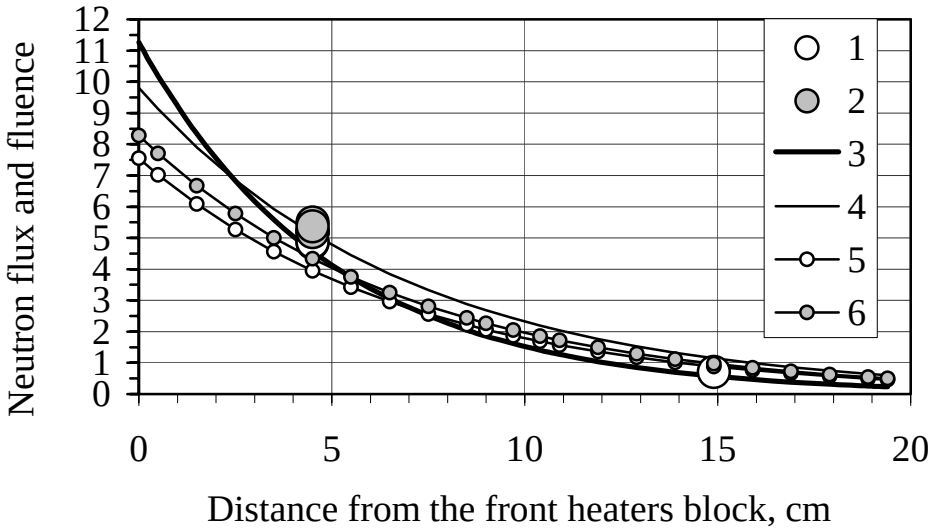

Figure 1. Change of neutron flux with energy E> 3.0 MeV (10^{11}cm^{-2} s^{-1}) and energy E> 0.5 MeV (10^{12} cm^{-2} s^{-1}) and neutron fluence with energy E> 0.5 MeV (10^{19}cm^{-2}) over thickness of samples blocks A and D:
1 and 2 - experimental values for cells No.13 and 23 (1) and 14 (2),
3 and 4 - results of the previous measurements for neutrons with energy E> 3 MeV (3) and E> 0.5 MeV (4),
5 and 6 - neutron fluence for ampoules CZR-2 and CZR-1.

Pseudo-Adjoint Model for Reactor Internals Analysis

Fero, A. H.
Westinghouse Electric Company
Nuclear Services
P. O. Box 158
Interstate 70, Exit 54
Madison, PA 15663-0158 USA

Perlov, Mary V.
University of Pittsburgh

As the US fleet of nuclear reactors ages, the operating utilities are applying to the US NRC for extensions to their operating licenses. The initial license extensions are from forty to sixty years of operation, but extensions to eighty years are being contemplated. This leads to questions of the effects of radiation exposure to structures located close to the reactor core, in particular the reactor internals structures.

Recent work [*1*] illustrated the importance of a detailed understanding of the operating environment seen by reactor internals structures in service. This includes the neutron exposure (fast neutron fluence, dpa, gas generation, etc.) and the temperature (which is strongly influenced by local gamma ray heating). This paper also illustrates the large variations that occur in the operating radiation environment that result from changes in fuel cycle design both within a given fuel cycle and from one fuel cycle to the next. A direct consequence of the need for detailed (as opposed to "design basis") analysis is that a very large number of (typically 3D) transport calculations are required. This level of effort may be impractical for many situations.

Historically, one method of reducing the level of effort was to run adjoint transport calculations. If one can limit the question to a few points (such as the peak flux location on the reactor vessel) and/or to a limited number of responses (fast fluence or iron atom displacements), then the adjoint method may prove useful. However, where there are many responses of interest and where data is needed for the majority of space in the model, the adjoint method is simply impractical. This has led to the development of a pseudo-adjoint approach to analyzing the reactor internals.

In a true adjoint the "source" is the response function of interest located at the point where the results are desired. The result of the transport calculations is the importance of each space mesh in the problem to the response at the point. Post-processing codes may then be employed to fold a core power distribution (neutron source distribution) with the importance function to obtain the result that corresponds to that power distribution.

The pseudo-adjoint approach uses a series of conventional forward transport calculations, each of which is run with a piece of the total source. Specifically, for PWR reactor internals analyses, the transport problem would be a 3D TORT model of the reactor (or a portion of the reactor). Each "source" would be a single fuel assembly. For peripheral fuel assemblies, the power distribution within the assembly

includes the shape across the assembly that is largely leakage driven. The relative assembly power is set at 1.0. Reactor coolant boron concentrations representative of beginning of life (BOL), middle of life (MOL), and end of life (EOL) conditions are considered. Each fuel assembly is analyzed separately. In order to obtain results for a given fuel cycle, the individual fuel assembly results are scaled by the relative power for that assembly during that cycle and are then combined by a post-processing code resulting in all responses of interest at all points in the model. This allows great flexibility in easily examining a large number of fuel cycle parameters.

This paper will discuss the sensitivities of the pseudo-adjoint approach to variations in reactor coolant temperature (density), boron concentration, and neutron source spectrum, as well as differing treatments of the axial core power distribution. The paper will also discuss the advantages and disadvantages of smaller, local models that focus on a component (such as a core former plate) versus a larger model that includes the entire core and the surrounding reactor internals structure.

REFERENCE

1. A. H. Fero and D. R. Forsyth, "Determination of Baffle Bolt Operating Parameters", in *Reactor Dosimetry in the 21st Century*, (J.Wagemans, et al., Ed.) World Scientific, London (2003) pp 233-241.

Measurements and Monte Carlo Calculations of Gamma and Neutron Flux Spectra inside and behind Steel-Water Configurations[1]

Boehmer, B., Konheiser, J., Noack, K., Stephan, I.,
Forschungszentrum Rossendorf e.V., Institut für Sicherheitsforschung,
PF 510119, 01314 Dresden, Germany

Hansen, W., Hinke, D., Unholzer, S.
Technische Universität Dresden,
01062 Dresden, Germany

Grantz, M., Mehner, H.-C.
Hochschule Zittau/Görlitz, Fachbereich Maschinenwesen,
Theodor-Körner-Allee 16, 02763 Zittau, Germany

INTRODUCTION

Gamma radiation can substantially contribute to the embrittlement of reactor structural materials. Material tests of surveillance probes of the High Flux Isotope Reactor (HFIR) at the Oak Ridge National Laboratory showed that the level of the measured radiation embrittlement exceeded that which was expected from the fast neutron fluence around the factor six. The observed displacements per atom (DPA) well agree with calculated values if the gamma irradiation is taken into consideration [1]. This observation at the HFIR clearly demonstrated the necessity to develop and to validate transport calculation methods and nuclear data sets for gamma fluence determination. Both have been evaluated to be on an essentially lower quality level than those for the determination of neutron fluences [2].

The Monte Carlo transport code MCNP is capable to calculate coupled neutron/gamma problems and is widely used together with nuclear data on the base of ENDF/B data libraries. But, a systematic verification for gamma spectra calculations in this field has not yet been reported on. The Monte Carlo transport code TRAMO developed by Forschungszentrum Rossendorf especially for reactor dosimetry flux/fluence calculations now has been extended to coupled neutron/gamma and gamma transport problems. The code, which uses nuclear data in an energy group representation, also waits for verification by comparing with experimental data. The neutron/gamma transmission experiments that hitherto were performed and partly are still going on give the measured data for the verification of both Monte Carlo codes.

EXPERIMENTS

Two zero power training and research reactors were chosen for the investigations. Both reactors differ in core design, experimental possibilities and neutron and gamma field characteristics. The AKR of the Technical University Dresden (Fig. 1, left) with a nominal power of 2 W has a small compact core consisting of a homogeneous mixture of fuel and polyethylen as solid moderator. The ZLFR of the University of Applied Sciences Zittau/Görlitz (Fig. 1, right) is a light water moderated and reflected reactor of

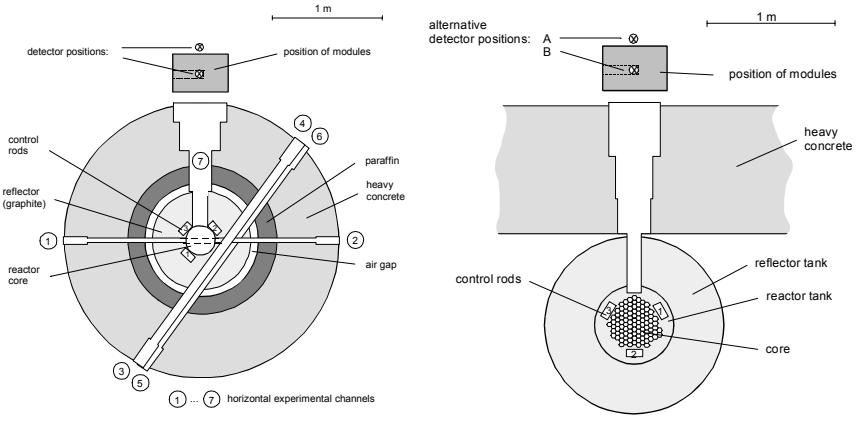

Figure1. Horizontal cross section of the AKR (left) and ZLFR (right)

[1] The research work was supported by Deutsche Forschungsgemeinschaft.

tank type with 36 % enriched UO_2 fuel.

The transmission modules were composed by plates of normal steel and stainless steel (SS) and welded water tanks of various thickness. Numerous combinations of steel or SS slabs with water tanks have been investigated. The modules were arranged outside of the irradiation channels. All measurements and calculations should be compared to an absolute scale of the neutron source intensity. Therefore, the absolute monitoring of the neutron flux in the cores of AKR and ZLFR was necessary. It has been done by a calibrated fission chamber and different activation detectors. For the simultaneous measurements of neutron and gamma spectra a NE 213 scintillation spectrometer [3] was applied. The spectra were measured mostly behind and sometimes within the transmission modules. The energy response ranges between about 1 and 20 MeV for neutrons and > 0.3 MeV for gamma rays. In addition, measurements with a ^{3}He detector were carried out.

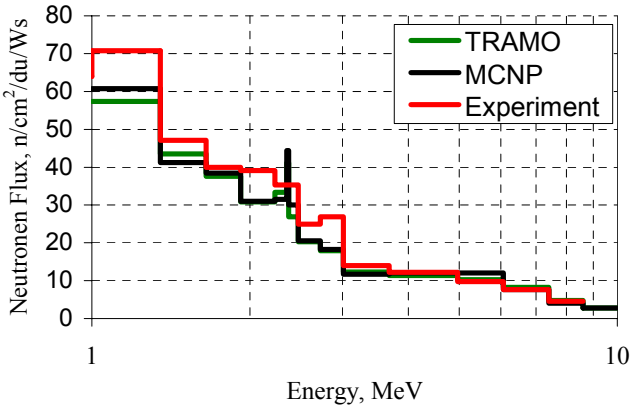

Figure 2. Comparison of neutron flux spectra

CALCULATIONS

The neutron and gamma energy spectra were calculated by means of the Monte Carlo codes MCNP and TRAMO. Both codes used nuclear data from the ENDF/B-VI library. The MCNP calculations used the energy point data representation of the cross-sections whereas the TRAMO calculations used effective group data that were generated with help of the NJOY code for the BUGLE-96 energy group structure. For efficiency reasons the calculations were carried out in two steps:

1. A criticality calculation by means of MCNP was done in which surface sources for neutrons and gammas were determined on a plane located outside the channel near to the exit.
2. Neutron and gamma transport calculations for the various modules starting from the same surface sources.

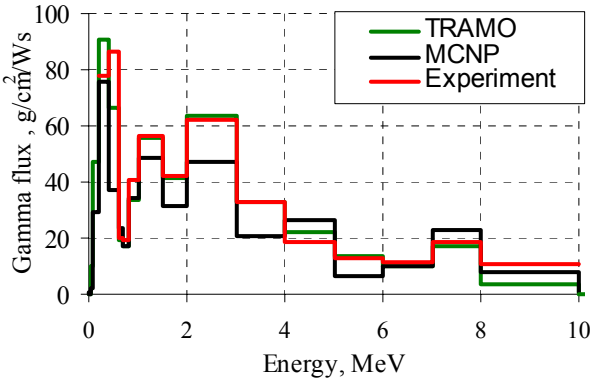

Figure 3. Comparison of gamma flux spectra

RESULTS

Measured and calculated flux spectra are compared in the energy group structure of BUGLE-96 on absolute scale of reactor power. As example, figures 2. and 3. show the spectra of the neutron and gamma fluxes, respectively, behind the module that was composed of: 3.4 cm water, 14.6 cm SS, 12 cm water and 15 cm steel. The investigations show that the neutron and gamma flux spectra measured in the performed steel-water transmission experiments in most cases agree with the spectra calculated by means of MCNP and TRAMO also on an absolute scale within the expected range of discrepancies given mainly by uncertainties in nuclear data and in the experimental methods.

REFERENCES

1. R. D. Cheverton et al., *Evaluation of HFIR pressure-vessel integrity considering radiation embrittlement*, ORNL/TM-10444, (1988)
2. NEA Nuclear Science Committee, *Report on Computing Radiation Dose to Reactor Pressure Vessel and Internals*, NSC/DOC(96)5 (1996)
3. S. Unholzer, et al., "The measurement of neutron and neutron induced photon spectra in fusion reactor related assemblies", Nucl. Instr. Meth., A476, 160 (2002)

Advances in Calculation of Fluence to Reactor Structures

Lippincott, E. P.
1776 McClure Road, Monroeville, PA 15146

Manahan, M. P., Sr.
MPM Technologies, Inc.
2161 Sandy Drive, State College, PA 16803-2283

Accurate calculation of fluence to reactor structures involves integration of exposure over time taking into account changes in operating conditions and also estimation of the uncertainty in the calculation process. This paper reports on recent improvements we have made in calculation techniques and also on validation of those techniques by benchmarking against measurements in operating boiling water reactors (BWRs).

Operating conditions are continuously changing in power reactors and this is especially true for BWR fuel cycles where significant changes in both power distribution and water density occur during a fuel cycle. To obtain suitable average conditions over a fuel cycle, we have investigated the changing operating conditions to divide the cycle into subparts with consistent parameters. By suitable averaging of the water density over the cycle, and taking the average power from the cycle burnup, we have shown in multiple cases that the cycle can be well represented by a single cycle statepoint calculation. Results for the single statepoint calculation have been compared with more detailed analyses that break the cycle into 6-10 subparts, and these comparisons indicate that using our averaging process gives results that agree within 1-2% with the detailed analysis.

We have benchmarked our BWR calculational results against dosimetry measurements from operating plants for 9 cases and achieved excellent results. The average calculated-to-measured (C/M) ratio for these cases is 1.01 with a standard deviation of 6%. This result indicates that present models and calculational methods produce accurate results, and also indicates consistency of analysis and measurement.

Most surveillance analyses and benchmarking have been performed at locations lying radially outside the core and axially in the beltline region between the top and bottom of the fuel. For some applications, most noteworthy for determination of BWR shroud and top guide welds exposures, it is necessary to calculate fluence in regions where simple symmetries are no longer valid. Although three-dimensional calculations are now practical with modern computer workstations, transport calculations of neutron fluence to reactor structures are still typically made using two-dimensional S_n calculations. The use of two-dimensional models is convenient for calculation of the effects of changing fuel loadings and changes in other conditions that may occur with changes in fuel burnup. In order to estimate the fluence in the three-dimensional geometry, the following synthesis equation may be used to evaluate the flux φ for each case:

$$\varphi(R,\theta,Z) = \varphi(R,\theta) * \varphi(R,Z) / \varphi(R) \qquad (1)$$

In this equation, $\varphi(R,\theta)$ is taken from an R,θ calculation (normalized to the power at midplane in the model region), and $\varphi(R,Z)$ is from an R,Z calculation normalized to the power in the entire core. A third calculation determines $\varphi(R)$ using a one-dimensional cylindrical model normalized at core midplane. This synthesis equation is recommended in the NRC Regulatory Guide 1.190.

In regions above and below the core, the separability of the azimuthal flux shape from the axial flux shape does not hold. Therefore, obtaining accurate fluence estimates in these regions requires a more complicated analysis. We have performed 3-dimensional calculations using the TORT code [*1*], and we have also developed an extension of the simple synthesis method in order to evaluate fluence to structures above and below the active fuel. The calculations were done for a BWR geometry similar to that described for the BWR benchmark calculation [*2*]. Comparisons were made between the TORT results and 2-D synthesis results using Equation 1 within the beltline region. An example is shown in Figure 1 which illustrates the generally good agreement between the 3-D and 2-D synthesis results in this region.

An example of the results from calculations performed outside of the beltline region is shown in Figure 2. In this figure, the fluence rate at the shroud inner radius at a point about 12.5 inches (32 cm) above the

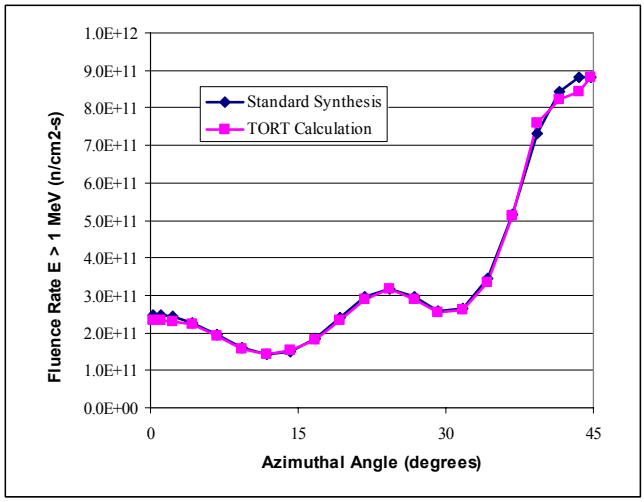

Figure 1. Fluence Rate vs. Azimuthal Angle at the Shroud Inner Radius at a Location 21 inches (53 cm) Below the Top of the Fuel

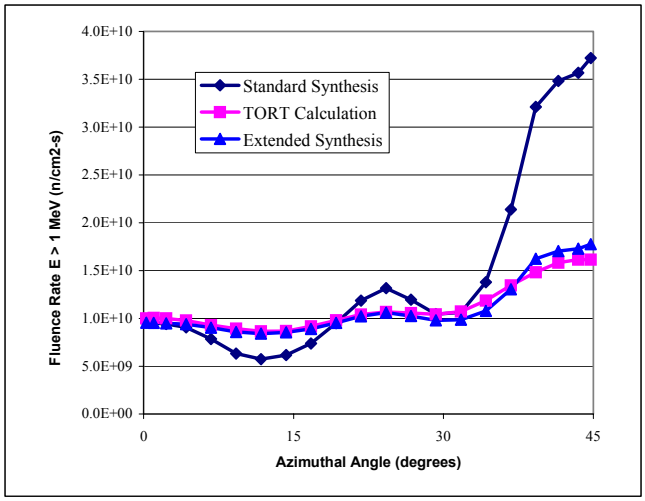

Figure 2. Fluence Rate vs. Azimuthal Angle at the Shroud Inner Radius at a Location 12.5 inches (32 cm) Above the Top of the Fuel

core is derived from the 2-dimensional calculations using both the standard and extended synthesis methods, and these are compared with the 3-dimensional result. It is seen that the standard synthesis greatly overpredicts the maximum fluence, but also underpredicts the fluence at the minimum. The agreement between the extended synthesis method and the 3-dimensional calculation is seen to be excellent. Similar results are obtained at other axial heights. Based on the results obtained it is concluded that the extended synthesis method can be applied to determine reasonable estimates of the neutron fluence to structures outside the beltline region. While we have only applied this method to BWR geometries, it may be anticipated that equally good results may be obtained in PWR applications.

REFERENCES

1. RSICC Computer Code Collection, CCC-650, "DOORS3.2a, One, Two- and Three-Dimensional Discrete Ordinates Neutron/Photon Transport Code System", available from the Radiation Safety Information Computational Center, Oak Ridge National Laboratory, Oak Ridge, TN, Updated October 2003.
2. Carew, J. F., Hu, K., Aronson, A., Prince, A., and Zamonsky, G., PWR and BWR Pressure Vessel Fluence Calculational Benchmark Problems and Solutions, NUREG/CR-6115 (BNL-NUREG-52395), Draft completed May 20, 1997.

Deterministic and Monte Carlo Neutron Transport Calculations for Greifswald-1 and Comparison with Ex-vessel Measured Data

Borodkin, G. I. and Khrennikov, N. N.
SEC NRS of GOSATOMNADZOR of Russia
Malaya Krasnoselskaya ul., 2/8, bld. 5, 107140 Moscow, Russia

Böhmer, B., Noack, K. and Konheiser, J.
Forschungszentrum Rossendorf e.V.
Postfach 510119, D-01314, Dresden, Germany

The VVER-440/230 type reactor of Greifswald-1 was shut down in 1990. The near core basic reactor equipment (pressure vessel, support constructions and internals) irradiated during 15 fuel cycles is suitable for structural material research by cutting out trepans at positions of interest [*1*]. The analysis of equipment material property degradation under irradiation is urgent in aspect of confirmation of safety of operating VVER units of similar type, and also in connection with an opportunity of operation prolongation (for example, in case of Russian units with VVER-440/230).

A necessary condition for the reliability of results of material property studies (for example, radiation embrittlement) is the validity of neutron dosimetry of tested material specimens. The improvement of the neutron and gamma dosimetry at the equipment of Greifswald-1 was one of the purposes of this work.

Another important aspect of dosimetry research on the Greifswald-1 reactor is the upgrading and validation of calculational methods used for the prediction of the end-of-life damage neutron fluence on the VVER-440 pressure vessel.

The paper deals with an analysis of a comparison of results of independent calculations by deterministic (DORT&BUGLE-96) and Monte-Carlo (TRAMO [*2*] &ENDF/B-VI) codes between themselves and with unpublished up-to-now experimental results. The calculations with the code TRAMO were carried out with two group libraries with largely differing numbers of energy groups: 47 neutron / 20 gamma groups in the first and 640 neutron / 20 gamma groups in the second case. Both libraries were derived in the same way from ENDF/B-VI allowing so to investigate the influence of the group approximation on the results.

The experimental results were available from an internal report [*3*] and data files of the predecessor institute of the Forschungszentrum Rossendorf. They were obtained in the late eighties under participation of one of the authors. The measurements and calculations were carried out for the 12^{th} fuel cycle characterized by a reduced reactor core resulting from the installation of dummy assemblies on the core periphery. During the 12^{th} cycle neutron-activation detectors were irradiated in the ex-vessel cavity at five azimuthal positions and for each azimuth at ten height levels evenly distributed over the core height. The analyzed dosimetry reactions were ^{58}Ni(n,p), ^{54}Fe(n,p), ^{46}Ti(n,p) and ^{63}Cu(n,α).
In the calculations the detailed three-dimensional distribution of neutron source, pin-to-pin power distribution in peripheral assemblies and variation of neutron-physical properties of fuel assemblies depending on burnup of fuel was taken into account. For each dosimetry position the detector activities for end of irradiation were calculated on the base of the power history. Used dosimetry cross section libraries were IRDF-90, rev.2, JENDL-D99 and RRDF-98.

The coincidence of absolute results of calculations among themselves in ex-vessel points of maximum of neutron fluence distribution is within 10 %. Measured and calculated activities of detectors agree within the range of ± 15 %. A coincidence of shapes of axial distributions of calculated and experimental activities for all detectors and azimuthal positions was observed. Found discrepancies are discussed.

REFERENCES

1. U. Rindelhardt, B. Böhmer, J. Böhmert, “RPV Integrity Assessment by Operational Feedback: Post Service Investigations of VVER-type NPPs.” *Transactions of ANS*, **88** (2003). p. 547.
2. H.-U. Barz, J. and Konheiser, FZR-245, Forschungszentrum Rossendorf, 1998.
3. H.-C. Mehner, B. Böhmer and I. Stephan, *Neutronendosimetrie an der Druckgefäßaußenwand des Blocks 1 im KKW Greifswald bei Einsatz von Abschirmkassetten*, Arbeitsbericht ZfK – RPM 6/88, Zentralinstitut für Kernforschung Rossendorf (December 1988).

Efficacy of Three-Dimensional Adjoint Biasing for a Cyclotron used for Medical Isotope Production in China

R. Pevey[1], L.F. Miller[1], B.J. Marshall[1], L.W. Townsend[1], and B. Alvord[3]
The University of Tennessee[1], Oak Ridge National Laboratory[2] and CTI[3]

Monte Carlo N particle (MCNP) and discrete ordinate calculations have been performed to determine the dose to various workers in a PET facility in China, where the radiation source is a cyclotron built by CTI to be used for the production of the isotopes necessary for Positron Emission Tomography (PET) scans. The energy dependent neutron source term is obtained by calculations with the ALICE code and compared to measurements obtained from Bonner Ball data.

The building that houses the cyclotron includes of labyrinth of walls to minimize dose to operators and to other building occupants. Walls that protect a radiochemistry laboratory and the wall between the control and scanner rooms are also modeled. The cyclotron is modeled as concentric cylinders surrounded by an annulus of copper. The outer wall of the cyclotron is an iron annulus, and the top and bottom of the cyclotron are iron disks.

A series of cylindrical phantoms composed of ICRU tissue standard are used for dose calculations. Each is used to represent a person and is 23 cm in radius and 1.8 m tall. A phantom the represents a maintenance worker is placed against the outside of the shield wall, and second phantom is placed in a chair at the control station. A third phantom is positioned just outside the building on the ground, and a fourth phantom is placed on the floor of the radiochemistry lab directly above the cyclotron.

Unbiased Monte Carlo calculations did not converge after more than one week of CPU time, whereas direction biasing alone resulted in convergence in several days. These calculations are accelerated with an automated technique that uses three-dimensional discrete ordinate calculations to obtain adjoint fluxes for use as weight windows biasing parameters for each detector modeled in the MCNP calculations. The option to use adjoint fluxes from discrete ordinate calculations is facilitated by the feature in MCNP5 that permits grids used in discrete ordinate calculations to be overlayed on the MCNP geometry definition.

The use of this computational methodology increases the computational speed of MCNP for the cited application by about a factor of one hundred. It is important to note that the capability for overlaying the grid for the discrete ordinates calculation onto the MCNP region description permits the biasing to take place on a much smaller spatial scale than when this capability was unavailable. The discrete ordinate calculations for this example are on a relatively course grid of about twenty centimeters; however, the improvement in computational time is quite noteworthy. Results from Monte Carlo calculations are also compared with two-dimensional discrete ordinate calculations.

Sensitivity Analysis and Neutron Fluence Adjustment for VVER-440 RPV

Belousov, S. I., Ilieva, Kr. D.
Institute for Nuclear Research and Nuclear Energy of Bulgarian Academy of Sciences
72 Tzarigradsko shosse, 1784 Sofia, Bulgaria

INTRODUCTION

The application of adjustment procedure is a way for more precise evaluation of reactor pressure vessel (RPV) neutron fluence. The least squares method [*1*] adjustment in reactor dosimetry is performed on the base of the discrepancies between measured and calculated neutron flux response values. The responses for the RPV fluence evaluation usually are the induced activity of ex-vessel (behind the vessel) detectors (iron, copper, and niobium). The sensitivity of responses to the main parameters (sources of uncertainty) of calculation needed for adjustment has been calculated for VVER-440 reactor with dummy cassettes core loading.

The adjustment has been performed using the relations presented in Ref. [*2*] and applied for the neutron fluence (with energy above 0.5 MeV) at the RPV inner wall of Kozloduy NPP Unit 1.

PARAMETERS AND MODEL DEFINITION

The parameters usually used for VVER and PWR neutron flux adjustment have been taken into consideration. The cross-section uncertainties data library LUND [*3*] created by Dr. G. Manturov has been applied. In our analysis have been taken into account the uncertainties of: inelastic, elastic and absorption cross section of iron and chromium, elastic cross section of hydrogen and oxygen; neutron source spectrum; neutron source spatial distribution; density of steel construction including baffle, basket, barrel, and RPV; moderator density, i.e. water density in the gap between the baffle and the basket, the basket and the barrel, and in the downcomer; the RPV inner radius. In addition to these sources of uncertainties the activation cross-section uncertainties have been included into consideration for calculation of the ex-vessel detectors' responses uncertainties.

The mentioned sources of uncertainties have been included into simplified one-dimensional calculation model of the VVER-440 reactor with dummy cassettes core loading.

SENSITIVITY CALCULATION

The relative sensitivities of the RPV neutron fluence and the ex-vessel detector responses to the neutron cross-sections have been calculated by the MCNP4C [*4*] code. The sensitivities to all other mentioned sources of uncertainties except the neutron cross-sections have been calculated by the DORT [*5*] code with multigroup cross section library BGL440 [*6*].

ADJUSTMENT TRANSFORMATIONS

The MATLAB [*7*] system has been used for creation of software procedure package for interface operations and adjustment calculation. The adjustment has been performed using the data of the discrepancy between calculated and experimental data for ex-vessel detectors' activity responses that has been obtained for cycle 20 of Unit 1, Kozloduy NPP. Before the adjustment the consistency of the data applied has been tested by the weighted sum of squared residuals. This testing shows a good consistency, especially when activation cross-section uncertainty is taken into account, of the adjusted data according to the χ^2 distribution with 3 degrees of freedom.

RESULTS AND ANALYSIS

The contribution of different sources of uncertainty to the calculated RPV neutron fluence (with energy above 0.5 MeV) and ex-vessel detector's responses before the adjustment is presented in Table 1.

Table 1. Contribution of the sources of uncertainty to the RPV neutron fluence with energy above 0.5 MeV and ex-vessel detector responses before adjustment

Source of uncertainty	Fluence, %	Cu detector, %	Fe detector, %	Nb detector, %
Iron XS inelastic	6.1	28.	24.	10.
Iron XS elastic	3.5	4.3	6.6	7.9
Iron XS absorption	0.80	5.3	2.7	1.3
Chromium XS inelastic	4.1	5.4	5.3	4.5
Chromium XS elastic	1.5	0.66	1.1	1.5
Chromium XS absorption	0.09	0.35	0.20	0.11
Hydrogen XS elastic	2.3	1.3	1.7	2.2
Oxygen XS elastic	2.5	1.6	2.2	2.5
Source Spectrum	4.3	11.	7.1	4.9
Source Spatial Distribution	3.9	3.3	3.6	3.9
Steel Density	1.1	2.4	2.5	2.0
Moderator Density	4.3	2.8	3.3	4.0
RPV inner radius	8.3	4.0	3.4	0.35
Activation XS	-	5.	5.	5.
Total	14.	32.	28.	17.

The values estimated by adjustment of the related responses $\delta\hat{r}$ for the ex-vessel detectors and the values $\delta\hat{F}$ for the RPV neutron fluence are presented in Table 2 together with their standard deviations.

Table 2. Estimated values and standard deviations of the RPV neutron fluence with energy above 0.5 MeV and ex-vessel detector responses after adjustment

Fluence		Cu detector		Fe detector		Nb detector	
$\delta\hat{F}$, %	STD, %	$\delta\hat{r}$, %	STD, %	$\delta\hat{r}$, %	STD, %	$\delta\hat{r}$, %	STD, %
-13.	10.	-14.	4.2	-10.	4.2	-28.	6.3

The results show that after the adjustment we obtain estimated detector response uncertainty values which are lower than the experimental ones. The adjustment by the applied set of ex-vessel detector data decreases the RPV neutron fluence level with about 13% and permits to reduce about one and a half times the RPV fluence uncertainty.

CONCLUSIONS

As a result of adjustment application the uncertainty of neutron fluence has been reduced rather significantly. This adjustment approach application could be useful for fluence evaluation of Kozloduy Unit 3 and 4 for RPV lifetime précising.

REFERENCES

1. W. Hamilton, Statistics in Physical Science, The Roland Press Company, New York, 1964.
2. S. Belousov, Kr. Ilieva, D. Kirilova, “Sensitivity Analyis and Neutron Fluence Adjustment for VVER-1000 RPV.” *Proc. of 11th Int. Symp. On Reactor Dosimetry*, Brussels, Belgium, (2002), pp. 436-443
3. G. Manturov, “Influence of Neutron Data Uncertainties on the Accuracy of Prediction of Advanced Reactor Characteristics”, *Proc. Int. Conf. Nucl. Data for Sci. and Technology*, Gatlinburg, Tenn, (1994) **II**, pp. 993-999
4. I. F. Briesmeister, Ed., “MCNP -A General Monte Carlo N-Particle Transport Code, Version4C,” LA-13709-M (April 2000)., RSICC ORNL, Code Package, CCC0700, 2000
5. DOORS3.2, RSICC ORNL, Code Package CCC-650, 1998
7. MATLAB is a copyright software product of The MathWorks, Inc. 24 Prime Park Way, Natick, MA 01760-1500, USA.
14. J. Bucholz, S. Antonov, S. Belousov S., “BGL440 and BGL1000 Broad Group Neutron/Photon Cross Section Libraries Derived from ENDF/B-VI Nuclear Data”, *IAEA, INDC(BUL)*-15, April 1996.

Generalized Linear Least Squares Adjustment, Revisited

Broadhead, B. L., Williams, M. L.
Oak Ridge National Laboratory, P.O. Box 2008,
Oak Ridge, TN 37830-6170 USA

Wagschal, J. J.
Racah Institute of Physics, Hebrew University of Jerusalem,
Edmond Safra Campus, Givat Ram, 91904, Jerusalem, Israel

INTRODUCTION

Over twenty years have passed since the LEPRICON methodology[1] was first proposed for the adjustment of pressure vessel fluence estimates by consolidating neutron transport calculations and surveillance dosimetry measurements. The generalized linear least-squares (GLLS) method has since been recognized as a comprehensive and technically correct approach to the analysis of reactor dosimetry data. The crux of the LEPRICON methodology is the simultaneous adjustment of: a) dosimetry measurements in benchmark fields, b) surveillance dosimetry measurements in the reactor field under test, c) dosimetry cross sections , and d) the transport-calculation parameters. This procedure results in the adjustment not only of the fluence *at the surveillance position* but also of the calculated fluence at any point *within the vessel steel*, in particular at the point of estimated maximum damage to the pressure vessel. The GLLS procedure also provides a rigorous estimate for the response uncertainties. This is of particular importance since the latest NRC regulatory guide[2] emphasizes the need for uncertainty analysis in vessel fluence computations, although there is no well defined rigorous approach specified for the analysis.

In order to perform the adjustment each measured quantity must be accompanied by the corresponding calculated value, the experimental uncertainty and possible correlations with other measured quantities. Uncertainty matrices of the dosimetry cross-sections as well as of the transport-calculation parameters are also needed. Such a procedure also necessitates the calculation of sensitivity profiles of the calculated fluences to the transport parameters at the surveillance position and at any other location of interest in the field under test. The inclusion of benchmarks in the adjustment requires the evaluation of the uncertainty matrix associated with the fluences in the benchmark experiments in addition to the evaluation of the uncertainty matrix associated with the field under test, and the cross-uncertainty matrices linking them all. Unfortunately, applications[3] of the methodology have been few and the original code package has not been maintained.

NEW GLLS CODE

Recently a similar methodology has been applied to criticality safety analysis and a GLLS code has been developed within the SCALE code system frame[4] to determine biases and uncertainties in neutron multiplication factors by consolidating differential data and benchmark integral experiments. The adjustment code uses the GLLS method to consolidate a prior set of integral responses measured in critical benchmark experiments and a corresponding set of calculated values obtained using the SCALE code system. The code improves the initial estimates for calculated and measured responses by varying the nuclear data used in the transport calculations as well as the values of the measurements, taking into account their correlated uncertainties, so that the most self-consistent set of data is obtained. This approach forces the refined estimates of the calculated and measured responses to agree, while at the same time constraining the data variations to minimize a generalized chi-squared parameter representing the sum of the squared differences in the data variations measured in units of their uncertainties. This insures maximum overall consistency in the set of calculated and measured responses for a specified set of data and experimental uncertainties, thus the posteria results represent the “best estimates” for the true response values. Consolidation of the original integral experiment data and calculated results reduces the prior uncertainty in the response estimates, since additional information has been incorporated compared to either the measured or calculated results alone. Computed responses may also be input for one or more “applications” for which no experimental measurements are available. The code computes an updated estimate for the application responses, as well as their reduced uncertainty. This new code, has many interesting input features allowing, inter alia, the use of reasonable internally generated covariance matrices for parameters with no entries in the covariance libraries. The features of the code and the experience gained using it for criticality safety applications will be discussed in the full paper.

CONCLUSION

Because the code development and its use are sponsored by the criticality safety community , it has a fair chance to be widely distributed and could be easily extended to pressure vessel dosimetry applications.

REFERENCES

1. J.J. Wagschal, R.E. Maerker and Y. Yeivin, "Extrapolation of Surveillance Dosimetry Information to Predict Pressure Vessel Fluences", *Trans. Am. Nucl. Soc.,* **34**, pp. 631-632,. (1980). See also R.E. Maerker, B.L. Broadhead and J.J. Wagschal, *Nucl. Sci. and Eng*., **91**, 369. (1985).
2. *Calculational and Dosimetry Methods for determining Pressure Vessel Neutron Fluence*, Regulatory Guide 1.190, U.S. Nuclear Regulatory Commission (March 2001).
3. R.E. Maerker, B.L. Broadhead, B.A. Worley, M.L. Williams and J.J. Wagschal, *Nucl. Sci. and Eng*., **93**, 137. (1986).
4. *SCALE*: *A Modular Code System for Performing Standardized Computer Analysis for Licensing and Evaluations*, Rev. 7, ORNL/NUREG/CSD-2/R7), Vols. I, II, II, CCC-545, Radiation Safety Information Computational Center, U.S. Nuclear Regulatory Commission (May 2004).

Retrospective Measurement of Neutron Activation within the Pressure Circuit Steelwork of a Magnox Reactor and Comparison with Prediction

Thornton, D. A., Thiruarooran, C, Allen, D.A., Harris, A. M.,
British Nuclear Group, Berkeley Centre, Berkeley,
Gloucestershire, GL13 9PB, United Kingdom.

Holmes, C. G., Harvey C. R.,
BNFL, Nuclear Sciences and Technical Services, Springfields, Salwick,
Preston, Lancashire, PR4 0XJ, United Kingdom.

INTRODUCTION

This paper describes a comparison of measured and predicted neutron activation rates within steel components of the pressure circuit of the reactors at the Wylfa nuclear power plant, using retrospective measurements performed on an irradiated thermocouple cable.

As part of a recent Periodic Safety Review (PSR) of Wylfa, the structural integrity of pressure vessel standpipe penetrations was re-assessed to demonstrate adequate temperature margins to embrittlement. Neutron dose recommendations expressed in displacements per atom (dpa) have formed an important input to this assessment. Consistent with the methodology for recommending doses for the UK Magnox reactors with steel pressure vessels [1, 2, 3], it was decided that the doses recommended for the structural integrity assessment of the Wylfa standpipes would be supported by neutron activation measurements.

PLANT DESCRIPTION

Wylfa is the latest and largest of the UK's fleet of Magnox power stations. Commissioned in 1971, its two reactors each operate with a thermal power of 1600 MW. The reactor coolant is carbon dioxide (CO_2) at a pressure of 27 bar, contained within a pre-stressed concrete pressure vessel (PCPV). Steel standpipe penetrations provide access to the reactor core, which enable the on-load re-fuelling of each reactor's 6156 channels. There are 397 standpipes per reactor.

The standpipes comprise vertical penetrations into the top of the pressure vessel and consist of steel annuli joined by axial and circumferential welds. The gap between the annuli contains PCPV cooling water to protect the surrounding concrete from the hot gas within the penetration. The combination of cool temperature and relatively high neutron dose rate makes welds in this region potentially susceptible to embrittlement.

Approximately one quarter of the standpipes contain instrumented fuel elements with thermocouples attached to the magnox fuel can. The thermocouple cables run from the fuel element, upwards through the associated standpipe assembly and out to the pile-cap. The cables were identified as the most readily accessible source of material for performing a measurement of neutron activation within the standpipes at Wylfa.

DESCRIPTION OF THERMOCOUPLE SAMPLES

Because of their additional complexity, channels containing instrumented fuel elements are re-fuelled off-load, during reactor outages. Normally, the attached cables are routinely disposed of during re-fuelling. However, a predetermined length of one of these cables was recently retained for performing activation measurements. The thermocouple cables consist of an entwined 'rope' of 4 thermocouple wires. Each of these wires comprises two alloy electrodes embedded in a magnesium oxide (MgO) insulator and surrounded by a stainless steel sheath. In the reactor, the thermocouple cables follow a complicated route between the pile-cap and the host element. This involves passing over a set of two movable pulleys, which ensure that the cable remains taut.

MEASUREMENT TECHNIQUE

The essential requirements of the measurement were accurate, absolute activation measurements in addition to the accurate positioning of the measurements within the reactor geometry. The approach taken was to determine

axial activation profiles of relative activation rates along the length of the cable and to normalize these against accurate 'spot' measurements. In this way axial profiles of absolute activation rates from the following neutron reactions were obtained:

Fast neutrons:	$^{54}Fe(n,p)^{54}Mn$	Thermal / epi-thermal neutrons:	$^{59}Co(n,\gamma)^{60}Co$
	$^{58}Ni(n,p)^{58}Co$		$^{58}Fe(n,\gamma)^{59}Fe$
			$^{50}Cr(n,\gamma)^{51}Cr$

The axial distribution of thermal neutron activation showed a clear thermalization peak corresponding to the coolant water in the standpipe. This was used to identify the position on the wire where it passed through the bottom of the standpipe and the absolute 'spot' measurements were performed on samples taken from around this location.

The 'spot' measurements required chemical separation of the sheath from the remainder of the cable, and the radioactive counting of the sheath samples followed by elemental analysis by Inductively Coupled Plasma Optical Emission Spectrometry (ICP-OES).

CALCULATIONS

Monte Carlo calculations were used to model the transport of neutrons from the top of the core, into the standpipe penetration and beyond. Using the MCBEND radiation transport code, a detailed model was created of a single standpipe and the reactor components beneath it; from the pile-cap down through the pressure vessel and above-core steelwork to the upper fuel elements in the core. Reflecting boundary conditions applied to this 'supercell' meant that a radially infinite reactor had, in effect, been modeled.

The calculations were performed without using variance reduction techniques other than to reduce the calculation to two stages. Activation rates corresponding to the measured reactions were produced in a fine axial / radial mesh.

The 'supercell' approximation was justified by the reactors' highly repetitive structures and very large size. However, the imposition of reflecting boundaries precludes any loss of neutrons from the sides of the model and it was acknowledged that the approximation would result in some over-prediction. For the purpose of dose prediction, this was recognized to be a conservative assumption.

RESULTS

Predicted and measured activation rates were interpreted in terms of equivalent fission and equivalent Westcott fluxes, and fluxes from each of the 5 reactions were compared. Both predicted and measured thermal neutron fluxes show a distinct thermalization peak corresponding to the cooling water contained within the standpipe. This was used to confirm the irradiation positions of the samples within the standpipe geometry.

All reactions were found to be over-predicted by the MCBEND model, confirming that dose predictions are conservative. Uniform levels of over-prediction for fast, epi-thermal and thermal fluxes suggests that the model predicts without significant spectral bias, giving confidence in the dpa dose data recommended from its predictions.

ACKOWLEDGMENTS

This paper is published with the permission of British Nuclear Group.

REFERENCES

1. J.R. Mossop, D.A. Thornton, T.A. Lewis , "Validation of Neutron Transport Calculations on Magnox Power Plant" *Proceedings of the 8th International Symposium on Reactor Dosimetry*, ASTM Special Publication 1228 (1994), pp. 384-391.
2. T.A. Lewis, S.E. Hopper, J.R. Mossop, D.A. Thornton, "The Prediction of Fast and thermal Neutron Dose Rates for the Pressure Vessels of Magnox Power Plant" *Proceedings of the 9th International Symposium on Reactor Dosimetry*, World Scientific (1996), pp. 600-607.
3. T.A. Lewis , D.A. Thornton, "A Decade of Dosimetry for Magnox Reactor Plants", Proceedings of the 9th International Symposium on Reactor Dosimetry, World Scientific (2003), pp. 269-277.

Comparison of Predicted and Measured Helium Production in US BWR Reactors

L. R. Greenwood and B. M. Oliver
Pacific Northwest National Laboratory, Richland, WA USA

Retrospective dosimetry, helium, and boron measurements are being performed for samples obtained from various locations in US BWR reactors. Samples are obtained by drilling small divots in components during reactor outages or by sectioning of components that have been removed from reactors. The stainless steel or inconel samples have been analyzed in order to determine the neutron fluence, helium content, and boron content. Activation products including ^{54}Mn, ^{55}Fe, ^{58}Co, ^{60}Co, ^{63}Ni, and ^{93m}Nb are determined by gamma spectrometry or chemical separations and beta or x-ray counting. The helium content is determined by isotope dilution gas mass spectrometry and the boron is determined by additional neutron irradiation to burn out some of the remaining ^{10}B followed by a second helium measurement. Original boron content in the material can then be determined by correcting for burnup which has occurred over the BWR lifetime. The composition of the starting material is determined by energy dispersive x-ray analysis.

The activation measurements are used to determine the thermal, epithermal, and fast neutron fluences at each reactor location taking into account the reactor irradiation history, corrected for local variations as appropriate. The spectral-averaged cross sections for the fast neutron fluence determinations are calculated from available neutron spectral calculations. If several different thermal reactions can be measured, then the thermal and epithermal fluences can be determined. Agreement between reaction products with different half-lives also provides a test of the power history corrections. Multiple threshold reaction measurements offer some information regarding the consistency and accuracy of the fast neutron spectral estimates.

The calculated thermal, epithermal, and fast neutron fluences can be used to predict the helium production in the reactor components for direct comparison with the direct helium and boron measurements. Helium is produced by burnup of the ^{10}B as well as threshold (n,alpha) reactions in the steel components. Helium production from ^{10}B is typically comparable to the fast neutron helium production. At higher neutron fluences, additional helium may also be produced from the ^{59}Ni(n,alpha) reaction, as ^{59}Ni is produced by the ^{58}Ni(n,gamma)^{59}Ni reaction. All of the required cross sections and fluences are readily determined by the retrospective dosimetry measurements and the original ^{10}B content is determined independently by the helium measurements.

Generally, good agreement has been obtained between the predicted and measured helium values at locations near the pressure vessel for a number of different BWR reactors. However, some differences have been seen at other reactor locations. Some of these differences can likely be attributed to sampling variability and sample heterogeneity. However, additional measurements and calculations are being performed in an attempt to understand any remaining differences between the predictions and measurements.

Shielding Calculations for the Upgrade of the HFIR Beam Line HB-2

C. O. Slater
D. L. Selby
J. A. Bucholz
J. L. Robertson
M. L. Crow

Oak Ridge National Laboratory
Oak Ridge, Tennessee

INTRODUCTION

The High Flux Isotope Reactor (HFIR) at the Oak Ridge National Laboratory (ORNL) began operation in 1966. It has one of the highest neutron flux levels in the world, and this flux has been used to produce various radioisotopes for medical and industrial applications. Its normal operating power is 85 MW and its design power is 100 MW. In recent years, the HFIR has undergone upgrades to its experimental facilities, including the enlargement of beam tubes to provide more neutrons at the experimental stations. For the radial beam tube, HB-2, the upgraded monochromator drum was placed about 4.5 m from the location of the previous drum (which was located at the HFIR biological shield). This placement allowed the inclusion of three additional experimental facilities on this beam line [a powder diffractometer, a residual stress diffractometer, and a wide-angle neutron diffractometer (WAND)]. In addition, a triple-axis spectrometer is tied to the monochromator drum. Bulk top, bottom, side, and end shields were placed around the beam to protect the instruments and the experimenters from background radiation. Shielding calculations were performed to determine dose rates outside of the bulk shielding as well as at heterogeneous regions of the shielding, such as beam shutters which penetrate the shields, shielding for scattering crystal hangers, and gaps at the junctions of shield sections. The calculations were designed to determine the adequacy of proposed shielding designs and indicate the direction of changes to the shield design (i.e. whether more or less shielding is required). This paper describes the shielding calculations for HB-2 and the comparison of calculated and measured results.

SOURCE FOR THE CALCULATIONS

Neutrons and photons leaking from the core into the beryllium reflector provide the source for the beam tube calculations. J. A. Bucholz of ORNL performed MCNP[1] calculations on a 3-D model of the HFIR and its beam tubes and determined equivalent point sources that could be used to perform shielding calculations for each of the beam tubes.[2] Using these point sources, one would calculate essentially the same spectrum at reference locations along the axes of the beam tubes as one would calculate using MCNP. The normalized HB-2 point source spectrum was the basis for the subject shielding calculations.

CALCULATIONS

The beam tube, portions of the HFIR vessel and biological shielding, the monochromator drum, and the beam line bulk shielding were modeled with the combinatorial geometry package of the MORSE Monte Carlo computer code.[3] Initial calculations consisted of a MORSE calculation coupled with DORT[4] calculations (either R-Z or X-Y) at the inner walls of the bulk shields. However, final calculations were performed entirely with the DORT code, since a full energy spectrum could be calculated using this procedure. A first-collision source calculated within the 3-D geometry and averaged over the DORT 2-D R-Z geometry provided the source for the DORT calculation. A second first-collision source and DORT calculation were performed for the monochromator drum. In addition, DORT calculations were performed for the shield gaps and the shielding for the scattering crystal hangers, and TORT[5] calculations were performed for the beam line shutters. These calculations used directional fluxes from the first DORT calculation as boundary sources.

RESULTS

The DORT calculation for the side shield yielded a maximum dose rate of 4.0 mrem/h on the outside surface of the bulk shield, and localized calculations for the penetrations yielded various dose rates. Measurements were made at several locations around the beam line shields, and calculated results are compared with some of those measured results in Table 1. Except for the location near the interface of the reactor biological shield and the beam line shield, the calculated and measured results are in good or acceptable agreement. For the location with the large disagreement, the high measured dose rate indicates a possible streaming path. There is no such path in the calculational model. The agreement for the open shutter is surprisingly good, since the calculated result was obtained using a source that consists of the thermal-neutron source from the guide and the background from the tunnel. A significant portion of the background source comes from neutrons and photons scattering through a nearly 90-degree angle in the glass of the beam guide, and the 90-degree scattering angle is one of low probability.

CONCLUSIONS

Calculations were performed in support of the design of shielding for the upgrade to the HFIR HB-2 beam line. Calculated results were compared with measured results and were in generally good agreement. The adequacy of the shield design was confirmed, and the design is not overly conservative.

Table 1 Comparison of calculated and measured dose rates for the HFIR HB-2 beam line

Measurement Location	Total Dose Rate (mrem/h)[a]		Ratio: Meas./Calc.
	Calculated	Measured	
Back of HB-2D Monochromator Drum	32	33	1.0
Basic Shield Tunnel	3	3.5	1.2
Interface with Biological Shield Wall	10	60.0	6.0
Shield Tunnel Roof	1	0.6	0.6
HB-2B Shutter Hole with Shutter Closed	10	9.0	0.9
HB-2B Shutter Hole with Shutter Open	32,000	36,000	1.1
HB-2C Shutter Interface with Shield Wall	30	12	0.4
HB-2C Shutter Hole with Shutter Closed	2.0	2.0	1.0
Roof Plug over Monochromator Crystal	6.5	4.5	0.7

[a]The total dose rate is the sum of the neutron and photon dose rates

REFERENCES

1. J. F. Briemeister, Editor, *MCNP – A General Monte Carlo N-Particle Transport Code, Version 4B*, Los Alamos National Laboratory Report LA-12625-M, March 1997.

2. J. A. Bucholz, “Source terms for HFIR beam tube shielding analyses, and a complete shielding analysis of the HB-3 tube,” Oak Ridge National Laboratory Report ORNL/TM-13720, July 2000.

3. E. A. Straker, W. H. Scott, and N. R. Byrn, “The MORSE-Code with Combinatorial Geometry,” DNA-2860-T, May 1972.

4. W. A. Rhoades and R. L. Childs, “The DORT Two-Dimensional Discrete Ordinates Transport Code," *Nucl. Sci. & Eng.*, **99** (1) 88-89, May 1988.

5. W. A. Rhoades and R. L. Childs, "The TORT Three-Dimensional Discrete Ordinates Neutron/Photon Transport Code," Oak Ridge National Laboratory Report ORNL-6268, November 1987.

NEUTRON RESPONSE FUNCTION FOR BC-523A SCINTILLATION DETECTOR IN ENERGY RANGE 0.5 to 20 MeV

F. Cvachovec, Military Academy Brno, J. Cvachovec, Masaryk University Brno,
S. Posta, Research Center Řež, B. Osmera*, Nuclear Research Institute Rez, Czech Republic
* corresponding author (e-mail osm@ujv.cz)

The results of calculation of the response function for BC-523A detector are presented. The response function was calculated using a (new) Monte Carlo code NEUBD - 7. It is a modification of the NEU-7 program [1] which was designed for stilben and NE-213 scintilators. To calculate BC-523A response funetion the interactions of neutrons with ^{11}B, ^{11}B and Oxygen have been added.

The scintillation detectors of a full neutron energy absorption, i.e. boron doped BC-523A can be used for fast neutron spectrometry because of their capability to suppress undesirable background applying coincidence techniques. The detector response function is a necessary input to unfolding procedure.
The NEUBD-7 code has been created with following assumptions:

- The parallel neutron beam incidents on the cylindrical detector. The neutron flight path direction regarding to the scintillator axis can be arbitrarily chosen as well as the diameter and the length of the detector. The response function corresponding to a multidirectional neutron field can be determined
- Considered interaction: neutron capture on boron 10, boron 11, elastic neutron scattering with hydrogen, carbon, oxygen, boron 10, boron 11, inelastic scattering with carbon, oxygen, boron 10, boron 11, reactions (n, α), (n, 3α, n') with carbon in energy range (0.5 - 20) MeV
- The protons escape from detector is included
- The neutron cross section data were compiled from ENDL, ENDF/B-IV,V and PTB Braunschweig publications
- (The proton light output, response function and detector energy resolution were verified for monoenergetic neutrons 2.8 MeV, 14.8 MeV). An ideal response function is smoothed by the Gaussian function using the full width at half maximum value determined from experiment
- A maximum number and type of interactions for each neutron can be set up

The output file contains:

- Numerical data for the ideal and smoothed response functions in proton and photon energy scale
- Detection efficiency depending on energy
- The contributions of the considered phenomenon
- Graphical and numerical representation of all response functions

The unknown neutron flux density spectrum from Fredholm equation is calculated (unfolded) by iteration algorithm with Maximum Likelihood criterion. The unfolding procedure is programmed in the MATHEMATICA® system. A high rejection of gamma background makes the boron loaded scintillator interested to low level neutron flux density measurement in mixed field e.g. in the vicinity of nuclear reactor.

Reference

[1] F. Cvachovec, J. Cvachovec, P. Tajovský: Anisotropy of light output in response of stilbene detector, Nuclear Instruments and Methods in Physics Research A 476 (2002)200-202

Development of a Silicon Calorimeter for Dosimetry Applications in a Water-Moderated Reactor

Luker, S. M[1], Griffin, P. J., King, D. B., DePriest, K. R., Naranjo, G.E.,
Sandia National Laboratories, MS 1146
Albuquerque, NM 87185-1146, USA.

Keltner, N.
Ktech Corporation
Albuquerque, NM 87123, USA

Suo-Anttila, A.J.
Alion Science and Technology
Albuquerque, NM 87110,USA

OBJECTIVE

High fidelity active dosimetry in the mixed neutron/gamma field of a research reactor is a very complex issue. For **passive** dosimetry applications, the use of activation foils addresses the neutron environment [1] while the use of low neutron response CaF_2:Mn thermoluminescent dosimeters (TLDs) addresses the gamma environment [2]. Approaches to high fidelity **active** neutron or gamma dosimetry are still being developed. A radiation-hardened diamond photoconducting detector (PCD) has been developed that provides a very precise fast response (picosecond) dosimeter [3] that can provide a time-dependent profile for the radiation environment. However, the quantification of the relative neutron/gamma response of the PCD depends on the resolution of several technical issues. In order to address the research reactor experimenter's need for a dosimetry that reports silicon dose and dose rate at a test location during a pulsed reactor operation, a silicon calorimeter has been developed. This dosimeter can be used by itself or in conjunction with the diamond PCD. This paper reports on the development, testing, and validation of this silicon calorimeter for applications in water-moderated research reactors.

APPROACH

In this calorimeter design, a Type E 1-mil diameter thermocouple is sandwiched between two silicon disks. The thermocouple is used to measure the temperature rise in the silicon disks. Figure 1a shows the components of the calorimeter. Figure 1b shows a partially assembled calorimeter. The measurement is a change in silicon temperature that can be converted into a rad(Si) metric using the specific heat for silicon. The temperature-dependent specific heat of the (undoped) ultrasil silicon used in the calorimeter has been measured with an accuracy of ~1%. The exact mass of the silicon disks is not important since this term cancels out. The silicon disks are supported on three thin thermally isolating alumina (Al_2O_3) pegs so that the heat is not lost due to conduction. Thermal radiation loss is still a consideration and is addressed in the uncertainty quantification of the dosimeter response. The thermal inertia of the thermocouple is designed to be small so that it does not significantly affect/delay the temperature measurement. A 1-mil thermocouple is used in order to minimize the delay due to heat transfer to the thermocouple. The gamma heating of the thermocouple material itself is a potential interference, but, since the thermocouple has a very small mass, this term is not a serious interferent. The calorimeter is a primary dosimeter and does not require a calibration. The response uncertainty is dominated by the knowledge of the material specific heat and the thermal diffusion issues. The interpretation of the calorimeter response and the validation of the uncertainty analysis has been accomplished by fielding the calorimeter is the Hermes-III bremsstrahlung x-ray field with a full width at half maximum (FWHM) pulse width of ~20 ns. When the calorimeter is used to determine the gamma dose, corrections need to be applied to account for heating due to neutrons in the mixed reactor environment. The neutron correction is ~10% for a pulse in the free-field central cavity of the water-moderated Annular Core Research Reactor (ACRR) at Sandia National Laboratories (SNL). The temperature rise in the silicon of the calorimeter when fielded in this environment is about 0.111 K/MJ from gammas and 0.0126 K/MJ from the neutrons.

This silicon calorimeter is designed to report the gamma-ionizing dose at a time immediately after a reactor pulse. Figure 2a shows an example of the time-dependent silicon calorimeter response and the ACRR power profile (determined by a Cd-

[1] This work was supported by the United States Department of Energy under contract DE-AC04-94AL85000. Sandia is a multiprogram laboratory operated by Sandia Corporation, a Lockheed Martin Company, for the United States Department of Energy.

based self-powered neutron detector located next to the fuel rods) for a 32-MJ reactor pulse with a FWHM of ~65 ms. The dosimeter response can be differentiated to produce a time-dependent silicon dose rate, as shown in Figure 2b, but the signal noise makes the direct use of this dose rate of marginal value. The main application for this silicon calorimeter is as a very accurate silicon integral dose measurement just after the reactor pulse that can be used to normalize the time-dependent transient profile from the PCD or other reactor power metric. The calorimeter is useful for ACRR pulses out to the pulse peak plus 3 FWHM.

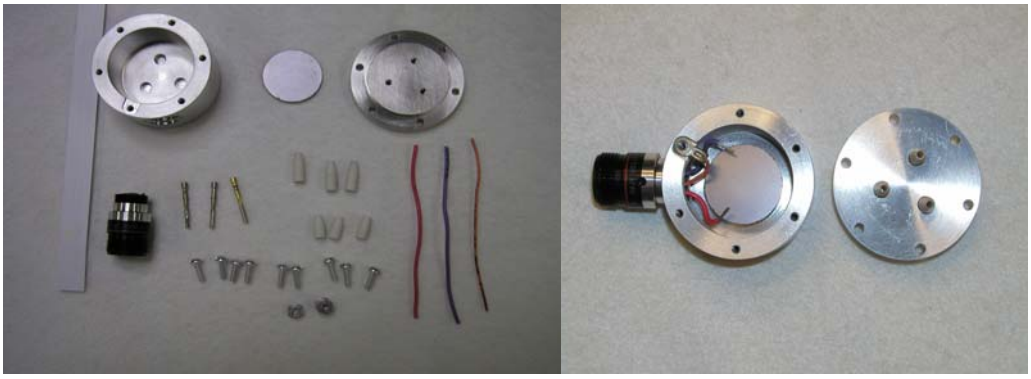

Figure 1. Silicon Calorimeter: (a) Components, (b) Partially Assembled Calorimeter

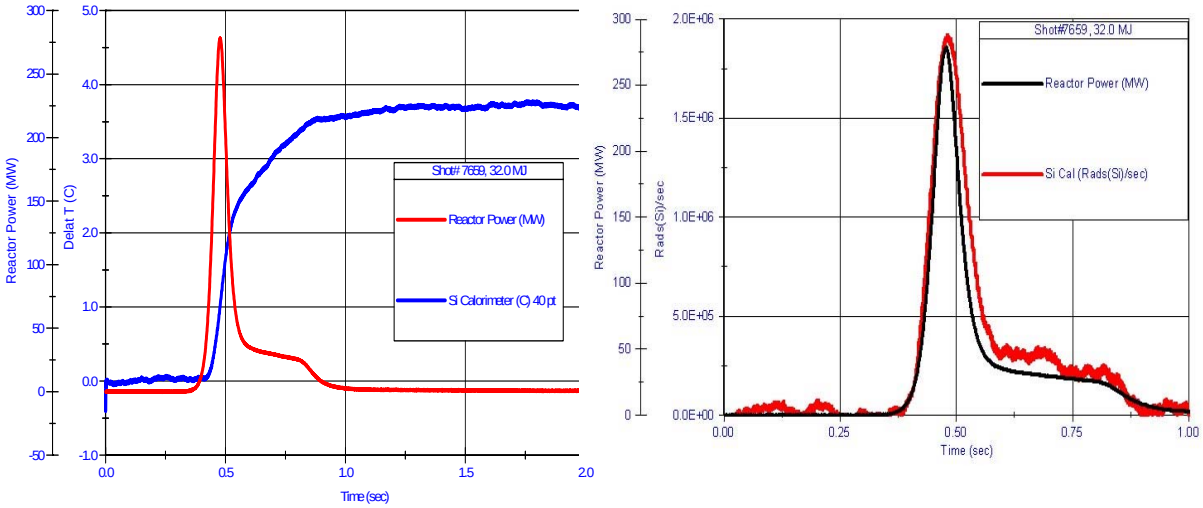

Figure 2. Comparison of Reactor Power and (a) Response of the Calorimeter (b) Derivative of Calorimeter Response

REFERENCES

1. P. J. Griffin, J. G. Kelly, "A Rigorous treatment of Self-Shielding and Covers in Neutron Spectra Determinations," *IEEE Trans. On Nuclear Science*, **42** (1995). pp. 1878-1885.
2. K. R. DePriest, P. J. Griffin, "Neutron Contribution to CaF2:Mn Thermoluminescent Dosimeter Response in Mixed (n/γ) Field Environments," *IEEE Trans. On Nuclear Science*, **50** (2003). pp. 2393-2398.
3. P. J. Griffin, et al., "Diamond PCD for Reactor Active Dosimetry Applications," presented at NSREC conference and submitted for publication in *IEEE Trans. On Nuclear Science*, **42** (2004).

Measurement and Calculation of WWER-440 Pressure Vessel Templates Activity for Support of Vessel Dosimetry

Vikhrov V.I., Erak D.Yu., Kochkin V.N., Brodkin E.B., Egorov A.L., Zaritsky S.M.
RRC "Kurchatov Institute"
Kurchatov sq. 1, 123182 Moscow, Russia

Activity of templates (specimens), which were cut out from inner surface of Kola-1 and Kola-2 WWER-440 reactor pressure vessels (RPV), was measured in order to support the RPV dosimetry.

12 weld and 2 base metal templates of Kola-1 RPV were cut out after 25 fuel cycles. The standard core loading was in the first 10 fuel cycles; burned fuel assemblies were located in the core periphery in the 11^{th} cycle and in 19-25 cycles; besides 36 steel shielding assemblies were located in the core periphery instead of fuel assemblies after 11 fuel cycles. Kola-1 RPV was annealed after 15 fuel cycles.

13 weld and 2 base metal templates of Kola-2 RPV were cut out after 24 fuel cycles. The standard core loading was in the first 8 fuel cycles; burned fuel assemblies were located in the core periphery in the 9-10 and in 16-24 cycles; besides 36 steel shielding assemblies were located in the core periphery instead of fuel assemblies after 10 fuel cycles. Kola-2 RPV was annealed after 14 fuel cycles.

The dimensions of each template were equal to 55x100 mm. Micro-Charpy samples were made from template material for mechanical testing.

Probes were taken from four corners of each template for dosimetry measurements. Activity of ^{54}Mn in each probe was measured and average activity of template material was evaluated. Nb was separated from several probes and ^{93m}Nb activity was measured also.

Calculations were carried out in P_3S_8 approximation of discrete ordinates method using DOORS 3.2 code package and BUGLE-96 nuclear data library. Calculated activities were compared with experimental ones (e.g. see Fig.1). Neutron flux density and fluence (for neutrons with E>0.5 MeV) were calculated and calculation uncertainty was evaluated basing on comparison of calculated and measured RPV templates activities and on some results of WWER-440 Mock-up experiments carried out earlier on the reactor LR-0.

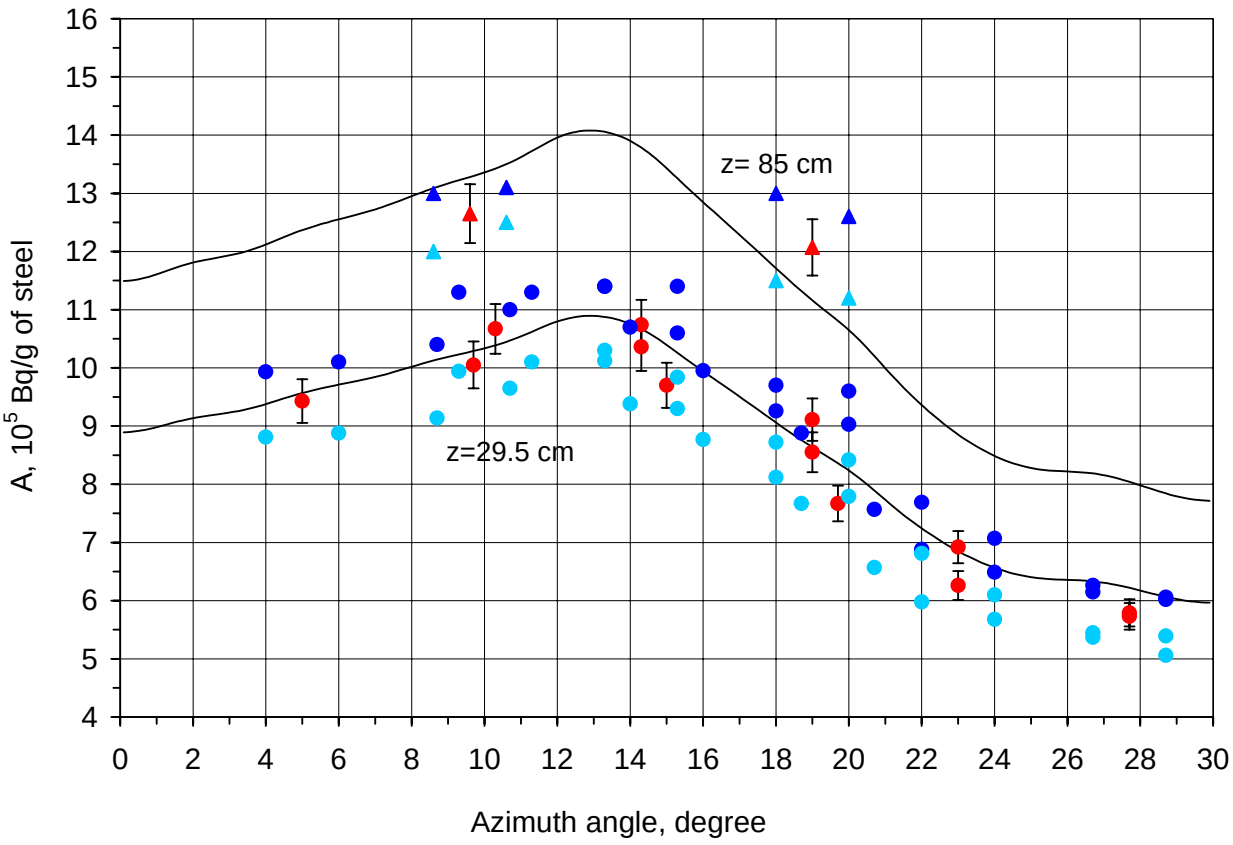

Fig 1. Calculation and experimental distributions of ^{54}Mn activity in templates of weld (z=29.5 cm) and base metal (z=85 cm) of Kola-2 RPV

Calculated curves and experimental points with error limits (at confidence level 0.95) are given for average activities of templates. Other experimental points are given for probes in corners of templates (see text).

Fast Neutron Dosimetry and Spectrometry Using Silicon Carbide Semiconductor Detectors

Ruddy, F. H., Seidel, J. G., Dulloo, A. R.
Westinghouse Electric Company
1332 Beulah Road Pittsburgh, PA 15235-5081, USA

INTRODUCTION

Silicon carbide (SiC) semiconductor radiation detectors [*1*] are being developed for a variety of neutron monitoring and dosimetry applications. [*2,3*] The wide band gap of SiC allows SiC detectors to operate at elevated temperatures. Furthermore, SiC detectors have been shown to be highly resistant to radiation effects due to prolonged exposures to gamma rays, fast neutrons, and charged particles. [*4,5*]

Initial fast-neutron response measurements were reported at the previous meeting in this series. [*6*] Neutron detectors based on a Schottky diode design were exposed to fast neutrons from ^{252}Cf, ^{241}Am-Be, cosmic-ray, and deuterium-tritium (D-T) sources. It was shown that the response was dependent on the incident neutron spectrum and that peaks due to specific neutron reactions could be identified in some cases.

A limitation of that work was that the active volume of the SiC neutron detector was only 10-μm thick, which represented the state-of-the-art at the time the detectors were manufactured. The neutron response of these detectors was consequently perturbed by finite-volume effects, because the ranges in SiC of some of the neutron-induced charged particle reaction products are not small compared to 10 μm. More recently, SiC devices with thick epitaxial layers up to 100 μm have become available, enabling the production of SiC neutron detectors with thicker active layers, larger active volumes, and higher intrinsic efficiencies. These larger-volume detectors are much less susceptible to finite-volume effects.

MEASUREMENTS

SiC p-i-n junctions were used for the measurements. A 90-μm epitaxial layer of n^- SiC doped with a nitrogen content of (1.5-2.5) x 10^{14}/cm^3 was applied to a 355-μm conducting SiC substrate layer with a nitrogen concentration of 5 x 10^{17}/cm^3. The n^- layer was covered with a 2-μm SiC p^+ layer containing an aluminum concentration of (5-8) x 10^{18}/cm^3 covered by a 0.5-μm SiC p^{++} layer with an aluminum concentration of >10^{19}/cm^3 and a 8-μm gold contact layer. The diode area is 4.4mm x 4.4 mm. When a reverse bias of -1000 volts is applied, the 90-μm n^- layer becomes fully depleted and serves as the active region of the detector. Neutrons are detected via silicon and carbon reactions that produce charged particles in the detector active volume. [*6*]

The SiC p-i-n neutron detectors were exposed to ^{252}Cf, ^{241}Am-Be, D-T (14.1-MeV), D-D (2.5 MeV), and ^{235}U(n,fission) neutrons.

RESULTS AND DISCUSSION

The response spectrum for 14.1-MeV D-T neutrons is shown in Figure 1. It can be seen that much more detail is evident in the neutron response spectra for the present larger-volume detectors than was observed previously [*6*] with smaller detectors. Multiple peaks are observed for the ^{28}Si(n,α)^{25}Mg reaction in addition to the ^{12}C(n,α)^{9}Be reaction peak reported previously [*6*]. The ^{28}Si peaks correspond to branches populating the ground state and excited states of ^{25}Mg. The known reaction Q-value and ^{25}Mg energy levels can be used to obtain a detailed energy response spectrum for the detector as shown in Figure 2. Note that the energy calibration point for the ^{12}C(n,α)^{9}Be reaction (only the ground state branch was observed) does not lie on the ^{28}Si(n,α)^{25}Mg calibration curve, because the pulse height defect will be more pronounced for ^{25}Mg ions than for ^{9}Be ions. The non-ionization part of the energy loss in SiC comprises a larger fraction of the total energy loss for ^{25}Mg, and, because the energy of both (n,α) reaction products is dependent on the reaction angle, pulse height defects will also contribute to the widths of the observed peaks, and in fact comprises the major component of the full width at half maximum (FWHM) of each peak. The FWHM values for the ^{28}Si(n,α)^{25}Mg peaks are about twice the value for the ^{12}C(n,α)^{9}Be peak.

Even though the observed reaction peaks are broadened by reaction kinematics effects on ionic stopping, the observed peaks are narrow enough to allow measurements of ion temperature in D-T fusion plasmas based on the temperature broadening of the peaks. Also, the peak energy positions and the internal detector energy calibration

based on the multiple peaks observed can be used to accurately measure the energy of D-T neutrons. Other features of the spectrum, such as the carbon and silicon neutron scattering continua contain recoil-ion spectrometry information, which, in principle, can be used to derive the incident neutron energy spectrum.

The use SiC detectors for fission-related neutron dosimetry and energy spectrometry will also be discussed.

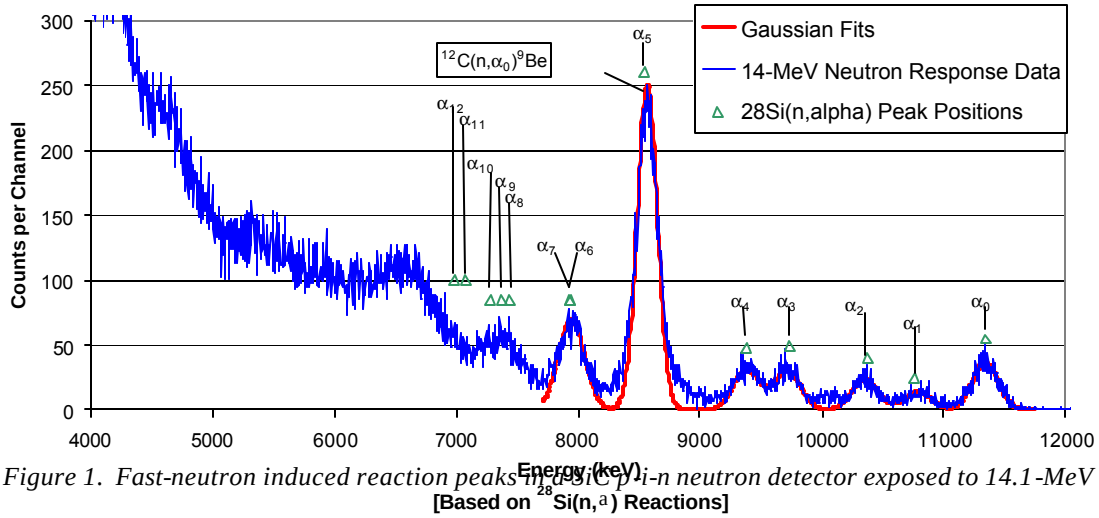

Figure 1. Fast-neutron induced reaction peaks in a SiC p-i-n neutron detector exposed to 14.1-MeV neutrons.

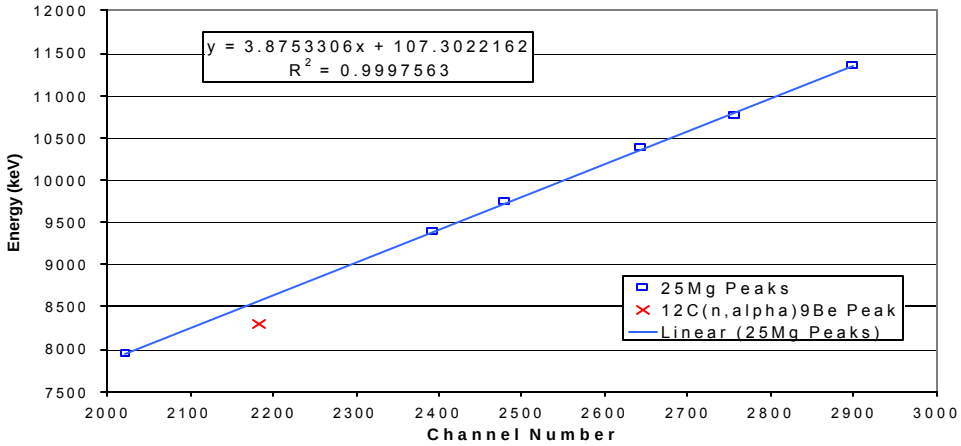

Figure 2. Detector energy calibration based on observed reaction peaks.

REFERENCES

1. F. H. Ruddy, A. R. Dulloo, J. G. Seidel, S. Seshadri, and L. B. Rowland, "Development of a Silicon Carbide Radiation Detector", IEEE Transactions on Nuclear Science **NS-45**, 536 (1998).
2. F. H. Ruddy, A. R. Dulloo, J. G. Seidel, F. W. Hantz, and L. R. Grobmyer, "Nuclear Reactor Power Monitoring Using Silicon Carbide Semiconductor Radiation Detectors",Nuclear Technology 140, 198 (2002)
3. T. Natsume, H. Doi, F. H. Ruddy, J. G. Seidel, and A. R. Dulloo, "Spent Fuel Monitoring With Silicon Carbide Semiconductor Neutron/Gamma Detectors", (this conference)
4. S. Seshadri, A. R. Dulloo, F. H. Ruddy, J. G. Seidel, and L. B. Rowland, "Demonstration of a SiC Neutron Detector for High Radiation Environments", IEEE Transactions on Electronic Devices **46**, 567 (1999).
5. F. H. Ruddy, A. R. Dulloo, and J. G. Seidel, "Study of the Radiation Resistance of Silicon Carbide Radiation Detectors", Trans. Am. Nuc. Soc. **90**, 348-349 (2004)
6. F. H. Ruddy, A. R. Dulloo, B. Petrovic, and J. G. Seidel, "Fast Neutron Spectrometry Using Silicon Carbide Detectors", in *Reactor Dosimetry in the 21st Century*, J. Wagemans, H. A. Abderrahim, P. D'hondt, and C. De Raedt (Eds.), World Scientific, London (2003) pp 347-355.

Retrospective Dosimetry of Fast Neutrons Focused on the Reactions ^{93}Nb (n,n')^{93m}Nb and ^{54}Fe(n,p)^{54}Mn

Voorbraak, W. P. and Woittiez, J. R. W
Nuclear Research and Consutancy Group, NRG, P.O. Box 25, Petten, The Netherlands
Wagemans, J. and Van Boxstaele, M.
SCK-CEN, Boeretang 200, B-2400, Mol Belgium
Kekki, T and Serén, T. O.
VTT Technical Research Centre of Finland, P.O. Box 1608, FI-02044 VTT, Finland.

An overview is given of practices for "retrospective" dosimetry (RetroD) based on the reactions ^{93}Nb(n,n')^{93m}Nb and ^{54}Fe(n,p)^{54}Mn. Both reactions are typical for the determination of the fast neutron fluence and the damage parameters derived from this fluence. The main problem of counting of structural material is the overwhelming presence of the nuclide ^{60}Co in the gamma-ray spectra of irradiated steels. Chemical separation of niobium and manganese is needed to determine the induced ^{93m}Nb and ^{54}Mn activities.

The applicability of the technique of RetroD based on the ^{93}Nb(n,n')^{93m}Nb reaction is mainly determined by the amount of niobium in the material. In general, the calculated neutron dose can only in limited cases be compared with measured data from monitor sets that are irradiated in surveillance capsules and sometimes in the cavity close to the reactor vessel outside the reactor. Therefore RetroD could give valuable information about the fast neutron fluence at critical positions of the reactor construction where no monitors are present.

RetroD is a well known procedure [*1*],[*2*],[*3*]. Unfortunately no detailed information has been published about the actual approach of RetroD on laboratory scale. The challenge to develop a procedure, status 2000, applicable at normally equipped radiochemical laboratories was picked up in a joint exercise of NRG, Petten, The Netherlands, SCK•CEN, Mol, Belgium and VTT Processes, Espoo, Finland, sponsored by the European Commission (Contract FIKS-CT-2000-91).

In principle, the neutron fluence should be derived from the activity induced in small amounts of the structural material that has been obtained by scraping or nibbling a few milligrams of reactor material at the location of interest. In order to develop our procedures we used reactor pressure vessel cladding material from surveillance capsules irradiated in VVERs in Finland and the Czech Republic and base material (15kH2MFA) irradiated in the HFR in Petten. The materials had different irradiation and cooling times, varying from 2 to 12 years, to investigate the influence of the disturbing nuclide ^{60}Co, and contained different amounts of niobium, varying from 1 per cent to 50 ppm. The samples were subdivided into smaller amounts to investigate 1) the influence of the homogeneity in niobium of the samples and 2) the reproducibility of the procedure.

The partners in the project investigated chemical separation procedures of niobium in parallel. Column chromatographic anion exchange has been applied to eliminate the spectral interference of ^{60}Co.
The determination of the amount of niobium in dissolution obtained after the separation has also been investigated in parallel. Techniques have been applied determined by local situation, viz. the presence of a small reactor, which can be used for Instrumental Activation Analysis or an Inductively Coupled Plasma - Mass Spectrometer (ICP-MS). The accurate counting of the very weak X-rays of ^{93m}Nb was tackled also. Different methods like counting of a few drops of a niobium solution deposited on filter paper, counting of niobium in solution and application of liquid scintillation counting (LSC) have been tested. The results were compared and in general very good agreement was achieved.

This report should be considered as the conclusion of the project and gives information on the different procedures that have been addressed. Advantages, disadvantages and the accuracy that can be achieved are reported. Details are given in the references [*4*] to [*8*].

The most important conclusion is that RetroD is a useful tool for determining the neutron fluence at locations inside a NPP e.g. at the welds of a RPV. Procedures are available to remove the ^{60}Co activity. The only condition is the presence of sufficient niobium. For cladding materials, typical for VVERs containing 8 mg Nb/g, an accuracy of ~ 5% can be achieved. At least 50 μg Nb/g in a sample of 100 mg is required to achieve an accuracy of 10 %.

The chemistry can be performed in normally equipped radiochemical laboratories. Availability of ICP-MS equipment or a nuclear reactor with counting equipment close to the reactor may be beyond the capability of some laboratories.

Besides ^{93m}Nb, also manganese can be isolated by extension of column chromatographic anion exchange. Measuring of the nuclide ^{54}Mn thereafter is a standard procedure. The spectrum index $\alpha(^{93m}\text{Nb})/\alpha(^{54}\text{Mn})$ gives information about the fast part of the neutron spectrum and can also be used as parameter for quality control.

Finally, the ^{94}Nb activities induced by the thermal neutron reaction ^{93}Nb(n,γ) were also measured and compared. The long half-life (2.03E4 years) and fairly high response in the upper epithermal region makes this reaction also useful. Little extra effort is needed because ^{94}Nb is easily measurable by conventional gamma spectroscopy after chemical separation of the niobium.

Combination of reaction rates of all these reactions could be a powerful tool to collect information about the neutron spectrum above 100 keV, being responsible for neutron damage. Therefore this report is completed with a separation procedure for manganese also.

REFERENCES

1. L.B. Bärs and E.K. Häsänen: Neutron Flux Estimation Based on Niobium Impurities in Reactor Pressure Vessel Steel, Reactor Dosimetry Methods, Application and Standardization, ASTM STP 1228, H. Farrar IV, E. Lippincott, J.G. Williams and D.W. Vehar, Eds, ASTM, Philadelphia, 1994.
2. J. van Aarle et al.: Fast neutron Dosimetry of Nuclear Power Plants by Means of Scraping Samples using ^{93}Nb(n,n')^{93}Nb^{m} Reaction, Reactor Dosimetry, ASTM STP 1398, John G Williams, David W. Vehar, Frank H. Rudy and David M. Gilliam, eds, American Society for Testing Materials, West Conshohocken, PA, 2000.
3. L.R. Greenwood and B.M. Oliver: Retrospective Reactor Dosimetry for Neutron Fluence, Helium and Boron Measurements; Proceedings of the 11th International Symposium on Reactor Dosimetry: Reactor Dosimetry in the 21st Century, editors J. Wagemans, H. Ait Abderahim; P. J. d'Hondt and Ch. De Raedt, World Scientific, ISBN 981-238-448-0.
4. W.P. Voorbraak, T. Kekki, T. Serén, M Van Boxstaele, J. Wagemans, J.R.W.Woitiez: Retrospective Dosimetry of fast neutrons focussed on the reactions ^{93}Nb(n,n')^{93}Nb, 20576/03.53641/C, NRG Petten, May 2003.
5. W.P. Voorbraak, J.K. Aaldijk and J.R.W. Woittiez, Retrospective Dosimetry of fast neutrons focussed on the reactions ^{93}Nb(n,n')^{93}Nb^{m} and ^{54}Fe(n,p)^{54}Mn, Contribution of NRG, 20576/03.53535/C, NRG, Petten May 2003.
6. J.R.W. Woittiez, B. Beemsterboer, O. Zwaagstra: RETROSPEC; Contribution of NAMS; Radioactive vessel steel: Separation of Nb and Mn from Co and determination of the Nb, K5160/03.53122/I, April 2003.
7. J. Wagemans, M. Van Bocxstaele, M. Gysemans and K. Van der Meer: Retrospective Dosimetry based on the ^{93}Nb(n,n') ^{93m}Nb reaction. Techniques applied at SCK•CEN, SCK•CEN-BLG-948, May 2003.
8. T. Serén and T. Kekki, "Retrospective Dosimetry based on Niobium Extraction and Counting; VTT's Contribution to the RETROSPEC Project , VTT Research Notes 2203, Espoo, 2003.

Space Reactor Shadow Shielding Experiments using Lithium Hydroxide[1]

Williams, J. G.,
University of Arizona,
PO Box 210119, Tucson, AZ 85721-0119, USA

Jun, I.,
Jet Propulsion Laboratory/California Institute of Technology,
4800 Oak Grove Dr., Pasadena, CA 91109, USA, and

Sallee, W. W.
US Army Systems Test and Assessment Directorate.
White Sands Missile Range, NM 88002, USA

SUMMARY

Experiments and calculations have been performed of radiometric monitor response and neutron fluence behind neutron shadow shields of lithium hydroxide monohydrate ($LiOH.H_2O$). These data are of interest for design of the neutron shield for a space vehicle powered by a fast fission reactor. For an unmanned mission, the main function of the shield would be to prevent damage to the electronics of the mission payload from fast reactor neutrons. Leakage neutrons from the Fast Burst Reactor (FBR) at White Sands Missile Range (WSMR) were used as the source in the experiment. The experiment was created as a benchmark to test the accuracy of MCNP simulations, and ENDF B/VI data files, used to model shadow shields of candidate materials. Lithium hydroxide monohydrate was chosen for these experiments because of its chemical stability, compared with lithium hydride.

The WSMR FBR was used to provide a source of fission neutrons leaking from a small source, resembling the source from a postulated space reactor. The FBR is a bare cylindrical fast reactor composed of enriched uranium metal, alloyed with a small percentage of molybdenum. The reactor is air-cooled and can operate at a steady-state power of 8 kW (thermal). The source strength of a space reactor operating at 1 MW thermal power will be about one hundred times larger than that of the WSMR FBR operating at 8 kW. The FBR core is cylindrical in shape, with its axis vertical, and has height and diameter each less than 20 cm. For target distances larger than one meter from the center, a point-source model of the reactor is adequate for most purposes. The reactor operates within a concrete room. In neutronics modeling of experiments inside the room, it is necessary to include the effect of neutrons returned from the walls, floor, and ceiling.

In the experiment, detectors were placed at a radius of 3.2 meters from the core center, at the height of the core midplane. This is about one tenth of the distance presumed for the payload of a space reactor. Since the space reactor will have a much larger neutron source strength, the fluence rate at the detector position is nearly the same as in the postulated space reactor configuration, in the absence of shield materials. In this respect the experiment can be thought of as a scale model of the reactor-powered space vehicle. The detectors used were radiometric monitors (activation foils), using neutron transmutation reactions in sulfur, aluminum, copper, nickel, indium, depleted uranium, and neptunium. Radiometric monitors have been selected because of their low sensitivity to gamma radiation, bearing in mind that gamma shielding is not part of the objective of the present work. The fission detectors (U-238 and Np-237) were enclosed in a spherical shell of boron-10 carbide, 4.8 cm in diameter, to suppress their thermal and epithermal neutron response. The sulfur pellets were 5.7-cm diameter disks, approximately 6 mm thick. The indium, copper, nickel and aluminum foils were discs 5.1 cm in diameter. Apart from the sulfur, all detectors produce discrete gamma emission from their induced activity and were counted by gamma spectrometry, calibrated using a 5.1-cm diameter mixed radionuclide source. The sulfur pellets were beta counted using a proportional counter. Calibration of the sulfur counting was done by transfer of the calibration of a 1.9-cm diameter sulfur pellet of a type previously calibrated at NIST. The three metal discs (Ni, Cu, In and Al) were

[1] The authors would like to acknowledge the Jet Propulsion Laboratory Director's R&D Fund program for the funding of this work. A part of the research described in this paper was carried out at the Jet Propulsion Laboratory, California Institute of Technology, under a contract with the National Aeronautics and Space Administration.

stacked together. This stack and the sulfur pellet and the boron ball enclosing the neptunium were irradiated side-by-side at 3.2 meters radially from the reactor core.

Detectors exposed with no shadow shield present were compared with similar packages exposed with different thicknesses of shielding between the detectors and the reactor. The largest shield thickness that could be used was less than the full thickness of the desirable space reactor shield, because of insufficient detection sensitivity for such low neutron fluences. The shield material was in powder form, packed into polycarbonate boxes in the form of square slabs 10-cm thick, and 40-cm wide. The width was chosen to ensure that the detector package and its enclosing shield (to be described below) could be completely occulted from the direct neutron source paths. The shield slabs were supported in a light frame constructed to allow the pieces to be mounted at various positions between the reactor and the detector package. The total length of the shadow shield assembly, including internal gaps, can be up to 1.5 meters.

The detectors were shielded from wall-return neutrons. These would otherwise dominate the detector response when a thick shadow shield is present. The detector shielding consists of a rectangular box of high-density polyethylene, with an opening at the front, and elsewhere with walls 15 cm in thickness. The front opening is designed to ensure that only neutrons that have emerged from the back surface of the shadow shield can directly reach the detectors. The entire width of the detector shield box falls within the width of the region protected by the shadow shield from direct source neutrons. The box enhances somewhat the sensitivity of the detectors to neutrons entering its front opening, and the detector shield should be thought of as part of the detector package. A schematic diagram of these arrangements is shown in Fig.1.

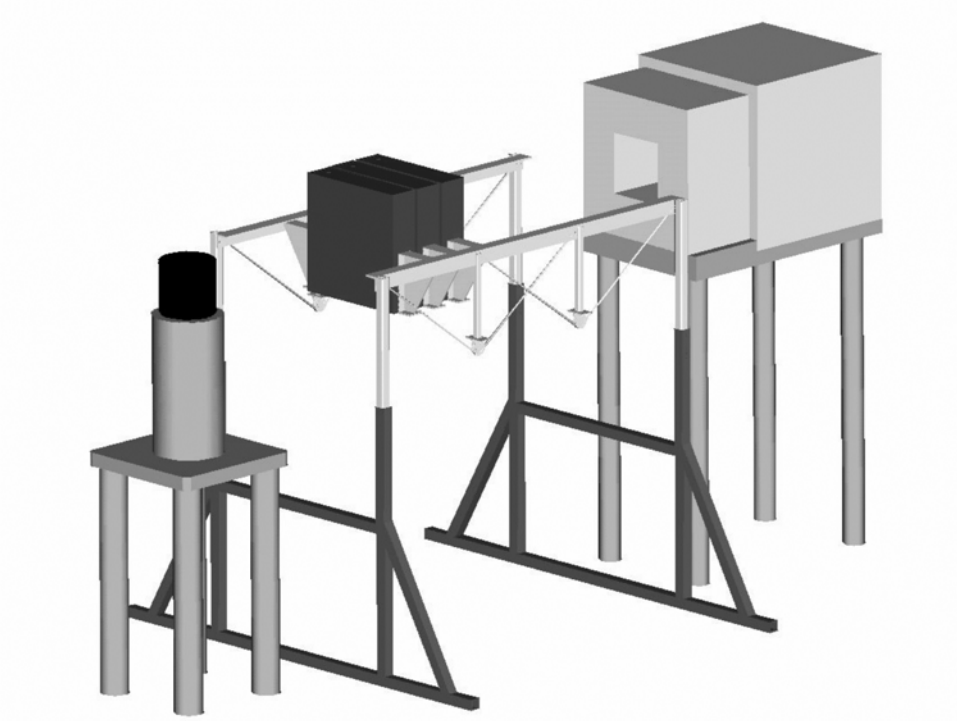

Figure 1. Experimental layout. The reactor is at the left, the detector shield at the right, and the shadow shield in the center.

Some relative neutron transmission values and C/E ratios from these experiments have been reported [1]. In this paper we shall report absolutely normalized reaction probabilities, both from calculation and experiments, comparisons with previous reference data for leakage neutrons from the bare reactor at WSMR, analysis of the direct and wall-return components of the neutron response, uncertainty analysis for the experimental data, and some sensitivity analysis for assessment of calculational uncertainties. These results are intended to be available to the community as benchmark data, and will be documented for that purpose.

References

1. J. G. Williams, I. Jun, W. W. Sallee and M. Cherng, "Benchmark Experiments for Space Reactor Neutron Shielding of Mission Electronics," *IEEE Trans. Nucl. Sci*., 51, No.6, 3658-3663, December 2004.

An International Evaluation of the Neutron Cross Section Standards

Carlson, A. D.
National Institute of Standards & Technology
Gaithersburg, MD USA.

Badikov, S. A.
Institute of Physics & Power Engineering
Obninsk, Russia.

Zhenpeng, Chen
Tsinghua University
Beijing, China.

Gai, E.
Institute of Physics & Power Engineering
Obninsk, Kaluga Region, Russia.

Hale, G. M.
Los Alamos National Laboratory
Los Alamos, NM, USA.

Hambsch, F.-J.
Institute for Reference Materials and Measurements
Geel, Belgium.

Hofmann, H. M.
Erlangen-Nürnberg University
Erlangen, Germany.

Kawano, T.
Los Alamos National Laboratory
Los Alamos, NM, USA.

Larson, N. M.
Oak Ridge National Laboratory
Oak Ridge, TN, USA.

Oh, Soo-Youl
Korean Atomic Energy Research Institute
Yuseong, Daejeon, Republic of Korea.

Pronyaev, V. G.
International Atomic Energy Agency
Vienna, Austria.

Smith, D. L.
Argonne National Laboratory
Argonne, IL, USA.

Tagesen, S.
Vienna University
Vienna, Austria.

Vonach, H.
Vienna University
Vienna, Austria.

The use of neutron cross section standards greatly simplifies the process of making neutron cross section measurements. These reference standards eliminate the need to measure the neutron fluence in a cross section measurement. Improvements in these standards increase the accuracy of all measurements made relative to them. The last complete evaluation of the standards, which was done for the ENDF/B-VI library, was completed in 1987. These standards were accepted internationally to ensure that all evaluation projects were using the same set of standards. Significant experimental activity on the standards has occurred since that evaluation was completed, which will cause changes in new evaluations of the standards. In response to the need for improved evaluations of the standards, working groups were formed by a number of nuclear data organizations. The U.S. Cross Section Evaluation Working Group formed a Task Force, the Working Party on International Nuclear Data Evaluation Cooperation of the Nuclear Energy Agency Nuclear Science Committee established a Subgroup and the International Atomic Energy Agency formed a Coordinated Research Project (CRP). These groups have worked cooperatively to update the previous work by including standards measurements made since the ENDF/B-VI standards evaluation was completed and to improve the evaluation process.

The primary effort on the evaluation has been done by the CRP. Important areas of concern have been improving the R-matrix evaluation methodology for light-element standard cross sections and obtaining a better understanding of the uncertainties observed in R-matrix model fits of experimental data. An improved procedure has been developed for combining an R-matrix evaluation with a model independent least squares fit to produce evaluations for both the light- and heavy-nuclei standards. The CRP has made significant progress toward achieving the goal of producing new standards by the end of 2004, so that they can be used as the basis for the preparation of new evaluated data libraries. Maintaining this schedule is important for the upcoming ENDF/B-VII library.

Significantly improved evaluations are being produced from this process for the ^{6}Li(n,t), ^{10}B(n,α), ^{10}B(n,α_1), ^{197}Au(n,γ), ^{235}U(n,f), and ^{238}U(n,f) standard reactions as well as the ^{238}U(n,γ) and ^{239}Pu(n,f) reactions that are simultaneously evaluated along with the standards due to the strongly coupled databases for these two reaction categories. Also independent R-Matrix evaluations are being produced for the H(n,n) and ^{3}He(n,p) standard cross sections. A new evaluation for the C(n,n) standard cross section is not being done due to the consistency of the new measurements with the existing evaluation. The need for standards above 20 MeV has led to extensions of the energy range of the H(n,n), ^{235}U(n,f), and ^{238}U(n,f) standards to about 200 MeV. Many of the cross sections being evaluated are used in neutron dosimetry for fluence determination.

The general trend observed for the evaluations is an increase in the cross sections for most of the reactions from fractions of a percent to several percent compared with the ENDF/B-VI results. Extensive work on tests and comparisons will be presented.

Analysis of the VENUS-3 PWR Pressure Vessel Surveillance Benchmark Using TRIPOLI-4.3 Monte Carlo Code

Lee, Y. K.
CEA/Saclay, DEN/DM2S/SERMA/LEPP
91191 Gif sur Yvette Cedex, France

ABSTRACT

This paper presents the analysis of the VENUS-3 PWR Pressure Vessel Surveillance Dosimetry Benchmark using the French 3D continuous-energy Monte Carlo code TRIPOLI-4.3. VENUS-3 benchmark specification is taken from the 2004 release of the International Database for Integral Shielding Experiments (SINBAD) of OECD/NEA. Nuclear data library for Monte Carlo transport calculations is from ENDF/B-VI.4. Detector cross-sections for $^{27}Al(n,\alpha)$, $^{58}Ni(n,p)$ and $^{115}In(n,n')$ from IRDF-90.v2 and ENDF/B-VI.4 are tested. Two ^{235}U fission spectra, continuous Watt spectrum and 581 groups ENDF/B-VI.4 spectrum are experienced. To improve the figure of merit (FOM) of TRIPOLI-4.3 simulation and to predict the large axial (50 cm) and azimuthal (0°-90°) variation of the fluence for core barrel measurement points, new variance reduction techniques (cylindrical surface biasing and cylindrical meshes) are applied. Values of C/E at different locations will be presented. About 10% C/E tolerance margin should be accepted when different detector cross-sections and ^{235}U fission spectra are used and when the uncertainty of the nuclear data library and the uncertainty of the 3D map of the neutron source power distribution are excluded.

VENUS-3 BENCHMARK

The Venus Criticality Facility is a zero-power reactor with a cruciform-shaped core located at SCK/CEN, Mol, Belgium. From 1983 to 1988, the VENUS mock-ups simulated the reflector geometry and the core boundary shape of a generic 3-loop PWR reactor. VENUS PWR mock-ups are widely used to qualify radiation transport calculation methods and nuclear data for PWR pressure vessel surveillance dosimetry applications. Three core loading configurations were considered in VENUS PWR mock-ups: VENUS-1, simulating a PWR fresh core loading, VENUS-2, simulating a low-leakage core loading, and VENUS-3, simulating the Partial Length Shielded Assembly (PLSA) concept in which part of the axial length of the fuel is replaced by steel in the outermost fuel rows [*1*].

VENUS-3 core is made up of twelve 15 x 15 subassemblies. The pin-to-pin pitch 1.26 cm remains typical of the 17 x 17 subassembly. Pressure vessel internal components of VENUS-3 mock-up are listed as follows: the core outer baffle (2.858 cm thick), the water reflector (minimum thickness 2.169 cm and 45° thickness 17.5 cm), the core barrel (4.99 cm), the first water gap (5.8 cm) and the thermal shield (average thickness 6.72 cm).

TRIPOLI-4.3 MONTE CARLO SIMULATION RESULTS

Figure 1 shows the plan view of the VENUS-3 core quadrant as simulated with TRIPOLI-4.3 code. Using the lattice features of TRIPOLI-4.3, the 650 fuel rods, including central stainless steel clad 4% enriched UO_2 rods, peripheral zircaloy clad 3.3% enriched UO_2 rods, PLSA rods and 11 Pyrex absorber rods, are pin-by-pin defined in 3D way. Measurement positions located in inner baffle, outer baffle, water reflector and core barrel zones are also shown.

Figure 2 shows the C/E ratios and statistical error bars at 38 measurement positions for the $^{27}Al(n,\alpha)$ detector where detectors 1 and 2 correspond to inner baffle; 3 to 5, outer baffle; 6 to 8, water reflector and 9 to 38, outer baffle (10 azimuthal positions from 0.7° to 89.3°, and 3 axial levels). The results in Fig. 2 show that the high energy tail of the ^{235}U fission spectrum from ENDF/B-VI.4 is helpful to improve the C/E ratios for the ^{27}Al detector comparing with continuous ^{235}U Watt fission spectrum. This conclusion confirms the previous TRIPOLI-4.3 calculations on the Oak Ridge National Laboratory Pool Critical Assembly (ORNL PCA) Pressure Vessel Facility Benchmark [*2*]. Another interesting point concluded from Fig. 2 is that the detector cross-sections from IRDF90.v2 give higher and better C/E ratios than those from ENDF/B-VI.4. Both libraries use the same evaluation but, between 5 –20 MeV, more energy groups are found in IRDF90.v2 and different interpolation methods are used.

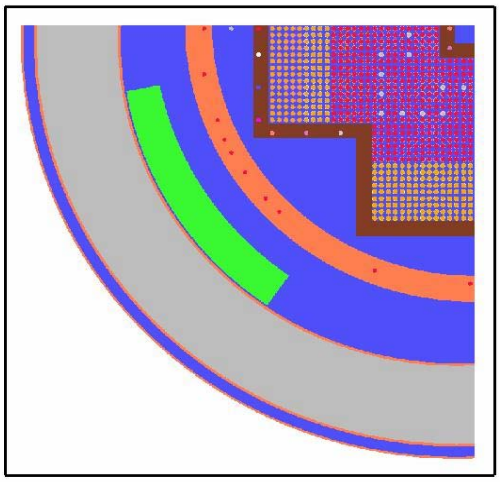

Figure 1. VENUS-3 core quadrant (with all measurement points located in inner baffle, outer baffle, water reflector and core barrel) as simulated with TRIPOLI-4.3

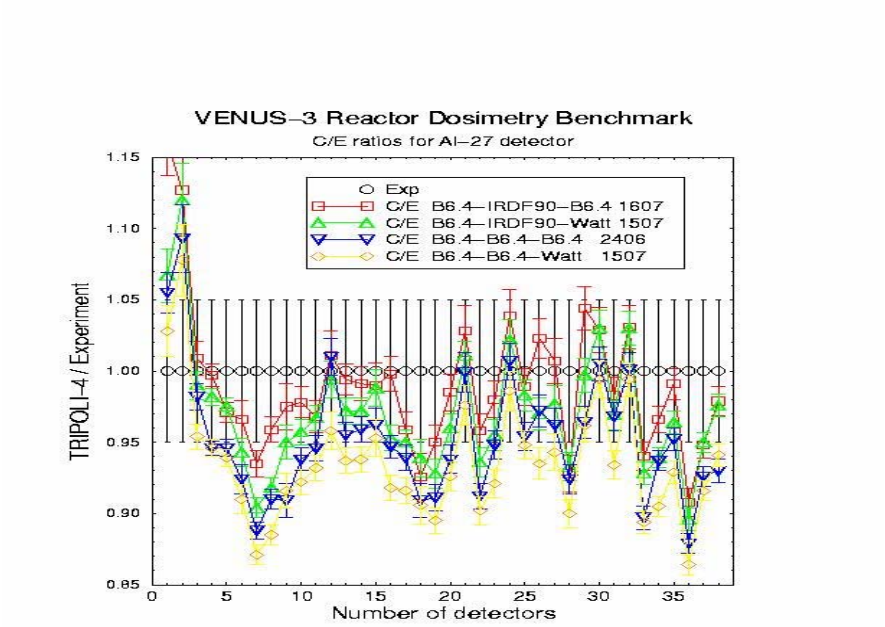

Figure 2. The C/E ratios and statistical error bars at all measurements locations for detector ^{27}Al (Red square: ENDF/B-VI.4 – transport calculation, IRDF90 - detector cross-sections and fission spectrum from ENDF/B-VI.4)

REFERENCES

1. "SINBAD – an International Database for Integral Shielding Experiments", http://www.nea.fr/html/science/shielding/sinbad/venus3/ven3-abs.htm (May, 2004).
2. Y. K. Lee, "Analysis of the NRC PCA Pressure Vessel Dosimetry Benchmark Using TRIPOLI-4.3 Monte Carlo Code and ENDF/B-VI.4, JEF2.2 and IRDF-90 Libraries." *Nuclear Mathematical and Computational Sciences: A Century in Review, A Century Anew*, M&C 2003, Gatlinburg, Tennessee, April 6-10, 2003.

Validation of the Neutron Fluence on the VVER-440 RPV Support Structure

K. Ilieva, S. Belousov, D. Kirilova, B. Petrov
Institute for Nuclear Research and Nuclear Energy of Bulgarian Academy of Sciences,
72 Tzarigradsko shosse, 1784 Sofia, Bulgaria,

E. Polke
Framatome ANP GmbH, 91058 Erlangen, Germany

SUBJECT

The neutron fluence of the RPV support structure has been evaluated in order to assess the lifetime of the reactor vessels of Kozloduy NPP Units 3 and 4. The accuracy of the neutron fluence calculation is limited by the uncertainties of the nuclear data and so of the constructional data of the inhomogeneous reactor medium which are used in the neutron transport calculations. That is why a validation of the neutron fluence based on comparison of calculational with measured induced activity has been done. The ratio of calculational to experimental activity values has been used as a measure for the uncertainty estimation of calculated neutron fluence.

MEASUREMENTS

Activation detectors of iron, copper and niobium have been irradiated during the 17th fuel cycle of Unit 4. The detectors have been installed in the area of the support structure in two positions (Fig.1): Position 1 - detectors positioned horizontally in the air cavity over the support structure, over the RPV flange; Position 2 - detectors positioned vertically at the top of the air cavity between RPV and water tank, under the support structure.

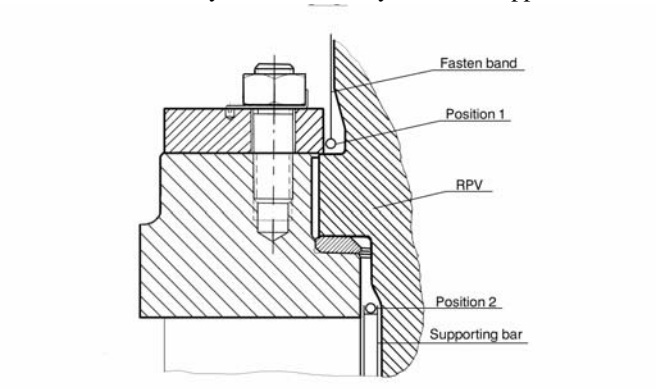

Figure 1. Positions of the detectors in the area of the RPV support structure of Kozloduy NPP Unit 4

CALCULATIONS

The three-dimensional calculations in (r,θ,z) mesh have been performed with the TORT code [*1*] using a model of the reactor system and support structure of VVER-440 reactor. The neutron fluence on the support structure and the activities of irradiated detectors from the reactions Fe54(n,p)Mn54, Cu63(n,α)Co60, and Nb93(n,n')Nb93m have been calculated taking into account the history of the local distribution of the neutron source. The BGL440 multigroup cross section library [*2*] has been used. This library has been produced by collapsing the fine-group library VITAMIN-B6 [*3*] (199 neutron and 42 gamma groups) to 67-group structure (47 neutron and 20 gamma groups). The scattering order P5 and the angle discretisation set S12 have been applied. The geometry model for calculation of the fluence on the support structure contains: core, baffle, moderator (water), core basket, barrel, downcomer, RPV with cladding, air cavity, thermal insulation, water tank, protection tube system, and support structure. A pin-wise neutron source (reactor core) presentation is used for the periphery assemblies and assembly-wise for the other part of the core.

COMPARISON OF THE RESULTS

Comparison of the measured and calculational induced activities results has been done (Fig.2-3). The calculated activities of all copper and niobium detectors irradiated above the support structure as well as of niobium detectors irradiated under the support structure are higher than the measured ones. Moreover the mean deviation for all detectors is positive. These results show that the calculated neutron fluence is conservative in the support structure area. The uncertainty on the activity measurement does not exceed 15%.

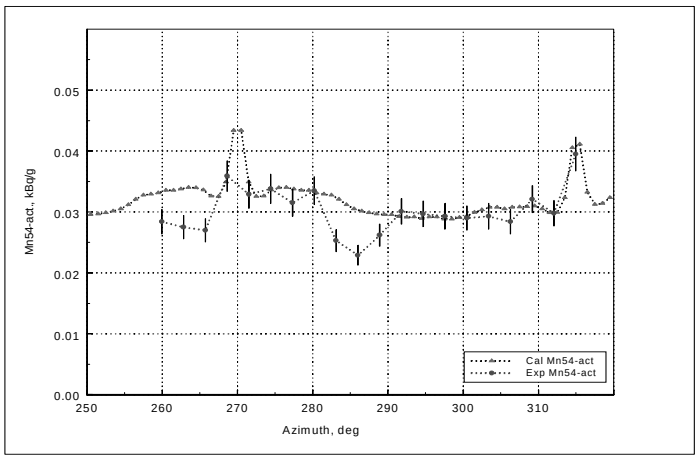

Figure 2. Calculated and measured (with uncertainty) Mn54-activity values of detectors irradiated above Support Structure, Position 1, during 17th cycle of Unit 4

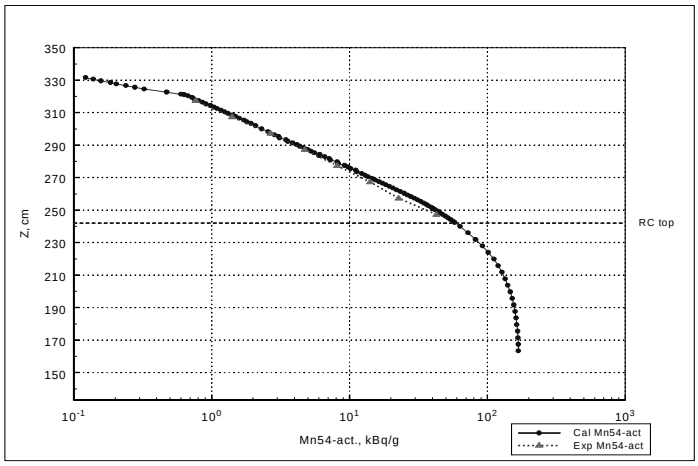

Figure 3. Calculated and measured Mn54-activity of detectors irradiated behind RPV, Position 2 , from the technological break to the end of cycle 17, Unit 4

ACKNOLEDGEMENTS

This work has been done under the Framatome ANP GmbH contract with KNPP “Evaluation of the RLT of Units 1-4 of NPP Kozloduy”.

REFERENCES

1. Rhoades, W.A., Childs, R.L., *TORT Three-Dimensional Discrete Ordinate Neutron/Photon Transport Code with Space-Dependent Mesh and Quadrature*, ORNL-6268 (Nov. 1987).
2. J.A.Bucholz, S.Y.Antonov, S.I.Belousov, *BGL440 and BGL1000 Broad Group Neutron/Photon Cross-Section Libraries Derived from RNDF/B-VI Nuclear Data*, INDC(BUL)-15, Distrib.:G, (Nov. 1996)
3. D.T.Ingersoll et al., *Production and Testing of the VITAMIN-B6 Fine-Group and the BUGLE-93 Broad Group Neutron/Photon Cross-Section Libraries Derived from ENDF/B-VI Nuclear Data*, ORNL-6795 (Draft Febr. 1994)

An Approach to Determining the Uncertainty in Reactor Test Objects using Deterministic and Monte Carlo Methods[1]

Keith, R.E.
ITT Industries, Advanced Engineering & Sciences
Colorado Springs, CO 80949-1990, and
Colorado School of Mines, Department of Physics
Golden, CO 80401

A study effort has been underway to quantify reasonable uncertainty bounds for the response of sensitive portions of a test-object exposed to a reactor neutron environment. Both discrete ordinates based approaches and a Monte Carlo based approaches are being pursued. The goal of the study was to not simply perform a series of calculations for a single series of tests, but rather to establish procedures that can be used for general, and perhaps complicated test objects. The lessons learned and a critique of the advantages and disadvantages of the two approaches are the subject of this paper.

The possible contributors to the uncertainty of an estimate of the response of a portion of a test-object can be grouped into the following categories: (1) source uncertainties, (2) cross-sections uncertainties, (3) geometrical inaccuracies, (4) thickness and density uncertainties, (5) numerical inaccuracies, and (6) response function uncertainties. Under these broad categories, many specific terms contribute to the overall uncertainty, and these can be combined to get a variance of the response using the familiar expression given in Eq.(1).

$$\sigma_R^2 = \sum_i \sum_j P_i \cdot rcov(i,j) \cdot P_j \tag{1}$$

Where, σ_R is the relative standard deviation of the response, P_i is the sensitivity of the response to some parameter referenced by i, and $rcov(i,j)$ is the relative covariance of the parameter referenced by i with the parameter referenced by j.

If R is the response, and x_i is a parameter referenced by i, the sensitivity can be expressed as in Eq.(2).

$$P_i = \frac{\partial R}{\partial x_i} \cdot \frac{x_i}{R} \tag{2}$$

The quest to find the variance in the response becomes a quest to identify the relative covariances and to determine the sensitivities P_i. Depending on whether a discrete ordinates or a Monte Carlo approach is being used, the form of the sensitivity calculation differs. For the sensitivity calculations, the discrete ordinates toolset included DOORS[1], DANTSYS[2] and SUSD3D[3], and the Monte Carlo calculations were performed using MCNP[4], Geant4[5], and custom software.

For each of the general broad categories, the transport method chosen has large effects on the specific procedure that must be employed. This can be illustrated for the important case of the contribution to the total variance due to cross-section uncertainty.

In this case, Monte Carlo calculations introduce a statistical uncertainty into the problem that must be propagated, but more importantly, exclude some very useful techniques. Perhaps most useful discrete-ordinates technique that is used to find the sensitivity of the response to a specific cross section is to fold the forward and adjoint fluxes together with the cross section as in Eq.(3). This procedure requires that the forward and adjoint fluxes be known at all locations where the reaction x can operate, and this is not normally possible with Monte Carlo. This method is very powerful in determining the effect that various reactions can have on the response, and is quite useful in scoping out the effect impurities might have - since as long as the basic adjoint and forward fluxes are not greatly affected due to the impurity, the sensitivity can be determined for the response to a reaction for an isotope not even in the original transport calculations.

[1]This work was supported by the United States Department of Energy under contract DE-AC04-94AL85000 with technical management by Sandia National Laboratories. Sandia is a multiprogram laboratory operated by Sandia Corporation, a Lockheed Martin Company, for the United States Department of Energy.

$$P_x(E) = \frac{1}{R} \cdot \int d\vec{r} \int d\vec{\Omega} \Big\{ - \Sigma_T^x(\vec{r}, E) \cdot \Phi(\vec{r}, \vec{\Omega}, E) \cdot \Phi^*(\vec{r}, \vec{\Omega}, E) + \int_{\vec{\Omega}'} d\vec{\Omega}' \int dE' \Big[\Sigma_s^x(\vec{r}, \vec{\Omega} \rightarrow \vec{\Omega}', E \rightarrow E') \cdot \Phi(\vec{r}, \vec{\Omega}, E) \cdot \Phi^*(\vec{r}, \vec{\Omega}', E') \Big] + \Sigma_D(\vec{r}, E) \cdot \Phi(\vec{r}, \vec{\Omega}, E) \Big\} \quad (3)$$

Where, $\Sigma_T^x(\vec{r}, E)$ is the total cross section for reaction type x at $\vec{r}$ with energy E, $\Sigma_s^x(\vec{r}, \vec{\Omega} \rightarrow \vec{\Omega}', E \rightarrow E')$ is the scattering cross section for reaction x,$\Sigma_D(\vec{r}, E)$ is the response function, $\Phi(\vec{r}, \vec{\Omega}, E)$ is the forward flux at $\vec{r}$, and $\Phi^*(\vec{r}, \vec{\Omega}, E)$ is the adjoint flux at $\vec{r}$.

To determine the sensitivity using a Monte Carlo transport code, a differential operator can be used (such a differential operator is available in MCNP). By setting a small perturbation ($\Delta\Sigma_x$)to a cross section for a reaction x (Σ_x), the change in response is calculated (ΔR), and this change in response can used to approximate the sensitivity via Eq.(4).

$$P = \frac{\Delta R}{\Delta \Sigma_x} \frac{\Sigma_x}{R} \quad (4)$$

Although this Monte Carlo differential operator technique allows for the calculation of the sensitivity, it is not without significant cost. For the detailed calculation of the variance of the activation of nickel-58 (^{58}Ni) foils in a test sphere, a recent calculation used over 150 separate perturbations. A 10 % increase in run time is projected for each perturbation[4]. Pre- and post- processing software was developed to effectively handle the large number of entries involved.

In general, the primary advantage of the Monte Carlo method is that the geometries involved can be arbitrarily complicated, and the uncertainty can still be determined. The discrete-ordinates method is powerful for the problems that can be readily addressed, but this technique has drawbacks related to the ease of modeling complicated test objects properly.

REFERENCES

1. RSIC, Oak Ridge National Laboratory, *DOORS3.2 discrete ordinates transport code system*, 2002. ccc-650.
2. R. E. Alcouffe, R. S. Baker, F. W. Brinkley, D. R. May, R. D. O'Dell, and W. F. Wlaters, *DANTSYS: A Diffusion Accelerated Neutral Particle Transport Code System.* Los Alamos National Laboratory, June 1995. LA-12969-M.
3. RSIC, Oak Ridge National Laboratory, *SUSD3D: A Multi-Dimensional, Discrete-Ordinates Based Cross Section Sensitivity and Uncertainty Analysis Code System*, 2000. ccc-695.
4. Los Alamos National Laboratory, *MCNP: A General Monte Carlo N-Particle Transport Code*, April 2000. LA-13709-M.
5. Centre Europen de Recherche Nuclaire, *Geant4 User's Guide*, 2002.

Influence of the Multigroup Approximation on VVER-1000 RPV Neutron/Gamma Flux Calculation

S. Belousov, D. Kirilova, M. Mitev, K. Ilieva
Institite for Nuclear Research and Nuclear Energy of Bulgarian Academy of Sciences
72 Tzarigradsko shosse, 1784 Sofia, Bulgaria

OBJECTIVES

Calculations of neutron and gamma group fluxes and radiation damage in terms of dpa have been carried out for VVER-1000 Mock up [*1*] at LR-0 Czech assembly in order to evaluate the contribution of the gamma radiation to the radiation embrittlement of VVER-1000 RPV by means of model calculations. Two methods have been applied: Monte Carlo method with continuous description of energy dependence, and discrete ordinates method with multigroup energy dependence approximation.

To estimate the influence of different multigroup cross section libraries application one-dimensional calculation have been carried out for the same VVER-1000 Mock-up.

CALCULATIONS

One-dimensional transport calculations have been carried out with the Monte Carlo code MCNP4C [*2*] and discrete ordinates codes DORT [*3*]. Continuous energy representation of the neutron cross-sections from the library DLC200/MCNPDATA [*2*] has been used in the modeling of neutron transport with the MCNP4C code.

The BGL1000 [*4*] and SAILOR-96t (BUGLE96) [*5*] (47 neutron and 20 gamma groups) microscopic cross section libraries have been used in DORT calculations. BGL1000 is a problem-oriented multigroup library for VVER-1000 type of reactor, and the library SAILOR-96t for PWR reactors both created by collapsing of the fine group library VITAMIN-B6 [*6*].

The neutron and gamma integral fluxes, and radiation damage in terms of dpa [*7*] have been evaluated in different positions of VVER-1000 Mock up (point: 2 – behind the barrel; 3 – on the RPV; 4 – at 1/4 of the RPV thickness; 5 – at 1/2 of the RPV thickness; 6 – at 3/4 of the RPV thickness; 7 – behind the RPV).

COMPARISON OF THE RESULTS

The comparison (Table 1) of the fast neutron fluxes, En>0,111MeV, of the results calculated by DORT with BGL1000 (BGL) as well as those calculated with SAILOR (SLR) library, with those calculated by MCNP shows a good consistency of both of them with the MCNP ones. The consistency for the other responses such as the total neutron fluxes, gamma integral fluxes and dpa, is better for those calculated with BGL1000 than those calculated with SAILOR.

Table 1. Comparison between DORT and MCNP results - (DORT/MCNP-1), %

Point	2		3		4		5		6		7	
Energy, MeV	BGL	SLR	BGL	SLR	BGL	SLR	BGL	SLR	BGL	SLR	BGL	SLR
NEUTRON												
E<4.14E-7	33.93	-42.4	63.43	-53.5	71.19	-37.9	39.0	-11.8	6.81	10.9	-0.10	2.68
E>0.111	4.33	3.58	-0.36	-2.43	4.63	2.43	6.46	4.10	5.39	2.79	-2.66	-6.39
E>0.498	5.32	3.77	-1.34	-3.98	0.74	-2.20	1.15	-2.25	0.04	-3.89	-4.91	-10.0
E>1	4.98	4.43	-1.87	-3.86	-1.44	-3.83	-2.04	-5.05	-3.05	-6.70	-6.17	-10.1
E>3	1.84	0.10	-3.55	-5.63	-4.50	-6.34	-5.16	-7.51	-5.85	-8.17	-6.17	-9.67
E>5	3.43	2.11	-1.32	-2.32	-1.83	-2.98	-3.17	-4.35	-3.59	-5.45	-3.76	-6.54
TOTAL	3.43	2.11	-1.32	-2.32	-1.83	-2.98	5.85	3.59	4.67	2.81	-1.69	-4.35
dpa	5.31	3.89	-0.40	-3.39	2.05	-0.74	5.31	3.89	-0.40	-3.39	2.05	-0.74

Table 1. Continue

GAMMA												
E>1	1.31	-33.0	-6.41	-32.5	-6.56	-32.3	-8.31	-32.4	-10.8	-32.7	-12.8	-29.0
E>3	6.32	-24.3	5.20	-20.3	3.77	-21.7	1.83	-22.6	-0.59	-23.9	-4.39	-22.0
E>5	7.69	-24.9	8.98	-20.4	7.44	-21.3	4.95	-22.2	1.88	-23.3	-1.94	-20.6
TOTAL	-5.58	-23.6	-27.7	-25.4	-18.2	-37.6	-18.9	-39.7	-20.6	-40.0	-22.0	-35.7
dpa	6.66	-27.3	5.83	-23.5	4.09	-23.8	1.87	-24.3	-0.97	-25.3	-3.82	-22.3

The differences between DORT results (BGL and SAILOR) are shown in Table 2. The consistency between the results for neutrons with E>0.1 MeV and dpa is very good, within 1%. The discrepancy for thermal neutrons flux is significant for points 2, 3 (up to 71%), 4 and point 5. The discrepancy for gamma fluxes and dpa values is significant for all points (up to about 30% in point 2). The BGL gamma flux and dpa results are greater than the SAILOR ones.

Table 2. Comparison between DORT results - (SLR/BGL-1),%

Energy,MeV	POINT2	POINT3	POINT4	POINT5	POINT6	POINT7
NEUTRON						
E<0.4 eV	-56,6	-70,9	-62,6	-33,8	4,31	5,59
E>0.1	0,63	0,07	0,06	0,08	0,10	0,22
E>0.5	0,05	-0,48	-0,46	-0,49	-0,54	-0,40
E>1.0	1,18	-0,15	-0,26	-0,28	-0,26	0,35
E>3.0	-0,43	-0,35	0,01	0,05	0,00	0,05
E>5.0	-0,26	-1,10	-0,96	-0,90	-0,81	-0,75
TOTAL	-12,6	-21,0	-2,72	-0,29	-0,04	0,30
dpa	0,42	-0,63	-0,24	-0,20	-0,19	0,03
GAMMA						
E>1.0	-33,2	-27,3	-26,5	-24,6	-22,6	-16,4
E>3.0	-28,1	-23,5	-23,4	-22,5	-21,5	-16,5
E>5.0	-29,4	-25,8	-25,2	-24,1	-22,7	-17,0
E>0.0	-18,1	4,08	-22,5	-23,9	-22,3	-15,0
dpa	-31,0	-26,9	-25,6	-24,1	-22,5	-16,7

CONCLUSION

The obtained relation between the one-dimensional results of MCNP and DORT permit to estimate the influence of multigroup approximation used in DORT calculations, and is useful in comparison analysis of the three-dimensional calculational results. On the basis of the results obtained, the BGL1000 library has been chosen as more appropriate for three dimensional calculation of neutron/gamma transport for VVER-1000 Mock up task.

ACNOWLEDGEMENT

This work was carried out under the REDOS project of 5FP, Euratom.

REFERENCES

1. B Osmera, S. Zaritsky, *VVER-1000 Mock-up Experiment in LR-0 Reactor Mock-up Description and Experimental Data,* REDOS project of 5FP, Euratom, R(01)/December 2002/Issue 01
2. J. Briesmeister, Ed. MCNP: *A General Monte Carlo N-Particle Transport Code, Version 4B,* LA-12625-M, March,1997, RSICC ORNL, Code Package, C00700ALLCP01, 2001 [3]
3. Rhoades W.A., R.L. Childs. *DORT*, Nucl. Sci. Eng. **99**, 1, pp. 88-89 (May 1988)
4. J.A.Bucholz, S.Y.Antonov, S.I.Belousov, *BGL440 and BGL1000 Broad Group Neutron/Photon Cross-Section Libraries Derived from RNDF/B-VI Nuclear Data,* INDC(BUL)-15, Distrib.G, (Nov. 1996)
5. BUGLE-96: *Coupled 47 Neutrons, 20 Gamma-Ray Group Cross Section Library Derived from ENDF/B-VI for LWR Shielding and Pressure Vessel Dosimetry Application*. RSIC DATA LIBRARY, DLC-185.
6. D.T.Ingersoll et al., *Production and Testing of the VITAMIN-B6 Fine-Group and the BUGLE-93 Broad Group Neutron/Photon Cross-Section Libraries Derived from ENDF/B-VI Nuclear Data,* ORNL-6795 (Draft Feb.1994)
7. J. Kwon and A.T. Motta, Neutron and Gamma DPA-cross sections. *Ann. Nucl. Energy* 27 (2000) 1627-1642

Precision Neutron Total Cross Section Measurements for Natural Carbon at Reactor Neutron Filtered Beams

Gritzay, O. O., Kolotyi, V. V., Klimova, N. A., Kalchenko, O. I., Gnidak, M. L., Vorona, P. N.
Institute for Nuclear Research
Kyiv, 03680, Ukraine

INTRODUCTION

This investigation is devoted to the precise measurements of total neutron cross section for natural carbon. This element is well known as reactor structure material and at the same time as one of the most important scattering standards, especially at energies of less than 2 MeV, where the neutron total and elastic scattering cross sections are essentially identical.

The best experimental data in the area 1-500 keV have the uncertainty 1-4% [*1*,*2*]. However, the difference between these data and those founded within R-matrix analysis and unified for all ENDF libraries is evident (Fig.1), especially in the energy range 1-60 keV.

The use of the technique of neutron filtered beam developed at the Kyiv Research Reactor makes possible to reduce the uncertainty of the experimental data to 1% and less. These high precision data on natural carbon could stimulate the new run of the R-matrix analysis for C-12.

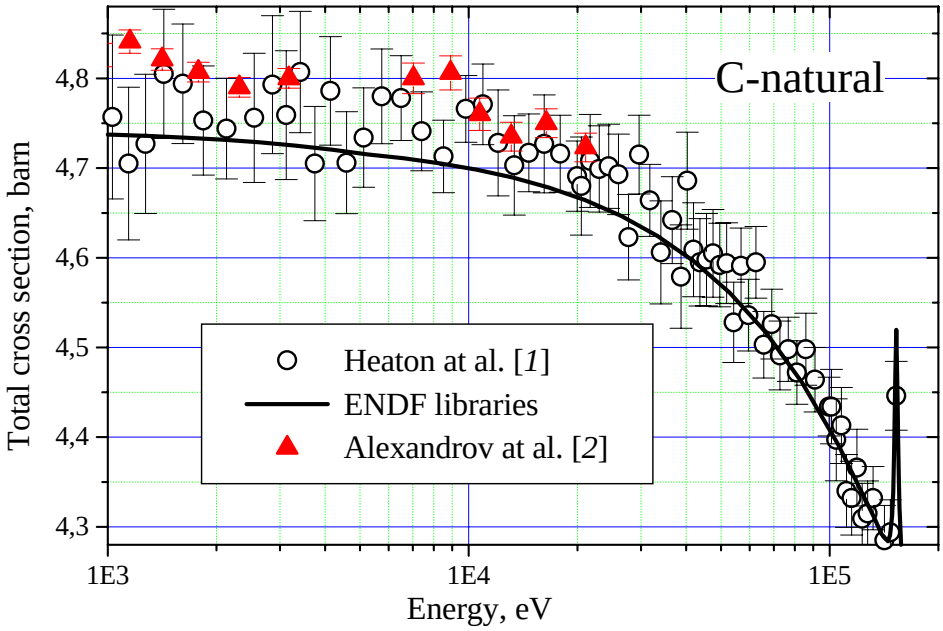

Figure 1. Natural carbon neutron total cross sections.

SUMMARY OF EXPERIMENTAL RESULTS

In our measurements we used the intense neutron filtered beams with average energies 24, 59 and 148 keV. All measurements were fulfilled using transmission technique and proton recoil counters. Experimental installation is similar to one for the Cr-52 cross section measurements, published in [*3*]. To optimize a composition of these filters and to obtain their neutron spectrum shape, the calculations with modified code FILTER_L [*4*] were carried out.

Components of the 24 keV filter were natural Fe (236.22 g/cm^2), Al (112.81 g/cm^2), S (62.1 g/cm^2), and the 85% enriched B-10 (1.0 g/cm^2). The part of main line 24.0 keV was 99.84%, other additions to the main spectra were negligible: 73 keV – 0.14%, 351keV – 0.02%. The limits of 95% response function for 24 keV

This research was supported by LLNL under the contract B513819

filter spectrum were defined as 22.25-24.97 keV. Three samples of reactor carbon (99.9%) with thickness 0.1275925, 0.1751940 and 0.3027865 at/barn were used in these measurements. The final value of total neutron cross section, averaged over all samples was 4.687± 0.006 barn (relative accuracy 0.13%). It is in a good consent with result by R. Block [*5*] - 4.684 ± 0.009 barn, measured with Fe-Al filter and time-of-flight at Linac spectrum.

Components of the 59 keV filter were: the enriched to 83.3 % isotope Ni-58 (83.3 g/cm^2), natural S (133.0 g/cm^2), V (18.33 g/cm^2), Al (5.4 g/cm^2), Pb (28.34 g/cm^2), and the 85% enriched B-10 (0.2 g/cm^2). The main filter line 58.7 keV constituted 98.43 %, contributions to the filtered spectrum of additional neutrons amounted to 0.02% for line at energy 83 keV and 1.5% for a group of lines in the energy range 345-368 keV. Three samples of C were used: 0.0437451, 0.0870349 and 0.2100811 at/barn. The averaged over samples total cross section value was 4.480±0.039 barn (relative accuracy 0.87%). Previous measurements at our reactor [*6*] with somewhat other filter on the basis of Si (energy about 55 keV) gave the value 4.497±0.089 barn.

Components of the 148 keV filter were the following materials: natural Si (197.18 g/cm^2), Ti (12.3 g/cm^2), and the 85% enriched B-10 (1.0 g/cm^2). The part of main line 147.8 keV is 93.72%, contribution of higher energy lines is negligible – 0.02 %. The low-energy lines in the region of 1 keV, 22 keV and 54 keV make more considerable contributions – about 0.3%, 0.05% and 5%, but in process of treatment they may be separated due to the proton recoil counter spectroscopy abilities. The limits of 95% response function for 148 keV filter line were defined as 116.15-156.74 keV. The sample with thickness 0.1275925 at/barn was used for this measurement. The obtained total cross section value is 4.2910 ± 0.0057 barn (relative accuracy 0.13%). Earlier data received at our reactor with the same type of Si filter [*6*] was 4.309±0.018 barn.

REFERENCES

1. H. T. Heaton, J. L. Menke, R. A. Schrack and R. B. Schwartz, “Total Neutron Cross Section of Carbon from 1 keV to 15 MeV.” *Nucl. Sci. Eng*., **56** (1975). pp. 27-31.
2. Yu. A. Alexandrov, I. S. Guseva, A. B. Laptev, N. G. Nikolenko, G. A. Petrov, O. A. Shcherbakov, *Measurement of the Neutron Total Cross Sections for Bi, C, Si, Pb*, Reprint JINR-E3-213, 1997, Dubna.
3. O. Gritzay, V. Kolotyi, O. Kalchenko, P. Vorona, M. Gnidak, “High Precision Measurements of Cr Total Cross Section at Neutron Filtered Beams.” *Journ. Nucl. Sci. Tech*., Supp. 2, **1** (2002), pp. 389-392.
4. O. O. Gritzay, V. V. Kolotyi., O. I. Kalchenko, *Neutron Filters at Kyiv Research Reactor*, Reprint KINR-01-6, 2001, Kyiv.
5. R. C. Block, Y. Fujita, K. Kobayashi, T. Oosaki, “Precision Neutron Total Cross Section Measurements Near 24 keV.” *Journ. Nucl. Sci. Tech*., **12** (1975). pp.1-11.
6. L. Litvinsky, V. Libman, A. Murzin, *Elastic and Inelastic Scattering Neutron Angular Distributions on the Neutron Filter Facility*”, KINR-85-35, 1985, Kyiv.

This research was supported by LLNL under the contract B513819

A New Derivation of the Perturbation Operator Used in MCNP[1]

Keith, R.E.
ITT Industries, Advanced Engineering & Sciences
Colorado Springs, CO 80949-1990, and
Colorado School of Mines, Department of Physics
Golden, CO 80401

Frequently it is desirable to determine the effect that a small change in a cross section, or geometric dimension might have on the result of a transport calculation. For deterministic calculations, this can be accomplished by running a perturbed case, or for cross section perturbations, by using a folding of the forward and adjoint fluxes with the cross section of interest. For Monte Carlo calculations the solution can be more involved. MCNP employs the perturbation operator formalism originally describe by Hall[1]. The MCNP manual[2] and perturbation-operator verification technical report[3] provide a derivation suited to the MCNP coding. In this method the change in a calculation tally result R due to a perturbation of a transport parameter (ν) is calculated using a Taylor series expansion as in Eq.(1).

$$\Delta R = \frac{dR}{d\nu}\cdot(\Delta\nu) + \frac{1}{2}\cdot\frac{d^2R}{d\nu^2}\cdot(\Delta\nu)^2 + \cdots + \frac{1}{n!}\cdot\frac{d^nR}{d\nu^n}\cdot(\Delta\nu)^n + \cdots \tag{1}$$

A new derivation of the derivatives ($\frac{dR}{d\nu}$, etc.) of this expansion has been completed that reproduces the first-order derivative formalism in MCNP exactly, and arrives at a simpler second-order derivative than is found in MCNP. This simpler second-order derivative can be shown to be exactly equal to that in MCNP, but consists of four terms rather than the eight in MCNP.

The formulation of the derivative terms follows along the lines of the actual coding in MCNP. Rather than formulating the derivatives using the microscopic cross sections and determining the change in the tally result due to the microscopic cross sections, the macroscopic cross sections will be the perturbed parameter [ν in Eq.(1)], and the microscopic cross sections will be held constant. A grouping of the microscopic cross section is made such that each group of microscopic cross sections is perturbed by the same factor Eq.(2) shows this grouping for some macroscopic cross section Σ_x. There is also a group of cross sections that is not involved in the perturbation [represented by the zero subscripted group in Eq.(2)].

$$\Sigma_x \equiv \rho_0 \sum_i^{N_0} \sigma_i^0 + \sum_j^n \rho_j \sum_i^{N_j} \sigma_i^j \tag{2}$$

Where Σ_x is the macroscopic cross section, ρ_0 is the unmodified density of the material, the N_0 cross sections σ_i^0 form the group of cross section that are not perturbed, and the σ_i^j values form n groups of cross sections that vary through perturbations of the densities ρ_j.

From this point the derivation of the expression to determine the derivative terms follows the basic pattern used in the derivation found in the MCNP documentation[2][3]. It can be shown that the tally result can be regarded as the sum of the tallies R_ξ of the individual paths (ξ) divided by the number of paths, and that the tally of a specific path can be given by:

$$R_\xi = \sum_j f_\xi \prod_k^{n_\xi} r_{k\xi_k} \tag{3}$$

Where f_ξ is a response multiplier, $r_{k\xi}$ is the particle weight of path segment k of the n_ξ segments that make up path ξ. The determination of the derivative of the tally result becomes the summation of the derivatives of the tallies multiplied by a constant, which in turn becomes the determination of the derivative of the path segments $r_{k\xi}$.

In MCNP, the first derivative $\frac{dr_{k\xi}}{d\Sigma_x}$ consists of four terms. The full derivation along the lines of the summary above reproduces these four terms.

[1]This work was supported by the United States Department of Energy under contract DE-AC04-94AL85000 with technical management by Sandia National Laboratories. Sandia is a multiprogram laboratory operated by Sandia Corporation, a Lockheed Martin Company, for the United States Department of Energy.

As stated above, this new derivation produces a second order term that consists of four terms, rather than the eight found in MCNP. But a closer examination of the eight in MCNP reveals that these eight terms can be expanded out to be identically the four derived in this study. The four terms in the second-order derivative can be shown to be consistent with physical intuition. For example, it can readily be shown that the first and second order derivatives are independent of the specific geometric modeling used, but are dependent only on the distribution of the material. That is, that the results are not dependent on whether a specific material was described by one region, two regions, or several regions.

An additional advantage to this derivation is that it is easy to obtain higher order derivatives for a single perturbation, and to derive the expression for the second order cross derivatives. The third and fourth derivative terms have been derived, and were implemented in a local version of MCNP5. The utility of these terms is admittedly somewhat limited by the nature of a Taylor series expansion, the expansion converges readily for small parameter changes - $\Delta\nu$ in Eq.(1) - but for larger changes the increasing exponent on the change in parameter can keep the expansion from converging. However, there are cases where the perturbation is such that the first and second derivative terms do not well represent the change in the tally result, but the higher derivative terms bring the calculated change result back toward expected values. A sample result (INP10 from the MCNP verification document[3]) is shown in Fig. 1, the red curve represents the change seen from different MCNP calculations, the green curve shows the change using the first and second order terms, and the blue curve shows the change using up to the fourth order terms. It should be noted that at the large change in copper density coupled with the high sensitivity of the result to density in makes this result somewhat surprising as the basic assumption of small perturbations has been violated.

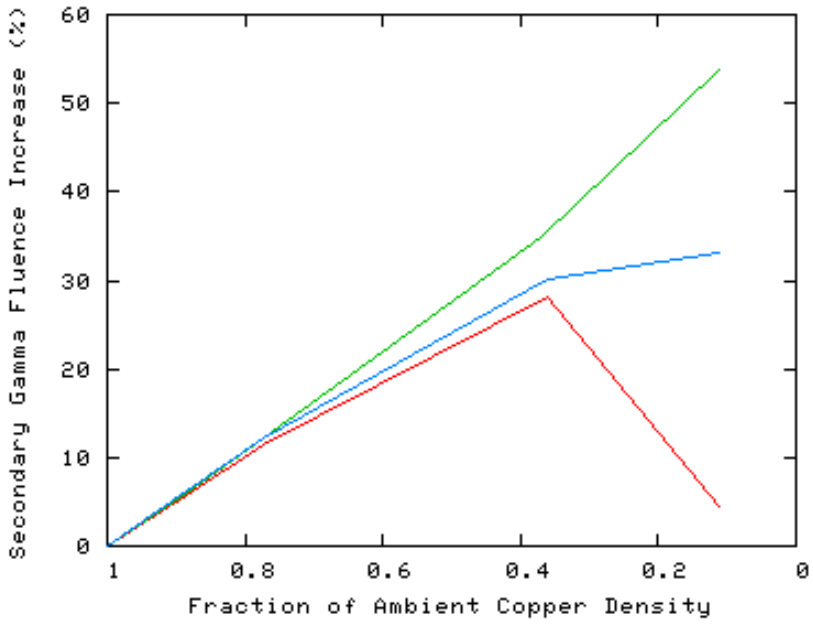

Figure 1: Change in secondary γ fluence in verification case INP10, red curve is "actual" change, the green curve uses up to second order terms, and the blue curve uses up to the fourth order terms.

REFERENCES

1. M. Hall, "Cross-section adjustment with monte carlo sensitivities: Application to the winfrith iron benchmark," *Nucl. Eng. and Sci.*, vol. 81, no. 3, pp. 423–431, 1982.
2. Los Alamos National Laboratory, *MCNP: A General Monte Carlo N-Particle Transport Code*, April 2000. LA-13709-M.
3. G. McKinney and J. L. Iverson, "Verification of the monte carlo differential operator technique for mcnp," Study Results LA-13098, Los Alamos National Laboratory, Los Alamos National Laboratory, Los Alamos, New Mexico 87545, U.S.A., February 1996.

Improved surveillance program realizing at the WWER-1000 reactor of Rovno NPP Unit 4

Grytsenko, O. V., Vasylyeva, E. G., Bukanov, V. N., Dyemokhin, V. L., Pugach, S. M.
Institute for Nuclear Research, Prospect Nauky, 47,
Kyiv, 03680, Ukraine.

The surveillance program (SP) is an important source of information about changing of reactor pressure vessel (RPV) metal properties under NPP operation conditions. At the same time regular SP that is carried out on majority of Ukrainian NPP units with WWER-1000 reactors has essential shortcomings. To eliminate them it was decided to improve SP program for putting into operation Rovno NPP Unit 4. As a result of modernization some shortcomings were eliminated because:

- surveillance specimens (SS) were located in plane containers;
- container assemblies (CA) orientation to the reactor core was optimized to decrease flux gradient on working parts of SS irradiated in the same container;
- dosimetry part of SP was improved.

Plane container orientation to the core ensuring minimal flux gradient at expected SS locations was determined by means of special calculation methodology before modernized CA installation into reactor.

The methodology is based on program package MCSS [*1*], in which Monte-Carlo method is used for neutron transport calculations to the SS locations in WWER-1000 reactor.

For calculation of neutron flux functionals (NFF) at the expected SS locations in WWER-1000 reactor of Rovno NPP Unit 4 the mathematical model of modernized CA was designed. In this model the plane containers with SS were the right parallelepipeds (9.8×3.3×7.2 cm) conditionally divided into five parts by their width and height and into two parts by their thickness. Each of container parts arisen after such division was separate calculational detector.

Calculations of NFF at the expected locations of modernized CA in reactor of Rovno NPP Unit 4 were performed for the set of given orientations of plane containers with SS to the core. First of all container models were located in such a way that the angle between the normal to plane of SS location and the radius of RPV crossing the container center was 0 degree.

Calculation results showed that in this case difference of fluxes with E_n>0.5 MeV along horizontal in SS location plane had reached 15% excluding CA L3 for all sets.

Then container models of modernized CA were turned around the axis parallel to the reactor pintle to fixed angles and for each location the NFF on SS were determined.

Calculation result analysis allowed the determination of the optimal plane container orientation to the core. This orientation ensured minimal, not exceeded some percent, difference of fluxes with E_n>0.5 MeV along horizontal in SS location plane.

It should be mentioned that independently of container locations to the core the difference of fluxes with E_n>0.5 MeV obtained for first and second SS rows was ~15%.

The scheme of neutron activation detectors (NAD) installation into containers was designed taking into account results of NFF calculations at the expected locations of modernized CA in WWER-1000 reactor of Rovno NPP Unit 4. According to this scheme there were installed the lengthy NAD in the form of wires from metallic iron, niobium, copper in all containers of both upper and lower floors of each CA for determination of neutron fluences on SS working parts.

Lengthy NAD were installed in aluminum fillers of containers on the levels of SS working parts and also in the space formed by V-notches of adjacent Charpy SS. In addition NAD were located in the middle of both upper and lower parts of Charpy and COD SS. It allowed the determination neutron fluences on working parts of reconstructed SS in case of SS reconstruction technology applying.

The methodology for determination of neutron fluences with E_n>0.5 MeV on SS working parts was based on using of calculated neutron field characteristics at the locations of irradiated SS and results of measurements of specific activities for products of $^{93}Nb(n,n')^{93m}Nb$, $^{54}Fe(n,p)^{54}Mn$, $^{63}Cu(n,\alpha)^{60}Co$ reactions.

Use of lengthy NAD provided calculation the neutron flux gradient along SS location plane in containers.

Thus, the scheme of modernized CA location in reactor of Rovno NPP Unit 4 described above allows the minimization of neutron flux gradient along SS location plane and dosimetry of the program allows a reliable determination of neutron fluences with E_n>0.5 MeV on working parts of irradiated SS.

REFERENCES

1. Bukanov, V. N., Dyemokhin, V. L., Gavriljuk, V. I., Grytsenko, O. V., Nedyelin, O. V., Vasylyeva, E. G., *Overview of the Surveillance Dosimetry Activities in Ukraine*, Reactor Dosimetry: Radiation Metrology and Assessment, ASTM STP 1398 (Proc. 10th Intern. Symp. on Reactor Dosimetry, Osaka, Japan, 12-17 Sept. 1999.) –ASTM, West Conshohocken, PA, 2001. pp. 61-68.

TRACK DETECTOR MEASUREMENTS IN RPV OF WWER-1000 MOCK-UP IN THE LR-0 REACTOR

B. Ošmera, S. Pošta, NRI Řež, Czech Republic , osm@ujv.cz
N.I. Karpunin, S.S. Lomakin, SEC GOSATOMNADSOR, Russia

ABSTRACT

The fission rates measurements were carried out with track detectors in the WWER-1000 Mock-up assembled in the experimental reactor LR-0.

Solid-state track detectors consist of the targets with fission isotopes and the mica foil detectors of the fission products fragments.

The ^{238}U and ^{236}U isotopes with the energy thresholds approximately 1.5 MeV and 0.8 MeV respectively were used; the number of target nuclei was not less than 4.9 10^{17}. The tracks were counted by means of photomicroscope with digital camera controlled by PC with corresponding software.

The WWER-1000 model [1] in this experiment was equipped with a simulator of the surveillance specimens box which was situated at the LR-0 tank, perpendicularly to the model core axis. The detectors were positioned before the RPV (reactor pressure vessel) and in one quarter of the RPV simulator in the central plane of the model core along the model axis. The total exposure was about 24 hours in five time intervals. The tracks was counted in both laboratories, SEC and NRI, to compare the evaluation methodologies.

The track detectors were positioned in the points where the neutron and photon spectra were measured with stilbene spectrometer. The power was monitored with two, fixed and movable, low noise measuring channel equipped with fission chambers. The system can cover four orders in neutron flux distribution (power). The measured values (absolute fluxes) used to be evaluated per count of the fixed monitoring chamber.

The fission rate ratio of ^{236}U and ^{238}U will have been evaluated in both measuring points as well as the fast neutron fluxes, attenuation factors. The results, measured with different techniques will have been compared. According to the preliminary evaluation the fast flux above 0.5 MeV measured before RPV simulator with stilbene detector differs from flat one evaluated from ^{238}U (n, f) trash detector in 10 %. The results are correlated via the spectrum shape of the stilbene measurement which was used for ^{238}U (n, f) integral cross seetiction calculation. The BUGLE 96 ^{238}U (n, f) cross section have been used. The correction for photofission will have been included.

[1] B. Ošmera, S. Zaritsky, Review of Experimental Data for WWER Reactor Pressure Vessel Dosimetry Benchmarking, paper presented to 11th ISRD, Brussels, 2002

Reactor Dosimetry Study of the Rhode Island Nuclear Science Center

Holden N. E., Reciniello R. N., Hu J.-P.
Brookhaven National Laboratory
Upton, NY 11973, USA

Leith J., Tehan T. N.
Rhode Island Nuclear Science Center
Narragansett, RI 02882, USA

The Rhode Island Nuclear Science Center facility (RINSC [*1*]) is a 2 mega-watt thermal, light water, open-pool type reactor. It is light water moderated and has beryllium and graphite elements surrounding the fueled core as neutron reflectors. The experimental ports include six beam tubes, a thermal column, a gamma-ray experimental facility and two pneumatic tubes. The reactor core residing at the center of the critical assembly has fourteen low enrichment uranium fuel elements (LEU, 19.75% ^{235}U plates) located in a grid box at twenty-six feet below the pool surface. The plate-type fuel is aluminum clad in the form of U_3Si_2Al. The total amount of ^{235}U in the fresh LEU core is 3.85 kilograms.

The reactor's thermal column is a graphite pile, which is 56 inches by 56 inches by 8 feet long within a concrete biological shield. There is a three-inch lead shield and a two-inch aluminum cooling plate (31 inches downstream of the lead shield) between the reactor core and the thermal column, which extends to the outer face of the concrete shield. The thermal column is made up of consecutive graphite blocks, each being four-inch by four-inch in cross section. Near the centerline of the thermal column, a two-inch by two-inch air beam hole has been designed to accommodate samples and apparatus for experimental usage. Since 1996, several measurements of the thermal and the epithermal neutron flux have been performed along this beam hole, using indium foils and cadmium covers.

Calculations of the thermal and the epithermal neutron fluxes at six-inch intervals along the air beam hole in the thermal column have been made using a Monte Carlo based program, MCNP[*2*]. Comparison between the measured and calculated neutron fluxes shows good agreement (< 10% uncertainty) in the thermal energy range (E_n < 0.5 eV), and acceptable agreement (< 20% uncertainty) in the epithermal energy range (0.5 eV < E_n < 10 keV). The results are shown in figures 1 and 2.

In figure 3, the MCNP calculated photon flux at six-inch intervals along the thermal column is shown.

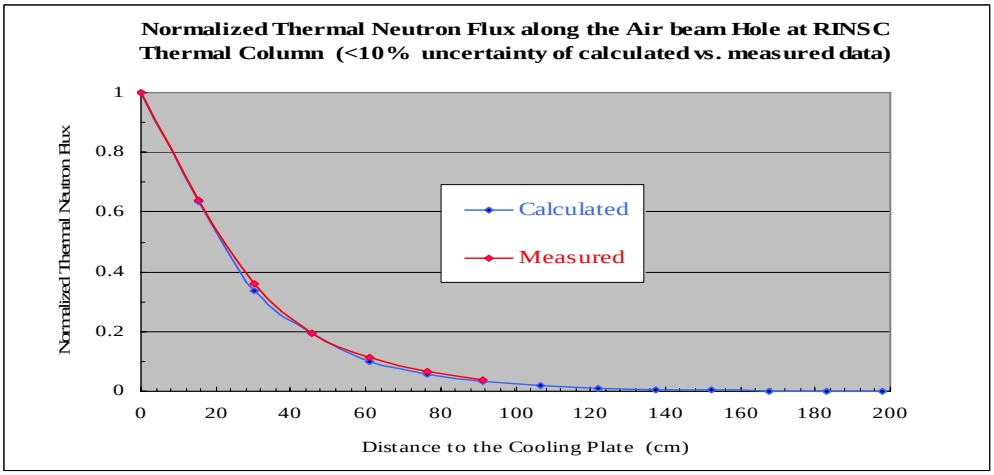

Figure 1. Comparison of MCNP calculated versus foil measured thermal neutron flux along the central air beam hole at RINSC thermal column.

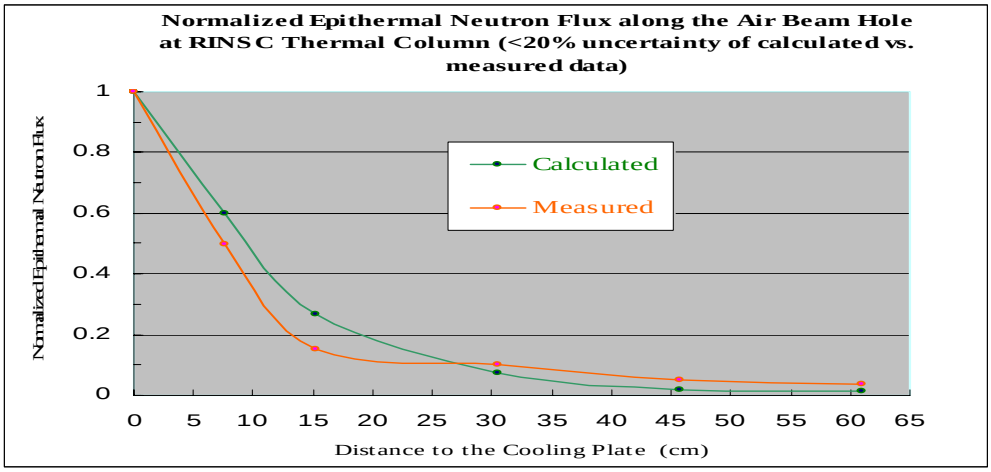

Figure 2. Comparison of MCNP calculated versus foil measured epithermal neutron flux along the central air beam hole at RINSC thermal column.

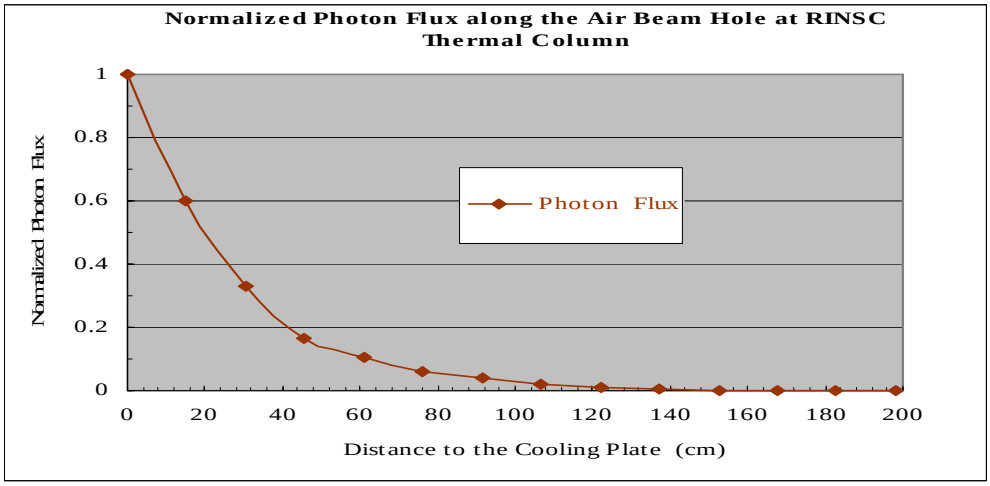

Figure 3. MCNP calculated photon flux along the central air beam hole at RINSC thermal column.

1. Rhode Island Nuclear Science Center (RINSC), edited in the Research, Training, Test and Production Reactor Directory – United States of America (1st edition), pages 1091-1112, published by the American Nuclear Society (1980).
2. J. F. Briesmeister (editor), MCNP – A Monte Carlo N-Particle Transport Code (version 4B2), developed by the Los Alamos National Laboratory (LA-12625-M), and distributed by the Oak Ridge National Laboratory (CCC-660) (1997).

Surveillance Specimen Programmes in Czech NPPs

Brumovký, M., Marek, M., Zerola, L., Rataj, J., Novosad, P., Kytka, M.
Nuclear Research Institute Rez plc
250 68 Rez, Czech Republic

Hogel, J., Brynda,J.
SKODA Nuclear Machinery plc
316 00 Plzen, Czech Republic

Surveillance specimens programmes from reactor pressure vessel materials are one of the most important parts of in-service inspection programmes that are necessary for realistic and reliable assessment of reactor pressure vessel residual lifetime. Structure, volume, type of specimens, withdrawal schedule and testing procedures depend, first of all, on time when reactor was designed, and also, on volume and other possibilities of reactor pressure vessel construction. Thus, these surveillance programmes represent, on one side, knowledge (state-of-the-art) of assessment of resistance against failure and of irradiation embrittlement, and on the other side, possibilities of individual pressure vessel internal part locations.

Two types of reactors are in operation in the Czech Republic – VVER-440 MW/V-213C type and VVER-1000 MW/V-320C type. Both types are characterized by small vessel radius as a result of the requirement for their transportation by land. Thus, surveillance programmes are designed and realised in different way than in PWR type RPVs.

VVER-440/V-213 type reactors were originally designed with the Standard Surveillance Programme, which lasted practically only five years due to its high lead factor (13 for base metal and 18 for weld metal). Monitoring of RPV material changes in realistic conditions required implementation of Supplementary Surveillance Programme – changes in container design, specimens design and manufacturing, adding materials from austenitic cladding as well as insertion of so-called dosimetry chains are described in the paper. Substantial changes in neutron dosimetry in individual containers using activation and fission monitors in foil as well as wire form allow to determine neutron fluence field within the whole container and thus also neutron fluence for each specimen. Comparison of location and type of monitors in the Standard and Supplementary Programmes is given in Figs. 1 and 2.

VVER-1000/V-320 type reactors were originally designed with Standard Surveillance Programme that was located above the reactor active core where irradiation conditions are not representative – different neutron energy spectra, higher temperature and steep neutron flux gradient as well as small number of neutron monitors. Thus, Modified Surveillance Programme was designed for Czech NPP in Temelin (and Bulgarian in Belene) where containers were located on the inner RPV wall in beltline region – all specimens for one withdrawal are irradiated at once and are supplied by several sets of foil and wire monitors of activated and fission type (with and without shielding).

The paper describes individual surveillance programmes in detail together with analysis of their advantages and disadvantages. Detailed attention is given to neutron dosimetry and some examples are also given.

The Modified Surveillance Programme for VVER-1000/V-320C type in NPP Temelin was proposed and then chosen as a “host” reactor for the Integrated Surveillance Programme for several VVER-1000 units operated in the Czech Republic, Ukraine and Bulgaria.

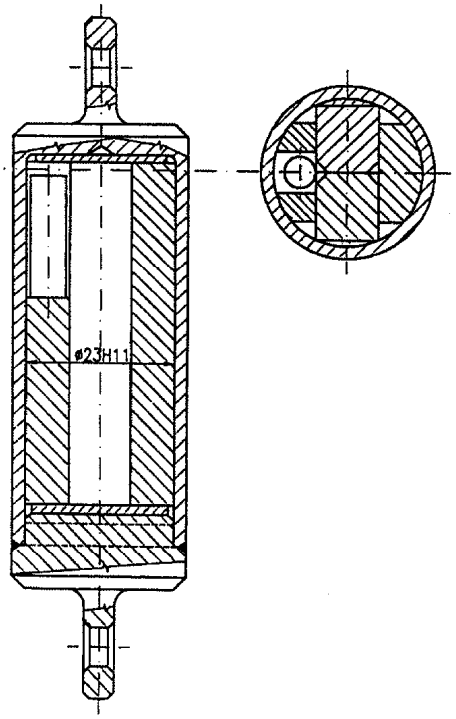

Fig. 1 Scheme of a container from the Standard Surveillance Program

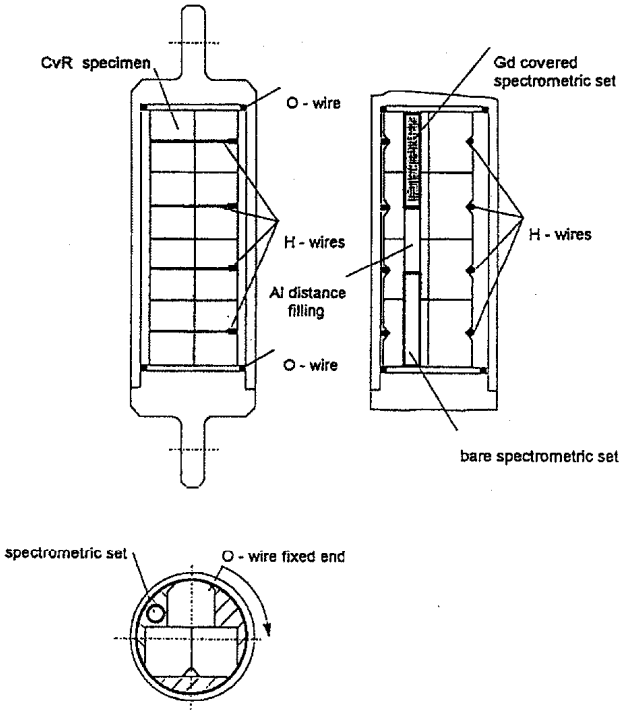

Fig. 2 Scheme of a container from the Supplementary Surveillance Program

Calculation of Neutron Fluxes for Radioactive Inventory Analysis of Magnox Power Plant

Allen, D.A, Lewis, T.A., Thiruarooran, C., Thornton, D.A.,
British Nuclear Group, Berkeley Centre, Berkeley,
Gloucestershire, GL13 9PB, United Kingdom.

Bird, A.J., Ryecroft, S.,
Serco Assurance, Winfrith Technology Centre, Dorchester,
Dorset, DT2 8DH, United Kingdom.

INTRODUCTION

In 2000, BNFL Magnox announced closure dates for each of its Magnox power plants, and preparations for decommissioning are now well underway. Radioactive inventory assessments are requirement for the efficient future management of the decommissioning process and neutron fluxes for the estimation of activation are an important component of that inventory assessment.

This paper describes radiation transport calculations performed to provide the neutron flux input data for the calculation of radioactive inventories for the UK's Magnox reactors using a methodology based closely upon that developed for the dosimetry assessments of the reactor pressure vessels of the Magnox plant [1, 2, 3].

REQUIREMENTS

The current radioactive inventory analyses for Magnox power plant require neutron flux data grouped as thermal and epi-thermal. In subsequent analysis, these data are combined with 2200 ms^{-1} cross sections and resonance integrals to estimate the required reaction rates.

The neutron flux estimates are required for every component of the reactors. The larger components are split into regions as there may be marked differences in activation across them, which may ultimately affect their disposal route.

MONTE CARLO MODELS

Detailed models of the Magnox reactors were originally developed for the assessment of neutron doses to the steel reactor pressure vessels (RPV) using the UK radiation transport code MCBEND. These semi-explicit models were successfully validated against fast and thermal neutron activation measurements performed within and just outside the RPV [1, 2, 3]. Having given C/M (calculated / measured) ratios within 25% of unity, there is a high degree of confidence in the predictions of these models.

In order to use the models for the purpose of calculating fluxes for inventory analyses, it was necessary to extend them in order to improve the representation of plant out to the outer edges of their biological shields. Attention has been paid to key streaming pathways within ex-RPV components. In addition, being the most massive components in the reactor, the biological shields have been sub-divided into four layers.

METHODOLOGY

While the calculations were performed in 'continuous energy', the results of the calculations have been provided in two groups: thermal flux (Westcott), and epi-thermal flux ($E_n > 0.5eV$), consistent with the requirements of the radioactive inventory analysis. Initial Monte Carlo calculations demonstrated that fluxes defined in these groups are capable of giving activation rates for the reactions of interest to within ±25%. This is easily adequate for the requirements of the analysis.

The calculations were broken down into regions below the core, to the side of the core and above the core. Calculations in each of these regions were split into stages. Use of variance reduction proved impracticable, and was consequently not used, except for the use of multiple stages enabling multiple use of Monte Carlo samples reaching

the stage interfaces. Lengthy run times were necessary for some of the biological shield calculations. Results from each stage, and each of the three regions, were then combined to give mean component fluxes in the two groups.

RESULTS

Neutron fluxes have been successfully provided for modeled components of the plant, including the biological shield. Because the method scored regionally averaged fluxes, attenuation within components is taken into account. For the massive, outer regions of the biological shield, the fluxes calculated in this way are dominated by the scoring samples in the high flux locations of the shield region. Provided the material is uniform, the absence of scoring samples in low flux locations of a region will not affect the accuracy of its predicted activation rates.

It has been possible to exploit the staging of the calculations in order to illustrate and compare the attenuation of the two flux groups through the biological shield. These have provided meaningful flux data for biological shield penetrations of up to 2m.

Additional sensitivity studies have been performed to determine the significance of modeling accuracy. One of the most important parameters is the water content of the concrete, which is currently uncertain. Neutron fluxes in the outer layers of the shield are so sensitive to this that it will probably be necessary to rely upon measurements.

Notwithstanding uncertainties associated with the water content of the concrete of the biological shield, it is estimated that fluxes calculated are accurate to a factor of two within the inner surface of biological shield and up to a factor five into the shield.

ACKOWLEDGMENTS

This paper is published with the permission of British Nuclear Group.

REFERENCES

1. J.R. Mossop, D.A. Thornton, T.A. Lewis , "Validation of Neutron Transport Calculations on Magnox Power Plant" *Proceedings of the 8th International Symposium on Reactor Dosimetry,* ASTM Special Publication 1228 (1994), pp. 384-391.
2. T.A. Lewis, S.E. Hopper, J.R. Mossop, D.A. Thornton, "The Prediction of Fast and thermal Neutron Dose Rates for the Pressure Vessels of Magnox Power Plant" *Proceedings of the 9th International Symposium on Reactor Dosimetry,* World Scientific (1996), pp. 600-607.
3. T.A. Lewis , D.A. Thornton, *"A Decade of Dosimetry for Magnox Reactor Plants", Proceedings of the 9th International Symposium on Reactor Dosimetry,* World Scientific (2003), pp. 269-277.

Radiation Damage Calculation and Database

W. Lu and M. S. Wechsler
Department of Nuclear Engineering, North Carolina State University, Raleigh, NC 27695

A radiation damage database is in preparation at NCSU in collaboration with investigators at the Los Alamos National Laboratory. The database is to contain primarily damage energy, displacement, helium, hydrogen, and heavier transmutation-product cross sections (CS's). Also, it is anticipated that information may also be present concerning experimental observations that serve to evaluate the validity of the calculations. Other items that may be included are proton and neutron fluxes and spectra at nuclear facilities, recoil and damage energy spectra, neutron yields upon proton bombardment, threshold displacement energies, and radiation damage literature compilations.

CS's for damage energy, displacements, helium, and hydrogen have now been calculated or downloaded from other sources for protons and neutrons on about 22 elemental targets extending from Mg to U for energies from 1E-8 MeV or lower to 3.2 GeV. We discuss these CS's as follows:

Low-energy CS's (1E-8 MeV or lower to 20 MeV)

The neutron CS's are derived from ENDF-6 [*1*] and SPECTER [*2*]. Typical results are shown in FIG. 1 for the damage energy CS for neutrons on Al. The ENDF CS's show large sharp swings in value due to resonance reactions in the energy range from about 0.01 to 1 MeV. The SPECTER CS's are largely in agreement with the ENDF data, but the swings are averaged out. For energies below 1E-4 MeV, we see a linear region (on the ln-ln plot) with slope of -1/2, presumably due to energy transfer from n-gamma recoils.

For low-energy transfers due to protons, we use SRIM [*3*]. FIG. 2 shows damage energy CS's for protons on a number of targets from Mg to W. The slopes of the lines in FIG. 2 indicate a 1/E dependence on proton energy, consistent with Rutherford scattering. SRIM is based solely on elastic interactions.

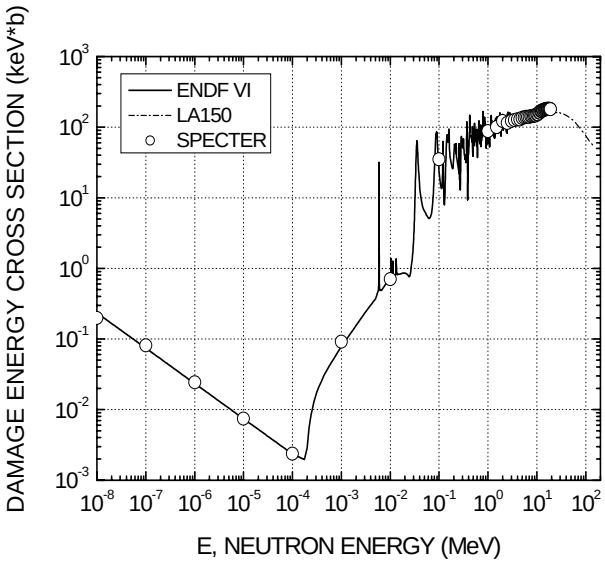

FIG. 1. Damage energy cross section vs neutron energy for Al, as calculated by ENDF, SPECTER, and LA150.

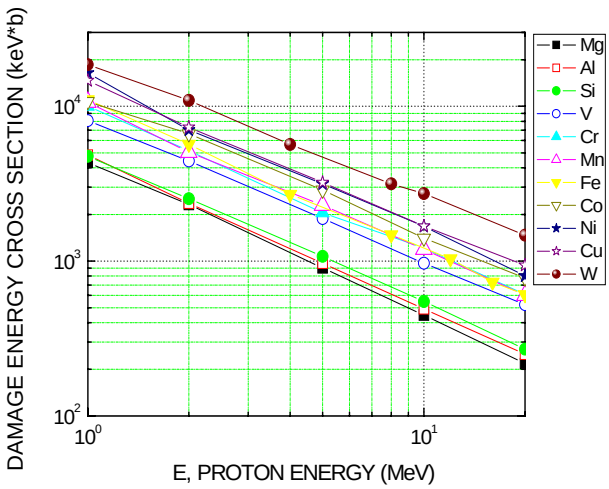

FIG. 2. Damage energy cross section vs proton energy for Al as calculated by SRIM 2003.

Medium-energy CS's (20 to 150 MeV)

For this range of energies, we use the LANL-based LA150 CS's [*4*]. FIG. 1 shows reasonable agreement between LA-150 CS's and ENDF-6 or SPECTER at 20 MeV for neutrons on Al. This agreement has generally also been found to be the case for the other targets. FIG. 3 shows the LA150 CS's again for comparison with the high-energy CS's.

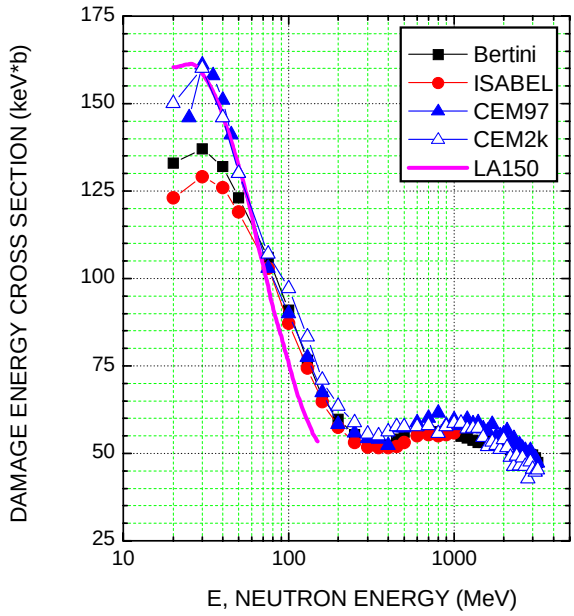

FIG. 3. Damage energy cross section vs neutron energy for aluminum, as calculated byLA150 and by MCNPX using the Bertini, ISABEL, and CEM INC models.

High-energy CS's (150 MeV to 3.2 GeV)

The high-energy CS's are based on our calculations with LAHET [*5*] within MCNPX, which includes three intranuclear cascade (INC) models: Bertini, ISABEL, and CEM [*6*]. In addition, for the first two of these there are three level-density formulations (GCCI, HETC, or Juelich) to be chosen and a multistage pre-equilibrium model (MPM) may be set on or off, but these choices affect mostly the He and H CS's, not damage energy and displacements. FIG. 3 shows damage energy CS's from 20 MeV to 3.2 GeV, as calculated with Bertini and ISABEL INC's and with two versions of CEM. The three INC models give somewhat different values below about 70 MeV, but are in approximate agreement above 70 MeV. Also, CEM agrees with the LA150 values below 70 MeV, but lies above LA150 curves above 70 MeV. On balance, the current thinking is to use LAHET/CEM2k above 150 MeV and LA150 from 20 to 150 MeV.

We have presented in this summary results concerning damage energy CS's for Al. In the full paper, displacement, He, and H CS's will also be covered for a representative range of targets that have been studied, including experimental findings that help to validate the calculations. The ultimate objective of the database is to make available to the nuclear community a useful, authoritative, and convenient source of radiation damage information.

References

1. V. McLane, Editor, ENDF-102, *Data Formats and Procedures for the Evaluated Nuclear Data File ENDF-6*, BNL-NCS-44945-01/04-Rev., National Nuclear Data Center, Brookhaven National Laboratory, Revised April 2001.
2. L. R. Greenwood and R. K. Smither, *SPECTER: Neutron Damage Calculations for Materials Irradiations*, ANL/FPP/TM-197, Argonne National Laboratory, Argonne, Illinois, 60439, January 1985.
3. http://www.srim.org.
4. M. B. Chadwick, H. G. Hughes, R. C. Little, E. J. Pitcher, and P. G. Young, "Nuclear Data for Accelerator-Driven Systems." *Progress in Nuclear Energy*, **38** (2001) pp. 179-219.
5. R. E. Prael and H. Lichtenstein, *User Guide to LCS: The LAHET Code System*, LA-UR 89-3014, Radiation Transport Group, Los Alamos National Laboratory, Los Alamos, NM, September 1989.
6. S. G. Mashnik, A. J. Sierk, O. Bersillon, and T. Gabriel, Cascade-Exciton Model Detailed Analysis of Proton Spallation at Energies from 10 MeV to 5 GeV, *Nucl. Instr. Meth.* A414 (1998) 68-72. Also, Report LA-UR-97-2905, Los Alamos National Laboratory, Los Alamos, NM, 1997.

Extensive Revision of the Kernel-based PREVIEW Program and its Input Data

Serén, T. O.
Wasastjerna, F.
VTT Technical Research Centre of Finland
P.O.Box 1608
FI-02044 VTT, Finland

INTRODUCTION

The kernel-based PREVIEW program has been extensively and successfully used as a convenient tool in the surveillance dosimetry for the Loviisa VVER-440 reactors [*1*], [*2*]. It calculates many quantities of interest, such as fluences, reaction rates and activities, taking into account the detailed local irradiation history. An adjustment library based on a large number of activation measurements and spectrum adjustments at different locations has been developed [*3*]. A major revision of the code has been carried out and its database of dosimetry and damage cross sections is being updated. The tools for updating the cross sections have been developed and will be applied to the IRDF-2002 library as soon as it is released [*4*].

REVISION OF THE CODE

The user input has been extensively revised and simplified. The output formats have also been revised and more complete information on the fine-group neutron spectra is given. To facilitate the editing and modification of the kernel file it is now read in only in text form, since disk capacity and speed is no longer an issue. Some features of the Fortran 90 standard have replaced previously system-dependent code so that it should now be completely portable between compilers and operating systems.

The dosimetry and damage cross sections were previously part of the large kernel library, which made it tedious to make any changes to the cross sections. Thus common condensed cross sections in the 47-group BUGLE-80 structure were used for all radial locations (surveillance position, RPV inner surface, RPV quarter-thickness and cavity). This is somewhat questionable if the best possible accuracy is desired. The dosimetry and damage cross sections are now read in from separate dedicated files, which are much easier to adapt to different locations and configurations (e.g. Cd or Gd covers). The adjustment library has also been moved from the code itself into a separate file for easier modification.

LOCATION-SPECIFIC CROSS SECTION FILES

Weighting spectra for all the radial locations of interest have been constructed based on typical 47-group spectra calculated with PREVIEW and applying the adjustment library [*3*]. For the cavity location the adjusted spectra from the 1998-99 irradiation in Loviisa 1 [*5*] were used directly. A least-squares spline approximation on log-log scale [*6*] was applied to expand the 47-group spectra to a point representation at the 641 SAND-II group boundaries, with Maxwellian and Watt-type extensions at the lower and upper end, respectively. Special attention was paid to the choice of effective neutron temperatures in the thermal region. The four weighting spectra are shown in Fig. 1.

These spectra will be applied to selected cross sections from the IRDF-2002 library to produce location-specific 47-group cross section files. This will provide an opportunity to test and compare different codes for cross section condensation, such as FLXPRO from the LSL-M2 package [*7*], X333 from the NMF-90 package [*8*] and the JANIS software [*9*]. This work will be completed as soon as the IRDF-2002 library is released. Preliminary investigations indicate that the influence of different weighting spectra on the total response is usually small (<1 %), but may be larger in some energy groups, which may be important in spectrum adjustments.

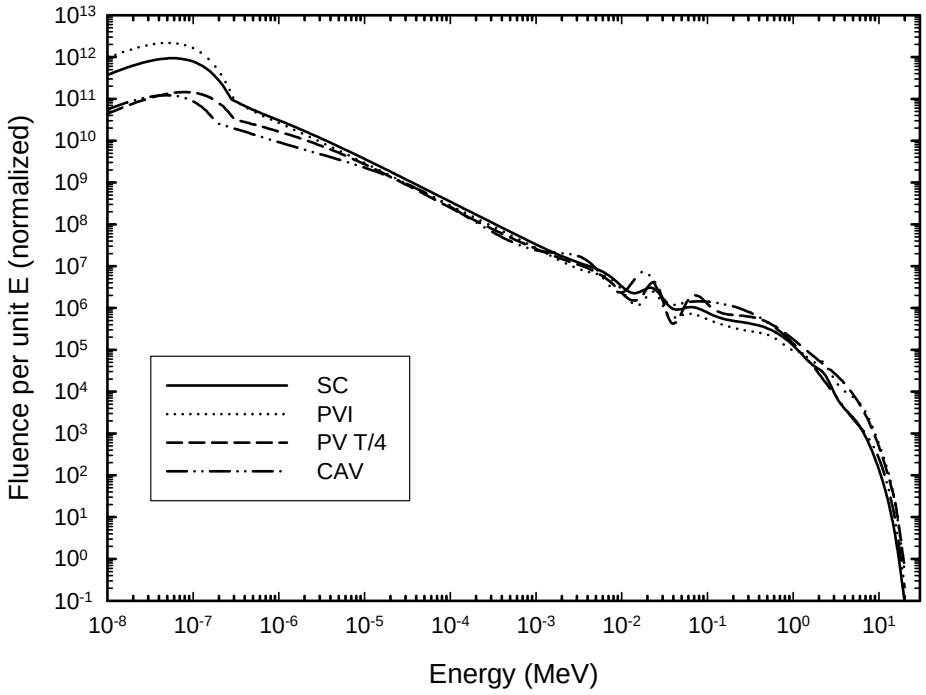

Figure 1. Weighting spectra constructed for four radial locations in the Loviisa VVER-440 reactors.

REFERENCES

1. F. Wasastjerna, "PREVIEW – A Fast Kernel-based Program for Calculation of Pressure Vessel Irradiation." *Proceedings of the ANS Topical Meeting on New Horizons in Radiation Protection and Shielding*, Pasco, Washington, April 26 – May 1, 1992.
2. L. B. Baers and T. O. Serén, "Revision of Neutron Dosimetry for the Loviisa VVER-440 Reactors: Principles and Application." *Reactor Dosimetry, Proceedings of the 8th ASTM-Euratom Symposium on Reactor Dosimetry*, Vail, Colorado, August 29 – September 3, 1993, ASTM STP 1228, Philadelphia 1994, pp. 45-54.
3. T. O. Serén, "Development of an Adjustment Library for the Kernel-based PREVIEW Program." *Proceedings of the 9th International Symposium on Reactor Dosimetry*, Prague, Czech Republic, 2-6 September 1996, World Scientific, Singapore 1998, pp. 278-285.
4. R. Paviotti-Corcuera *et al.*, "International Reactor Dosimetry File: IRDF-2002." *Reactor Dosimetry in the 21st Century, Proceedings of the 11th International Symposium on Reactor Dosimetry*, Brussels, Belgium, 18-23 August 2002, World Scientific, Singapore 2003, pp. 654-661.
5. T. Serén, J. Högel and W. P. Voorbraak, "Post-Annealing Ex-Vessel Dosimetry at Loviisa 1 – An International Exercise." *Reactor Dosimetry in the 21st Century, Proceedings of the 11th International Symposium on Reactor Dosimetry*, Brussels, Belgium, 18-23 August 2002, World Scientific, Singapore 2003, pp. 18-25.
6. B. J. Thijsse, M. A. Hollanders and J. Hendrikse, "A Practical Algorithm for Least-Squares Spline Approximation of Data Containing Noise." *Computers In Physics*, **12** (1998), pp. 393-399.
7. F. W. Stallmann, *LSL-M2: A Computer Program for Least-Squares Logarithmic Adjustment of Neutron Spectra*, NUREG/CR-4349 (ORNL/TM-9933), ORNL (March 1986).
8. E. J. Szondi and H. J. Nolthenius, *User's Guide to the Cross Section Processing Code X333*, BME-NTI 222/95, Technical University of Budapest (May 1995).
9. N. Soppera *et al.*, *JANIS User's Guide*, OECD Nuclear Energy Agency, Paris (July 2004).

Reactor Pressure Vessel Radiation Exposure Monitoring at Khmelnitskaya NPP Unit 2 and Rovno NPP Unit 4 Which Are Set into Operation

Bukanov, V. N., Dyemokhin, V. L., Grytsenko, O. V., Vasylyeva, E. G., Pugach, S. M., Pugach, A. M.
Institute for Nuclear Research, Prospect Nauky, 47,
Kyiv, 03680, Ukraine.

The safe operation of WWER-1000 reactor, realization of safety life management program for main equipment of reactor facility require to develop and introduce at the NPP the systems that should provid the registration of neutron-physical parameters influencing the capacity for work of Unit's first loop elements on the modern scientific and engineering level. The system for monitoring of radiation exposure onto reactor pressure vessel (RPV) belongs to such systems.

The systems for monitoring of radiation exposure onto RPV were installed at the units Khmelnitskaya NPP Unit 2 and Rovno NPP Unit 4 which are set into operation. They are to determine of irradiation conditions, current and accumulated radiation exposure of specific RPV zones.

To the specific WWER-1000 RPV zones belong:

- RPV upper shell welds zones (weld №3 and №4);
- RPV zones where current and / or accumulated radiation exposure has maximum value. As a rule these zones are located little above the level of the most powerful layer of reactor core.

The irradiation conditions are characterized by a set of values of neutron flux functionals onto RPV to which first of all belong:

- neutron fluence with energy above 0.5 MeV;
- reduced to nominal power and averaged over the fuel cycle integral neutron flux with energy above 0.5 MeV;
- spectral index which is calculated as a ratio of neutron fluence with energy above 0.5 MeV to neutron fluence with energy above 3.0 MeV;
- dpa caused by neutrons with energy above 0.5 MeV and reduced to nominal power and averaged over the fuel cycle dpa rate.

The current RPV radiation exposure is the maximum fast neutron fluence onto the inner surface of specific RPV zones or the maximum dpa caused by neutrons with energy above 0.5 MeV over the fuel cycle. The accumulated RPV radiation exposure is the maximum fast neutron fluence onto the inner surface of specific RPV zones or the maximum dpa caused by neutrons with energy above 0.5 MeV over all time of Unit operation.

Neutron flux functionals characterizing the WWER-1000 RPV irradiation conditions will be determined around perimeter of RPV specific zones onto the cladding, the inner RPV surface and in the depth of 1/4 and 3/4 wall thickness for each Unit fuel cycle.

The basis of system for monitoring of radiation exposure onto RPV for Khmelnitskaya NPP Unit 2 and Rovno NPP Unit 4 is the methodology which includes numerical neutron transport calculations within WWER-1000 reactor near-vessel space and ex-vessel dosimetry by neutron-activation method.

Code package MCPV is intended for numerical neutron transport calculations. The main package module is transport code that is performing the calculation of neutron flux functionals within reactor near-vessel space by the Monte-Carlo method in multigroup approximation of neutron transport theory.

Special equipment allows to locate neutron-activation detectors from niobium, iron, titanium and cooper at the outer RPV surface. Main elements of it were installed in the under-reactor room. Equipment construction was determined by the degree of units' readiness at the moment of beginning of system for monitoring of radiation exposure onto RPV creation.

Detectors were made of certified materials for neutron dosimetry and look like discs with diameter 5 mm and thickness from 0.1 to 1.0 mm.

Neutron-activation detector sets are located at the outer RPV surface on the specific zone levels for irradiating during fuel cycle. Azimuth detector location scheme at these levels is determined by fuel loading characteristics. Special methodology is intended for allocation of point coordinates where neutron-activation detectors were placed during irradiation.

Specific activities at the end of irradiation for products of activation reactions $^{93}Nb(n,n')^{93m}Nb$, $^{54}Fe(n,p)^{54}Mn$, $^{nat.}Ti(n,x)^{46}Sc$, $^{63}Cu(n,\alpha)^{60}Co$ are used as reference values during RPV radiation exposure determination.

Ten sets of neutron-activation detectors from niobium, iron, titanium and cooper were located at the outer RPV surface before the first fuel cycle of Khmelnitskaya NPP Unit 2 beginning at the each level: weld №3, weld №4 and the level of expected maximum radiation exposure.

Moreover four detectors from iron were located at each level additionally to allocate point coordinates where neutron-activation detectors were placed during irradiation.

Eleven sets of neutron-activation detectors from niobium, iron, titanium and cooper were located at the outer RPV surface before the first fuel cycle of Rovno NPP Unit 4 beginning at the each level: weld №4 and the level of expected maximum radiation exposure. Six sets were located at the weld №3 level.

In addition six iron detectors were located at the weld №3 level and four iron detectors were placed at the each other levels.

Detector location schemes were determined by fuel loading characteristics for reactors of Khmelnitskaya NPP Unit 2 and Rovno NPP Unit 4.

Neutron-activation detector location schemes for following fuel loadings of each Unit will be determined by means of analysis of data obtained for the first fuel cycles.

Uncertainties of specific RPV zones radiation exposure monitoring results should be evaluated within a few years of Khmelnitskaya NPP Unit 2 and Rovno NPP Unit 4operation. This evaluation is needed for reliability comparison of surveillance specimens and RPV irradiation conditions in order to transpose the irradiated specimens testing results onto the RPV metal.

Investigation of Radiation Transport Modeling Trends in the WSMR MoLLY-G Environments[1]

Sparks, M.H., Sallee, W.W., Flanders, T.M.
White Sands Missile Range
White Sands, NM 88002-5158, USA.

Radiation transport calculations provide the backbone for the spectrum characterization used to support experimenters at research reactors. The radiation transport calculations provide the *a priori* neutron spectrum that is used in least squares spectrum adjustment. In addition, calculations are often the sole source of baseline neutron spectra data when an experimental test object substantially perturbs the free-field spectrum. Given these applications, it is crucial that analysts provide high fidelity uncertainty quantification for the spectrum calculations. There are several sources of uncertainty in a spectrum calculation including; 1) Monte Carlo statistical sampling and discrete ordinate numerical convergence; 2) modeling uncertainties, e.g. densities, dimensions; and 3) underlying nuclear data, e.g. transport cross sections. The first uncertainty source, statistical sampling and numerical convergence, can be quantified by estimates routinely provided by the transport codes. The second source of uncertainty can be probed with sensitivity analysis tools that are becoming more available and easier to use. The status of the third source of uncertainty, the underlying nuclear data, is improving with respect to dosimetry reactions, where energy-dependent covariance matrices are routinely available, but little progress has been made in getting quantified uncertainties for transport cross sections or in propagating the transport uncertainties through complex geometries.

SCOPE

This paper investigates the systematic trends that can be seen in calculated spectra at a fast burst reactor facility. At the White Sands Molly-G fast burst reactor, experimenters can get a wide range of fast neutron spectra by varying their experimental location from a close 6-inch distance from the center of the ^{235}U core to a distant 100-inch location next to a facility wall. Fine-grouped (621 energy point) energy-dependent calculated neutron and gamma spectra have been calculated using the MCNP5 Monte Carlo code [3] and the latest ENDF/B-VI release 8 cross sections [4]. Integral metrics, spectrum-averaged cross sections for dosimetry-quality reactions, have been measured at the various experimenter locations. The latest IRDF-200 dosimetry cross sections [5] are folded with the calculated spectra to obtain ratios of the measured cross sections. These ratios are then compared to the calculated spectrum-averaged cross sections ratios. This comparison is designed to highlight trends in the C/E ratios that may shed light on deficiencies in the transport cross sections or in the details of the facility modeling.

SPECTRUM CALCULATIONS

Figure 1 shows the calculated neutron spectra at the 6-inch reactor position. The figure shows a 621-energy group representation of the spectrum. This calculation was produced using the

[1] Approved For Public Release; Distribution Is Unlimited OPSEC Review Conducted On: 9 Sept 04.

MCNP5 code and over 2E9 source particles. The Monte Carlo sampling uncertainty in the energy groups is ~x%. An inspection of the figure shows some structure from 10 – 100 keV. These structures have been tentatively identified as correlating with resonance structures in the aluminum cross section. The aluminum is present in the experimenter table that surrounds the reactor. This preliminary identification will be confirmed in the main paper by artificially removing the resonance features from the aluminum transport cross sections and then repeating the calculations to confirm that the features have then been eliminated.

Figure 1

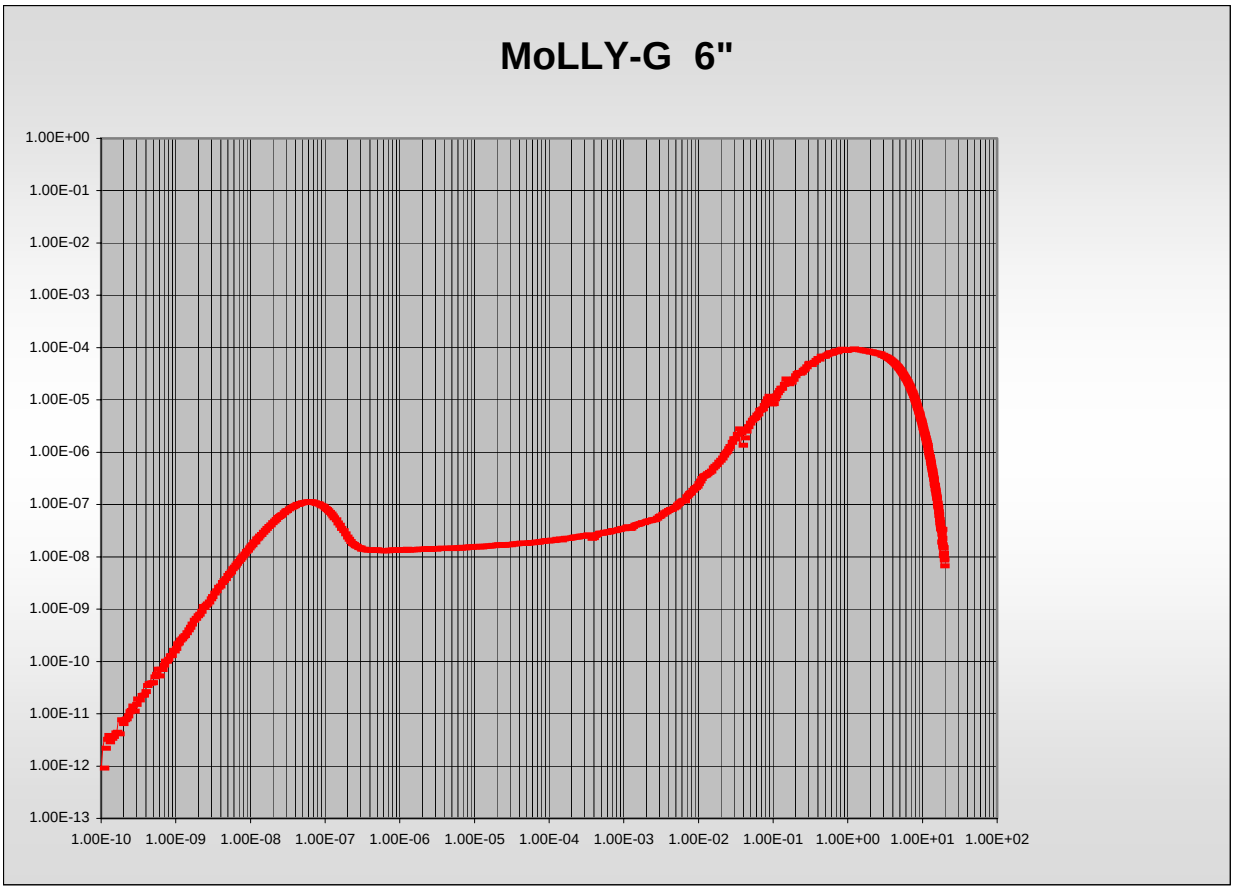

Interlaboratory Ex-Vessel Dosimetry Measurements and Calculations on VVER-440 of Kola-1

Borodkin, G.I., Khrennikov, N.N., Stolbunov, A.Yu.
SEC NRS of GOSATOMNADZOR of Russia
2/8, bld. 5, Malaya Krasnoselskaya ul., 107140 Moscow, Russia

Vikhrov, V.I., Erak, D.Yu., Kochkin, V.N., Brodkin, E.B., Egorov, A.L., Zaritsky, S.M., Geraschenko S.S.
RRC "Kurchatov Institute"
Kurchatov sq. 1, 123182 Moscow, Russia

Tsofin, V.I., Rozanov, K.G.
FSUE EDO "GIDROPRESS"
21 Ordzhonikidze str., 142103 Moscow district, Russia

Measurements and calculations, which are discussed in the paper, were carried out on Kola-1 VVER-440 in order to increase the reliability of reactor pressure vessel (RPV) dosimetry. In accordance with the Safety Guide [*1*] of the Nuclear, Industrial and Environmental Authority of Russia (former Gosatomnadzor of Russia) evaluated uncertainty of dosimetry parameters (for example, neutron fluence above 0.5 MeV) should be taken into account on examination of RPV lifetime. The final goal of dosimetry methods development and experimental justification is real decreasing of conservatism in evaluation of RPV residual lifetime.

Altogether 40 neutron activation monitor sets (MS) were located on the RPV outer surface (ex-vessel MS). Two sets were located inside the ionization chamber channel in the water tank (specific component of biological shield of VVER-440/230 type reactor) located behind the reactor thermal insulation not far from the outer RPV surface. Ex-vessel MS were placed on a special support frame, which was put into narrow gap between RPV and thermal insulation. Two groups of MS (12 MS in each group) were located on the two horizontal frame sections inside 36-degree sector at the core midplane level and at 95 cm below the core midplane (level of RPV weld # 4). Additional two groups of MS (12 and 4 MS) were located on the two vertical frame sections installed at different azimuth directions and covered approximately 250 cm along RPV vertical axis. Thus rather representative region of RPV outer surface was covered by monitors. MS were irradiated during 122.3 effective full power days from October 01, 2002 to February 14, 2003 in time of 26 fuel cycle.

Monitor activities were measured independently in two laboratories, and each laboratory used own monitors. The following monitors and reactions were used in the experiment by two laboratories:
SEC NRS - $^{237}Np(n,f)^{137}Cs$, $^{93}Nb(n,n')^{93m}Nb$, $^{238}U(n,f)^{137}Cs$, $^{58}Ni(n,p)^{58}Co$, $^{54}Fe(n,p)^{54}Mn$, $^{46}Ti(n,p)^{46}Sc$, $^{63}Cu(n,\alpha)^{60}Co$, $^{59}Co(n,\gamma)^{60}Co$,
and RRC KI - $^{93}Nb(n,n')^{93m}Nb$, $^{58}Ni(n,p)^{58}Co$, $^{54}Fe(n,p)^{54}Mn$, $^{63}Cu(n,\alpha)^{60}Co$.
Nb monitors of both laboratories contained less than 3 ppm Ta.

Intercomparison of absolute measured results has shown good agreement for $^{54}Fe(n,p)$ and $^{63}Cu(n,\alpha)$ reactions (1 – 4 %). Much more discrepancies were observed in separate space positions for $^{58}Ni(n,p)$ reaction (up to 9 %) and $^{93}Nb(n,n')$ reaction (more 12 %).

Different independent calculations were carried out by methods routinely used in VVER pressure vessel dosimetry. Three-dimension neutron field functionals (activities, reaction rates and fluence rates) were synthesized from two- and one-dimension distributions calculated by discrete ordinates method using DORT (SEC NRS), DOTIII+ANISN (RRC KI and FSUE EDO "GIDROPRESS") and DOORS-3.2 (RRC KI) code package. Neutron cross section libraries BUGLE-96 and BGL-440 were used for calculations. Results of independent calculations are compared between themselves and with experimental ones. Discrepancies of results are analysed and discussed in detail.

ACKOWLEDGMENTS

This work is carried out under financial support of Kola NPP. The authors express their thanks to Kola NPP staff, personally to Pytkin Yu.N. and Goloschapov S.N.

REFERENCES

1. “Safety Guides. Recording of Fast Neutron Fluence at VVER Pressure Vessels and Surveillance Specimens for Ulterior Prediction of RPV Radiation Lifetime (RB-007-99).” *Bulletin of GOSATOMNADZOR of Russia*, **3** (5) (1999). pp. 2-14.

Proton Induced Activation of Mercury: Preliminary Comparison of Calculations and Measurements

I. Remec, D. C. Glasgow, J. O. Johnson, and J. R. Haines

Oak Ridge National Laboratory, Oak Ridge, TN, USA

(E-mail: remeci@ornl.gov)

Abstract

The Spallation Neutron Source (SNS), currently under construction at Oak Ridge National Laboratory, will use a high-energy proton beam to produce neutrons in a mercury target. To facilitate the target design an experiment was conducted at the LANSCE-WNR facility at Los Alamos National Laboratory in which the stainless steel container filled with mercury was exposed to a series of proton pulses. The main objective was to measure the pressure waves in the mercury and the strains in the container. The secondary goal of the experiment was to provide information about the activation of the mercury. For this purpose a small sample of mercury was withdrawn from the target after the irradiation. The sample was analyzed using a high-resolution germanium-detector gamma-ray spectrometer. The gamma spectroscopy was performed about 24 days after the end of irradiation, which limited the measurements to longer-lived isotopes. Nevertheless, due to numerous isotopes still present, the measurement was difficult and only 11 radioisotopes were identified. About half of them were identified with high confidence, while activities of the others were less reliable.

To predict the activities of these isotopes the calculational methodology used for the SNS design was applied. The isotope production rates were obtained from the MCNPX simulation of the experiment and were forwarded to the OriHet95 code for subsequent activation calculations. An important aspect of the analysis was the calculation of the gamma ray self-shielding corrections for the mercury sample, which had a volume of about 1 cm^3.

An alternative simulation of the proton beam interaction with the mercury target using PHITS code will also be completed and the comparison of MCNPX and PHITS results will be provided.

The results obtained with MCNPX showed that for six of the measured isotopes, e.g., Hg-203, Au-198, Au-196, Au-195, Au-194, and Ag-105 the calculated and measured activities agreed within 40%. For Au-199 and Ag-105m the calculations were ~3 times higher and 4 times lower, respectively, than the measurements. For the remaining three isotopes Ir-188, Os-185, and Ag-110m, no agreement between the calculations and measurements was obtained. While the measurement of Ir-188 was considered questionable because its predecessor was not identified in the spectrum, and the Os-185 measurement suffered from potential interferences, no significant concerns were identified for the Ag-110m measurement.

While the experiment showed encouraging agreement with the calculations for some isotopes it has also spotlighted the difficulties involved in the measurements of the Hg activation in the SNS target. More experiments would be beneficial to benchmark the calculations and potentially allow improvement in the calculational methodology.

The Effect of the Undefined Positioning of the RPV Surveillance Capsules at the VVER-440 NPP Reactors on the Uncertainty of the Reactor Dosimetry Results

Fehér S., Zsolnay É. M., Czifrus Sz.
Institute of Nuclear Techniques, Budapest University of Technology and Economics,
Műegyetem rkp. 3-9., H-1111 Budapest, Hungary

ABSTRACT

At the VVER-440 NPP reactors the RPV surveillance specimens and the neutron monitors are situted in the surveillance capsules behind each other and without any orientation to the geometrical construction of the capsules. At the same time, during the insertion of the surveillance chains to the irradiation channels, the capsules can turn around their geometrical axis with different, undefined angles, and move radially and horizontally ±5 mm from the center of the irradiation channel, relative to the active core [1]. MCNP calculations show that all these circumstances result that the neutron exposition of two specimens in the same capsule can differ even 20% from one another, while the difference between the maximum and the minimum exposition of the neutron monitors can be as large as 37% for the same capsule, depending on the above mentioned geometrical conditions. The method of retrospective dosimetry – by sampling from the irradiated specimens – combined with Monte Carlo calculations was used to determine the geometrical configuration of the different specimens and monitor sets to the active core, during irradiation. The results have shown that the possible configurations of the different irradiation capsules were randomly distributed in a surveillance chain, i.e. any angle of the capsules' turning relative to the active core was equally possible. The effect of the above mentioned geometrical discrepancies on the uncertainty of determining the neutron exposition of the specimens was investigated in separate runs by a special Monte Carlo code developed for this purpose. The exposition rates of the specimens and of the neutron monitors within the same capsule were determined and analysed. The results have shown that an important decrease can be reached in the uncertainty of the exposition rate of the specimens and the neutron monitors by averaging the corresponding data of more capsules irradiated in the vicinity of the position with the maximum neutron fluence rate.

This paper presents the method applied in the investigations and the results obtained.

REFERENCES

[1] Results of the RPV surveillance investigations of the first, second, third and fourth reactor blocks of the Paks NPP from the point of view of irradiation embrittlement, after the first, second, third and fourth reactor cycles. Reports for restricted distribution. Paks NPP Company, Nuclear Directory. Paks, 1985-1992.

Neutronics Tools for the Design of a Spallation Neutron Source

F. X. Gallmeier, T. A. Gabriel, P. D. Ferguson, E. B. Iverson, I. I. Popova

The contribution aims at outlining the code systems typically used for the simulation of high energy accelerator environments in contrast to fission reactor applications and give the perspective of future developments in this area.

Monte Carlo transport codes are the particle transport work horses in radiation transport, dosimetry and shielding of accelerator environments. Historically, codes like LAHET, CALOR, SHIELD, NMTC, PHITS are used to perform the high energy physics transport and interface below about 20 MeV neutron and gamma transport into reactor physics transport codes. Modern Monte Carlo transport codes combine high energy charged particle transport with low energy neutron and photon transport as realized in FLUKA, MARS, MCNPX and also GEANT4 and the modernized CALOR.
Common to all these codes is the use of nuclear reaction models in the high energy domain of the code that phases into a cross section library based domain for the below 20 MeV neutron and photon transport. Detector responses are for this reason often a sum of a directly simulated contribution and a contribution of folding a response function with flux spectra.

Discrete ordinates codes like ANISN/DORT/TORT, can not directly be used in accelerator environment calculations because of the lack of charge particle transport, but can be of great use for determining the dominating neutron/gamma radiation fields through thick shields. They start typically with boundary sources far from target areas that originate from MC calculations. Coupling tools facilitate the generation of these boundary. Essential for the usage of the discrete ordinates codes is the availability of high energy neutron cross section libraries. The recently released coupled neutron/gamma multigroup library HILO2k developed at ORNL for the SNS replaces the widely used HILO86 library and extends its applicability to 2GeV of neutron energy.. A similar library is being generated in Japan for the J-PARC project extended up to 3 GeV.

Schemes for calculating activity buildup and decay via isotope production rates from direct simulation fed into activation codes like CINDER’90, ORIHET or DCHAIN2 become increasingly feasible due to increased CPU capabilities and improved event generators. Efforts are on the way to merge the activation code into the transport code to enable one-code high energy driven activation analyses as already realized by the MCB code for reactor burnup and accelerator transmutation of waste predictions. Alternative ways are the use of omega-factors with star-densities as performed in MARS, or the use of semi-empirical recipes of Silberberg and Tsao to yield the isotope production rates.

Coupled neutron-gamma calculations for the LR-0 experimental benchmark

Gábor Hordósy
KFKI Atomic Energy Research Institute
Budapest, Hungary

The lifetime of a nuclear power plant is ultimately restricted by the degradation of the mechanical properties of the reactor pressure vessel. Generally it is supposed that this is mainly determined by the time integral of the fast neutron flux. Recently, the possible role of the gamma flux in the degradation is also investigated. For this reason, the validation of the computer codes and nuclear data used for the calculation of space- energy dependent neutron and photon flux has grate importance, especially by measurements on mock-ups with dimensions close to the real-life applications.

Unique mock-up of a WWER-1000 reactor was developed on the reactor LR-0 in NRI Rez (Czech Republic). This mock-up included an axially and azimuthally shortened part of a WWER-1000 core (1.25 m active height, 60 degree symmetry sector) and radialy full-scale simulators of reactor externals, i.e. baffle, barrel, downcomer, pressure vessel and biological shielding. The radial dimensions and material compositions from the core boundary to the biological shielding are completely identical with the power reactors.

Coupled neutron-gamma calculations have been performed by the Monte Carlo code MCNP for the detailed model of the mock-up described above. The neutron source was specified pin-by-bin details in the 32 assemblies of the mock-up. The integral fluxes, attenuation factors, neutron and gamma spectra in SAILOR group structure have been evaluated at different locations. Also, the photon spectra have been evaluated from 0.2 MeV till 10 MeV by 0.1 MeV steps, for comparison with measurements. The combination of different variance reduction methods have been used to speed up the calculations.

The neutron and photon spectra were measured and calculated in all representative points of the mock-up: at the barrel (P2), before pressure vessel (P3), at ¼, ½, ¾ thickness of the pressure vessel (P4, P5, P6) and after the pressure vessel (P7). The measured and calculated neutron attenuation factors between these points and above different threshold energies are compared in the next table. Here Q is the ratio of the calculated and measured values while R is their difference relative to the common statistical error. The calculations were performed by the ENDF/B-VI. Rel. 2 library.

Table 1. Comparison of calculated and measured attenuation factors

	P2/P3		P3/P4		P4/P5		P5/P6		P6/P7		P3/P7	
E_{thr}	Q	R	Q	R	Q	R	Q	R	Q	R	Q	R
E>3.012 MeV	1.15	4.15	0.85	-4.6	0.94	-1.9	0.95	-1.4	1.05	1.29	0.80	-6.1
E>1.003 MeV	1.18	6.04	0.88	-4.2	0.97	-1.0	0.99	-0.4	1.03	0.88	0.87	-4.3
E>0.498 MeV	1.17	5.28	0.86	-4.3	0.96	-1.2	0.97	-0.8	1.01	0.31	0.80	-5.6
E>0.111 MeV	1.16	4.99	0.86	-4.2	0.95	-1.2	0.98	-0.6	1.00	0.13	0.81	-5.6

It can be seen from the Table 1, that using this library the attenuation is overestimated in water (P2/P3) and underestimated in the steel of pressure vessel (P3/P7). The ratio of the photon flux above 1 MeV to neutron flux above 1 MeV is also underestimated at all points by about 10 %.

These calculations were repeated using the FENDL 2.0, JEF 2.2 and JENDL 3.3 libraries. The main findings can be summarized as the FENDL increases the attenuation booth in the water and in the steel, while JEF 2.2 and JENDL 3.3 decreases the attenuation in the water and increases in the steel at most energies. Detailed comparison of calculated and measured neutron spectra as well as neutron spectra calculated with different libraries will be given in the final paper.

The photon spectra were calculated for points 2-7 by the libraries ENDF/B-VI. Rel. 2 and FENDL 2.0. For direct comparison with measurements, the calculated spectra were broadened with the detector resolution. The spectra calculated by ENDF/B-VI. Rel. 2 are shown on Figure 1 without broadening for points 2-7. The calculated and broadened photon spectra are shown together with the measured one on Figure 2 at the half width of the pressure vessel (point 5).

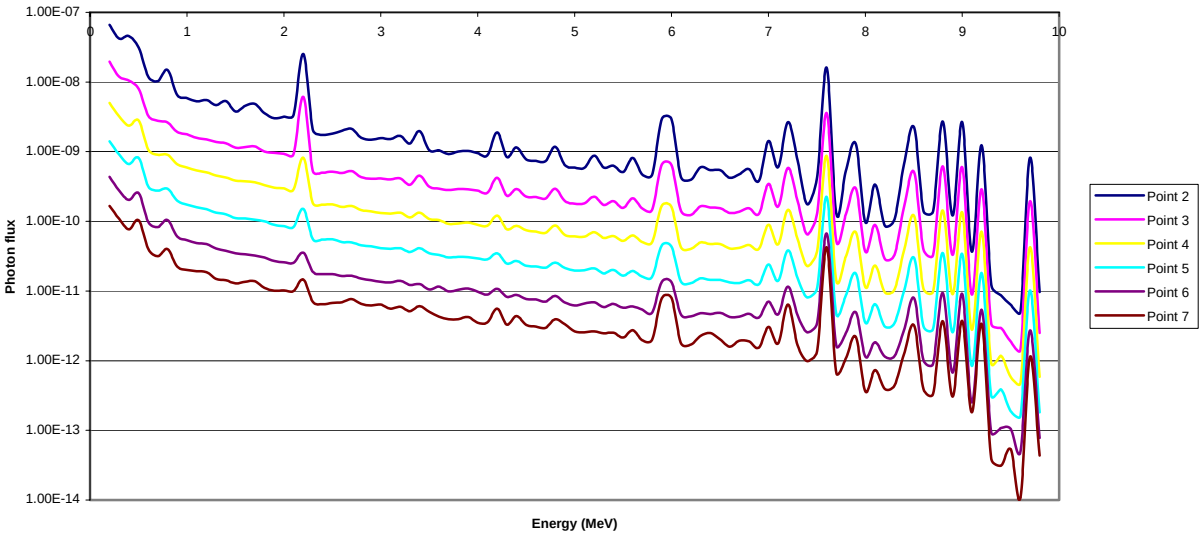

Figure 1. Photon spectra calculated by ENDF/B-VI.2 for points 2-7

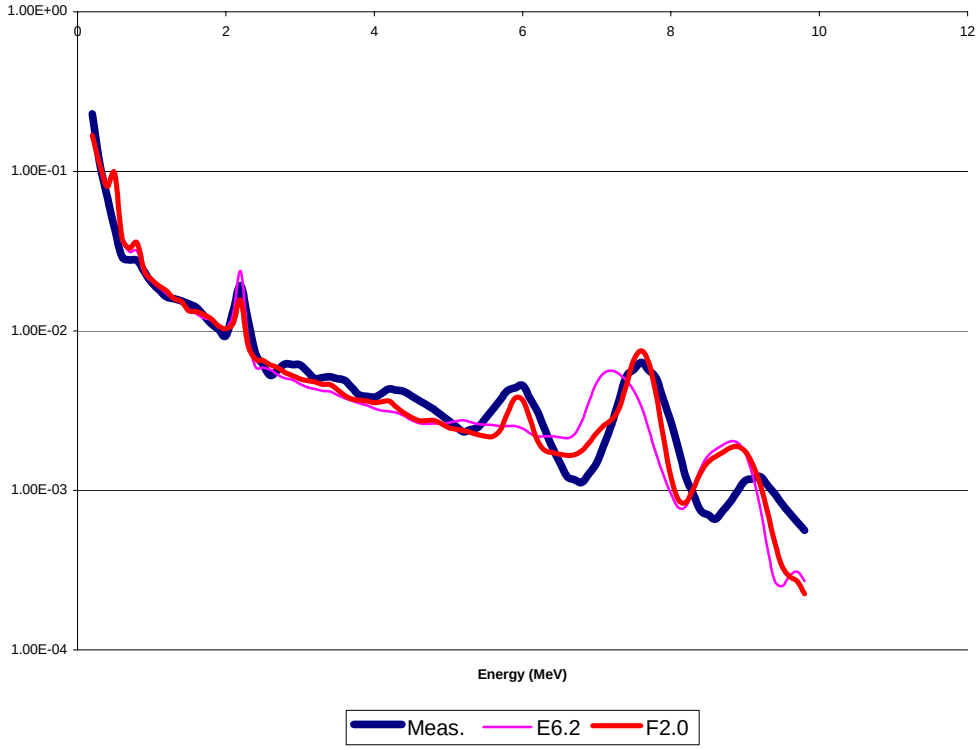

Figure 2. Comparison of measured and calculated (ENDF/B-VI and FENDL 2.0) neutron spectra at the half with of the pressure vessel. The detector resolution is taken into account in the calculated curves.

It can be seen, that calculation with FENDL 2.0 can reproduce the measured peaks at 6 MeV and 7.6 MeV, while ENDF/B-VI doesn't produce peak at 6 MeV at all, and it produces a peak at about 7.2 MeV instead of 7.6 MeV.

Comparison of the Results of the Calculational and Experimental VVER-440 Pressure Vessel Dosimetry at Paks NPP for Lifetime Extension

G. Hordósy, Gy. Hegyi, A. Keresztúri, Cs. Maráczy, L. Szalmás, P. Vértes
KFKI Atomic Energy Research Institute, Budapest, Hungary

É. Zsolnay
Budapest University of Technology and Economics, Institute of Nuclear Technique, Budapest, Hungary

E-mail: hordosy@sunserv.kfki.hu

At Paks NPP, Hungary, a major project was launched to investigate the possibility of lifetime extension of units of Paks NNP up to 60 years. Recently, detailed calculational and experimental investigations are going on to determine of the pressure vessel radiation load during this period.

For the accurate calculation of the fluence a large number of shielding calculations should be performed. To speed up these calculations the surface source method described in [1] has been used. The neutron source on the outer surfaces of the outermost assemblies is determined. This source is given as sum of a linearly and a quadraticaly anisotropic terms. The weight of the two terms (i.e. the angular spectrum) and the energy spectrum of booth component depend on the position along the outer surface of the reactor core. The transport of the neutrons from this surface through the pressure vessel is calculated by the MCNP Monte Carlo code.

Validation of the calculations will be performed using the results of measurements made by the activation foils located around the detector core. There are a large numbers of such measurements; some part of them still should be evaluated. In this summary some preliminary results of comparison for the 8th cycle of Unit II. of Paks NPP is described. The calculated and measured activities are given for such foils which were removed from the reactor after one cycle. The fast reactions ^{93}Nb(n,n') and ^{54}Fe(n,p) is examined at surveillance positions and in the cavity at different axial heights. The comparison of calculated and measured values is shown on Figures 1-4.

The agreement is fairly good at surveillance positions and in the case of the ^{54}Fe(n,p) in the cavity. In the case of ^{93}Nb(n,n') the differences in the cavity are significantly higher than that could be explained by statistical and measurement errors. Keeping in mind the good agreement for the same reaction at the surveillance position, this may be due to the error of the iron cross section.

The error introduced by the uncertainties of the iron cross section was calculated using the sensitivities and covariance data. The results are summarized in the next table.

Table 1. Uncertainty of the calculated reaction rates due to the iron cross section error

	SURV. POS.	CAVITY
^{54}Fe(n,p)	8 %	20 %
^{93}Nb(n,n')	6 %	14 %

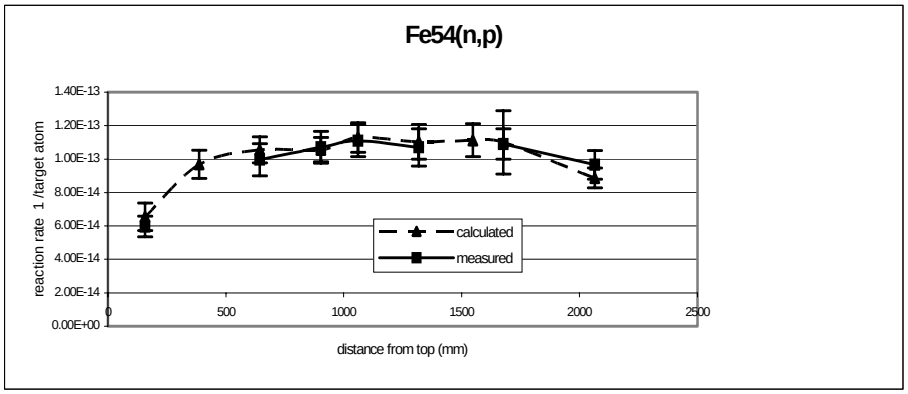

Fig. 1. Calculated and measured values of Fe54(n,p) rates at surveillance positions

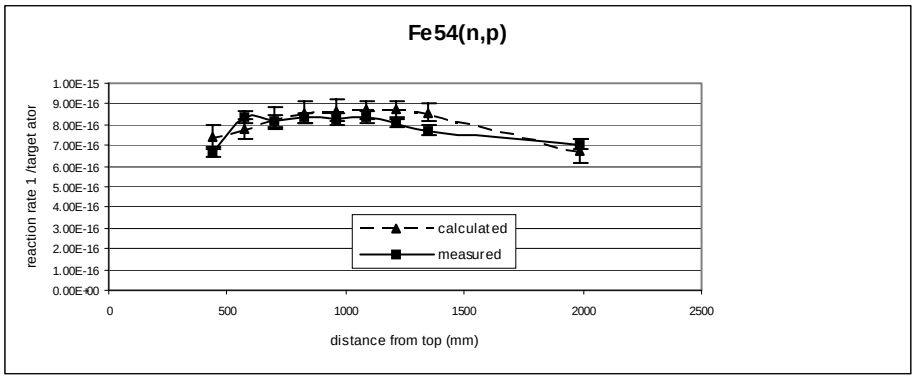

Fig. 2. Calculated and measured values of Fe54(n,p) rates in the cavity

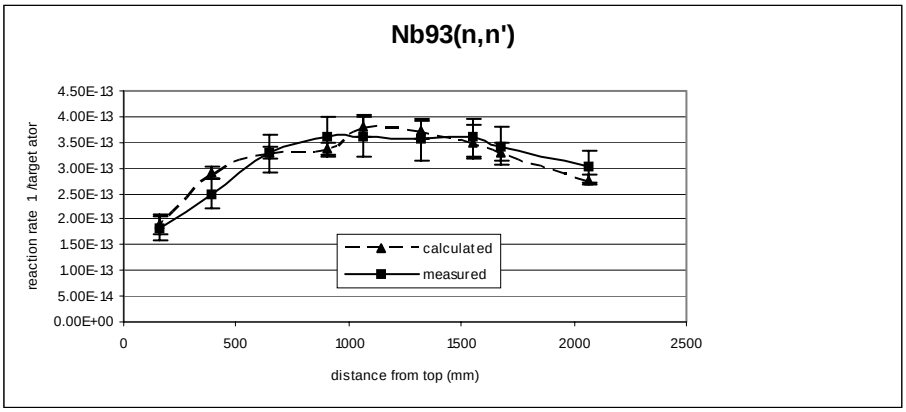

Fig. 3. Calculated and measured values of Nb93(n,n') rates at surveillance positions

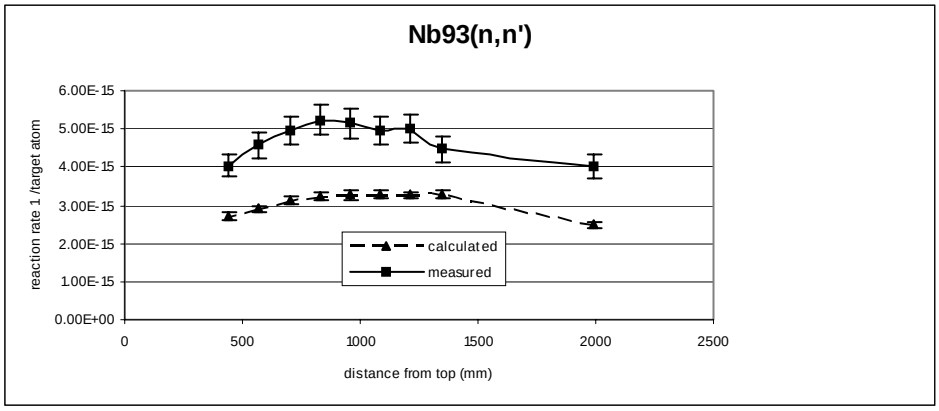

Fig. 4. Calculated and measured values of Nb93(n,n') rates in the cavity

As it is expected, the error is essentially higher in the cavity than at the surveillance positions. In the case of the ^{93}Nb(n,n') the error is 14 % in the cavity. This value is still a little low to explain the difference of measured and calculated values in the cavity. Further investigation is done to understand this deviation and complete the comparison of calculation with measurements.

[1] G. Hordósy, Gy. Hegyi, A. Keresztúri, Cs. Maráczy, E. Temesvári, P. Vértes ; É.Zsolnay: Pressure Vessel Calculations for Vver-440 Reactors, Proc. of the 11th Int. Symp. on Reactor Dosimetry, August 18-23, 2002 Brussels, Belgium

Use of CPXSD for Generation of an Effective Multigroup Library for PV Fluence Calculations

Alpan, F. A.
Oak Ridge National Laboratory
P. O. Box 2008, MS-6171
Oak Ridge, TN 37831-6171, USA.

Haghighat, A.
University of Florida
Nuclear and Radiological Engineering Department
202 Nuclear Sciences Building
Gainesville, FL 32611, USA.

INTRODUCTION

Deterministic methods, such as the discrete ordinates (S_N) method, require the use of multigroup (broad-group) cross sections. The standard way of generating broad-group cross sections can be given in the following 3 steps [1].

Step 1: Evaluated nuclear data are processed to obtain fine-group cross sections (generally in the order of hundreds).

Step 2: Fine-group cross sections are energy self-shielded to include the effect of resonances in cross section averaging.

Step 3: Fine-group data are collapsed to broad groups (generally in the order of tens) using scalar flux collapsing.

On generating the broad-group library, one of the major factors that cause inaccuracies is the multigroup structure. There are several broad-group libraries commonly used for shielding applications such as the 47-group BUGLE library. However there is no publicly available methodology that generates problem- and objective-dependent group structures. For this purpose, the Contributon and Pointwise Cross Section Driven (CPXSD) methodology [2] was developed.

THE CPXSD METHODOLOGY

The CPXSD methodology is an iterative method that constructs effective fine- and broad-group structures for a problem of interest, depending on the objectives of the problem. This new methodology derives group structures by refining an initial arbitrary (e.g., evenly partitioned in energy) group structure. Refinement of the initial group structure is performed according to the importance of the groups in the initial group structure, depending on the objectives of the problem of interest. The importance of groups can be determined based on the group-dependent response flux formalism as given in Eq. (1).

$$C_g = \sum_{s \in D} V_s \sum_{l=0}^{L} \sum_{m=0}^{l} \frac{2l+1}{4\pi} \Psi_{l,g,s}^{m} \Psi_{l,g,s}^{m,+} \qquad (1)$$

In Eq. (1), s refers to a materially uniform sub-domain in domain D, V_s is the volume of the sub-domain, l and m are polar and azimuthal indices for the spherical harmonic polynomial, and g refers to energy group. Ψ is the angular flux and Ψ^+ is the adjoint function. The group-dependent "contributon" in Eq. (1) gives the importance of a neutron at an energy group g for an objective.

After the importance of groups is determined, the most important group is identified. Depending on the cross sections of an important isotope/material in the problem of interest, sub-groups are placed in the most important group considering the resonance and non-resonance behavior. After the number of sub-divisions in the most important group is determined, the number of sub-divisions in other groups is calculated based on the ratio of their C_g to the C_g of the most important group. Sub-divisions in remaining groups are placed using cross section information of the important isotope/material and a new group structure is formed. The refinement process continues until a convergence criterion is met on the calculated objectives.

EFFECTIVE GROUP STRUCTURE CONSTRUCTION WITH CPXSD

New group structures were developed using CPXSD for pressure vessel dosimetry problems using the TMI-1 reactor. The objective is to generate broad-group structures for fast neutron and gamma dosimetry applications. For fast neutron calculations six dosimetry reactions sensitive to energies above 0.1MeV were considered including $^{63}Cu(n,\alpha)$, $^{54}Fe(n,p)$, $^{58}Ni(n,p)$, $^{46}Ti(n,p)$, $^{237}Np(n,f)$, and $^{238}U(n,f)$. For gamma production in thermal energies, $^{1}H(n,\gamma)$ and $^{56}Fe(n,\gamma)$ reactions were considered.

To calculate the importance of groups, the response flux formulation given in Eq. (1) was used in the fast, transfers from epithermal to thermal groups were used in the epithermal, and reaction rates per unit energy and transfers within thermal groups were used in the thermal energy range. ^{56}Fe was selected as the most important isotope in the problem, and its cross sections were used to determine sub-group boundaries in the refinement procedure of CPXSD. A convergence criterion of 1% was used on the objectives, i.e., reaction rates, to obtain the final group structures.

The 450-fine-group LIB450 library was generated for fast neutron dosimetry calculations using CPXSD. The 16-group LIB16 and 15-group LIB15 broad-group libraries were generated from LIB450 using scalar flux and bi-linear adjoint [3] weighting techniques. The broad-group to LIB450 reaction rate ratios of the aforementioned reactions were calculated and given in Table 1.

Table 1. – Broad- (LIB16 and LIB15) to fine-group (LIB450) reaction rate ratios

Response	LIB16 / LIB450	LIB15 / LIB450
$^{63}Cu(n,\alpha)$	.9882	1.006
$^{54}Fe(n,p)$	.9884	.9924
$^{58}Ni(n,p)$	.9888	.9946
$^{46}Ti(n,p)$	.9896	1.005
$^{237}Np(n,f)$	.9996	1.012
$^{238}U(n,f)$	.9992	1.003

For gamma production in thermal energies, the 589-group LIB589 was generated using CPXSD. LIB589 was collapsed to the 35-group LIB35 and 34-group LIB34 libraries using scalar flux and bi-linear adjoint weighting approaches, respectively. Reaction rate ratios of the broad-group to LIB589 results in the thermal energy range are given in Table 2.

Table 2. Broad- to Fine-Group Reaction Rate Ratios in the Thermal Energy Range

Response	LIB35 / LIB589	LIB34/ LIB589
$^{1}H(n,\gamma)$	0.9880	0.9984
$^{56}Fe(n,\gamma)$	0.9829	0.9920

CONCLUSIONS

The new broad-group cross section libraries generated with CPXSD are in excellent agreement with the fine group libraries that they were derived from, especially for bi-linear weighted cross sections in LIB15 and LIB35 for fast and thermal neutron reaction rate calculations, respectively. It was shown that CPXSD generated broad-group libraries effectively produce comparable results as their fine-group libraries.

REFERENCES

1. ANSI/ANS-6.1.2-1989, *Neutron and Gamma-Ray Cross Sections for Nuclear Radiation Protection Calculations for Nuclear Power Plants* (1989)
2. F. A. Alpan, *An Advanced Methodology for Generating Multigroup Cross Sections for Shielding Calculations*, Ph. D. Thesis, Nuclear Engineering, The Pennsylvania State University (May 2003)
3. H. L. Hanshaw, *Multigroup Cross Section Generation with Spatial and Angular Adjoint Weighting*, M.S. Thesis, Nuclear Engineering, The Pennsylvania State University (August 1995)

Benchmarking of PENTRAN-SSn using the VENUS-2 MOX Problem

G. Longoni, A. Haghighat, C. Yi, & J. Huh
Department of Nuclear and Radiological Engineering
University of Florida
Gainesville, FL 32611

The discrete ordinates method (Sn) is the most widely used technique to obtain numerical solutions of the Linear Boltzmann Equation, and therefore to evaluate radiation fields and dose rates in nuclear devices. However, it is well known that this method suffers from slow convergence for problems characterized by optically thick media and scattering ratio close to unity. To address this issue, a number of acceleration techniques for the Sn method have been developed in the past, such as synthetic methods, and rebalance algorithms. However, the application of these acceleration methods to large 3-D problems characterized by material heterogeneities has been hindered by limited applicability mainly due to inherent instabilities of the methods.

In order to overcome these limitations, we have developed and analyzed a new preconditioning method based on the Even-Parity SSn (EP-SSn) equations. The new method is based on the Flux Acceleration Simplified Transport (FAST) algorithm which is implemented into the PENTRAN-SSn code system. The main philosophy behind the new algorithm is to use a simplified model like the EP-SSn equations to calculate an initial solution which is introduced as initial guess into a transport calculation. In our new methodology, the EP-SSn equations resolve the low-frequency domain of the solution, while the Sn method is used to correct this initial solution with high-frequency components. It is worth noting that the EP-SSn equations are a higher order approximation to the Sn equations; therefore, the new preconditioning algorithm is suitable for problems characterized by strong transport effects.

The FAST preconditioning algorithm is designed for parallel computing environments, with spatial, angular and hybrid (spatial/angular) domain decomposition strategies. The algorithm is fully integrated into the PENTRAN-SSn 3-D parallel transport code, and from a user stand-point, the new preconditioning system is totally transparent, requiring only a very limited number of parameters to be executed. In the past, we have tested PENTRAN-SSn with the C5G7 MOX Fuel Assembly benchmark, issued by OECD/NEA, without spatial homogenization, and we have obtained accurate results with a speed-up ranging between ~3 and ~5 compared to a standard transport calculation.

In this paper, our objective is to test the accuracy and performance of the new preconditioning system for a 3-D shielding calculation based on the VENUS-2 MOX benchmark problem, issued by OECD/NEA. We will compare calculated reaction rates for several dosimeters throughout the VENUS-2 facility with experimental data and a reference Monte Carlo calculation. For the Monte Carlo calculation, we will use the A^3MCNP (Automated Adjoint Accelerated MCNP) code system. This study will provide detail information on the accuracy and efficiency of the PENTRAN-SSn code system for performing real-world shielding problems.

Benchmark Experiments/Calculations of Neutron Environments in the Annular Core Research Reactor *

K. Russell DePriest
Applied Nuclear Technologies, Org. 6871
Sandia National Laboratories
Albuquerque, NM 87185-1146

A series of benchmark experiments using spherical test objects were performed in the central cavity of Sandia National Laboratories' Annular Core Research Reactor (ACRR). The ACRR is a pool-type reactor that is equipped with a large 9-inch diameter dry central cavity suitable for fielding experimenter test objects. The ACRR facility also has the capability of inserting spectrum-modifying buckets into the dry cavity for tailoring the neutron/gamma environment that a test object will encounter. The experiments were performed with 4-inch and 7-inch aluminum (Al6061) and high-density polyethylene (HDPE) spheres that were essentially solid with cavities scrolled out along the equator to allow the insertion of activation foils and/or sulfur pellets. The cavities in the spheres were configured such that there were no radiation streaming paths or large void volumes. In addition to the foils located in the interior of the spheres, an external Ni activation foil was attached to the equator on the exterior of each sphere. The external Ni foil provides normalization back to the free-field reactor spectrum characterization and allows comparison from one reactor operation to another. The neutron monitor foils were selected to cover a wide range of reaction energies. Table 1 shows the neutron monitors that were used in the irradiations. The effective energy response range found in Table 1 corresponds to approximately 90% of the neutron energies found in the ACRR Central Cavity [*1*].

Table 1: Neutron monitors used for benchmark experiments

Monitor Reaction	Effective Energy Response Range
^{58}Ni (n, p) ^{58}Co	1.9 - 7.4 MeV
^{32}S (n, p) ^{32}P	2.0 - 7.2 MeV
Cd-covered ^{197}Au (n, γ) ^{198}Au	5.4 x 10^{-7} - 1.0 MeV
^{45}Sc (n, γ) ^{46}Sc	6.3 x 10^{-9} - 5.75 x 10^{-6} MeV
Cd-covered ^{59}Co (n, γ) ^{60}Co	5.4 x 10^{-7} - 1.35 x 10^{-4} MeV
^{nat}Ti (n, X) ^{47}Sc, ^{48}Sc	1.6 - 7.5 MeV 6.0 - 12.5 MeV

The irradiations were performed in two environments (the bare central cavity and a spectrum-modifying lead boron [Pb-B_4C] experimental bucket) that are well defined and characterized [*1*]. The irradiation environments were selected to provide a "clean" geometry for modeling the experiments. Additionally, the materials for the spheres were chosen to provide a baseline calculation (Al6061) and a stressing calculation (HDPE). The reactor environments were modeled in detail using MCNPX [*2*]. The MCNPX model includes the ability to move control rods to match the experiment positions so that the neutron flux profile within the reactor will be calculated more accurately (see Fig. 1).

This paper presents the results of benchmark experiments in the spherical test objects for ACRR irradiations of neutron monitors in 4-inch and 7-inch spheres composed of Al6061 and HDPE. The experimental results are then compared to the Monte Carlo calculations of the reaction rates of each of the foils at various depths in the spheres produced by MCNPX. The comparison between calculation and experiment includes a Calculation to Experiment (C/E) ratio and a complete treatment of the calculation uncertainties. The calculation uncertainties considered include the Monte Carlo statistical uncertainty, the uncertainty in the experiment configuration, the uncertainties in the nuclear data (reaction cross section and material cross sections), and the uncertainties in the physically measurable quantities (e.g., material densities and size of the spheres).

* Work supported by the United States Department of Energy under contract DE-AC04-94AL85000. Sandia is a multiprogram laboratory operated by Sandia Corporation, a Lockheed Martin Company, for the United States Department of Energy.

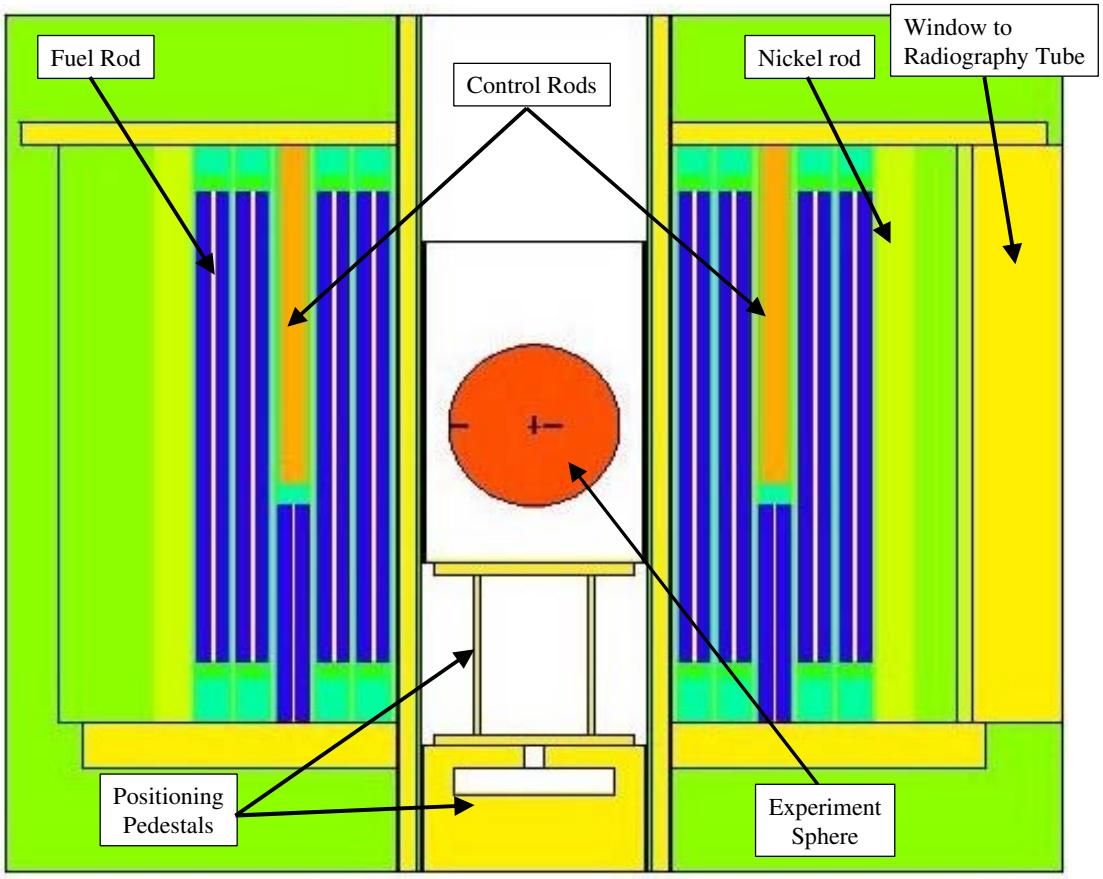

Figure 1: MCNPX model of benchmark experiments

References

1. P. J. Griffin, J. G. Kelly, D. W. Vehar, *Updated Neutron Spectrum Characterization of SNL Baseline Reactor Environments, Vol. 1: Characterization*, Sandia National Laboratories, Albuquerque, NM, report SAND93-2554, April 1994.
2. L. S. Waters (Editor), *MCNPX User's Manual, Version 2.4.0*, LA-CP-02-408, Los Alamos National Laboratory, Los Alamos, NM, September 2002.

Spent Fuel Monitoring with Silicon Carbide Semiconductor Neutron/Gamma Detectors

Natsume, T.
Mitsubishi Heavy Industries, LTD.
Wadasaki-cho 1-1-1, Hyogo-ku, Hyogo-ken, 652-8585, JAPAN

Doi, H.
Nuclear Development Corporation
622-12, Funaishikawa,Tokaimura Ibaraki, 319-1111, JAPAN

Ruddy, F. H., Seidel, J. G., Dulloo, A. R.
Westinghouse Electric Company
1332 Beulah Road Pittsburgh, PA 15235-5081, USA

INTRODUCTION

Previously, neutron and gamma-ray response measurements in simulated spent fuel environments using silicon carbide (SiC) semiconductor detectors were reported. [*1*] In the present paper, measurements carried out in an actual PWR spent nuclear fuel pit using a SiC detector are presented and discussed. The purposes of the measurements were to confirm the separability of neutron and gamma-ray pulses in an actual spent nuclear fuel environment, which has a large gamma-ray background, and to demonstrate the stability of the neutron and gamma-ray responses during long-term exposure to the spent-fuel radiation field. Neutron and gamma-ray dosimetry measurements on spent fuel assemblies are useful for characterization of parameters such as fuel burnup.

MEASUREMENTS

The measurements were carried out at the spent fuel pool of Nuclear Development Corporation (NDC), which has gamma-ray intensities up to about 10 Gy/h and has neutron fluence rates up to about $2x10^2$ cm^{-2}-s. The measurement geometry is shown in Figure 1. The detector was contained within a tungsten case and placed in a water-proof tube adjacent to a fuel assembly. The SiC detector has a 28 mm^2 active area and was placed adjacent to a 25-μm thick ^{6}LiF foil to enable thermal and epithermal neutron detection. [*1,2*] The detector assembly was movable in the axial direction. Periodic measurements in a constant position as well as axial distribution measurement were carried out. Neutron and gamma-ray sensitivity measurement were carried out in established radiation fields in a graphite pile and in a Co-60 facility, and measurements to determine the separability of the neutron and gamma-ray pulse-height responses were also performed.

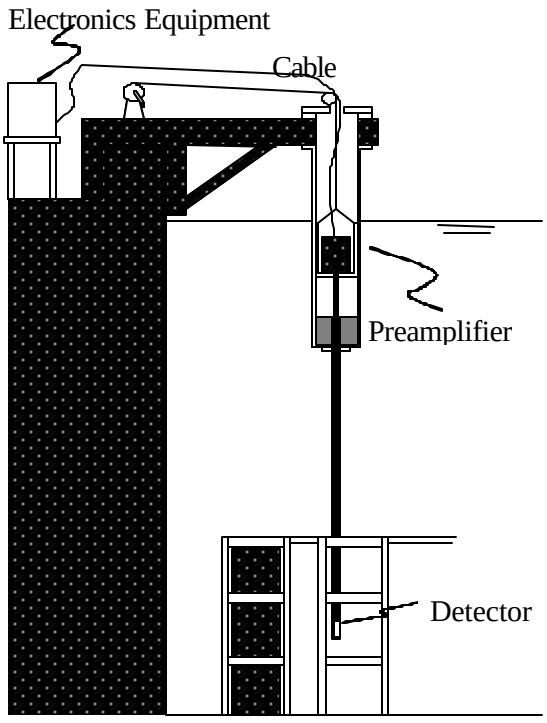

Figure.1 Measurement geometry

RESULTS AND DISCUSION

The measured neutron and gamma-ray response spectrum at a gamma dose of 1.9Gy/hr is shown in

Figure 2. The neutron response is clearly separated from the gamma-ray response, enabling simultaneous neutron and gamma-ray intensity measurements. The gamma-ray response was found to have good linearity in a comparison with a fiber-optic gamma-ray detector. From the neutron measurement results in strong gamma-ray fields we can conclude that the neutron response is completely separable from the gamma-ray response up to a gamma-ray dose of 400Gy/hr. At a dose of approximately 2000Gy/hr the gamma-ray response overlapped 50% of the neutron response. For comparison, in a boron-lined proportional counter with a sensitivity of 4 cps/nv, approximately 50% of the neutron response spectrum is obscured by the gamma-ray response at a dose of about 10 Gy/hr.

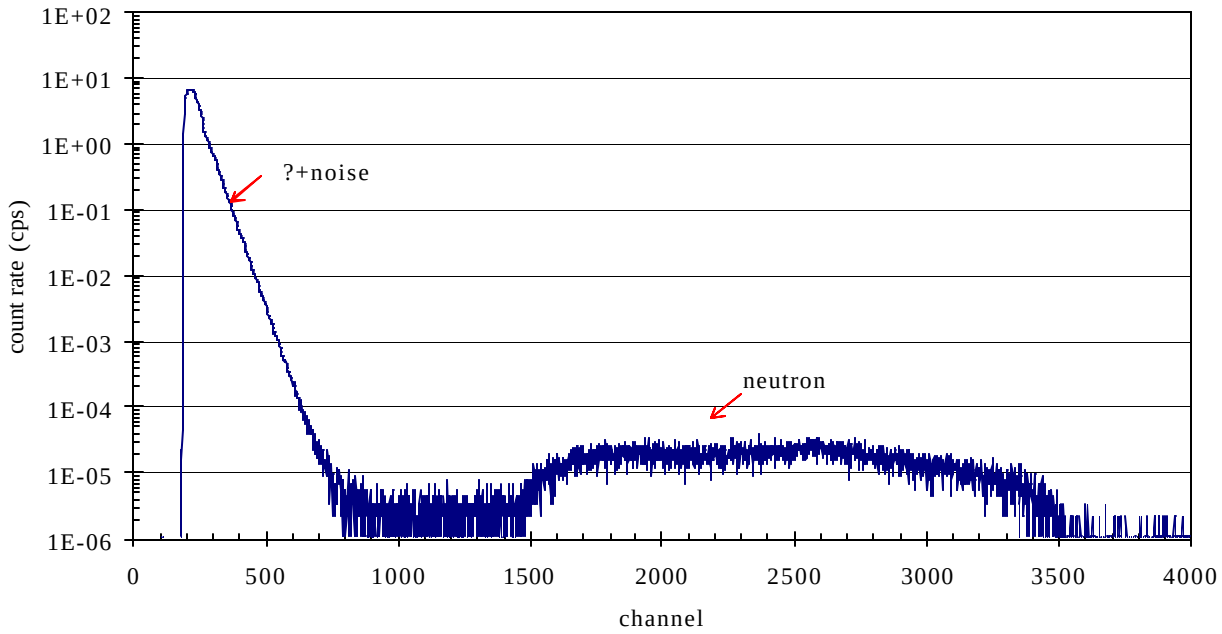

Fig.2 Neutron and gamma Measurement result for actual spent nuclear fuel

Based on measurements in an established radiation field in a graphite pile, the neutron sensitivity for the single 48-mm^2 SiC detector is 0.0015cps/nv. Higher sensitivities are obtained by using arrays containing multiple SiC detectors.

The measurements confirmed that the SiC detector can simultaneously measure both neutron and gamma-ray intensities in the radiation field surrounding a spent nuclear fuel assembly. Furthermore, both the neutron and gamma-ray sensitivities were found to be stable during prolonged exposure to the spent fuel radiation field over a period of almost four months.

REFERENCES

1. A. R. Dulloo, F. H. Ruddy, J. G. Seidel, T. Flinchbaugh, C. Davison, and T. Daubenspeck, "Neutron and Gamma Ray Dosimetry in Spent-Fuel Radiation Environments Using Silicon Carbide Semiconductor Radiation Detectors", in *Reactor Dosimetry: Radiation Metrology and Assessment, ASTM STP 1398*, John G. Williams, David W. Vehar, Frank H. Ruddy, and David M. Gilliam, Eds., American Society for Testing and Materials, West Conshohoken, PA, 2001, pp 683-690.
2. A. R. Dulloo, F. H. Ruddy, J. G. Seidel, J. M. Adams, J. S. Nico, and D. M. Gilliam, "The Thermal Neutron Response of Miniature Silicon Carbide Semiconductor Detectors", Nuclear Instruments and Methods A, **498**, (2003) pp 415-423.

Measurement of Helium Generation in AISI 304 Reflector and Blanket Assemblies after Long-Term Irradiation in EBR-II

F. A. Garner, B. M. Oliver, and L. R. Greenwood
Pacific Northwest National Laboratory, Richland, WA

Far from the active core regions of a small fast reactor it becomes somewhat difficult to calculate the helium generation in stainless steel components of the reflector and blanket regions. This is particularly true for components that served many years in EBR-II while the core and reflector regions underwent many modifications, or for components which were moved and sometimes rotated during their lifetime.

In an experiment directed toward determination of the effect of displacement rate on void swelling of AISI 304 stainless steel, it was important to insure that observed differences in void swelling were primarily in response to displacement rate and not other important variables such as the helium/dpa ratio that might exhibit time-dependent or position-dependent variations. Rather than relying only on calculations of expected helium content for such complicated histories, the helium content was measured directly using an isotopic dilution mass spectrometry method known to be very accurate. Five specimens spanning a large axial range about the core center-plane were removed from each of the inboard and outboard faces (relative to the core centerline) of five separate hexagonal subassemblies irradiated in rows 8, 9, 10 and 14 of EBR-II.

Since some significant fraction of the helium in these relatively soft spectral regions might arise from transmutation of boron it was necessary to determine the unknown boron content using an archive specimen of the identical heat. Accurate determination of the boron content in the samples was made using a method similar to neutron activation. Here, the samples were exposed to a known dose of thermal neutrons in order to convert a known fraction of the ^{10}B isotope to helium via the ^{10}B (n, α) ^{7}Li reaction. After irradiation, the helium generated from the irradiation was accurately measured, and used to determine the ^{10}B content at the beginning of the irradiation. Neutron dosimetry samples, in the form of a well characterized Al-^{6}Li alloy were included in the irradiation assembly to determine the thermal neutron fluence via the ^{6}Li (n, α) ^{3}H reaction. The thermal neutron cross sections for the ^{10}B and ^{6}Li samples are well known.

After separating the boron contribution from the total measured helium it was possible to determine the contribution from various fast and thermal neutron interactions with the other major elements in the steel and compare the helium generation with predicted values. One important conclusion of the study is that the range of He/dpa ratios over the five subassemblies is not very large, allowing the observed changes in swelling to be attributed primarily to variations in displacement rate and temperature.

Development and Test Program for Radiation Hardened Diamond PCDs

King, D. B., Luker, S. M., Naranjo, G. E., Griffin, P. J., Hohlfelder, R. J.
Sandia National Laboratories, MS 1146
Albuquerque, NM 87185-1146, USA.

PURPOSE

Experimenters often need active measurements of the ionizing dose rate during the testing of electronic parts in pulsed reactor fields. Silicon PIN diodes are typically used for this application by the radiation testing community. However, PINs, including the most radiation-hardened PIN available from commercial sources, show significant neutron damage effects (ranging from increases in leakage current to actual device failure) even during single pulses in TRIGA reactors. This paper reports on a program to develop and test a neutron-hardened diamond photoconducting detector (PCD) that has the potential for a stable response over many (> 25) reactor pulses for dose rate measurements over the region from 10 – $1x10^{12}$ rad(C)/sec.

FABRICATION AND OPERATION

A photoconductive detector consists of a photoconductive material fitted with two ohmic contacts [*1*, *2*]. When a voltage is applied across the contacts, an equilibrium current flows that is proportional to the free carrier concentration in the photoconducting material (determined by the material bandgap). When the active material is exposed to ionizing radiation, the free carrier concentration increases and a current flows with a characteristic time determined by the charge carrier lifetime. A short free carrier concentration lifetime is required to maintain fast device response to a time varying radiation pulse, but this short lifetime results in a small gain and signal. High bandgap or high resistivity materials are desired for these detectors, but maintaining this resistivity requires great care in fabricating true ohmic contacts.

Diamond is a good material for detecting ionizing radiation [*3*, *4*, *5*]. Diamond is a wide band-gap semiconductor and has the potential of "outstanding radiation hardness, fast charge collection, and low leakage current that will allow them to be used in high radiation ... aggressive environments." [*6*]. Diamond has many good properties for use as a photoconductive device, including 1) a large band-gap material (~5.6eV); 2) low leakage; 3) ability to operate at high temperatures; 4) high dielectric strength so it can operate at high fields; 5) high carrier mobilities and saturated carrier velocities; 6) low dielectric constant (low capacitance), and short lifetime (nanosecond response time). Type II diamonds have been observed to show a wide variation in their response. Hence, the diamond PCD application protocol used here requires that each dosimeter be individually tested and calibrated.

The diamond PCD reported here uses a 1x1x2 mm single crystal Type IIa industrial diamond chip, metallized on the 1x1 faces, that has been pre-damaged with an ACRR exposure of ~$1x10^{16}$ n/cm^2. The neutron pre-damage step, used to minimize the degradation of the PCD to further neutron exposures, will introduce additional trapping sites, decrease carrier lifetime, and reduce the signal from the PCD. The packaged PCD uses RTV as a potting material and Peek in the adaptors/connectors that convert from Lemo to BNC in order to prevent dielectric breakdown during operation and to minimize connector dose-related degradation during reactor exposures. The packaged dosimeter is a cylinder with a radius of 0.477 cm and a length of 3.3 cm.

CALIBRATION AND TESTING

For calibration, the PCD is configured as a two-port device with one port biased at 750 VDC and the second for signal output. For detector calibration at Hermes-III bremsstrahlung source and other fast-pulse acquisitions, the signal is terminated into a 50 Ω load at the digitizer input to match the transmission line impedance. For low frequency applications (< 1 MHz bandwidth), such as a Co-60 source, the signal can be terminated into a resistance other than 50 Ω for use with an amplifier to improve the signal-to-noise ratio.

The general PCD calibration involves exposure at three high dose rate points in the Hermes-III bremsstrahlung environment (from $5x10^8$ – $2x10^{12}$ rad[CaF_2:Mn]/sec) and three low dose rate points (10 - 100 rad[alanine]/sec) at the SNL Gamma Irradiation Facility (GIF). The measurements from these calibration exposures are combined with calculated device response from coupled gamma/electron radiation transport calculations. The result is a device-specific calibration factor, in units of [mV-sec]/rad(C). Note that this calibration factor is a device response relative to the active material of the PCD.

The red curve in Figure 1 shows the PCD response in a small (24.8 MJ) ACRR reactor pulse. The normal

reactor power diagnostic is a Cadmium-based self-power neutron detector (SPND) and is shown in black. The PCD is a very small dosimeter and is co-located with experiments in the reactor exposure. The SPND is a large detector (~46 cm tall), has a small response - so it is located next to the reactor fuel elements, and is sensitive to thermal neutrons. The blue curve in Figure 1 shows the ratio of the PCD to SPND response. Over the main reactor pulse the neutron/gamma ratio is constant and the near constant shape of the PCD/SPND ratio indicates that the PCD does an excellent job in tracking the dose rate over the reactor pulse. The PCD has been compared to the SPND response for pulses from 20 - 300 MJ with similar good agreement.

One critical attribute for an active dosimeter in a reactor environment is its insensitivity to neutron damage. This is demonstrated for our dosimeter by calibrating a PCD and then conducting a series of ACRR reactor shots where each reactor exposure was followed by a Co-60 exposure. To date, twelve 12 ACRR/GIF tests have been completed. Five PCDs have been exposed to a neutron fluence of 6.2×10^{15} n/cm^2. The stability of the response between the separate Co-60 exposures (1.8 - 5%) thus far is proof of the absence of appreciable neutron degradation in the pre-damaged diamond PCD.

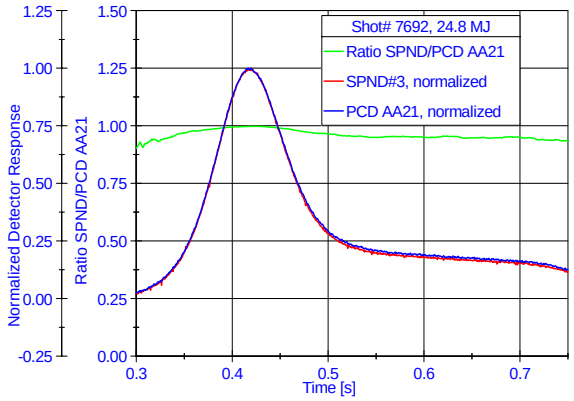

Figure 1.PCD and SPND response to ACRR reactor pulse.

CONCLUSION

This paper reports on the design, construction, and testing of a diamond PCD used for active dose rate measurements in test reactor environments. The use of pre-damaged diamonds produced a PCD whose response has not yet degraded with multiple reactor exposures. The PCD shows sensitivity to gamma dose rates over a range from 10 – 1E12 rad(C)/sec. The consistency of the normal reactor power diagnostics with the PCD dose rate over a reactor pulse confirms that the diamond PCD yield a good time profile for the ionizing dose over the reactor pulse.

ACKNOWLEDGMENTS

This project is partially supported by Sandia National Laboratories. Sandia is a multiprogram laboratory operated by Sandia Corporation, a Lockheed Martin Company, for the United States Department of Energy under Contract DE-AC04-94AL85000.

REFERENCES

1. Radiation Detection and Measurement, G. F. Knoll, Third Edition, John Wiley & Sons, 2000, pp. 491-492.
2. Castaldini, A., Cavallini, A., Polenta, L., Canali, C., del Papa, C., Nava, F., “The role of ohmic contact on the efficiency of gallium arsenide radiation detectors,” Nuclear Instruments and Methods in Physics Research, Vol. A 388, 1997, pp. 417-420.
3. Benny, A.H.B., Champion, F.C., “Some Effects of Neutron Irradiation of Diamond,” Nature, Vol. 173, pp. 1087.
4. Benny, A.H.B., Champion, F.C., “Neutron bombardment of counting diamonds,” Proc. R. Soc., Vol. 234, 432-440, 1956.
5. Keddy, R.J., Nam, T.L., “Diamond Radiation Detectors,” Radiat. Phys. Chem., Vol. 41, 1993, pp. 767-773.
6. Han, S., “New developments in photoconductive detectors,” Rev. Sci. Instrum., Vol. 68, January 1997, pp. 647-652.

Digital Multiparameter System for Characterisation of Neutron – Gamma Field in the Experimental Reactor LR-O

Z. Bures, J. Kroupa, F. Cvachovec, P. Celeda
Military Academy Brno,
B. Osmera
Nuclear Research Institute, 25068 Rez
Czech Republic
osm@ujv.cz

A digital multiparameter spectrometer with the organic stilbene or NE-213 scintillator for neutron and gamma spectra measurement is described. The developed system corresponds to the modern trends in nuclear electronics replacing the analog signal processing by the digital one. The control logic has been realized with the Field Programmable Gate Array. The spectrometer was tested in Nuclear Research Institute Rez. The measurements were performed in the VVER – 1000 Mock-up assembled in the LR-0 experimental reactor in NRI Rez. The measurements were done in the vicinity of the pressure vessel simulator.

The space-energy distribution of neutrons and gamma ray in the vicinity of it and over the pressure vessel thickness is particular objective of the REDOS project [1]. According to the REDOS project the spectrometer should measure the neutron and gamma spectra in the energy range of 0.5 – 10 MeV approximately. The evaluation of the ratio of gamma and neutron flux density has been requested.

The digital system allows to record several parameters of a detected particle as a characterisation of the detection event.

In this case two recorded parameters were chosen:

a) The pulse amplitude from the stilbene detector which includes the information about the energy of the detected particle.
b) The pulse rise time which characterises the type of detected particle, i.e. neutron or photon.

The new system relates to the previous one BUBULAK described in [2]. The BUBULAK consists of analog Pulse Shape Analysis (PSA) part and digital processing of PSA output and linear (amplitude) output. The analog modules of Pulse Shape Analysis (PSA) have been replaced by digital circuits in the new system. The main advantages of the digital PSA are:

- increase of "working" count rate, with the better recognition of the subsequent pulses (lower pile-up),
- better resistance against perturbation of measured data,
- replacing the analog PSD by the digital circuits with relating software enables to realize various PSD like comparison of slow and fast component of scintillation, evaluation of the pulse rise time, measurement of the time from the start of the pulse to the zero crossing time of double differentiated pulse, etc.
- replacing the analog circuits by the digital ones can miniaturize the device
- the system can be used also for other measurements, e.g. with the boron doped scintillators
- in general the off line (re) evaluation of the stored data is possible.

Unfortunately the time resolution of the nowadays avarable digital circuits is not fine enough to reach all goals. Nevertheless the progress in this field is very promising

[1] REDOS Project. The Fifth Framework Programme of the European Community 1998-2002
[2] Z. Bures, J.Cvachovec, F. Cvachovec, P.Celeda, B.Osmera: Multiparameter Multichannel Analyzer System for Characterization of Mixed Neutron / Gamma Field in the Experimental Reactor LR-0. Proceedings of the 11th International Symposium on Reactor Dosimetry "Reactor Dosimetry in the 21th Century", Brussels, Belgium, 18-23 August 2002, pp. 194-201, World Scientific

A Beam-monitor System for Neutrons and Gamma-rays in the Medical Irradiation Field of the Kyoto University Research Reactor

Sakurai, Y. and Maruhashi, A.
Kyoto University Research Reactor Institute,
Asashironishi 2-1010, Kumatori-cho, Sennan-gun, Osaka 590-0494, Japan

INTRODUCTION

The Heavy Water Neutron Irradiation Facility of the Kyoto University Reactor (KUR) was updated in March 1996 [*1*], as a medical irradiation field with multi neutron energy spectra, mainly for the improvement in neutron capture therapy (NCT). In December 2001, the first NCT clinical trial using the epi-thermal neutron irradiation was carried out for oral cancer. Simultaneously with the start of epi-thermal neutron irradiation, the several matters to be improved have been clarified in our present NCT. For one of those matters, the preparation and installation of beam monitors are urgently necessary. In this paper, our concept and study results are reported about a beam-monitor system for neutrons and gamma-rays in the medical irradiation field of the KUR.

CONCEPT AND EXPERIMENTS

The thermal, epi-thermal, fast and gamma-ray components must be separately measured in the beam-monitor system. The dose estimation consistent among the thermal, epi-thermal and mixed neutron irradiation modes is also needed. The multi-chamber method was adopted using the combination of four kinds of ionization chambers. Each chamber has a two-layer wall. The outer wall has a thickness sufficient for charged-particle equilibrium for gamma rays (a few mm), and it is employed as a neutron filter namely a local spectrum-shifter. The inner wall has a thickness sufficient for charged-particle equilibrium for neutrons (a few ten micron), and it is employed as a controller for the charged-particle generation due to neutrons. The response for each component can be adjusted also by regulating the chamber-gas components.

Some chamber walls were made for trial, for the IC-17M type chamber of Far West Technology, Inc.. Non-foamed polyurethane with LiF in 35 weight percent was selected as the outer-wall materials for the four chambers. The chamber volumes were 1 cc and the wall thicknesses were 5.3 mm. As the wall thicknesses were the same, the charged-particle equilibrium for gamma rays were also the same for the all chambers. For the chambers for neutrons, the neutron-filtering characteristics were controlled by changing the ^{6}Li ratio in LiF. The ^{6}Li ratio was adjusted by mixing enriched ^{6}LiF and natural LiF. The chamber walls with the ^{6}Li-enrichment of 7.5% (natural), 20%, 40%, 60%, 80% and 96%, were prepared. The experimental surveys were performed for the materials of the outer and inner walls, and the chamber gases.

RESULTS

The suitable ^{6}Li-enrichment was 96% for fast neutrons, 40% for epi-thermal neutrons, and 7.5% for thermal neutrons. For the inner wall, carbon paste was coated about 100-micron thickness on the inner surface of the outer wall. For the chamber gas, CO_2 gas was selected for gamma rays, N_2 gas for thermal and epi-thermal neutrons, and tissue-equivalent (CH_4 64.4%, CO_2 32.5%, N_2 3.1%) gas for fast neutrons. The characteristic experiment for the trial-made multi-chamber was performed using the several irradiation modes at the KUR-HWNIF. In the standard modes of thermal, epi-thermal and mix neutrons, which are applied for NCT clinical trials, it was confirmed that the coefficients of the respective chambers for the respective components could be fixed, and then the beam-monitoring consistent among the modes was possible.

REFERENCES

1. Y. Sakurai and T. Kobayashi, “Characteristics of the KUR Heavy Water Neutron Irradiation Facility as a Neutron Irradiation Field with Variable Energy Spectra” *Nucl. Instr. Meth. A*, **453** (2000). pp. 569-596.

Comparison of Boron-Based Solid State Dosimeter Schemes

M. S. Hallbeck[1], A. N. Caruso[1], S. Balkir[1], W. K. Pitts[1], J. I. Brand[1]

1. University of Nebraska College of Engineering
245NWSEC
Lincoln, NE 68588-0511

2. Pacific Northwest National Laboratories
Richland, WA 99352

The need for solid state based personal and portable neutron detectors is well established for applications in personal dosimetry, as well as national security, space applications, waste, and environmental monitoring [1]. Devices which can offer real-time, sensitive detectors of neutrons in a rugged, portable packaging have been proposed and are being tested. Tiny diodes or other collection geometries can be packaged with their electronics into dosimeters the size of cell-phones or wristwatches, with minimal power requirements, or handheld, ergonomically designed screening devices.

Boron-based solid-state devices are being developed as the heart of the detection systems due to the large capture cross section of ^{10}B for neutrons (~3850 barns for a thermal neutron of energy 0.025 eV), the charged reaction products and the availability of a semiconducting form of a boron rich material make it uniquely suitable for such a device. The interaction of a neutron with a ^{10}B atom is given by:

$$^{10}B + n \rightarrow {}^{7}Li\ (0.84\ MeV) + {}^{4}He\ (1.47MeV) + \gamma\ (0.48MeV)$$

or

$$^{10}B + n \rightarrow {}^{7}Li\ (1.02\ MeV) + {}^{4}He\ (1.78MeV)$$

with 94 and 6% probability respectively. Naturally occurring boron has a ^{10}B to ^{11}B ratio of about 1:4, and enriched ^{10}B substances are easilty available.

Boron devices to date have included a variety of geometries, including of enriched boron on gallium arsenide, enriched boron on silicon, boron phosphide thin films, and semiconducting boron carbide devices both on silicon and as heteroisomeric diodes, but not all boron devices are equivalent [2]. Especially for personal dosimetry where not only neutron detection, but dosage equivalence is important, the response characteristics of individual devices become significant. As shown in the Figure 1, below, the pulse height response various geometries [3-6] reveal significant differences in sensitivities, signal to noise, and signal discrimination. These spectra reflect the underlying physical parameters which indicate that the integrated semiconductor materials rather than the conversion layers, have significant advantages. Both boron carbide (in its many polytypes) and boron phosphide are excellent semiconductors, as shown in figure 2, below. Semiconducting direct detectors exhibit great potential for the development to marketable devices in the near future.

In this work, the neutron responses of these different geometries are investigated in detail, and compared to spectral response modeling. Both previously published results from the literature and new, unpublished spectra for novel geometries will be included. However, the technological challenges for dosimetry and other monitoring do not rest in the materials science alone. Fabrication, electronic circuitry, and wearability constraints are also important outside the physics laboratory. The results from the material and device evaluation are explained in light of implications for real-world dosimetry including optimal circuitry design, dosimeter packaging and the accuracy and reliability of dosage measurement. Implications for the ergonomics of the ultimate dosimeter are also addressed.

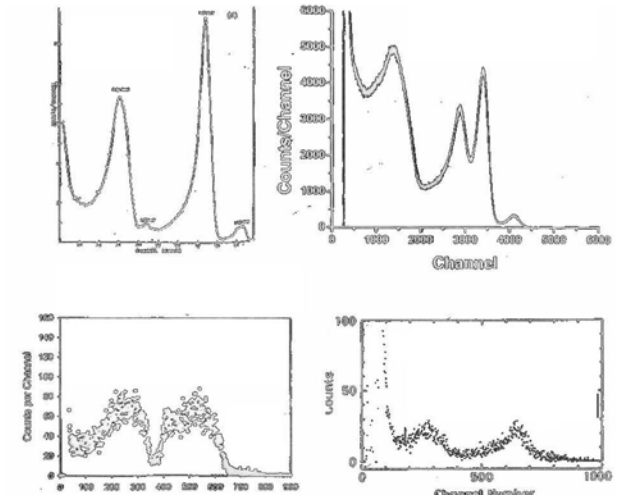

Figure 1 Pulse height spectra from boron-rich neutron detector geometries [3-6]

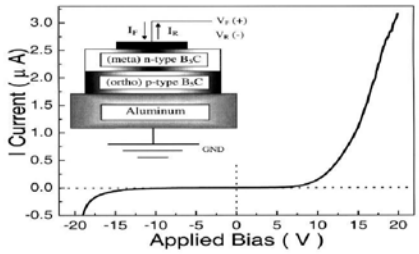

Figure 2 A semiconducting boron carbide heterosiometic diode [7]

References

1. F. d'Errico et al. / Nuclear Instruments and Methods in Physics Research A 505 (2003) 411–414 413
2. D.S. McGregor, J. Kenneth Shultis / Nuclear Instruments and Methods in Physics Research A 517 (2004) 180–188
3. D.S. McGregor, S.M. Vernon, H.K. Gersch, S.M. Markham, S.J. Wojtczuk, and D.K. Wehe: IEEE Trans. Nucl. Sci. **47** (2000) 1364.
4. N. Sato, O. Ishiwata, Y. Seki, and A. Ueda: Jpn. J. Appl. Phys. **29** (1990) 2526.
5. A. Rose: Nucl. Instrum. & Methods **52** (1967) 166.
6. B.W. Robertson, S. Adenwalla, A. Harken, P. Welsch, J.I. Brand, P.A. Dowben and J.P. Claassen: Appl. Phys. Lett. **80** (2002) 3644.
7. A.N. Caruso, R.B. Billa, S. Balz, J.I. Brand, P.A. Dowben. J. Phys.: Condens. Matter **16** (2004) L139–L146

Verification of MultiTrans Calculations by the VENUS-3 Benchmark Experiment

Kotiluoto, P.
VTT Technical Research Centre of Finland
P.O. Box 1608, FI-02044 VTT, Finland.

INTRODUCTION

The MultiTrans code has been developed at VTT for 3D radiation transport problems [*1,2*]. Adaptive tree multigrid technique is used as a deterministic solution method. This enables local refinement of the calculation grid combined with the use of effective multigrid acceleration on tree-structured nested grids: starting from a fast solution on coarse grid, successive solutions are obtained on finer and finer grids. In the MultiTrans code, simplified spherical harmonics (SP_3) are used as a radiation transport approximation.

In order to test the applicability of the new MultiTrans code to reactor dosimetry problems, LWR-PVS benchmark experiment VENUS-3 (with partial length shielded assemblies) [*3*] was chosen.

MATERIALS AND METHODS

The VENUS-3 benchmark geometry was constructed with commercially available CAD software based on benchmark specifications [*3*]. All material regions were modeled in detail, except that fuel pin, fuel cladding, and water regions were homogenized over each fuel zone. The external regions outside the jacket inner wall (air, jacket outer wall, reactor vessel, water, and reactor room) were left away from the model, as they can be assumed to have no significant effect to the responses at the measurement points.

The geometry of each material region of the model was exported from the CAD software as a stereolitography (STL) file. A three dimensional tree multigrid (octree grid) was generated directly from these STL-files, resulting in over 2.46 million cells. A horizontal cross section of the generated octree grid is illustrated in Fig 1., showing also the PLSA fuel region below the core mid-plane.

The venus3.src file from NEA-1517/69 SINBAD-VENUS-3 distribution CD was used as a fixed-source. Fission spectrum for ^{235}U was taken from BUGLE-96 library, which was also used in generation of the transport cross-sections.

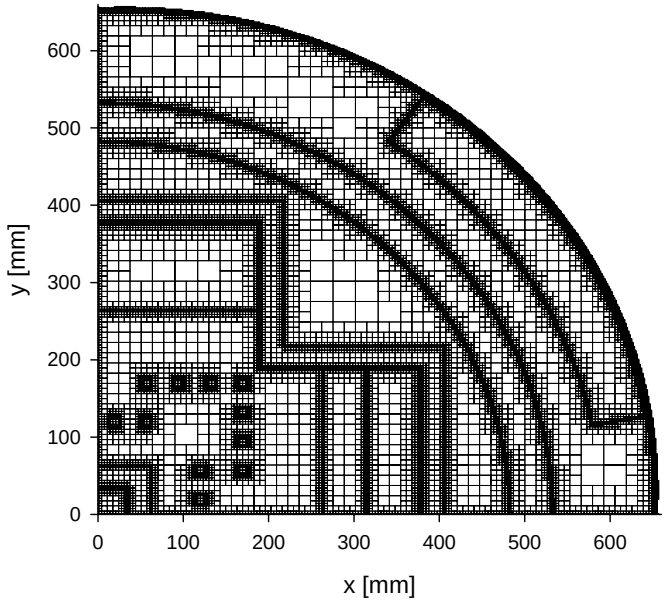

Figure 1. Horizontal cross section at the height of 120 cm (10 cm below the core mid-plane) of the octree grid representing the VENUS-3 benchmark geometry

For calculation of the reaction rates, ^{58}Ni(n,p), ^{115}In(n,n') and ^{27}Al(n,α) cross-sections were condensed into the BUGLE groups from IRDF-90 version 2 dosimetry library in SAND II energy group structure by using X333 utility program from the neutron metrology file NMF-90 [*4*] with combined Maxwell, 1/E, and fission weighting spectrum. Resulting fission spectrum averaged dosimetry cross-sections were 105.7, 186.3, and 0.726 mbarn for Ni, In, and Al.

RESULTS

Comparison of calculated and experimental reaction rates for VENUS-3 detector positions is given in Fig. 2. In general, reaction rates agree well with the experimental values: the majority of the values are within 5% for Ni and Al and within 7% for In. The deviation is larger than 20% only in 2 detector positions of Ni in uppermost PLSA region, and in 1 detector positions of In and Al in core barrel near the corner of the PLSA. Calculation time was 70 min for 47 BUGLE neutron groups on desktop PC running Windows XP with 3.0 GHz P4 CPU and with 3.62 GB of RAM.

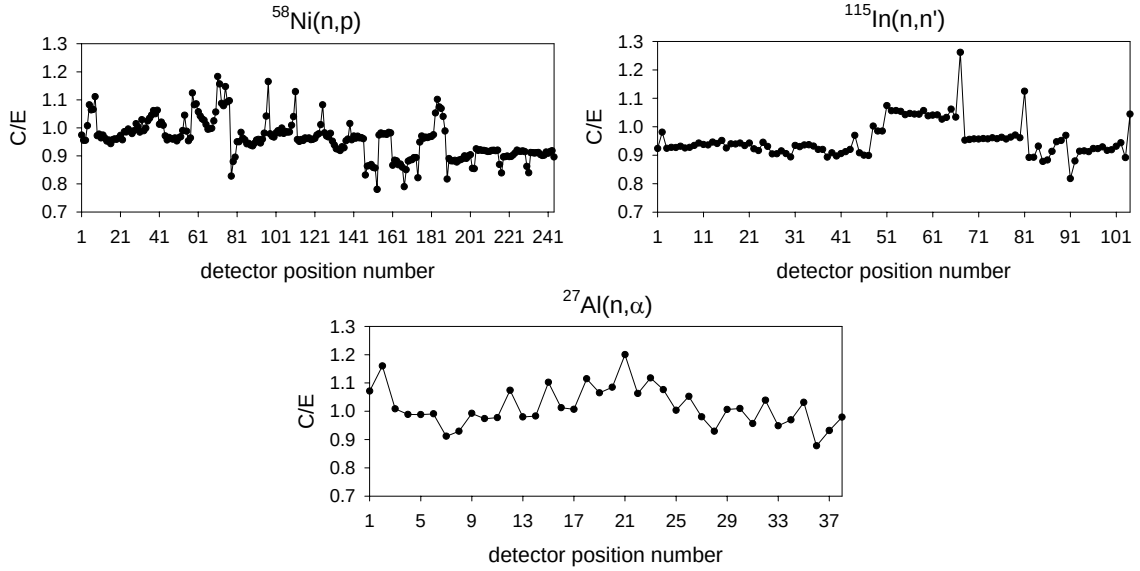

Figure 2. C/E values for ^{58}Ni(n,p), ^{115}In(n,n'), and ^{27}Al(n,α) reaction rates in VENUS-3 detector positions

DISCUSSION AND CONCLUSIONS

The MultiTrans results show good agreement to the experimental reaction rates of the VENUS-3 reactor dosimetry benchmark, demonstrating the applicability of the new MultiTrans code in reactor dosimetry.

ACKOWLEDGMENTS

I wish to acknowledge my colleague Tom Serén for help with the dosimetry cross sections and related utility programs, as well as for other valuable guidance.

REFERENCES

1. P. Kotiluoto, "Fast Tree Multigrid Transport Application for the Simplified P_3 Approximation." *Nucl. Sci. Eng.*, **138** (2001). pp. 269-278.
2. P. Kotiluoto, "Application of the New MultiTrans SP_3 Radiation Transport Code in Criticality Problems and Potential Use in Dosimetry." In: *Reactor Dosimetry in the 21st Century*, World Scientific (2002), pp. 580-587.
3. L. Leenders, *LWR-PVS Benchmark Experiment VENUS-3 (with Partial Length Shielded Assemblies)*, FCP/VEN/01, SCK/CEN (September 1988).
4. É. M. Zsolnay, E. J. Szondi and H. J. Nolthenius, *The Neutron Metrology File NMF-90*, IAEA-NDS-171 Rev.1, IAEA (January 1999).

Application of a Silicon Calorimeter in Fast Burst Reactors

Luker, S.M.[1], DePriest, R.J., Griffin, P.J., King, D.B., Naranjo, G.E., Suo-Anttila, A.J.
PO Box 5800, MS1146
Sandia National Laboratories

PURPOSE

Frequently in experiments at fast burst reactors (FBRs), experimenters need to know the dose and peak dose rate absorbed by a material in terms of dose to silicon. The dose to silicon cannot be reliably measured by a passive dosimeter in a mixed field environment, so we rely on the silicon calorimeter as the true standard. A silicon calorimeter has been developed for applications in a water-moderated pulsed reactor. This calorimeter development is reported in reference [1]. In this paper, the authors investigate the application of this silicon calorimeter in an FBR environment. Tests have been conducted at the White Sands Missile Range (WSMR) fast burst reactor to developed techniques to use this silicon calorimeter for a measure of rad(Si) and for coupling this metric to the response of a diamond photoconductive detector (PCD) in order to derive dose rate.

FBR-SPECIFIC ISSUES

In principle the measurement of the silicon dose in a reactor using the silicon calorimeter should be the most accurate dosimetry method since neutron and gamma absorbed energy will contribute to the integral dose for the material of interest. This is much higher fidelity than relying on calibrations of other detectors in inadequately characterized neutron and gamma spectra. However, several measurement issues make the use of the calorimeter more difficult to use at an FBR. Whereas the peak signal level from the silicon calorimeter in a large water-moderated reactor pulse is typically ~1.5 mV, the signal is much smaller in an FBR and the presence of noise sources can swamp the signal unless proper cabling, amplifier common-mode rejection and cable shielding techniques are chosen.

The silicon calorimeter was developed for applications in a water-moderated reactor with pulse widths from 10 – 100 ms. In a fast burst reactor, the pulse width can be as short as 50 μs and the heat transfer between the thermocouple wire and the silicon wafers can be significantly slower than the reactor pulse width. The slow equilibration of the thermocouple wire heating with the much more massive silicon wafers can interfere with efforts to recover pulse shape. In Figure 1 the thermocouple response is seen to equilibrate to the silicon temperature at about 3 ms after the fast 50 μs FBR pulse. This silicon heating can then be equivalenced to the PCD integral at this 3 ms time point. The PCD time profile can then be used to infer the time history dose rate. Once the thermocouple wire is equilibrated with the silicon wafers, the silicon calorimeter is seen to be stable against heat loss to the housing over times of tens of seconds. Figure 2 shows an expanded look at the derivative of the silicon calorimeter response. The actual PCD response (and the reactor power) is seen to be much shorter than the apparent rise in the early calorimeter response (which is attributed to the wire thermocouple heating). This difference in the temporal profiles is explained by the noise filtering in the data acquisition system that essentially time-averages the calorimeter response over intervals larger than the actual reactor pulse (~50 μs).

In early silicon calorimeter designs, several problems were encountered. These issues included 1) thermal conduction between the silicon wafers and the calorimeter housing; 2) a photocurrent generated in the silicon that delivered a small current between the bare thermocouple leads; and 3) electron emission between the silicon and the calorimeter housing. This paper will discuss our approach to these problems and how we ended with a calorimeter design where the silicon wafer diameter has been reduced from 2.54 cm to 0.952 cm.

[1] This work was supported by the United States Department of Energy under contract DE-AC04-94AL85000. Sandia is a multiprogram laboratory operated by Sandia Corporation, a Lockheed Martin Company, for the United States Department of Energy.

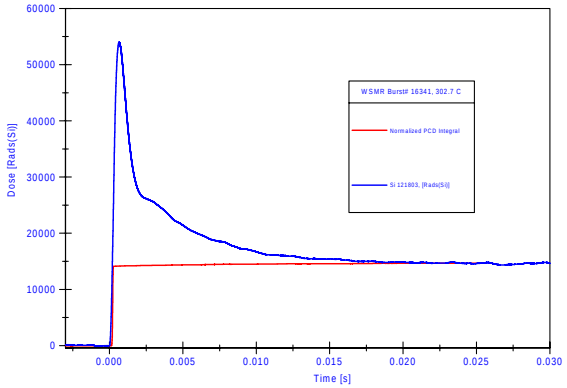

Figure 1. Calorimeter and Integrated PCD response at WSMR.

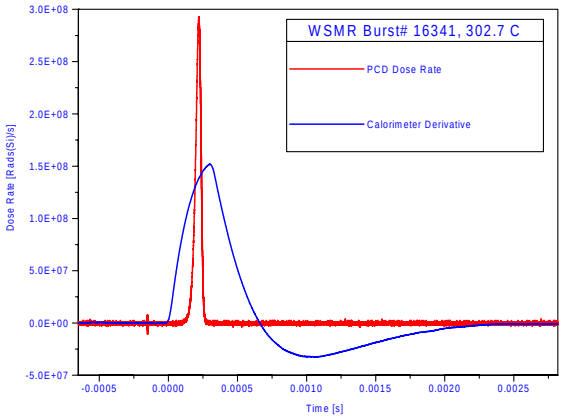

Figure 2. Reactor pulse shape from PCD compared with calorimeter response.

When using a silicon calorimeter, the reference dose is taken at a point during the pulse where the neutron-gamma ratio is known to be constant. The calibration dose at water-moderated reactors was taken at time-to-peak plus three full width half maximum pulse widths (TTP+3FWHM). This normalization point was then used in conjunction with a PCD time profile. When using the silicon calorimeter at a fast burst reactor, the calorimeter/PCD development criteria of matching the response at TTP + 3FWHM would not be appropriate because the pulse can be as small as 50 μsec. This paper discusses attempts to shorten the matching point while taking into account the early-time noise and the heating of the thermocouple wire itself.

REFERENCES

1. Luker, S.M., et al., **Development of a Silicon Calorimeter for Dosimetry Applications in a Water-Moderated Reactor,** Sandia National Laboratories, Albuquerque, submitted to the ISRD12.
2. Griffin, P.J., Kelly, J.G., Vehar, D.W., **Updated Neutron Spectrum Characterization of SNL Reactor Environments, Vol. 1: Characterization,** Sandia National Laboratories, Albuquerque, NM, SAND93-2554, April 1994.
3. Knoll, G.F., **Radiation Detection and Measurement,** Third Edition, John Wiley & Sons, 2000.

The Neutron Spectrum of NBS-1

Craig R. Heimbach
National Institute of Standards and Technology
100 Bureau Drive; Mail Stop 8461
Gaithersburg MD 20899

NBS-1 is the US national neutron reference. It was developed in the late 1940's as a stable, precisely-defined neutron source capable as serving as a calibration reference[1]. The source is driven by the gamma rays emitted from one Curie of radium. A photoneutron (as opposed to an alpha-neutron) reaction was chosen to avoid unknowns in the emission rate due to radium-beryllium mixing, and to avoid an increase in neutron emission as alpha-emitting polonium-210 built up over the years.

A disadvantage of the photoneutron source is the high gamma-ray background. This is due to two causes. There is a reaction threshold of 1.6 MeV, so that almost all the gamma rays produce no neutrons. Also, the reaction cross section for the gamma rays above threshold is on the order of only millibarns.

Figure 1 shows the construction of NBS-1. It consists of radium ($RaBr_2$) inside a PtIr cylinder which is inserted into the center of a beryllium sphere. The gamma rays from the radium interact with the beryllium to produce neutrons.

The neutron emission rate of NBS-1 has been documented by NIST over the years through measurement and through intercomparison with other neutron sources.

The neutron spectrum was measured by Eggler[2], using proton-recoil techniques with a hydrogen-based bubble chamber. The neutron spectrum is difficult to measure because of the relatively high gamma-ray background. Eggler found a spectrum with distinct neutron peaks corresponding to the gamma-ray energies of radium decay products.

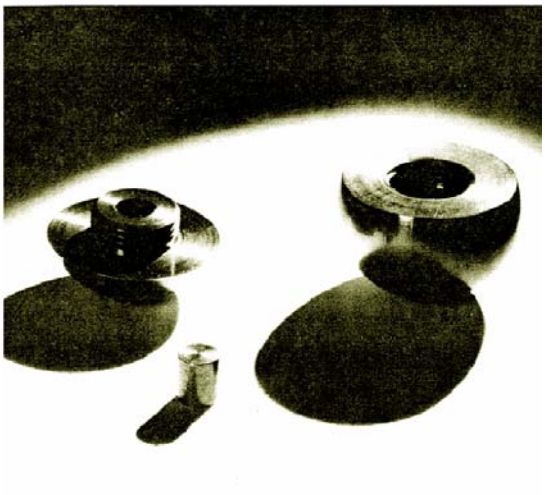

Figure 1. NBS1 disassembled.

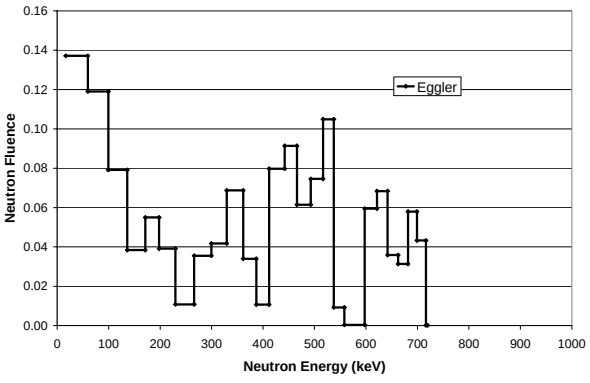

Figure 2. Measured neutron spectrum.

The International Atomic Energy Agency (IAEA) has recently[3] developed a set of photonuclear reaction cross sections which are available in Monte Carlo N–Particle (MCNP) format. The cross sections come with a warning that "they are provided for purposes of testing and validation, and they should be treated with caution."
Due to the clean separation of radium from beryllium in NBS-1, this source provides a good test of the photonuclear data. Also, any improvement in the knowledge of the neutron spectrum assists NIST in establishing its error budget for neutron fluence calibration.

A straightforward calculation would allow the modeling of all materials and the calculation of results. Unfortunately, photonuclear cross sections are available only for the beryllium. In addition, neutron cross sections are not available for radium. Of course, MCNP will not run unless all the appropriate cross sections are included with the problem.

MCNP has the option of substituting cross sections of known elements for cross section of elements with unknown cross sections. This may be done for just one type of interaction (e.g. photonuclear) while using the correct cross sections for other interactions. This technique allows the calculation to proceed, but caution must be taken to ensure that the substitution does not distort the results. One procedure for bracketing the results was to use zero-attenuation (zero-density) and infinite-attenuation (MCNP zero-importance zones) regions in addition to using substitute cross sections.

The equilibrium radium gamma-ray emissions of Sadari[4] were used as gamma-ray input to drive the photonuclear process. The source geometry is simple and was modeled precisely. Cross section approximations were used as appropriate, as stated above. The calculated neutron emission rate was calculated to be higher than the NIST value by about 30%. The calculated neutron spectrum did not show the prominent peaks as Reference 2, and had a neutron distribution substantially lower in energy than measured.

---

1. ***Absolute Calibration of the National Bureau of Standards Photoneutron Standard: I***, J. A. DeJuren, D. W. Padgett, L. F. Curtiss, Journal of Research of the National Bureau of Standards, Vol. 55, No. 2, August 1955.
2. ***The Neutron Spectrum of a Radium Beryllium Photo Source***, ANL-4476, 1950.
3. ***Handbook on Photonuclear Data for Applications***, IAEA TECDOC 1178, Final Report, Oct. 2000.
4. ***Gamma-ray emission probabilities in the decay of ^{226}Ra and its Daughters***, D. Sadari and T. D. MacMahon, Journal of Radioanalytical and Nuclear Chemistry, Vol. 244, No. 2 (2000) 463-469.

The Validity of the Use of Equivalent DIDO Nickel Dose for Graphite Dosimetry

Allen, D.A, Thornton, D. A., Harris, A. M.
British Nuclear Group, Berkeley Centre, Berkeley,
Gloucestershire, GL13 9PB, United Kingdom.

Sterbentz, J. W.
Idaho National Engineering and Environmental Laboratory,
Idaho Falls, ID 83414-3885, USA.

BACKGROUND

Equivalent DIDO Nickel Dose (EDND) is the UK standard unit for representing fast neutron dose to graphite. For a given location, in any specific reactor, EDND is defined as the nickel fluence in DIDO which would give rise to the same amount of graphite damage in DIDO as occurs at the given location in the reactor of interest. EDND is used as a correlation parameter to relate reactor core graphite properties to graphite properties measured from MTR and surveillance specimens.

The commonly used conversion factor between graphite damage in the reactor of interest and EDND has historically been given the value of 1.313×10^{-21} dpa/(n cm^{-2}) and is here denoted D_{DIDO}. This value is based on a published spectrum from 1962, which used very early nuclear data in its evaluation and, more significantly, the Thompson-Wright graphite damage weighting function. This energy-dependent weighting function represents the amount of graphite damage inflicted by fast neutrons and the validity of its use has recently been questioned. Several alternative response functions now exist, based on differing choices of carbon scattering cross-section and graphite damage weighting function. Clearly, if inconsistent use is made of different response functions for MTR samples and power reactor calculations, then the potential for miscalculation of graphite properties will arise. This paper presents work to investigate whether or not any such inconsistencies are significant.

DIDO

The materials test reactor, DIDO, was moderated with heavy water and fuelled using enriched uranium fuel tubes. These tubes were arranged concentrically and allowed the positioning of graphite, and other, specimens within their centres. The scaling factor D_{DIDO} is defined at the centre of a fuel tube located in the centre of the DIDO core. The scaling factor has been recalculated using the Monte Carlo radiation transport code MCBEND and modern nuclear data. A single cell model of a DIDO fuel element was constructed and graphite damage and nickel flux calculations were performed. Several alternative graphite damage response functions were used. The value of D_{DIDO} has been shown to be insensitive to the choice of either carbon scattering cross-section or graphite damage weighting function. All calculated results were within 3% of the standard historical value.

MAGNOX REACTOR GRAPHITE

A similar exercise has been undertaken for Magnox reactor core graphite. A MCBEND single cell model has been used to calculate the graphite damage within Magnox cores. Historically this has made use of the DAMSIG-84 response function, which is based on the Thompson-Wright damage weighting function. When alternative functions are employed the differences in calculated EDND are within 5% of those previously obtained using the DAMSIG-84 response.

INEEL ADVANCED TEST REACTOR CORE

As part of the programme of work for the Magnox graphite core safety cases, samples of graphite were subjected to accelerated irradiation and oxidation within the core of the INEEL Advanced Test Reactor. Graphite dosimetry and nuclear heating calculations have been performed by INEEL staff using the Monte Carlo code MCNP.

This core has a very different fast neutron spectrum from that found in Magnox reactors and it was necessary to investigate whether or not the choice of response function is significant in determining the calculated EDND. Results are presented, along with measured wire fluxes for validation.

CONCLUSION

It is concluded from this work that, although apparently significant differences exist between the available graphite damage response functions, the net effect is not significant in determining EDND. Therefore confidence in past calculations has been improved and continued use of previous methods is supported.

ACKOWLEDGMENT

This paper is published with the permission of British Nuclear Group.

Radiation Dosimetry in the BNCT Patient Treatment Room at the BMRR

Holden N. E., Reciniello R. N., Hu J.-P.
Brookhaven National Laboratory
Upton, New York 11973, USA

The Brookhaven Medical Research Reactor (BMRR) was a heterogeneous, tank-type, light water cooled and moderated, graphite reflected reactor, which was operated on demand at a power level up to 3 mega-watts (MW) for medical and biological research and became operational in 1959. The BMRR had a thermal neutron beam in the Thermal Neutron Irradiation Facility (TNIF) on the west side of the core and an epithermal neutron beam in the Epithermal Neutron Irradiation Facility (ENIF) on the east side of the core [*1*].

The primary use of the epithermal neutron beam in the ENIF was to perform clinical trials on patients with malignant brain tumors (glioblastoma multiforme). The treatment that was used in these clinical trials involved Boron Neutron Capture Therapy (BNCT). The patient was injected with a boron compound and subsequently irradiated with the epithermal neutrons in the ENIF. For the period from September 13, 1994 until March 26, 1999, a total of fifty-four patients had undergone such clinical trials in the patient treatment room (ENIF) of the BMRR. The BMRR was permanently closed down at the end of December 2000.

A series of measurements and calculations had been performed in the ENIF both prior to the beginning of the clinical trials, as well as during such patient treatment. The details and the comparison of the measurements and the Monte Carlo calculations are included in the following discussion.

Both bare foils and cadmium-covered gold foils, various threshold detector foils were used to determine the neutron flux values. Thermo-luminescent dosimeters (TLDs) and test TLD badges with ^{6}LiF and ^{7}LiF chips were utilized to provide experimental data on the neutron dose rates and gamma-ray dose rates. TLD test badges use LiF: Mg, Ti as the thermo-luminescent material in the form of solid chips. Three of the chips were TLD-700 material (enriched in ^{7}Li to 99.93%) and one chip is TLD-600 material (enriched in ^{6}Li to 95.6%). The badges also have filters of plastic, copper and thin aluminized mylar film of various thicknesses to separate and measure mixed fields of neutrons, beta particles and gamma-rays.

The MCNP code [*2*] was used to perform Monte Carlo calculations at various locations throughout the ENIF, to obtain energy dependent spatial distributions of gamma-rays and neutrons from thermal energies (0.001-0.04 eV) up to fast energies (0.1-10.0 MeV). MCNP has been used to mock up the geometry of the core, reflector, the shutter, the epithermal port, the collimator, and the patient treatment room.

In the ENIF, the neutron beam was located three feet above the floor in the center of the reactor wall. Radiation shielding in the beam port ended with a bismuth shield. In performing the BNCT, experimental comparisons were made with the patient in place, with a tissue equivalent head phantom in place to mock up the patient's head position and with the room empty to study the impact of the patient on the background flux and dose rate values. At 10.5 cm downstream of the bismuth shutter apex along the beam path, a removable six-inch thick, Li_2CO_3-based collimator is located. The collimator had a concave cavity 20 cm in diameter on the reactor side tapering to 12 cm on the room side, for an optimal beam focusing. When collimator is in place, the axial distribution of the thermal and epithermal neutron fluxes can be shown by the two curves in Figure 1 below. Note in Figure 1, although the epithermal flux decreases faster than the thermal flux, its absolute value is 27 times larger.

The effectiveness of the ENIF mechanical shutter was tested using an RO2A (at a full scale of 50 R/h) ionization chamber, and an ASP1 Rem-ball. The measured dose rate of neutrons and gamma-rays has provided the baseline reference data for the BMRR operation when BNCT is performed.

Additional results on the neutron fluxes, the gamma-ray fluxes, the neutron dose rate and the gamma-ray dose rate and the comparison with the MCNP calculations for the various room conditions will be presented.

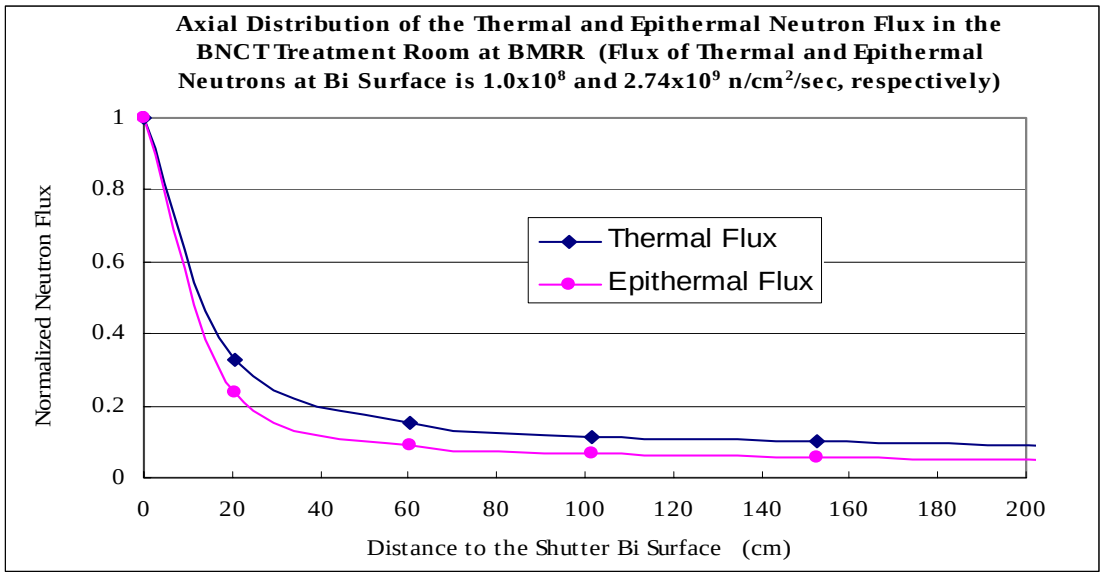

Figure 1. Axial distribution of the thermal and epithermal neutron flux along the beam path starting from the shutter Bi surface and passing through the Li_2CO_3-based collimator in the BNCT patient treatment room at BMRR.

1. N. E. Holden, J.-P. Hu, D. D. Greenberg, and R. N. Reciniello, Radiation Dosimetry for NCT Facilities at the Brookhaven Medical Research Reactor in "Frontiers in Neutron Capture Therapy", Hawthorne et al., (editor), Kluwer Academic / Plenum Publishers, New York, New York, 2001.

2. J. F. Briesmeister (editor), MCNP – A Monte Carlo N-Particle Transport Code (version 4B2), developed by the Los Alamos National Laboratory (LA-12625-M), and distributed by the Oak Ridge National Laboratory (CCC-660), 1997.

Predictions of Radiation Damage in Silicon Carbide Semiconductor Radiation Detectors for Nuclear Reactor Power Monitoring in the GT-MHR

Blue, T. E., Lohan, B., Khorsandi, B., Miller, D.W.,
Ohio State University, Nuclear Engineering Program
Columbus, OH 43202, USA.

INTRODUCTION

As a part of a DOE NERI project, we are evaluating the potential for using Silicon Carbide (SiC) Semiconductor radiation detectors, operating in the pulse mode, as power monitors for the Gas Turbine Modular Helium Reactor (GT-MHR) [*1*]. Locations for the power monitors will be selected considering acceptable detector count rates and lifetimes. Our intent is to characterize the radiation environment in various locations in the GT-MHR where detectors may be placed in terms of the 1 MeV equivalent neutron flux in SiC ($\phi^{Total}_{eq,1MeV,SiC}$). Then we will characterize the radiation field in Beam Port 1 (BP1) of the Ohio State University Research Reactor (OSURR) in these same terms, and correlate observed degradation of the SiC detectors in the OSURR to the degradation that can be expected for various detector locations in the GT-MHR. This paper describes the results of our efforts to characterize the radiation environment in various locations in the GT-MHR where detectors may be placed, in terms of $\phi^{Total}_{eq,1MeV,SiC}$.

METHODS

In placing the SiC detectors within the reactor, there is a conflict between achieving a high count rate, which is necessary to generate a scram in an appropriately small time, and degrading the detector as a consequence of radiation damage. In order to predict the detector count rate and to quantify the radiation exposure in terms that are technically precise and relevant to the observed radiation effect, we have calculated the neutron and gamma-ray radial flux distributions in the Reactor Cavity (RC) and in the Reactor Cavity Cooling System (RCCS) resulting from fission events within the GT-MHR core.

The GT-MHR reactor was modeled in 3-dimensions in MCNP[*2*] accounting for radial and axial variations of the core power distribution. Regarding the level of detail of the model, while various regions of the core were modeled as being physically distinct (most importantly the fueled region of the core was modeled as being distinct from the various reflector regions), the fueled region of the core was treated as a homogeneous mixture. The neutron and gamma-ray flux distributions, were calculated as a function of axial location for the following radial locations: 1) In the central reflector, for detector capsules located at radial distances R=117 and R=153 cm from the central reflector centerline, 2) In the RC at R=505 cm, and 3) In the RCCS at R=610 cm. We have used this data to predict the detector count rate and $\phi^{Total}_{eq,1MeV,SiC}$ at the respective detector locations.

The total 1 MeV equivalent neutron flux for SiC was calculated using the general expression given in Eq. (1),

$$\phi^{Total}_{eq,1MeV,mat} = \int_0^\infty \frac{F_{D,mat}(E)}{F_{D,1MeV,mat}} \phi(E) dE \qquad (1)$$

where $F_{D,mat}(E)$ is the damage function for the material of interest (SiC) evaluated at energy E, $F_{D,1MeV,mat}$ is the damage function for the material of interest (SiC) evaluated at energy E = 1 MeV, and $\phi(E)$ is the energy dependent neutron flux density function. Figure 1 presents the damage function for SiC ($F_{D,SiC}(E)$) that was used to calculate $\phi^{Total}_{eq,1MeV,SiC}$, as well as the damage function for Si ($F_{D,Si}(E)$), which is presented in the figure for the purposes of comparison.

Table 1 presents $\phi^{Total}_{eq,1MeV,SiC}$ for the GT-MHR, averaged over all axial layers of the core, with radius as a parameter.

Table 1. 1 MeV equivalent neutron flux in SiC at various locations within the GT-MHR

Detector Radial Location (cm)	117	153	505	610
$\phi^{Total}_{eq,1MeV,SiC}$ (n/cm^2-s)	3.50E+11	3.75E+12	9.68E+07	1.95E+07

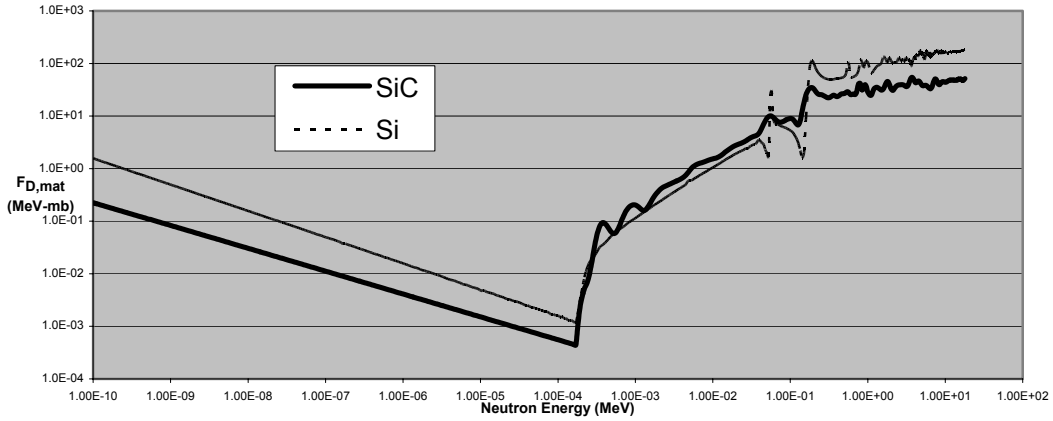

Figure 1. The damage functions for Si and SiC ($F_{D,mat}(E)$)

For purposes of comparison, $\phi^{Total}_{eq,1MeV,SiC}$ was calculated in the manner described above for Position 4 in the semi-conductor device characterization vessel in Beam Port 1 (BP1) of the OSURR. The values of $\phi(E)$ that were used in the calculations were determined using foil activation data and the SAND-II neutron energy spectrum deconvolution code. The results of the calculations are $\phi^{Total}_{eq,1MeV,SiC}$ = 7.20 x 10^{11} neutrons $cm^{-2}s^{-1}$ for operation at 500kW (nominal full power).

In conclusion, it can be seen by comparing the values $\phi^{Total}_{eq,1MeV,SiC}$ for the GT-MHR with the value of $\phi^{Total}_{eq,1MeV,SiC}$ for the OSURR, that SiC devices can be adequately tested in the characterization vessel in BP1 of the OSURR for the radiation damage that would be incurred over a refueling cycle for detectors placed in the GT-MHR RC and RCCS. Unfortunately, it appears that this is not the case for detectors located in-core in the GT-MHR.

ACKOWLEDGMENTS

This material is based upon work supported by the US Department of Energy under the NERI program Award No. DE-FG-07-02SF22620 and NERI Project Number 02-207. Any opinions, findings, and conclusions or recommendations expressed in this material are those of the authors and do not necessarily reflect the views of the Department of Energy.

REFERENCES

1. General Atomics, "GT-MHR Conceptual Design Description Report," Issued by General Atomics, U.S. Nuclear Regulatory Commission Project 716, San Diego, CA (August 2002).
2. MCNP: A General Monte Carlo N-Particle Transport Code, Version 5, Los Alamos National Laboratory, Los Alamos, NM (2003).

Measurements of Reactor Neutron Spectra Characteristics Using Activation Composite Monitors

Efimov B.V., Demidov A.M., Dikarev V.S., Ionov V.S.
RRC "Kurchatov Institute"
Kurchatov sq. 1, 123182 Moscow, Russia

The results of neutron spectra measurements in several experimental reactors are reported. All measurements were carried out using composite activation monitors developed in RRC "Kurchatov Institute". Each monitor was made of well homogenized composition contained a mixture of five isotopes: 164Dy, 55Mn, 197Au, 186W, and 81Br. It allows measuring spectra parameters in thermal and epithermal energy regions. Special irradiations together with standard samples (with well known isotope contents) and comparisons of their activity were carried out for determination of isotope contents in composite monitors. Induced γ- activity of monitors was measured by the γ-spectrometer with extra pure Ge-detector (crystal volume 150 cubic centimeters, ORTEC equipment).

Different modes of neutron spectra characteristics determination were used. System of five equations for reaction rates (in monitor isotopes) is solved taking into account corresponding thermal cross sections and resonance integrals, and thermal (*Fth*) and epithermal (*Fepi*) neutron flux densities are determined. According to alternative approach this equation system is treated as a system of linear regression equations. Both approaches give similar results. Effective temperature of thermal spectrum *Tn* is determined by iteration process using its functional dependence on ratio *Fth* / *Fepi* (see below).

First of all that methodology was verified in standard thermal neutron field in reactor F-1, for which metrological values of *Fth* , *Fepi* and *Tn* are known. Calibration of all composite monitors was carried out in this reactor. Reaction rates measured in the reactor F-1 were compared with calculated ones (Monte Carlo method, RRC KI code MCU) and satisfactory agreement was found.

An experimental technique developed was used also for fission reaction rate (*FRR*) measurements in reactor fuel elements.

The numerous measurements of *Fth* , *Fepi* and *FRR* were carried out in the various experimental nuclear reactors of RRC «Kurchatov Institute»: above mentioned uranium-graphite reactor F-1 (first Russian and today world oldest reactor, which is used for providing the standard thermal neutron field), water critical facilities P and SK-PHYS, and critical facility ASTRA (model of HTGR). Spectrum parameters distribution inside facility P core was measured and significant positive correlation between *Fth* and *Fepi* was found. Distributions of *Fth* , *Fepi* and *FRR* were measured inside ASTRA core. Measured and calculated values of *FRR* are in a good agreement.

Analysis of numerous experimental data obtained in different reactor types show that different spectral parameters can be represented as functions of spectrum "hardness" parameter $z = Fth / Fepi$. Such dependencies were shown for *Tn*, *Fepi*, and ratios of experimental (n,γ) reaction rates Dy/Mn, Dy/Au, Dy/W, Dy/Br. It is significant that these parameters depend only on *z* but not on reactor type.

TRIM Modeling of Displacement Damage in SiC for Monoenergetic Neutrons

Khorsandi, B., Blue, T. E., Windl, W.,
Ohio State University

INTRODUCTION

Silicon carbide (SiC) is a promising material to monitor the neutron power for nuclear reactors. SiC has very good thermal, chemical, neutronic and electrical properties, particularly at high temperatures. Compared to Si, SiC is a radiation hard material; however, its properties are changed by irradiation with a large fluence of energetic neutrons, as a consequence of displacement damage.

This paper describes the methodology that was used by the authors to predict the number of displacements resulting from neutrons using two codes (MCNP [*1*], and TRIM [*2*]) in combination. To the best of our knowledge, this modeling method is unique for SiC detectors.

CALCULATIONAL METHOD

In order to use the TRIM code to determine the number of displacements resulting from neutrons, a TRIM input deck (trim.dat) is required including the following characteristics of the Primary Knock-on Atoms (PKA): their types, energies, initial positions and direction cosines. Therefore, in order to model displacement damage in SiC from neutrons (indirectly ionizing radiation), using TRIM, one must use the output of another code that model the transport of neutrons through SiC (such as MCNP) to write the TRIM input file.

In our case, we are concerned with radiation damage in Schottky SiC semi-conductor diode detectors. These diodes are very thin (~ 300 μm). Consequently, the majority of neutrons that are incident upon the surface of the SiC diode pass through the SiC without interacting. The PTRAC card in MCNP was used to determine the conditional probability that a neutron entering the SiC volume will interact with a Si or C atom therein. Furthermore, a program was written to extract neutron characteristics (energy, position and direction cosines) before and after each collision, as well as the type of PKA from the PTRAC file that was created by MCNP. Based on the conservation of energy and momentum, the code also calculated the necessary PKA characteristics from the change in the neutron characteristics resulting from collisions.

The output (the PKA characteristics) of this program was used as an input for the TRIM code to estimate the number of displacements, including the number of C- and Si-vacancies, and replacements.

The semiconductor was modeled as a cylinder with 310 μm thickness (the active volume was assumed to have a thickness of 10 μm and the substrate was assumed to have a thickness of 300 μm). The semiconductor was modeled as an amorphous material (because of TRIM limitations). The SiC density was set to be 3.2 g/cm^3. E_d (the minimum energy to move an atom from its original site) was assumed to be 20 and 35 eV for C and Si, respectively, to be consistent with Weber et al [*3*].

RESULT

Figure 1 shows the displacements per atom per fluence (dpa/fluence) as a function of the neutron energy.

CONCLUSION

Two computer codes were used to determine the number of displacements, including C- and Si-vacancies and replacements, created by neutron irradiation in a thin SiC semiconductor detector. This methodology can be used to predict the number of displacements resulting from a reactor energy dependent neutron flux distribution as a basis for studying the distribution, nature, evolution and effect of neutron-induced damage in SiC or other semiconductors.

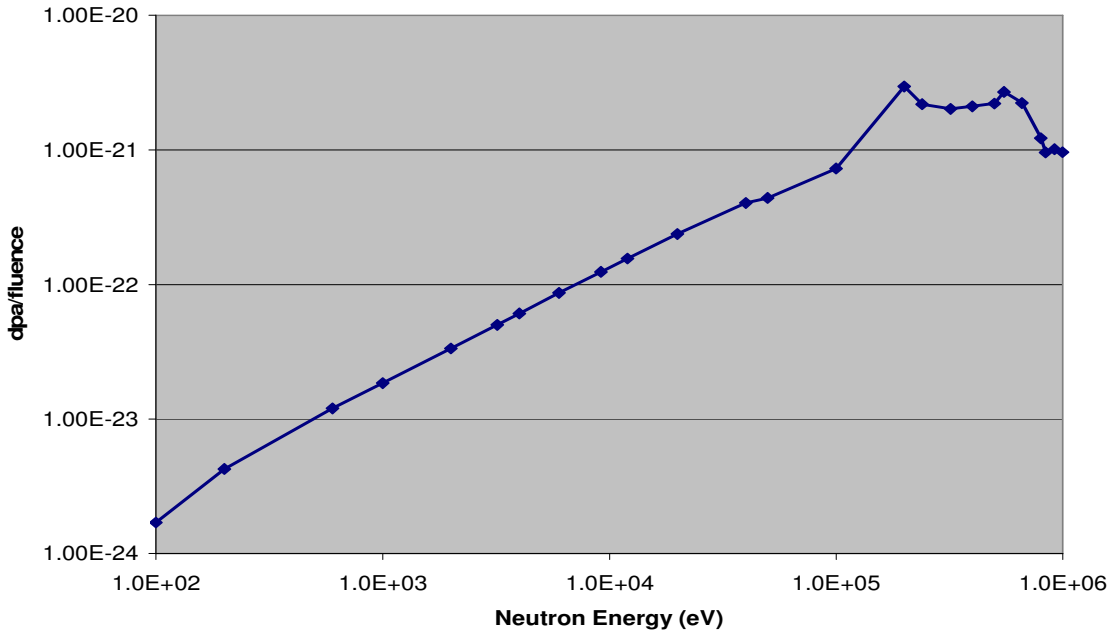

Figure 1. dpa/fluence for SiC detector as a function of the neutron energy

ACKOWLEDGMENTS

This material is based upon work supported by the US Department of Energy under the NERI program Award No. DE-FG-07-02SF22620 and NERI Project Number 02-207. Any opinions, findings, and conclusions or recommendations expressed in this material are those of the authors and do not necessarily reflect the views of the Department of Energy.

REFERENCES

1. *MCNP: A General Monte Carlo N-Particle Transport Code*, Version 5, Los Alamos National Laboratory, Los Alamos, NM (2003).
2. J. F. Ziegler, *Computer Code SRIM-2003,* http://www.srim.org.
3. W. J. Weber, and et al., "The Efficiency of Damage Production in Silicon Carbide," *Nuclear Instruments and Methods in Physical Research B,* **218** (2004). pp. 68-73.

Thermal and Epithermal Fluence rate Measurements in Multipurpose Reactors.

Voorbraak, W.P., Aaldijk, J.K. and Freudenreich, W.E..
Nuclear Research and Consultancy Group, NRG, P.O.Box 25, Petten, The Netherlands

INTRODUCTION

Material Test Reactors are more and more transformed to multipurpose reactors. Production of medical isotopes, silicon doping, even direct treatment of patients with thermal and/or epithermal neutrons play more and more an important role besides the original objective of the reactor, material testing. This means also a growing interest for an accurate characterisation of the thermal and epithermal neutron field.

A more accurate approach has been developed therefore. An existing computer code RESDETLINE [*1*] for solving the set of linear activation equations describing the activation by thermal and epithermal neutrons has been upgraded to RESDET2 [*2*]. Combinations of activation materials with suitable nuclear data have been sorted out for different irradiation intervals.

RESDETLINE CODE

If the neutron spectrum can be represented by a pure Maxwellian distribution coupled to a 1/E distribution, then, in principle, only two energy groups are sufficient to describe the activation of monitor material. Materials with suitable half-life are chosen of which cross-sections show generally an 1/v shape, on which a few resonance peaks may be superimposed to solve both, the thermal and epithermal fluence rate.

Unfortunately the solution of the 2 equations with 2 unknowns produces thermal and epithermal fluence rates with unknown accuracy. The code RESDETLINE had been developed therefore. RESDETLINE uses the reaction rates of more than 2 reactions. The solution of the equations is based on least squares analysis. Covariances in the measured reaction rates and in the cross sections are taken into account. Since the method of least squares leads sometimes to a matrix of coefficients of the normal equations, which can be very ill conditioned, the approach is not to solve these normal equations directly. Instead the so-called Householder transformation is applied first.

RESDET2 CODE

The upgraded code RESDET2 has been designed with a simple input and a simple output. For that purpose also a nuclear data library for different resonance reactions has been established; this library (RESLIB) contains values for cross-sections and resonance integrals, together with coefficients of variation and correlation coefficients. The values for the 2200 m/s cross-section and the resonance integral are taken from DOSCROS2001[*3*]. All data were based on the information present in the International Reactor Dosimetry File (IRDF-90) [*4*] and the more recent Japanese JENDL library [*5*]. The values for the correlation between the 2200 m/s cross-section, and the resonance integral are taken from the International Reactor Dosimetry File (IRDF-90) [*4*].

EXPERIMENTS

The approach with the computer code RESDET2 is demonstrated with combinations of:

- iron, cobalt and silver, the both latter diluted in aluminium, reactions $^{58}Fe(n,\gamma)\,^{59}Fe$, $^{59}Co(n,\gamma)^{60}Co$, $^{109}Ag(n,\gamma)^{110m}Ag$
- manganese-nickel, copper and gold diluted in aluminium, reactions $^{55}Mn((n,\gamma)^{56}Mn$ and $^{197}Au(n',\gamma)^{198}Au$.

- the ACORD monitor set type II [*6*], which supplies reaction rates for six thermal activation reactions: $^{45}Sc(n,\gamma)^{46}Sc$, $^{58}Fe(n,\gamma)\ ^{59}Fe$, $^{59}Co(n,\gamma)^{60}Co$, $^{93}Nb(n,\gamma)^{94}Nb$, $^{109}Ag(n,\gamma)^{110m}Ag$, and $^{235}U(n,f)F.P.$
- $^{59}Co(n,\gamma)^{60}Co$ irradiated with and without Cadmium absorber compared to a combination of $^{59}Co(n,\gamma)^{60}Co$ and $^{109}Ag(n,\gamma)^{110m}Ag$.

The measured reaction rates of these combinations of reactions have been used to determine the thermal fluence rate ϕ_0 and epithermal fluence rate per unit lethargy ϕ_{epi} at the position of the irradiated monitor materials.

CONCLUSIONS

Use of the code RESDET and sets of suitable monitor materials give an important reduction in the uncertainty of the epithermal fluence rate. Introduction is recommended of the reaction $^{197}Au(n',\gamma)^{198}Au$ for short irradiations and the reaction $^{109}Ag(n,\gamma)^{110m}Ag$ for irradiations up to a few months. Burn-up of ^{110m}Ag has to be noticed an corrected for. The reliability of results remeins strongly connected to the availability of nuclear data, their uncertainty and the covariances.

REFERENCES

[1] H.Ch. Rieffe: *Program description of RESDETLINE. R.M.G.* Note 72/08, RCN, Petten, June 1st, 1972.

[2] J.K.Aaldijk, *RESDET2, a computer program for solving linear equations for resonance detectors,* Report 20901/02.51120/I, March 2003

[3] W.E. Freudenreich: *Neutron Activation Cross Section Library DOSCROS2001,* Report 20689/01.40537/I.

[4] N.P. Kocherov, and P.K. McLaughlin: *The International Reactor Dosimetry File (IRDF-90),* IAEA-NDS-141, Rev. 2, October 1993.

[5] *JAERI Nuclear Data Center: JENDL Dosimetry File 99 (JENDL/D-99),* private communication (1999).

[6] W.P. Voorbraak, W.E. Freudenreich and A. Paardekooper, *Experimental Analysis of Neutron Field Parameters for 2 Surveillance Channels in Kola NPP Unit No.3. Results of ACORD monitor sets*. Report 21046/04.58978/P, Report 20901/02.51120/I, March 2003.

Comparison of Two Methods of Fast Neutron Fluence Measurements in WWER-1000 Surveillance Assemblies

Nikolaenko V.A., Zaritsky S.M., Bachuchin I.V.
RRC "Kurchatov Institute"
Kurchatov sq. 1, 123182 Moscow, Russia

The fast neutron fluence received by each WWER-1000 surveillance specimen is determined today using results of direct measurement of ^{54}Mn absolute activity in the material of specimen. The effective threshold energy of the ^{54}Fe(n,p)^{54}Mn reaction is approximately 3 MeV. The spectral index (ratio of integral neutron flux densities at thresholds 0.5 and 3.0 MeV) should be calculated with necessary precision in every specimen position in order to obtain fluence of neutrons with E > 0.5 MeV starting from fluence with E > 3 MeV.

The decay half time of ^{54}Mn is equal to 312 days and due to this fact it allows determining reliably the fluence only for approximately last 3 years of specimen irradiation. After a few years of irradiation the activity of ^{54}Mn in a specimen material is completely saturated and does not depend on fluence. The extrapolation is necessary for evaluation of fluence beyond this period. At that it is necessary to take into account the detailed local power distribution and its history in the upper parts of fuel assemblies, which are nearest to the surveillance assembly in consideration (WWER-1000 surveillance assemblies are located over the core on the baffle top).

Spectral index for a given specimen depends on surveillance assembly position and orientation. Orientation of surveillance assemblies with respect to the core should be evaluated taking into account the measured specimens activities and local power distribution in the nearest fuel assemblies. The orientation should be evaluated e.g. comparing the experimental and calculated ^{54}Mn activities, which were obtained using mentioned local power distributions.

Thus the standard method of fluence determination is rather complicated and it would be desirable to consider any alternative one in order to check the standard method and guarantee the necessary reliability of WWER-1000 surveillance dosimetry.

The diamond detectors, which are located inside surveillance containers, give other opportunity for fluence measurements. Neutron irradiation causes the extension of diamond crystal lattice: the more neutron fluence – the more lattice extension. That's why diamond detectors could be used for neutron fluence measurement after corresponding calibration. Diamond can summarize fluence over a long period, and information concerning local power history is not necessary in this case. The lattice extension depends also on temperature during irradiation, but recent special experiments showed, that WWER-1000 surveillance temperature is practically stable on a level 300 C.

Data obtained with 123 diamond detectors irradiated in 13 WWER-1000s (irradiation time from 315 days to 8.8 years) were used for their calibration. It was demonstrated that reasonable accuracy of fluence above 0.5 MeV measurements can be reached at diamond lattice extensions 0.4-2.0%. This extension interval is enough for fluence measurements during all RPV lifetime.

Results of fluence determination based on ^{54}Mn activity and diamond lattice extension measurements are compared for several surveillance sets – from 3.3 to 8.8 effective years of irradiation. Both methods give closed fluence values at relatively short irradiations but disagreements are significant in some cases at long irradiations of surveillance specimens.

Characterization of the Environment Inside a Graphite Thermal Column at the White Sands Fast Burst Reactor Facility[1]

Wesley W. Sallee, M. H. Sparks, T. M. Flanders[2]

The White Sands Fast Burst Reactor Facility (FBRF) has historically been used for the testing of fast neutron effects in electronics. The current work focuses on converting this essentially fission spectrum source into a heavily moderated, nearly thermal, neutron source by use of a specially constructed graphite pile. The modified environment is a pile of graphite approximately 20 cm thick, surrounded by 5 cm of polyethylene. There is a central cavity located approximately 58 cm from the core's vertical center line and approximately 35.5 cm above the horizontal center plane. The focus of this investigation was to determine the amount of thermalization achieved with this design and to characterize the non-thermal part of the spectrum.

Pure gold radiometric monitors (foils) and the procedures in ASTM standard E-261 and E-262 were used to determine the thermal neutron fluence in the pile. In addition, the fast and thermal gradients were measured within the central cavity test location using nickel and gold foils. Finally, a full spectrum measurement was made using a foil set which covered the entire energy range. The spectrum was compared to free field measurements (previously reported) at approximately the same location.

The central cavity area is essentially a 20x20 cm square, 5 cm deep. The gradient in the fast (energy > 3 MeV) part of the spectrum shows a sharp bottom to top gradient (Figures 1 and 2). A careful examination of the setup shows that the bottom of the pile's cavity is actually above the top of the FBRF's core. So, the top-to-bottom gradient in the cavity is to be expected. Two foil widths up or down is 7-10%. Fortunately, for a given plane within the cavity, the gradient is minimal. Because the fluence gradients in the nickel and gold monitors are not the same, it is safe to say that the spectral shift within the cavity is also significant. Thus, using a monitor foil activity ratio to adjust for the gradient during the spectral measurement was not deemed appropriate. These factors severely limit the available area for a spectral determination. The result of these physical limitations was that foil stacks and multiple runs were used during the spectral determination.

Table 1 is a list of the foils used during the initial spectral characterization. After examination of the activities, it was determined that a more extensive set of activities would be necessary which incorporate activities for Pu and Np inside a boron ball. (This set of data should be available shortly.) The foil set was limited by the amount of available space in the cavity as described above and is only applicable to the center plane of the cavity where the measurement was conducted. Because of the extreme amount of moderation, relative to the facility's normal free field environment, the high energy foils in the set have light activation. Where possible, 1% statistics for at least one count of each monitor was the goal. However, 3% counting statistics were more typical for the iron, magnesium and titanium monitors. By contrast, it was very easy to achieve the 1% goal for the counting statistics in the monitors covering the thermal and resonance region of the energy spectrum.

The foils for this measurement were located approximately 58 cm from the core's vertical center line. The best known test environment for this facility is 60.96 cm, 10 cm above the experimenter's table. Several high quality spectral determinations have been conducted for this location. Table 1 includes the activation data for the foils common to both the current work and the most recent (1998) free field 61 cm data. The activities are first compared by a ratio to the nickel activity in each data set. Then they are compared by taking the ratio between data sets. In effect, this double ratio uses the nickel activity to account for the difference between the irradiations. It assumes only that the nickel activity could be accurately measured for each data set. Using 1 keV as a metric of thermalization, the free field measurement has ~ 3% of it's neutrons below this threshold. The double ratio shows that the thermal column has done its job and produced a spectrum which has the vast majority of it's neutrons below 1 keV.

---

[1] Approved For Public Release; Distribution Is Unlimited OPSEC Review Conducted On: 9 Sept 04.

[2] The authors are members of the White Sands Fast Burst Reactor Physics Division. Commander, White Sands Missile Range, CSTE-DTC-WS-ST-SR, 100 Headquarters Blvd, White Sands Missile Range, NM 88002, USA (email: Wesley.Sallee@us.army.mil)

Figure 1. Inset for Dosimetry Shot: Graphite Thermal Column.

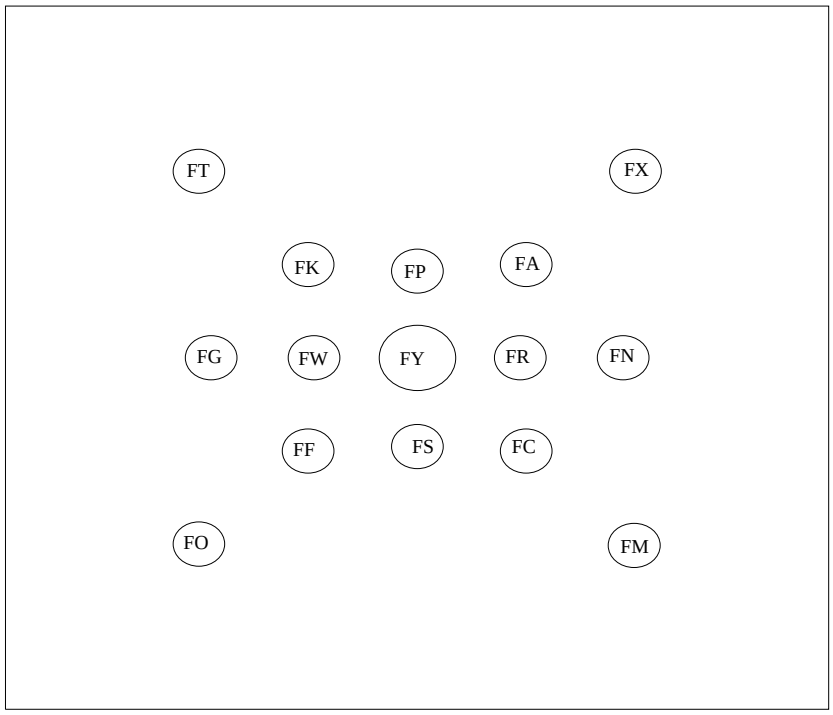

Insert is an ~20x20 cm (8"x8") square. In each row, the foils centers are separated by ~2.5 cm (1"). On the diagonals, the centers are ~3.8 cm (1.5") apart.

Figure 2: Gradient Base on Nickel Foil Monitors

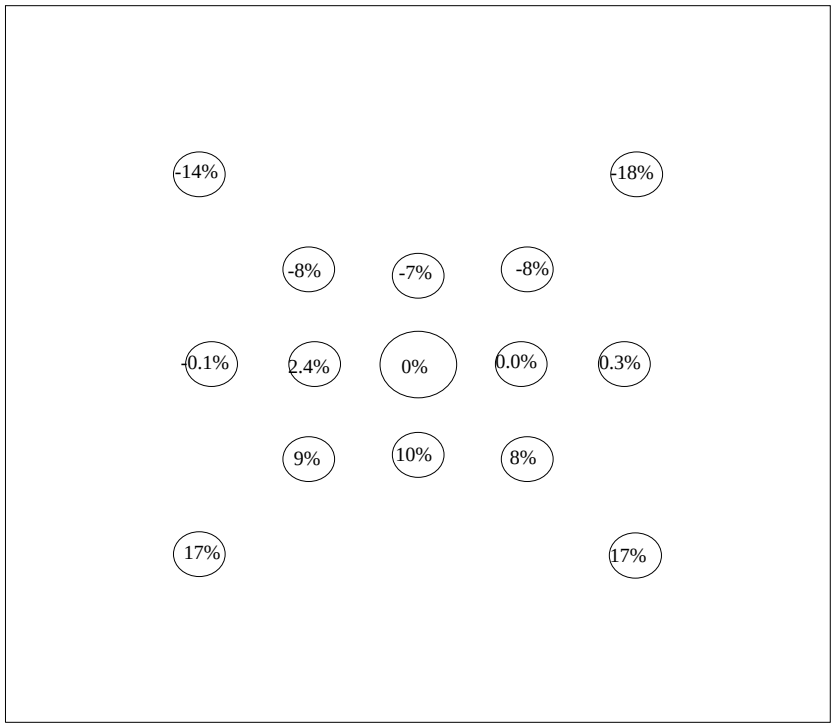

Table 1: Comparison of Heavily Moderated Activities at 58cm to Free Field at 61 cm

Reaction Probabilities

		400 kW-M 3000 sec @ 8kW 10 cm above the table 7/1/1998		Ratio to Nickel	273.6 deg C Burst 35.5 cm above the table 5/1/2004		Ratio to Nickel	Double Ratio Graphite:FF
		Free Field	Unc		Graphite	Unc		
MG27P		1.826E-14	0.7%	1.358E-02	4.052E-16	4.0%	1.849E-02	1.36
FE56P		1.384E-14	1.0%	1.029E-02	4.539E-16	4.0%	2.072E-02	2.01
NI58P		1.345E-12	1.0%	1.000E+00	2.191E-14	1.5%	1.000E+00	1.00
IN115N	Cd	2.670E-12	1.0%	1.985E+00	4.954E-14	1.0%	2.261E+00	1.14
MN55G	Cd	7.951E-13	2.0%	5.912E-01	1.420E-12	0.5%	6.481E+01	109.63
SC45G	Cd	6.205E-13	1.0%	4.613E-01	1.500E-12	0.4%	6.846E+01	148.40
IN115G	Cd	1.436E-11	3.0%	1.068E+01	4.603E-11	0.8%	2.101E+03	196.77
AU197G	Cd	4.590E-11	0.9%	3.413E+01	1.455E-10	1.0%	6.641E+03	194.59
AU197G		5.489E-11	0.9%	4.081E+01	5.825E-10	1.0%	2.659E+04	651.45
SC45G		3.909E-12	0.7%	2.906E+00	1.313E-10	1.0%	5.993E+03	2061.95
FE58G		NA			1.954E-14	1.5%		

Neutron and photon dosimetry at LR-0 using paired dosemeters

Fernandes, A. C., Santos, L., Cardoso, J. and Marques, J.
Nuclear and Technological Institute
Estrada Nacional 10, 2686-953 Sacavém, Portugal.

Novák, E.
Nuclear Research Institute Řež plc.
Husinec - Řež 130, 250-68 Řež, Czech Republic

INTRODUCTION

Neutron and photon doses in mixed radiation fields are frequently determined with two detectors having different neutron sensitivities, with one of them insensitive to neutrons. The complex radiation spectra and discrepancies in detector sensitivities reported in the literature are often responsible for a poor agreement between the results obtained.

In this work, ionisation chambers and thermoluminescent dosemeters have been used to measure neutron and photon doses at the LR-0 reactor (Nuclear Research Institute, Czech Republic), at points located inside the core and the vessel. The response characteristics of various detectors have been studied in reference photon fields and at the RPI reactor at ITN (Nuclear and Technological Institute, Portugal). Reference results obtained by independent methods [*1*,*2*] have been used to interpret the measuremements and to compare the two methodologies used.

DOSEMETER CHARACTERISTICS

Magnesium and tissue-equivalent (A-150 plastic) ionisation chambers were used to measure the photon and neutron doses, respectively. The Mg (Exradin M2) and TE (Exradin T2) chambers were flushed with high purity Ar and methane-based tissue-equivalent gas, respectively. The chamber responses as a function of dose rate, photon energy and gas temperature and pressure were investigated (Figure 1) in standard photon fields available at ITN (^{137}Cs, ^{60}Co and various X-ray qualities).

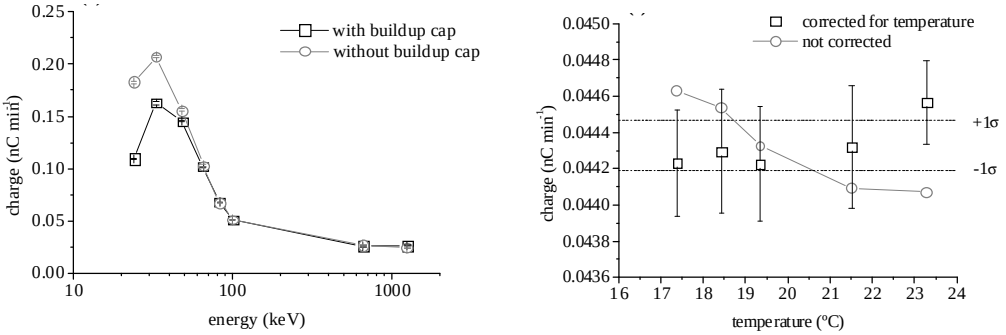

Figure 1. Response of the M2 chamber as a function of photon energy (left) and gas temperature (right).

For thermoluminescent dosimetry, ^{nat}LiF:Mg,Ti (TLD-100, Harshaw) and ^{7}LiF:Mg,Ti (TLD-700, Harshaw) were used to determine the neutron and photon doses, respectively. The glow curve, linearity, repeatability and neutron sensitivity were investigated in the standard photon fields and at the thermal column of the RPI reactor of ITN (Figure 2). The measured relative sensitivities to thermal neutrons (TLD-100: 1100 mGy ^{60}Co / 10^{10} n_{th} cm^{-2}; TLD-700: 20 mGy ^{60}Co / 10^{10} n_{th} cm^{-2}) are consistent with values reported in the literature [*3*]. However, it should be noted that the supralinear response and sensitivity loss observed for TLD-100 irradiated in the mixed-field will hamper its application at high thermal neutron fluences in a reactor.

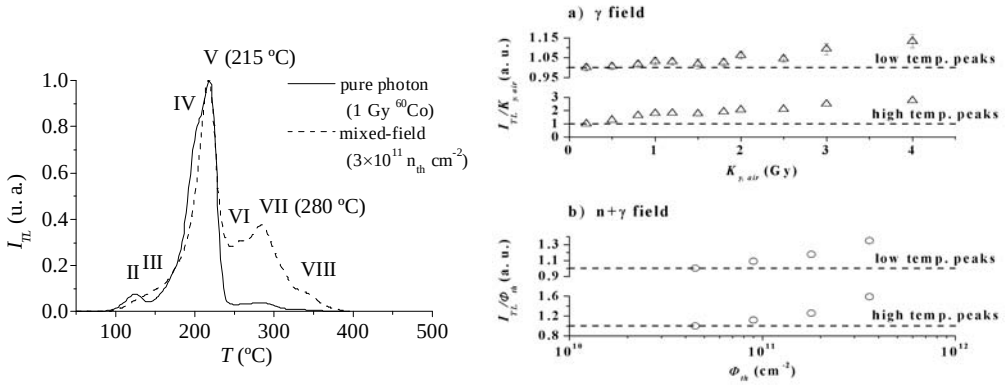

Figure 2. Glow curve (left) and dose response (right) of TLD-100 irradiated in a pure photon field and in a mixed field of thermal neutrons and photons.

MEASUREMENTS IN LR-0

Dose measurements were performed at various points in the LR-0 reactor, both in the core and in the reactor vessel. Table 1 shows the measured doses at the maximum reactor power. The neutron doses were calculated after subtracting the measurements obtained with the T2 and the M2 chambers, assuming that the relative neutron sensitivity of the T2 chamber is unity, for energies higher than 100 keV [*4*].

Table 1. Measured photon and neutron dose rates (μGy s^{-1}) in tissue.

Position	Location	Photon dose rate	Neutron dose rate
2	in core	7.4 ± 4%	8.3 ± 10%
3	3 cm from reactor vessel	1.8 ± 4%	0.16 ± 60%
4	10 cm from reactor vessel	0.36 ± 9%	~ 0.001

ACKOWLEDGMENTS

The present work was partly supported by the EC for shared-cost RTD actions: Support for Access to Research Infrastructures-Transnational Access to Research Infrastructures (project RENION no. FIR1-CT-2002-40157). A. C. Fernandes acknowledges the Foundation for Science and Technology (Portugal) for a post-doctoral grant (SFRH-BPD-14464-03).

REFERENCES

1. B. Ošmera and S. Zaritsky, *WWER-1000 Mock-up Experiment*, ÚJV č. 12036-R, Nuclear Research Institute, Czech Republic (May 2002).
2. B. Ošmera, F. Cvachovec and M. Mařík, *The Results of Photon Spectra Measurements Over the Reactor Pressure Vessel Simulator in WWER-1000 Model (Engineering Benchmark) in the LR-0 Experimental Reactor*, REDOS-R-06 / March 2004 / Issue 1, Nuclear Research Institute, Czech Republic (March 2004).
3. Horowitz, Y. S. *Neutron dosimetry*. In: Thermoluminescence and thermoluminescent dosimetry. Vol. II. Horowitz, Y. S., Ed. (Boca Raton, FL: CRC Press) (1984). pp. 90-114.
4. A. Kosunen, M. Kortesniemi, H. Ylä-Mella et al., "Twin Ionisation chambers for Dose Determinations in Phantom in an Epithermal Beam" *Radiat. Prot. Dosim.*, **81** (1999). pp. 187-194.

A New Methodology for Adjustment of Iron Scattering Cross Sections Using Time-of-Flight Spectroscopy

Wenner, M. T. & Haghighat, A.
University of Florida
Gainesville, FL 32608, USA.

Adams, J. M. & Carlson, A. D.
National Institute of Standards & Technology
Gaithersburg, MD 20899, USA.

Grimes, S. M. & Massey, T. N.
Ohio University
Athens, OH 45701, USA.

INTRODUCTION

This paper introduces a new methodology for adjustment of the iron scattering cross sections. The accuracy of the cross section data contained in the Evaluated Nuclear Data Files (ENDF) is paramount in performing accurate particle transport simulations. For pressure vessel fluence studies, the iron cross section is of highest importance. To assess the accepted values for the iron scattering cross section, we have developed a methodology combining measurements utilizing neutron transmission experiments through iron shells of different thicknesses, employing time-of-flight (TOF) spectroscopy and particle transport simulations to identify and adjust deficiencies in the scattering cross section of iron.

EXPERIMENTAL BACKGROUND

We perform TOF measurements utilizing the tandem Van de Graaff accelerator at the Ohio University Accelerator Laboratory. A unique feature of this facility is the "beam swinger,"[1] that permits experimental measurements to be made at various angles along a single well-defined flight path without the need to disturb the precision alignment of the neutron beamline.

Two accelerator-based neutron sources were utilized: ^{15}N(p,n) and D(d,n), in conjunction with two high-purity iron shells with different thicknesses of 3 cm and 8 cm. These thicknesses were selected based on the results of Monte Carlo calculations. These calculations provided information on maximizing the number of detected inelastically scattered neutrons[2]. Neutron sources were generated based on incident deuteron energies of 3 MeV, 5 MeV and 7 MeV projectiles with the D(d,n) source reaction as well as with an incident proton energy of 5.1 MeV with the ^{15}N(p,n) reaction with eight angular beam alignments (0°, 15°, 45°, 60°, 90°, 120° and 135°).

SIMULATION

The MCNP Monte Carlo code[3] was used on the parallel computing clusters of the Particle Transport and Distributed Computing (PTDC) Laboratory at the University of Florida Nuclear & Radiological Engineering (UFNRE) department. The source distributions used in the simulations were generated by using the TOF spectra without the presence of the iron shells. Since data is only available for eight angular beam alignments, a bilinear interpolation routine was applied to the available data to provide the missing data in the source spectrum[4].

Because of the limited experimental data, the interpolated source agrees well with the experimental data mainly at the peak locations of the TOF spectra. This is especially true for the zero degree D(d,n) cases since this reaction is highly forward peaked.

Comparison of measurement data and MCNP predictions for experiments with iron shells indicates differences in the TOF spectra. These differences can be from several sources: experimental and calculation statistics, source interpolation, detector resolution and cross section error. Comparing the zero degree D(d,n) case at 3 Mev, 5 Mev and 7 MeV source projectile energies, differences of ~8%, ~13%, and ~18% respectively, were observed in the peak regions. It was determined that since experimental and calculation errors are the lowest for these regions, some of the differences may be attributed to the errors in the iron scattering cross sections.

To examine further these differences, a utility code was developed to modify energy dependant cross sections, in ENDF-6 format. Since the differences observed were increasing with energy, we used an 'ad hoc' methodology for preliminary analysis by decreasing the Fe-56 inelastic cross sections at the peak energy regions by 21%, 29% and 35% for the 3 MeV, 5 MeV and 7 MeV D(d,n) cases respectively [5].

Using the adjusted ENDF files, continuous and Bugle-like multigroup cross sections were generated. MCNP simulations with the new cross sections show an ~40% decrease in the differences observed between experiment and calculation. To test the significance reactor pressure vessel (RPV) fluence calculations using the new multigroup cross section library in a 1-D RPV model (Figure 1), reaction rates for the 63Cu(n,α), 54Fe(n,p), 58Ni(n,p), 46Ti(n,p), 237Np(n,f), and 238U(n,f) interactions were determined at the cavity dosimeter. Our findings indicate RPV fluence might be underestimated based on the currently available libraries.

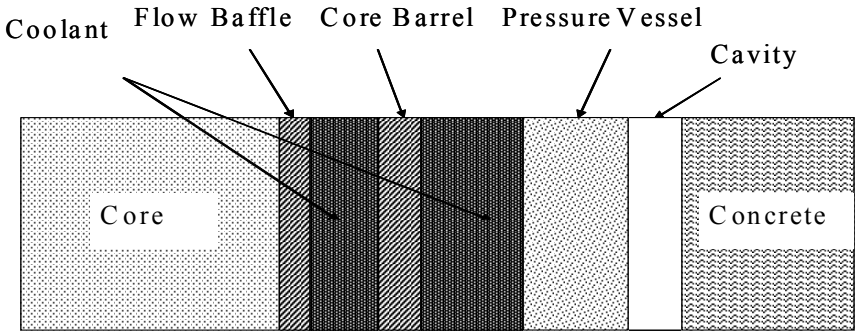

Figure 1. 1-D Reactor Pressure Vessel Model

REFERENCES

1. R.W. Finlay, C.E. Brient, D.E. Carter, et al., "The Ohio University beam swinger facility," Nucl. Inst & Meth., 198, 197 (1982).
2. S. Gardner, A. Haghighat, and A. Patchimpattapong, "Monte Carlo Analysis of Spherical Shell Transmission Experiment with New Tallying Methodology, presented at M&C 2001 – ANS Topical Meeting, Salt Lake City, Utah (2001).
3. J. F.Breismeister, "MCNP- A General Monte Carlo N-Particle Transport Code, Version 4C", LA 13709-M, Los Alamos National Laboratory, (2000).
4. M. Wenner, A. Haghighat, J. M. Adams, A. D. Carlson, S. M. Grims and T. N. Massey, "Monte Carlo Modeling of a Time-of-Flight (TOF) Experiment for Determination of Fe Scattering Cross Sections," Proceedings of PHYSOR 2004, April 25-29, 2004, Chicago IL.
5. M. Wenner, A. Haghighat, J. M. Adams, A. D. Carlson, S. M. Grims and T. N. Massey, "Development of a Methodology for Analysis of the Impact of Modifying Neutron Cross Sections," Proceedings of PHYSOR 2004, April 25-29, 2004, Chicago IL.

Reactor dosimetry with niobium

Wagemans, J., Willekens, M., Borms, L., Oeyen, J.
SCK•CEN
Boeretang 200, B-2400 Mol, Belgium.

Moens, A.
JRC-IRMM
Retieseweg, B-2440 Geel, Belgium

INTRODUCTION

Since several decades niobium has been recognised as a very favourable neutron activation material for reactor dosimetry purposes. The main advantages of this material are the long half life of its fast neutron activation product ^{93m}Nb, which allows neutron fluence determinations for long irradiations, and the low threshold energy of the ^{93}Nb(n,n')^{93m}Nb reaction, which makes it very suited for the determination of neutron induced damage fluences.

The disadvantages of using niobium as activation dosimeter are twofold: (i) pure niobium can become brittle under neutron irradiation; and (ii) special techniques are required for the detection of the low-energy X-rays that are emitted during the decay of ^{93m}Nb. A straightforward solution to the first difficulty would be the usage of low-purity niobium. This material however contains impurities of tantalum, and the decay gamma rays from its activation product ^{182}Ta induce X-ray fluorescence in niobium, which hampers a correct neutron fluence determination.

Both difficulties can be overcome applying special experimental techniques [1]. These techniques have been proven to be successful but they are less straightforward than measuring activation dosimeters as such. Moreover material embrittlement remains a problem. It was therefore decided to look for an alternative way of using niobium for reactor dosimetry. Wires of very pure niobium alloyed with aluminium (Al-10%Nb) were prepared and irradiated in the BR2 reactor at SCK•CEN (Mol, Belgium).

Finally, a third complication with using niobium for reactor dosimetry is the presence of a reliable reference source. From a recent intercomparison on retrospective dosimetry using niobium (see [2] and references therein), it appeared that the participating laboratories all use niobium calibration sources that are prepared from the same standard solution. Thus although the results from the intercomparison are in very good agreement, the absolute value of the specific ^{93m}Nb activities could be questioned. Therefore the first step in this investigation was the preparation of new ^{93m}Nb calibration sources.

EXPERIMENTS AND RESULTS

The experimental technique applied at SCK•CEN is the dissolution of the niobium dosimeter in a HF-HNO_3 mixture, the preparation of thin deposits from this solution and the measurement of the ^{93m}Nb X-rays using a suited germanium detector. The calibration of this detector is performed using deposits that were prepared from a standardised ^{93m}Nb solution in 1984, applying exactly the same technique. In order to verify the five existing standard sources, a new certified ^{93m}Nb standard solution (independent from the previous one) was purchased and from this five new deposits were prepared. Measurement of these deposits with the germanium detector (that is calibrated using the existing standard sources) shows an agreement with the nominal activities within 1.5%. In this way, the detector calibration is confirmed.

In order to solve the embrittlement problem, a Al-10%Nb alloy was prepared at IRMM and from this 1mm diameter wire dosimeters were made. In order to study the material behaviour and the activation properties of this new material, a dedicated irradiation in the BR2 reactor at SCK•CEN was set up. Al-10%Nb dosimeters were irradiated together with pure Nb to compare possible material embrittlement, and with Al-1%Co, Al-1%Ag, Fe and Ti to investigate its application as neutron dosimeter. Three irradiations were performed, with following targeted fluences:

- ~ 2E20 cm^{-2} fast neutron fluence and 2.5E20 cm^{-2} thermal neutron fluence;
- ~ 3E20 cm^{-2} fast neutron fluence and 3.5E20 cm^{-2} thermal neutron fluence;
- ~ 5.5E20 cm^{-2} fast neutron fluence and 6E20 cm^{-2} thermal neutron fluence.

Nor the pure Nb, nor the Al-10%Nb dosimeters have become brittle, even after the longest irradiation. This is a promising result for the Al-10%Nb material, but evidently it is not conclusive whether this material has a higher resistance against embrittlement than pure Nb. In order to verify this, a longer irradiation will be performed, possibly of thin foils of Al-10%Nb (the thinner the material, the faster it becomes brittle).

The homogeneity of the material was tested by measuring the ^{94}Nb activity of the entire wire and, after subdivision, of pieces of the wire. All results agree within the uncertainties hence the material is shown to be homogeneous.

The ^{93m}Nb specific activities of the irradiated pure Nb and Al-10%Nb have also been compared. For the pure Nb dosimeters, the normal target preparation and measurement procedure was followed. Thanks to the lower mass density of Al-10%Nb, the preparation of thin deposits is not a prerequisite for these dosimeters and therefore they have been measured as such. The agreement between the results obtained from both types of dosimeters is good, but nevertheless a dissolution procedure for Al-10%Nb is currently being investigated in order to obtain more accurate results.

Finally, analyses are ongoing to look at the applicability of the Al-10%Nb dosimeters for thermal and epithermal neutron fluence determinations. ^{94}Nb is formed through thermal (and epithermal) neutron capture and the ^{94}Nb decay gammas can be easily detected. Fluences obtained from Co-Ag, Fe-Ag and Al-10%Nb-Co dosimeter combinations are being compared. The advantages of using Al-10%Nb (compared to e.g. Ag) are its long half life, low flux depression and self-shielding effects, low burnup and the fact that the same dosimeter can be used for both fast and thermal/epithermal fluence determination.

CONCLUSION

New ^{93m}Nb calibration deposits have been prepared. In this way the absolute values of previously performed ^{93m}Nb activity measurements at SCK•CEN (and in other laboratories) are verified and confirmed.

A new type of niobium dosimeter has been developed and tested. This material has distinct advantages over other material types. Several positive results have already been obtained. Final analyses are currently ongoing and a long-term irradiation is scheduled for further testing.

REFERENCES

1. *Standard Test Method for Measuring Fast-neutron Reaction Rates by Radioactivation of Niobium*, ASTM E 1297.
2. W. Voorbraak, J. Woittiez, J. Wagemans, M. Van Bocxstaele, T. Kekki and T. Serén,*Retrospective Dosimetry of Fast Neutrons Focused on the Reactions ^{93}Nb(n,n')^{93m}Nb and ^{54}Fe(n,p)^{54}Mn*, these proceedings.